# Droppable oyster brood stock structure

Experimental study on the design for a flat oyster brood stock structure, that can be installed at the scour protection of Dutch offshore wind farms, via dropping from a vessel

*Eva Siderius*

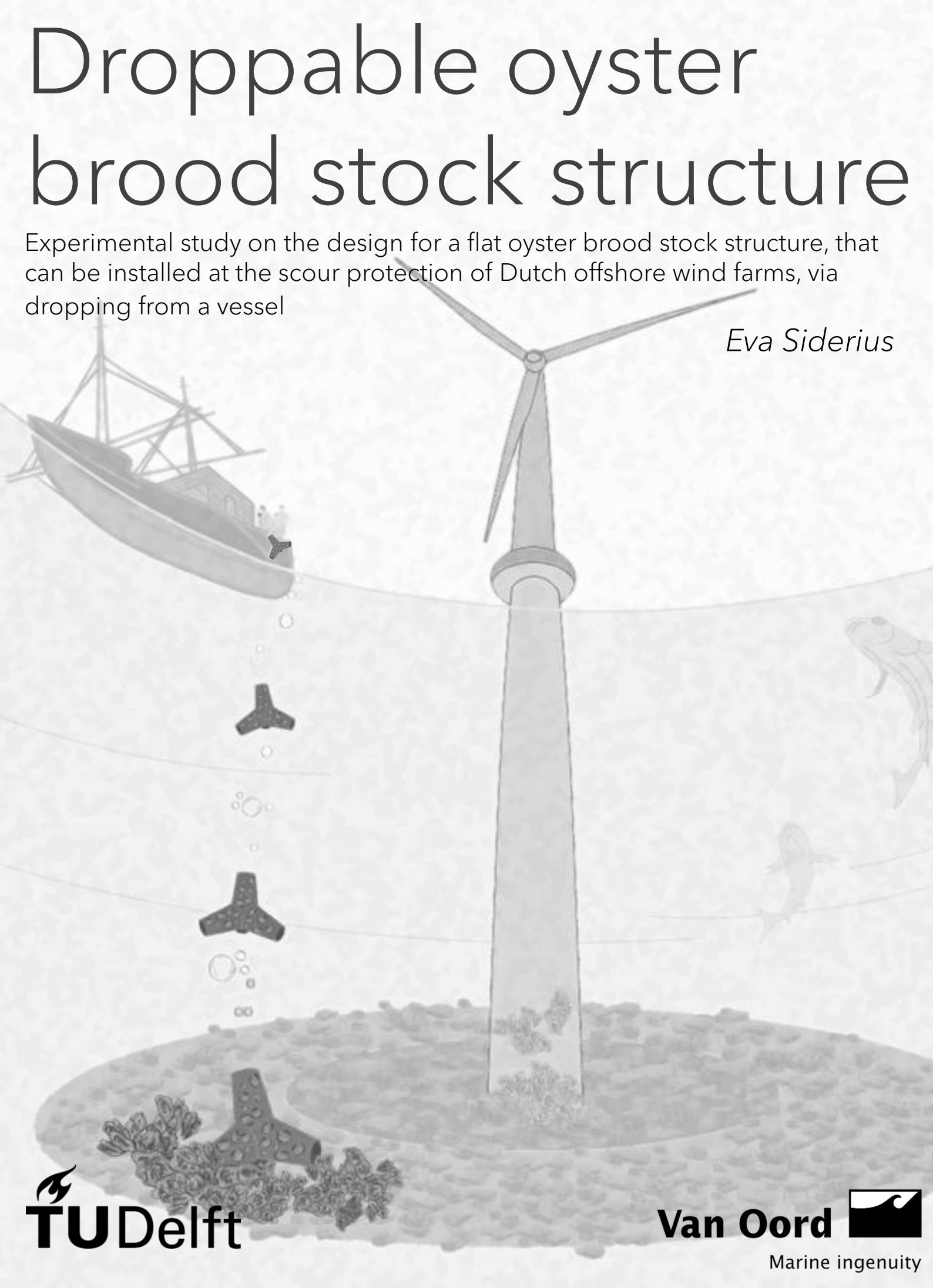

TU Delft

Van Oord

Marine ingenuity

# Droppable Oyster Brood Stock Structure

Experimental study on the design for a flat oyster brood stock structure, that can be installed at the scour protection of Dutch offshore wind farms, via dropping from a vessel

by

Eva Siderius

In partial fulfilment of the requirement for the degree of Master of Science in Hydraulic Engineering at the faculty of Civil Engineering and Geosciences at Delft University of Technology

| | | |
|---|---|---|
| Student number: | 4486536 | |
| Project Duration: | January, 2022 - Month, Year | |
| Institution: | Delft University of Technology | |
| Place: | Faculty of Civil Engineering and Geosciences, Delft | |
| Thesis committee: | Prof. dr. ir. Mark van Koningsveld (chair) | TU Delft & Van Oord |
| | Dr. ir. Bas Hofland | TU Delft |
| | Drs. Remment ter Hofstede | TU Delft & Van Oord |

An electronic version of this thesis is available at http://repository.tudelft.nl/.

TU Delft

Van Oord

Marine ingenuity

# Preface

This thesis was commissioned by the Delft University of Technology and was partly carried out in the Hydraulic Engineering Laboratory at the Faculty of Civil Engineering. The research involves eco-enhancing engineering, investigating a new type of oyster brood stock structure. The research was carried out in cooperation with Van Oord.

To execute this research on a subject that is becoming increasingly important in the development of offshore wind farms was very exciting. It gave me the opportunity to work in a dynamic environment and to have a look outside my study scope. Conducting the research has been a challenging, educational and extremely interesting experience for me.

There are a few people who helped and supported me throughout my research. I would like to thank these people in this preface.

First of all, I would like to thank my committee. I would like to thank Mark van Koningsveld for making this thesis possible. In addition, for trusting me while conducting the research and remaining enthusiastic about what I carried out. The feedback regarding the application helped a lot to see that sometimes it is good to take a step back and look at the bigger picture instead of getting stuck on small details. I would also like to thank Bas Hofland. The discussions with Bas helped me enormously, especially in terms of physical modelling and concept ideas. His inexhaustible energy and passion for the subject radiated. His keen eye for detail and critical questioning has taken my research to the next level. I would also like to express my gratitude to Remment ter Hofstede for his daily guidance during my research. Your keen interest in improving the structure and approach of my research elevated the report. Our weekly meetings helped me immensely to reflect on details about the research and also to discuss the overall process and planning. Your positive outlook also gave me the necessary confidence during uncertain stages of the process.

Secondly, I like to thank Van Oord, especially the Environmental Engineering department. My enthusiastic colleagues made my thesis writing enjoyable and interesting to discuss. Also, the opportunities they provided, such as attending a conference on wind energy and wildlife and lecturing, were a great experience.

I would also like to highlight the people working in the lab. Chantal, Arie, Pieter and Arno helped me greatly with the preparation and execution of the experiments. Also during some setbacks related to construction delays in the lab, they were very helpful and thoughtful in finding solutions.

Lastly, I would like to thank my friends and family for their support during the past months. I would like to acknowledge my housemates for staying enthusiastic and interested during my monologues about oysters and conducting tests. I thank Thom for listening to my complaints when something went wrong and also for the suggestions how to process my test results. Even though you had no idea about the content of the project, your suggestions were very beneficial. Finally, I thank my parents for the patience and support you showed with my graduation and also during the whole of my time at university.

*Eva Siderius*
*Delft, November 2022*

# Abstract

In 2050, the entire energy consumption in the Netherlands is foreseen to come from renewable sources. Offshore wind energy has the potential to enable this transition to a CO2-emission-free energy supply. Consequently, the development of offshore wind farms in the Dutch North Sea has been expanding enormously in the last decade. The Dutch Government is also ambitious to achieve biodiversity goals in the Dutch North Sea, by restoring ecosystem functions. The ecological value in the development of offshore wind farms is therefore considered an important aspect and its significance is only increasing. The European flat oyster is identified as a key species when restoring the biodiversity in the North Sea, because they embody a distinctive benthic community that provides a range of valuable ecosystem services. The environmental conditions in offshore wind farms have shown to be suitable to act as a habitat for the European flat oyster reefs, because of hard substrate and undisturbed areas. Multiple oyster recovery initiatives have been introduced in offshore wind farms, to kick-start oyster reef restoration. No larvae source is nearby, therefore oysters need to be introduced for oyster reefs to develop in offshore wind farms. These oysters are introduced by applying oyster brood stock structures, which are structures to which adult oysters are attached. The brood stock structures are installed by onboard cranes present at vessels, on the scour protection at offshore wind farms. A scour protection is a protection layer consisting of rocks, which is installed around a wind turbine to guarantee its stability. This crane installation method has shown to be complicated and costly, due to the vessel type and equipment required. These complications result in a challenging and therefore limited application. Hence, there is a need to look for an alternative installation method, that ensures a simple and cost-effective application. Deployment of brood stock structures via dropping from a vessel manually is selected, which ensures easy deployment, because it does not require a crane (and a vessel that can hold this crane). This would decrease the engaged expenses significantly. Such a new installation method requires a different design for the brood stock structure. Research is needed into a new design for a flat oyster brood stock structures, which is appropriate for the drop installation method. This leads to the following research objective for this master thesis;

*What is the design for a flat oyster brood stock structure, that can be installed at the scour protection at offshore wind farms, via dropping from a vessel, such that it will be stable and integer during deployment and operational lifetime?*

Based on literature study and consultation sessions with experts, a set of design criteria for the droppable brood stock structure are set. The design criteria considered, result in preferred properties for the design of the concept. These criteria lead to six suitable basic concept designs that are selected; Xblock, Tetrapod, Cube framework, Anchor, Open table and Reference block. However, two set design criteria result in specific requirements, which should be met; the positioning and stability criteria. The positioning criterion defines a requirement, that the maximum positioning accuracy for deployment is 5.5 meter. The stability criterion defines a requirement, that the brood stock structures should remain stable during a storm event with a return period of 10 years. Behavioural predictions are made for the performance of the concepts during the lifetime of the droppable broodstock structure by performing calculations. Three relevant situations during the lifetime are investigated; fall from the vessel until the scour protection, the landing on the scour protection, the stability during storm events. The behavioural predictions are used to select the most suited concept parameters (e.g. volume, dimensions) for the six basic concepts by an iterative process. Ten concepts emerged; Reference block, Xblock, Tetrapod, Cube framework, Piebox framework, Anchor long, Anchor short, Open table 1, Open table 2 and Open table 3.

Physical model tests were performed to test the behaviour of the ten selected concepts during the relevant situations. Three types of tests are executed; fall test, land test and stability test. The physical model tests are performed in the wave flume in the Hydraulic Engineering Laboratory at TU Delft.

The fall test investigated the fall of the structure from the vessel onto the scour protection, to define the dropping accuracy during the fall. This is done by dropping the prototypes in the wave flume and analysing the fall movement. The results are defined in horizontal displacement encountered during the fall, which are processed to full scale by extrapolation. Four concepts comply with the positioning requirement of a maximum horizontal displacement of 5.5 meters, based on the test results; Reference block, Tetrapod, Open table 1, Piebox framework.

The land test investigates the landing of the structure on the scour protection, by analysing the interaction between the prototypes and the stone layer after dropping them in the wave flume. The interaction observation is used to get insight in the amount of oyster damage encountered during the landing. An indication of the amount of oysters lost can define the number of structures needed per scour protection, to obtain the required oyster population for restoration. No valued requirement (arose from the design criteria) was defined by the design criteria with regard to the results obtained in the land test. However, minimal oyster loss and minimal number of structures are preferred. Four concepts scored best on these criteria; Cube framework, Piebox framework, Anchor long and Anchor short

The stability test investigates the stability of the concepts during extreme hydraulic conditions, by generating storm conditions in the wave flume. The conditions at which the concepts fail to remain stable are determined. The stability requirement implied that the brood stock structure should at least remain stable during a storm event with a return period of 10 years. Four concepts comply with this set requirement; Open table 2, Open table 3, Tetrapod and Anchor long.

The results obtained by physical modelling are used to calibrate the calculations performed to make behavioural predictions about the relevant situations.

To select the design for a droppable flat oyster brood stock structure, the ten concepts are analysed and assessed, using two methods. The first method entails a requirement analysis, which is fully dependent on the two set requirements (positioning and stability). Only the concepts that comply with these requirements are considered. Only the Tetrapod complies with both requirements. The Open table 2 only slightly exceeds the positioning requirement and is therefore also considered for the second assessment method. The second method entails a multi-criteria analysis, which uses all the defined design criteria to assess the remaining concepts on their overall suitability. This is a subjective method as the design criteria have been assigned a weighting factor, which are instinctively determined based on the preferences of this study. This method determines the Open table 2 to be better suited than the Tetrapod.

For the application of an oyster brood stock structure, the type of installation method and type of brood stock structure need to be determined.

The crane method ensures ecological value but is expensive. The drop method ensures easy installation, but part of the oysters will almost certainly be lost during deployment. The choice of a drop method versus a crane method is therefore a trade-off between financial and ecological value. Possible follow-up research could focus on a cost-benefit analysis of the two installation methods, including the corresponding structures, to make a well-informed decision for each application.

When a drop method is applied, a suitable concept must be selected. The most suitable concepts selected in this research, are determined based on preferences and requirements. These preferences and requirements have emerged from the design criteria set in this study and the specific conditions selected, for which the concepts have been tested. For each application, these preferences and conditions differ and should be adjusted for the specific situation. The selection of the concepts is to be redefined using this research, to obtain the design for a droppable flat oyster brood stock structure best suited.

# Contents

# List of Symbols

| Symbol | Definition | Unit |
|---|---|---|
| a | Wave amplitude | m |
| $A_{hit}$ | Surface of object hit relative to total surface | % |
| $a_0$ | Amplitude of orbital motion induced by waves | m |
| $A_a$ | Surface of armour layers | $m^2$ |
| $A_f$ | Surface of filter layer | $m^2$ |
| $A_{pile}$ | Surface of monopile | $m^2$ |
| $A_{sp}$ | Total surface of scour protection | $m^2$ |
| C | Chezy value | $\sqrt{m}/s$ |
| $c_f$ | Friction coefficient | - |
| $C_A$ | Added mass coefficient | - |
| $C_D$ | drag coefficient | - |
| $C_L$ | Lift coefficient | - |
| $d_{50}$ | Median grain size | m |
| $D_{n50}$ | Nominal diameter of concept | m |
| $d_{50n-a}$ | Nominal grain size armour layer | mm |
| $d_{50n-f}$ | Nominal grain size filter layer | mm |
| $\Delta$ | Relative density | - |
| dh | Drop height of falling structure | m |
| $D_i$ | Objects inside diameter | mm |
| $F_B$ | Bottom friction force | N |
| $F_D$ | Drag force | N |
| $F_G$ | Gravitational force | N |
| $\sum F_h$ | Horizontal force acting upon object | N |
| $F_I$ | Inertia force | N |
| $F_L$ | Lift force | N |
| $\sum M$ | Momentum force acting upon object | Nm |
| $F_r$ | Froude number | - |
| $\sum F_v$ | Vertical force acting upon object | N |
| $f_w$ | Friction factor | - |
| g | Gravitational acceleration | $m/s^2$ |
| H | height of the structure | m |
| h | Water depth | m |
| $H_{1\%}$ | Wave height which is exceeded by 1 % of the waves | m |
| $H_s$ | Significant wave height | m |
| k | Wave number | 1/m |
| $k_r$ | Bottom roughness | m |
| $k_s$ | Hydraulic roughness | m |
| KC | Keulegan-Carpenter number | - |
| L | Characteristic length of object | m |
| $L_0$ | Deep water wave length | m |
| $L_{max}$ | Maximal wave length | m |
| $L_{min}$ | Minimal wave length | m |
| M | Rotational forces on object | Nm |
| $N_n$ | Scale parameter for density scaling | - |
| P | Probability of occurrence | % |
| Re | Reynolds number | - |
| S | Projected area of object normal to the force direction | $N/m^2$ |

| Symbol | Definition | Unit |
|---|---|---|
| t | time | s |
| T | Return period | years |
| $t_a$ | Thickness of armour layer | mm |
| $t_f$ | Thickness of filter layer | mm |
| $T_p$ | Peak wave period | s |
| $T_s$ | Significant wave period | s |
| $t_t$ | Thickness of armour and filter layer | $m^2$ |
| u | Velocity of object relative to the fluid | m/s |
| $\bar{u}$ | Depth averaged flow velocity | m/s |
| $u_b$ | Flow velocity near the bottom | m/s |
| $u_c$ | Current velocity | m/s |
| $u_{c-1.5m}$ | Current velocity 1.5 meters above seabed | m/s |
| $\dot{u}$ | Fluid particle acceleration amplitude | $m/s^2$ |
| $u_r$ | Resulting flow velocity induced by current and waves | m/s |
| $u_{r-1.5m}$ | Resulting flow velocity induced by current and waves, 1.5 meters above the seabed | m/s |
| $u_w$ | Orbital motion induced by waves | m/s |
| $u_{w-1.5m}$ | Orbital motion induced by waves, 1.5 meters above the seabed | m/s |
| $U_{ursell}$ | Ursell number | - |
| V | Volume of object | $m^3$ |
| w | Equilibrium velocity | m/s |
| W | width of the structure | m |
| $w_a$ | Width of armour layer | m |
| $w_f$ | Width of filter layer | m |
| $WG_x$ | Distance between two wave gauges | m |
| x | x-coordinate | m |
| $x_h$ | Horizontal displacement | m |
| $x_{h-max}$ | Maximal horizontal displacement | m |
| $x_{h-mean}$ | Mean horizontal displacement | m |
| y | y-coordinate | m |
| z | z-coordinate | m |
| $z_0$ | Heigth above the bottom | m |
| $\kappa$ | Kappa coefficient | - |
| $\mu$ | Bottom friction coefficient | - |
| $\omega$ | Angular frequency | 1/s |
| $\phi$ | Angle between wave and current direction | ° |
| $\varphi$ | Fall angle | ° |
| $\psi$ | Shields parameter | - |
| $\rho_s$ | specific weight of object | $kg/m^3$ |
| $\rho_w$ | specific weight of water | $kg/m^3$ |
| $\theta$ | Settle angle of object | ° |
| $\tau_c$ | Shear stress induced by current | $N/m^2$ |
| $\tau_c r$ | Critical shear stress | $N/m^2$ |
| $\tau_r$ | Shear stress induced by current and waves | $N/m^2$ |
| $\tau_w$ | Wave induced shear stress | $N/m^2$ |
| $\upsilon$ | Kinematic viscosity | - |

# 1

# Introduction

## 1.1. Background information

In the last decade, the energy transition has rapidly evolved. The urge to replace fossil fuels with more sustainable energy sources has led to increasing interest in expanding the range of available and affordable low-carbon technologies. Offshore wind energy is currently considered one of the large-scale technologies for renewable energy production [RVO, 2021b]. The offshore wind energy supply is increased significantly in the last few years. The global offshore wind market has grown nearly 30% per year between 2010 and 2018 and over the next five years, about 150 new offshore wind projects are scheduled to be completed around the world, pointing to an increasing role for offshore wind in power supplies [Cozzi and Wanner, 2019]. At present, seven offshore wind farms are located in the Dutch North Sea, with a combined installed capacity of approximately 2.45 MW of electricity. Six offshore wind farms are under construction or in preparation and even more are planned [RVO, 2021a].

Wind turbines are constructed on monopile foundations [Desyani and Mungar, 2022]. A monopile is a slender subsea construction. Slender subsea structures change the existing flow patterns, which can cause local erosion or scour. Scour is the phenomenon that seabed sediments are eroding around the base of the foundation. This effect is caused by flow acceleration along the structure, followed by the deceleration of the flow downstream of the structure [Breusers et al., 1977]. This results in increased turbulence downstream of the structure, causing scour (see Figure 1.1)[Raudkivi et al., 1985]. This results in a scour hole around the monopile, which eventually can undermine the stability of the wind turbine.

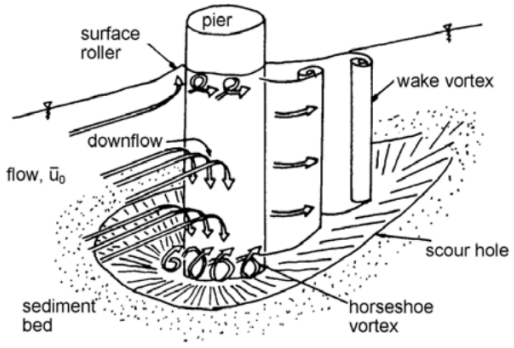


**Figure 1.1:** Scour around a cylinder [Raudkivi et al., 1985]

To ensure stability for the foundation, a scour protection is installed around the monopile [Raaijmakers et al., 2017] [Schiereck, 2003]. A scour protection consists of rock layers around the foundation, which can act as new hard substrate habitat [ove, 2019]. The scour protection type that is considered

in this report, consists of two types of rock layers. These two layers are placed before the wind turbine is installed, after which the wind turbine foundation is placed. The bottom rock layer is called the filter layer, which is placed on the seabed. The filter layer consists of a range of relatively small rocks that are placed in an oval or round shape around the monopile. An armour layer is placed in a round shape on top of this filter layer. The armour layer has a smaller radius than the filter layer and consists of a range of larger rocks [Blankenweg, 2017] [Tönis et al., 2013], [Desyani and Mungar, 2022]. This type of scour protection is broadly applied at offshore wind farms in the Dutch North Sea. A side and top view of a scour protection around a monopile in offshore wind farms is presented in Figure 1.2(a) and (b).

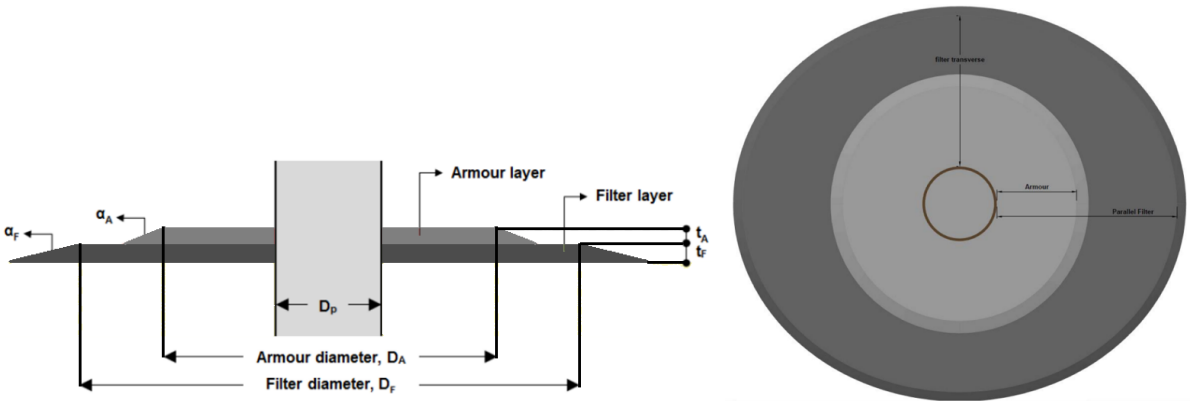


**(a)** Side view **(b)** Top view

**Figure 1.2:** Display of conventional scour protection around a monopile in offshore windfarm [Blankenweg and Elleswijk, 2017]

150 years ago, the bottom of the Dutch North Sea was covered with epibenthic shellfish reefs, of which approximately 30% were occupied by European flat oysters (*Ostrea edulis*), see Figure 1.4(a) [Olsen, 1883]. European flat oysters create hard substrates on otherwise flat soft sediment by creating reefs [Kamermans, 2018]. Oyster reefs provide a range of valuable ecosystem services: better water quality, local decrease of toxic algal blooms, increase in nutrient uptake, increase of benthopelagic coupling, increase in species richness, increase of biogenic structures which provide habitat, food and protection for numerous invertebrate and fish species [Pogoda, 2019] [Beck et al., 2011]. This indicates that the oyster reefs have an important role in the biodiversity and maintenance of marine ecosystems, which makes the flat oyster a valuable species in the North Sea.

The European flat oyster (*Ostrea edulis*) is an oyster species that is native to Europe, see Figure 1.3a. The original habitat of the European flat oyster is along the European coast from Norway to Morocco, across the Mediterranean and the Black Sea [Olsen, 1883] [Duren et al., 2016].

The European flat oyster has two valves (shells). The two valves are held together by a large muscle, which can close and open the valves. The oyster also has gills, which take in oxygen and filter algae from the water as food. If the suspended matter content is too high, the gills become clogged and less food is absorbed which can eventually lead to suffocation [Haelters and Kerckhof, 2009].

The average age of a flat oyster varies between 5 to 10 years, which is influenced by environmental conditions [Perry and Jackson, 2017]. Oysters start their lives as a male and become a female after approximately three years. From the first time they are female, they change sex generally twice during a single reproductive season [Foighil and Taylor, 2000], depending on the conditions [Walne, 1970]. Resulting in the fact that they can reproduce twice each breeding season. The reproductive season is dependent on water temperature and can therefore vary per location and season [Perry and Jackson, 2017]. When the larvae have been fertilised, they remain in the shell of the mother for a while [Smaal et al., 2017b]. Thereafter, they travel with the flow of the water for some time, which can vary from one to four weeks, before settling on a hard substrate they encounter [Muus et al., 1973]. Due to this relatively short 'swim' period, the larvae do not migrate far before they settle. Their spreading distance reaches on average about 1 km [Walne, 1970] and can reach a maximum of 10 km [Perry and Jackson, 2017]. The life cycle stages of European flat oyster are presented in Figure 1.3b.


**(a)** European flat oyster **(b)**

**Figure 1.3:** European flat oyster (a) and the stages of the European flat oysters life cycle [Didderen et al., 2019b] (b)

In the nineteenth century, the European flat oyster population has been declining rapidly in the Dutch North Sea, due to exposement to large-scale fisheries, overexploitation and pollution. The bottom of the Dutch North Sea is now merely consisting of sand. At present, flat oysters are scarcely present near the coast of Zeeland and above the Wadden islands [Airoldi and Beck, 2007] Figure 1.4(b). After 1985, only several dozen individual flat oysters were detected in the entire Dutch North Sea (which were not near offshore wind farms), see [Smaal et al., 2015].

The presence of certain diseases contributed greatly to this decline in the oyster population, for example *Bonamia ostreae*. In 1980, *Bonamia ostreae* was identified for the first time in Europe. *Bonamia Ostreae* is a parasite whose main target species is the flat oyster [Culloty et al., 2001]. Due to the exchange between oyster farms, the parasite quickly spread to all major flat oyster regions within Europe. Currently, the disease is still present in oyster banks in the Netherlands and also in numerous other oyster hatcheries in Europe, including the United Kingdom, France, Belgium and Norway [Smaal et al., 2015] [Engelsma et al., 2014]. When flat oysters are infected with the parasite, mortality can begin after four months. The most common age at which mortality occurs is two years. This means that the oyster has already died before it was able to reproduce [Lallias et al., 2008].

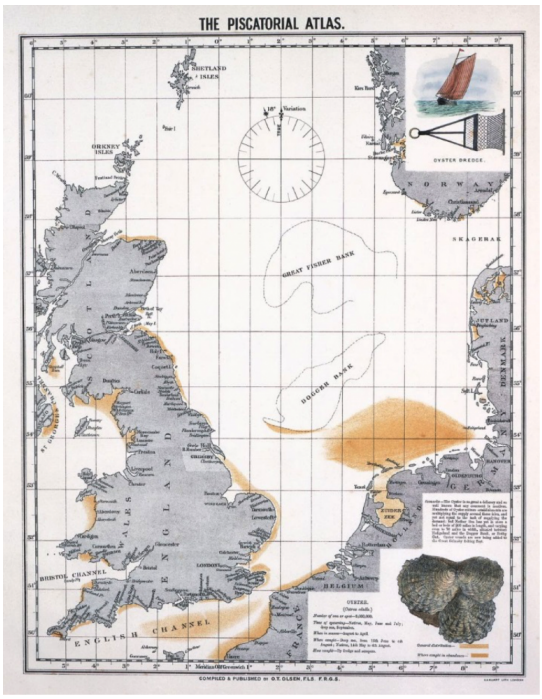


**(a)** Historical distribution of the flat oyster in 1883 [Olsen, 1883]

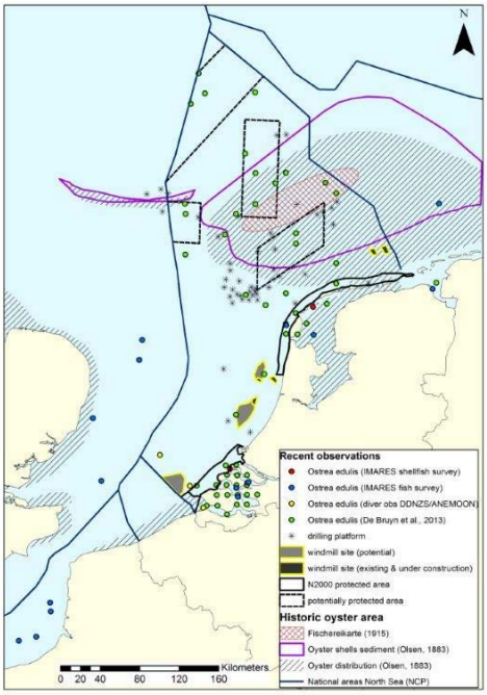


**(b)** Flat oysters observed in Dutch North Sea, in 1985 [Smaal et al., 2015]

**Figure 1.4:** European flat oyster distribution in the North Sea

The decline of the flat oyster population is acknowledged as problematic, due to their positive effect on the ecosystem, they are classified as threatened by the OSPAR convention [J. Haelters, 2009]. Multiple nature conservation organisations have identified the European flat oyster as a key species to restore the biodiversity in the North Sea [Duren et al., 2016]. The Dutch Government is ambitious to achieve biodiversity goals, restore ecosystem functions and enhance ecosystem services [nat, 2020], which also includes restoration of the European flat oyster reefs in the Dutch North Sea [Kamermans et al., 2018b].

## 1.2. Problem statement

Due to sensitive systems and expensive materials present at offshore wind farms, the crossing or navigation of fishing and leisure vessels is constrained and any fishing operations during their construction and (in many cases) operational phase are excluded. These constraints make the offshore wind farm areas effectively closed for navigation, which results in an undisturbed area for marine ecosystems [Schupp et al., 2021]. Offshore wind farms therefore provide new hard substrate and undisturbed areas in the North Sea. These factors indicate, that the offshore wind farms in the Dutch North Sea offer suitable locations for flat oysters to grow. These artificially created areas could therefore provide an opportunity to restore the flat oyster population [Kamermans et al., 2018b]. Offshore wind farms are usually far away from natural oyster reefs, which means there are no larvae nearby [Smaal et al., 2015] [Kennedy and Roberts, 2006] and also no *Bonamia Ostreae* infected oysters. To kick-start oyster reef development, oysters therefore need to be introduced at offshore wind farms. Various approaches can be used to introduce oysters [Bouma et al., 2017].

Across Europe, many projects have been initiated to kick-start the development of the native flat oyster reefs (at offshore wind farms), see Figure 1.5(a). These projects include testing different types of scour protection, spat recruitment, concrete structures which are attractive for larvae settlement, oyster cages and reef structures [NORA, 2017].

Several pilot projects to introduce flat oyster recovery have been executed in the Dutch North Sea. Relevant pilot projects for this research are outlined in Section A.2. An overview of the relevant

structures, focus points and lessons learned for the relevant pilots are displayed in Table 1.1. The locations of the pilot project can be seen in Figure 1.5(b).

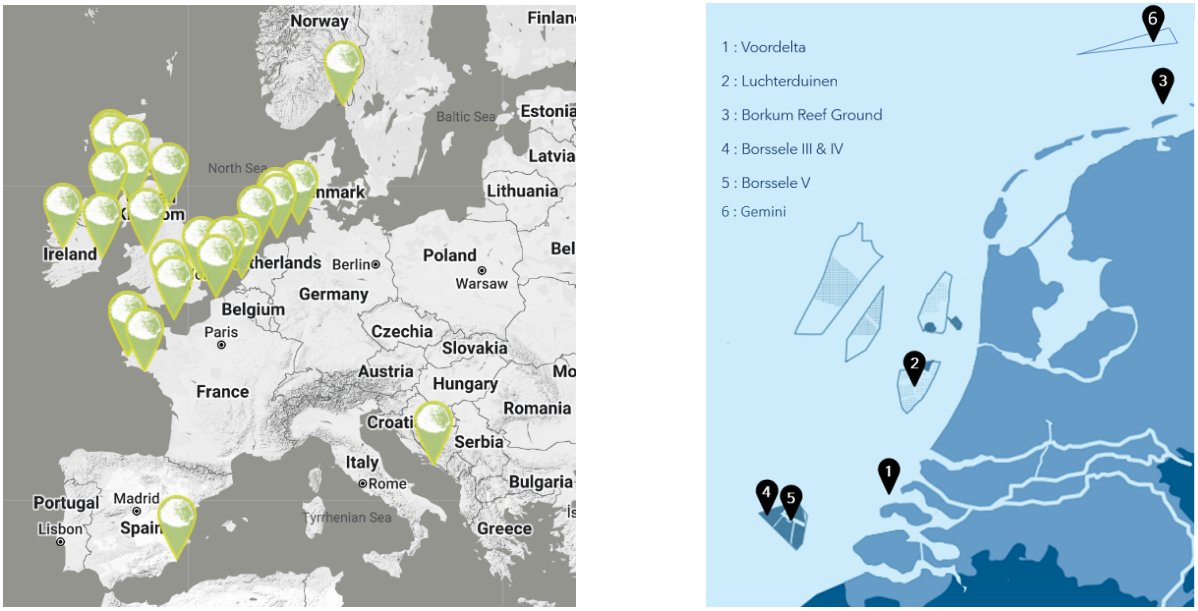


**(a)** Across Europe. From NORA.nl

**(b)** In the Dutch North Sea. Adjusted from rvo.nl

**Figure 1.5:** Locations of offshore flat oyster restoration pilot projects.

**Table 1.1:** Overview of pilot projects for flat oyster Restoration in Dutch offshore wind farms, with the relevant structures, focus points and lessons learned [Sas et al., 2016], [Didderen et al., 2019a], [Didderen et al., 2020], [Didderen et al., 2018], [Kardinaal et al., 2021], [Schutter et al., 2021].

| Pilot project | Relevant structure | Focus points | Lessons learned |
|---|---|---|---|
| *Voordelta* | - Oyster racks<br>- Substrate racks<br>- Spat collectors | - Design of structure<br>- Type of oysters<br>- Type of substrate<br>- Oyster survival<br>- Restoration location<br>- Disease-free oysters | - Disease-free oysters<br>- Low survival rate of adults<br>- Structure should be placed on hard substrate<br>- Stability was not maintained |
| *Luchterduinen* | - Oyster racks<br>- Substrate racks | - Design of structure<br>- Type of oysters<br>- Type of substrate<br>- Oyster survival<br>- Restoration location<br>- Disease-free oysters | - Disease-free oysters<br>- Promising reproduction<br>- Structure should be placed on hard substrate<br>- Stability was not maintained |
| *Borkum Reef Ground* | - Research racks | - Design of structure<br>- Type of oysters<br>- Type of adhesive<br>- Oyster survival | - Cages in racks got clogged<br>- High survival rate<br>- Stability was maintained<br>- Used adhesive not optimal<br>- Use large adult oysters |
| *Borssele III & IV* | - Research cages | - Design of structure<br>- Restoration location<br>- Oyster survival | Not yet evaluated |
| *Borssele V* | - Brood stock structure | - Design of structure<br>- Fabrication structure<br>- Type of adhesive<br>- Oyster survival | - Avoid sedimentation at the structure<br>- Avoid unnecessary weight of structure<br>- Assembling in dry conditions<br>- Stability was maintained |

Numerous lessons were learned from these pilot projects and improvements were made in each new project. Based on the executed pilot projects, the placement of brood stock structures is deemed to be a suitable approach to kick-start flat oyster reef growth at offshore wind farms [Didderen et al., 2019b] [Smaal et al., 2015]. A brood stock structure entails a structure on which adult oysters (of different age classes) are attached to. The oysters are meant to reproduce, which leads to a growing population and eventually a reef. In Figure 1.6, a couple of examples of brood stock structures used in previous pilot projects, are presented. Each project in which a brood stock structure was installed, contained its own focus points, e.g. the shape or size of the structure, the type of oysters, the type of substrate, the type of adhesive material, the manufacturability of the structure and the location.

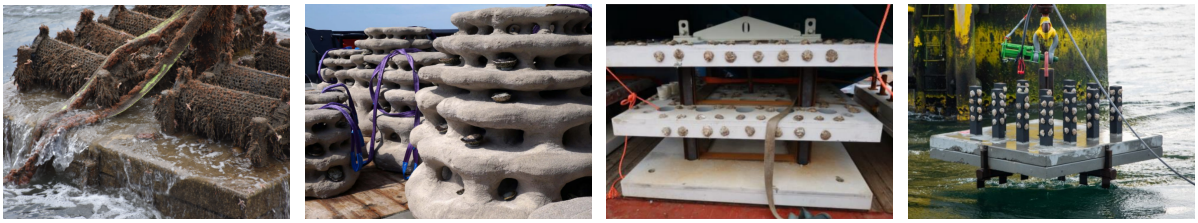

(a) (b) (c) (d)

**Figure 1.6:** Oyster brood stock structures used in previously executed pilot projects.

The pilot projects have shown that introduction of flat oysters within offshore wind farms by installation of oyster brood stock structures is promising and has the potential to reintroduce the flat

oyster population into the Dutch North Sea, because monitoring visits indicated disease-free oysters, high survival rates and reproduction of the oysters.

However, the projects have also shown that improvements in the design of the brood stocks are needed, to increase the oyster survival and reproduction rate [Didderen et al., 2019a]. The improvements are mainly related to preventing sedimentation on the structures, which leads to suffocation of the oysters. The size and shape of the structures also resulted in complications regarding the preparation of the structures, as they are not easily managed [Schutter et al., 2021]. These design limitations were enhanced by manufacturing issues, which resulted in last-minute design changes in some executed projects [Schutter et al., 2021].

Furthermore, during the installation of the brood stock structures complications were encountered. In all pilot projects, the brood stock structures were placed on the scour protection using onboard cranes. A vessel that is equipped with such a crane and that can come near monopiles is required for the installation. The structures are hung on these cranes from which they are put on scour protection. When they are hanging, the structures are swinging considerably due to weight and sea conditions, making it difficult to put the structures in the correct location. This swinging can also cause dangerous situations and damage to structures, oysters and equipment. Apart from the complications encountered, this deployment method is also very costly due to the type of vessel and equipment required.

As a result of these difficulties regarding the design, manufacturing and the installation of the brood stock structures, there is interest in exploring new design options and the use of alternative deployment methods. Based on consultations with ecological experts and hydraulic engineers, a manual dropping method is selected for investigation. Deployment of brood stock structures via manual dropping entails the structures being dropped from a vessel by people. This method does not require special equipment and should therefore ensure easy deployment. The engaged expenses are likely to decrease significantly, which would simplify application and provide opportunity.

The manual drop method is compared to the crane installation method, based on the most relevant advantages and disadvantages, in Table 1.2.

**Table 1.2:** Advantages and disadvantages per installation method

| | **Crane method** | **Drop method** |
|---|---|---|
| *Pros* | - Accurate positioning<br>- Oysters stay intact<br>- Few structures needed | - Less expensive<br>- Easy installation |
| *Cons* | - Specific installation vessel needed<br>- Expensive | - Less accurate positioning<br>- Partial loss of oysters |

The drop installation method, together with the existing limitations regarding design, lead to the need for investigation into a new design for a flat oyster brood stock structure that can be installed, using the manual drop method, at the scour protection in offshore wind farms. See Figure 1.7 for a situation sketch of the application of a droppable brood stock structure.

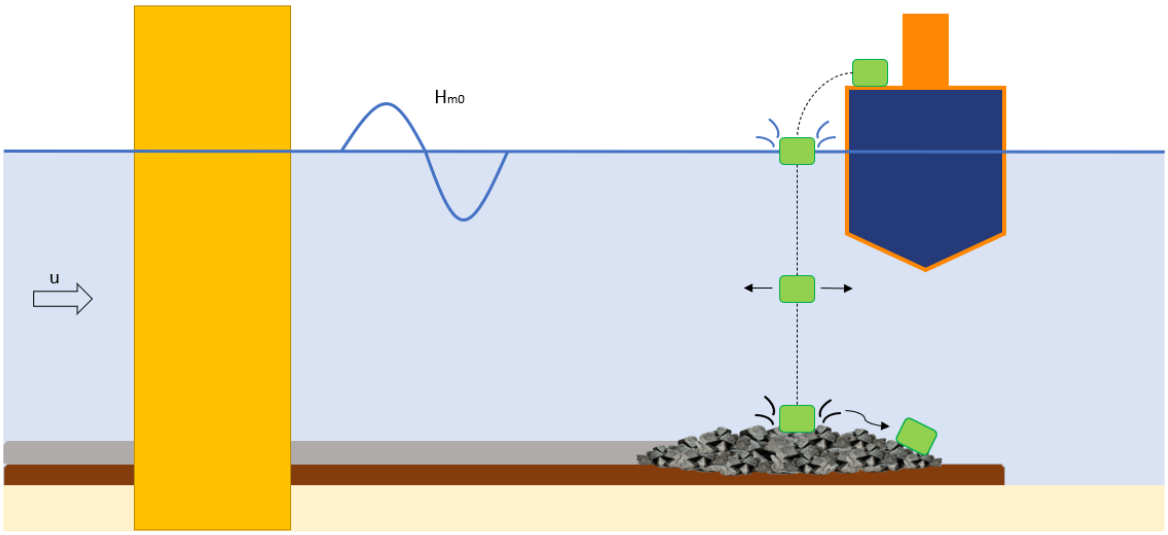


**Figure 1.7:** Situation sketch of droppable oyster brood stock structure. The structure is illustrated as a basic block in green.

Recently, a study has been conducted which investigates the design of a small product, where oyster larvae settle on, which also gets dropped in the ocean and naturally forms oyster beds. The product is designed to sink to the natural sea bottom and stays in place as much as possible [Raspoort, 2022]. The product has approximately the size of one oyster.

So studies into the design of an oyster brood stock structure have been done and also studies, where structures are dropped into the sea are executed. However, no study has been done to specifically investigate the design of a droppable oyster brood stock structure which should be installed at the scour protection in offshore wind farms.

## 1.3. Research objective

The objective of this research is derived from the problem statement;

*What is the design for a flat oyster brood stock structure, that can be installed at the scour protection at offshore wind farms, via dropping from a vessel, such that it will be stable and integer during deployment and operational lifetime?*

The dropping needs to be executed accurately due to the presence of sensitive equipment, such as energy cables and the monopile. The structure should be able to endure a drop in the water column onto the scour protection, and when the structure has settled on the scour protection, it must remain stable on its location.

This research question was subdivided into four sub-questions to aid in answering the main question.

1. *Which design criteria apply for a droppable oyster brood stock structure?*
2. *Which concepts can be designed for a droppable oyster brood stock structure, considering the design criteria?*
3. *What is the performance of the concepts to function as a droppable oyster brood stock structure?*
4. *Which concepts best meet the proposed design criteria of the droppable oyster brood stock structure, according to their performance?*

## 1.4. Research approach

The research objective of this study covers a design study. To indicate the design stage of the research, Technical Readiness Levels (TRLs) are used. This design study includes TRL 1 to 5.

*Technology Readiness Levels* (TRL) are a measurement system used to assess the readiness level of a particular technology. Each technology project is assessed on the parameters for each technology level and then given a TRL rating based on the progress of the project. There are nine levels of technology readiness, explained in Section A.3 in Table A.2 [Mankins, 1995].

To answer the research objective and the research questions, this master thesis is divided into 10 chapters. Chapter 1 is the introduction, in which relevant background information, the problem statement, the research objective and a summary of the approach are presented. In chapter 2, the design process to obtain the basic concepts of the droppable brood stock structure is elaborated, including the definition of relevant design criteria. TRL 1 is addressed in chapter 2. In chapter 3, the specific design parameters per basic concept are determined, which leads to a selection of suited concepts. The concept parameters are determined by behavioural prediction made for relevant situations by an iterative process. The behavioural predictions are made by calculations based on the relevant forces that act upon a droppable brood stock structure. The relevant situations entail the fall of the structure during the drop, the landing on the scour protection and the stability during storm events. Chapter 3 addresses TRL 2. In chapter 4, the applied physical model, to test the behaviour of the different concepts during the relevant situations, is presented. The scaling parameters, model set-up, test conditions and test runs are discussed. TRL 3 is addressed in chapter 4. In chapter 5, the results obtained during the fall, landing and stability tests are presented. TRL 4 is addressed here. In chapter 6, the raw data obtained from the tests is analysed and interpreted into useful data in reality. This includes data about the positioning accuracy of the concepts during the fall, the surface hit of the concepts during the landing and the thresholds of motion per concept. TRL 5 is partly addressed here. In chapter 7, the results obtained by physical modelling are compared to behavioural prediction results obtained by calculations in chapter 4. This comparison is used to calibrate the calculations. In chapter 8, the data obtained in chapter 6, together with the defined design criteria in chapter 2, are used to select the most suitable concept(s) to act as a droppable oyster brood stock structure based on the behaviour per tested concept. Chapter 9 addresses uncertainties and limitations that arose during the different research phases, with corresponding relevant results and implications. In chapter 10, the conclusions with regard to the research objective and questions are given. It also includes recommendations for future research based on the outcomes of this master thesis. The general outline of the research is illustrated in Figure 1.8

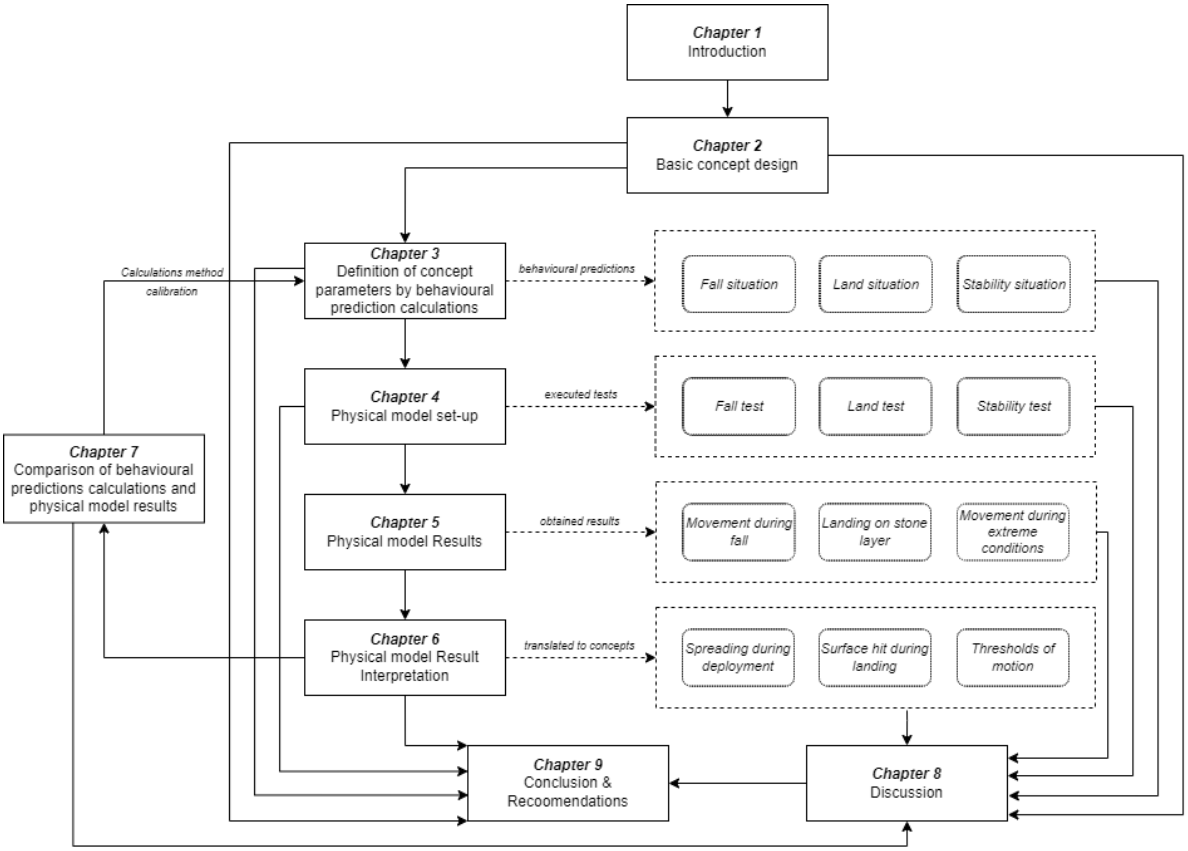


**Figure 1.8:** General outline of the research performed

## 1.5. Research scope

For the results of this study to be specific and relevant, a scope is defined for this study.

- For the brood stock population, the research focuses solely on the European flat oyster (*Ostrea edulis*).
- This study only focuses on the design of a flat oyster brood stock structure for the Dutch part of the North Sea. The environmental conditions which are considered in this research are based on this area.
- The study only focuses on the installation of an oyster brood stock structure at the scour protection of a Dutch offshore wind farm.
- The costs involved for the application of the concepts in practice are explicitly excluded.
- Group behaviour between structures during the drop is not considered in this study.

All assumptions made during this study are presented in Section A.4.

# 2

# Design of basic concepts

In this chapter, the design process of the basic concepts, that are considered in this research, is described.

*This chapter addresses Technical Readiness Level 1. TRL 1 entails that, research is carried out into the innovative idea and the basic principles of the innovation. This involves fundamental research and desk research. The basic principles are being examined.*

## 2.1. Relevant information for concept design

This section addressed relevant information necessary for concept development. This entails the conditions for which the concepts are intended and the critical mass required to kick-start oyster restoration.

### 2.1.1. Design conditions

First, the conditions for which the droppable brood stock structure should be designed are investigated. These conditions are divided into environmental conditions relevant for the flat oyster, the prevailing hydraulic conditions at offshore wind farms in the Dutch North Sea and scour protection dimensions.

**Environmental conditions**

European flat oysters exist within certain limits of abiotic factors and biotic factors. Based on these environmental conditions for a flat oyster habitat, design criteria and design requirements concerning the ecological aspects, can be defined [Smaal et al., 2017b]. These specific environmental conditions for flat oysters are addressed and are linked to (offshore wind farms in) the Dutch North Sea conditions, see Section B.0.1. The environmental conditions include; substrate, water depth, water temperature, flow velocity, oxygen content, salinity, food concentration, and predation. Based on the these environmental conditions, for the European flat oyster, it is concluded that the Dutch North Sea is suitable as a habitat for European flat oysters.

To indicate the conditions specifically at offshore wind farms in the Dutch North Sea, three locations of offshore wind farms are selected as reference locations. These wind farms are 'Gemini', 'Hollandse Kust West (HKW)' and 'Borssele V'. HKW offshore wind farm is planned to be developed, but is not constructed yet. These three wind farm locations are spread over the Dutch North Sea, from north to south, see Figure 2.1. For these three wind farms, the essential information is collected and averaged.


**Figure 2.1:** Offshore wind farms currently present and under construction in the Dutch North Sea. Adjusted from noordzeeloket.nl

**Hydraulic conditions**

The prevailing hydraulic conditions including current and wave data for offshore wind farms in the Dutch North Sea are discussed in this subsection. The hydraulic conditions information is given for four situations, see Table 2.3. This information is based on historic data.

The first situation provides information about the deployment conditions. These conditions entail maximum hydraulic conditions which are accepted when a broodstock structure or other comparable equipment is installed. These conditions are not related to one specific location, but indicate defined maximum conditions that are considered by installation vessels in the Dutch North Sea near offshore wind farms. Certain limits regarding the hydraulic conditions are set to when a vessel can sail out for installation of the broodstock structures. These hydraulic conditions entail the significant wave height, current and wind speed. The wind speed is not of importance, for the behaviour of a broodstock structure. Therefore the waves and currents are only considered. The maximum significant wave height, that may prevail during installation for such a structure at the Dutch North Sea, is defined at 1 meter. Based on averaged historical data measured at the North Sea during the usual installation months (April, May, September and October), a corresponding significant wave period ($T_s$) of 7 seconds is chosen [ODNM, 2021][Rijkswaterstaat, 2022]. These conditions stem from limits used by a market-leading dutch marine contractor. The accepted current velocity for deployment is dependent on the tide. Four times a day, the tide turns resulting in spring and neap tides. This leads to four turning points a day when the velocity is low, leading to deployment windows. The velocity of the water is measured with measuring equipment on the vessel to provide real-time data. The water velocity is monitored and when the velocity is low enough the structures can be deployed. A maximum velocity at the water surface of 0.3 m/s is usually applied. This velocity includes the tidal current and also the wind-driven current. A depth-averaged current ($\bar{u_c}$) of 0.3 m/s is considered. The current velocity is generally decreasing over depth (following a parabolic pattern), which makes this a safe assumption.

**Table 2.1:** Hydraulic conditions prevailing during 'deployment conditions'.

| **Parameter** | Value | Unit |
|---|---|---|
| $\bar{u_c}$ | 0.3 | $m/s$ |
| $H_s$ | 1 | $m$ |
| $T_p$ | 7 | $s$ |

The second, third and fourth situation provide hydraulic conditions that occur during storm events with a return period of 5, 10 and 50 years for each selected location. These situations are mainly relevant for determining the stability during the operational lifetime of the oyster brood stock structure, as extreme conditions are dominant for the stability. The information about the hydraulic conditions during storm events is obtained from scour protection design reports for HKW [Desyani and Mungar, 2022], Borssele V [Blankenweg, 2017] and Gemini [Tönis et al., 2013], which is based on historic data. The operational lifetime of an offshore wind farm in the Dutch North Sea is approximately determined to be 30 years [Blankenweg, 2017]. The probability of at least one storm event that exceeds the design limits during the expected life (30 years) per return period is presented in Table 2.2 [Jonkman et al., 2017].

The collected information for the three different wind farms is averaged and this provides the normative information for the design of the structure in the fourth column of Table 2.3. This averaged data will from now on be considered as the relevant environmental conditions for the design of the oyster brood stock structure. From these conditions, it can be concluded that the waves are present in transitional waters ($0.1 < h/L_0 < 0.5$) [Schiereck, 2003].

**Table 2.2:** The probability of at least one storm event that exceeds design limits during the expected life (30 years) of the structure. Determined using $R = 1 - (1 - (1/T))^n$, [Jonkman et al., 2017]

| Return period, T [years] | Probability of occurrence, P [%] |
|---|---|
| 5 | 0.99 |
| 10 | 0.96 |
| 50 | 0.45 |

**Table 2.3:** Hydraulic conditions at normative offshore wind farms, Hollandse Kust West (HKW), Borssele and Gemini. Information obtained from scour protection design reports for HKW [Desyani and Mungar, 2022], Borssele [Blankenweg, 2017] and Gemini [Tönis et al., 2013].

| **Parameters** | unit | **HKW** | **Borssele** | **Gemini** | **Averaged** |
|---|---|---|---|---|---|
| d | $m$ | 28 | 28.4 | 29.5 | 28.6 |
| *T = 5 year* | | | | | |
| $\bar{u_c}$ | $m/s$ | 0.5 | 1.19 | 1 | 0.9 |
| $u_{c-1.5m}$ | $m/s$ | 0.4 | 0.83 | 0.57 | 0.6 |
| $H_s$ | $m$ | 6.5 | 5.7 | 8.3 | 6.8 |
| $T_p$ | $s$ | 11.2 | 9.5 | 13.3 | 11.3 |
| *T = 10 year* | | | | | |
| $\bar{u_c}$ | $m/s$ | 0.5 | 1.65 | 1.05 | 1.07 |
| $u_{1.5m}$ | $m/s$ | 0.4 | 0.84 | 0.58 | 0.61 |
| $H_s$ | $m$ | 7 | 6.2 | 9.1 | 7.4 |
| $T_p$ | $s$ | 11.7 | 9.7 | 13.8 | 11.7 |
| *T = 50 year* | | | | | |
| $\bar{u_c}$ | $m/s$ | 0.5 | 1.25 | 1.15 | 1.3 |
| $u_{1.5m}$ | $m/s$ | 0.5 | 0.85 | 0.6 | 0.65 |
| $H_s$ | $m$ | 7.5 | 7 | 10 | 8.2 |
| $T_p$ | $s$ | 12.2 | 11.3 | 14.4 | 12.6 |

**Scour protection dimensions**
The scour protection conditions for the three considered wind farms and averaged values are presented in table 2.4. The information is obtained from scour protection design reports for HKW [Desyani and Mungar, 2022], Borssele [Blankenweg, 2017] and Gemini [Tönis et al., 2013], which is based on historic data. The parameters for each wind farm are averaged values used for the entire wind farm, as these differ per wind turbine.

**Table 2.4:** Scour protection information for reference offshore wind farms, Hollandse Kust West (HKW), Borssele and Gemini. Information is obtained from scour protection design reports for HKW [Desyani and Mungar, 2022], Borssele [Blankenweg, 2017] and Gemini [Tönis et al., 2013].

| **Parameters** | unit | **HKW** | **Borssele** | **Gemini** | **Averaged** |
|---|---|---|---|---|---|
| $A_a$ | $m^2$ | 660 | 380 | 316 | 452 |
| Armour grading | $kg$ | 5-40 | 5-40 | 40-200 | |
| $d_{50-a}$ | $mm$ | 225 | 225 | 432 | 294 |
| $t_a$ | $m$ | 0.5 | 0.47 | 1 | 0.66 |
| $A_f$ | $m^2$ | 1257 | 485 | 360 | 701 |
| Filter grading | $mm$ | 45/180 | 45/180 | 22/90 | |
| $d_{50-f}$ | $mm$ | 100 | 100 | 45 | 82 |
| $t_f$ | $m$ | 0.5 | 0.5 | 0.5 | 0.5 |
| $A_{pile}$ | $m^2$ | 64 | 43 | 40 | 49 |
| $A_{sp}$ | $m^2$ | 1321 | 528 | 400 | 750 |
| $t_t$ | $m$ | 1 | 0.97 | 1.5 | 1.16 |

### 2.1.2. Critical mass
The critical mass is defined as the number of individual flat oysters that need to be introduced to initiate oyster reef development in offshore wind farms.

In a previously executed pilot project (at Borssele V) and a future planned pilot project (at Luchterduinen), where oyster brood stock structures are placed, a population of 1000 oysters is introduced, divided over two scour protection sites [Schutter et al., 2021]. These brood stock structures are placed using an installation method that involves the use of a crane. This ensures minimal damage to the oysters (compared to a drop method). From these pilot projects it is assumed that a population of 500 intact oysters needs to be installed per scour protection. The kick-start amount of 500 oysters does not yet include the loss of oysters. The total number of individual oysters determines the number of brood stock structures that need to be dropped on the scour protection. The number of brood stock structures in turn is dependent on the maximum number of flat oysters that can be attached to one structure at which this loss percentage should be incorporated.

## 2.2. Basic concepts
As a first step into developing the basic concepts for the droppable oyster brood stock structure, inspiration is gained by existing subsea structures. Existing concrete armor units are considered. Some examples are presented in Figure 2.2 [Molines and Medina, 2015].

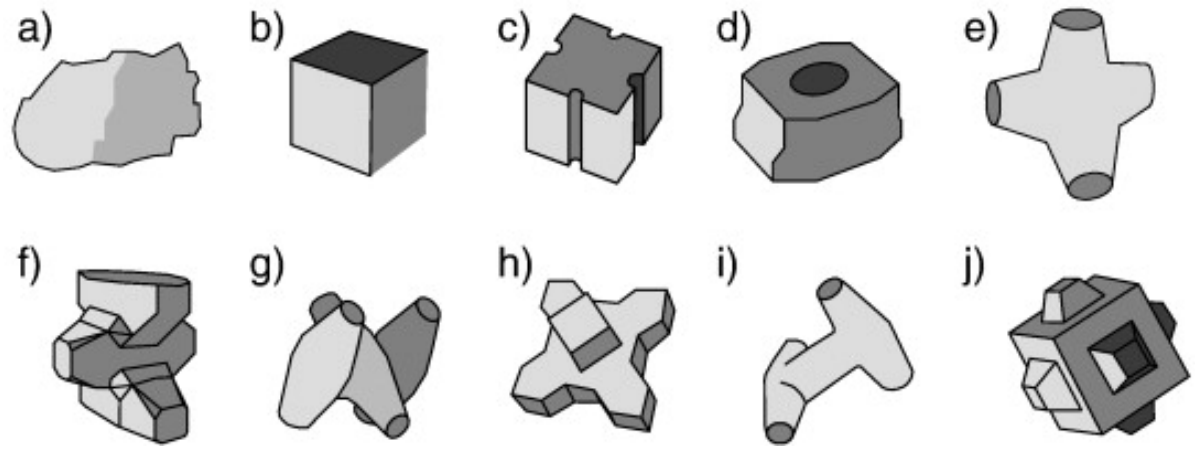


**Figure 2.2:** Concrete armor units [Molines and Medina, 2015]

Also, existing artificial reef enhancement elements are considered for inspiration. Some examples are presented in Figure 2.3. These reef structures are already used to enhance reef development for restoration. Mostly, they are intended for corals, but Figure 2.3e is used for oyster spat settlement in England [of South Hampton, 2022].

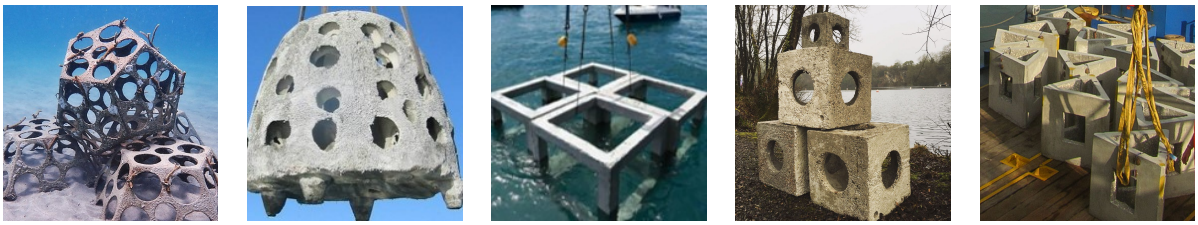

(a) (b) (c) (d) (e)

**Figure 2.3:** Artificial reef structures

These existing subsea structures are used as starting point for the basic concept development. Brainstorm sessions and consultations with different marine ecology experts and hydraulic and structural engineers are held, which have resulted in the development of twelve basic concepts.

The basic concepts are classified into three categories; open structures, structures with arms and penetrating structures.

The dimensions of all concepts are not yet considered in this section and will be addressed later on in this research (Chapter 3). The proportions may therefore also still change further in the design process.

## 2.2.1. Concepts with arms

Five concepts with arms are drawn up. These five concepts all have 'arms' that extend from the core. At and around the core and at the arms, the oysters can be attached. The oysters on these concepts are relatively exposed to damage.

**Xblock**

This concept consists of a 3D Xblock shape, with six arms. Xblock-shaped structures are already widely applied as breakwater elements, see Figure 2.4a.

**Tetrapod**

This concept has a tetrapod shape. The concept is symmetrical and it consists of three arms. Each arm has a round shape, with the radius increasing as it comes closer to the core. The tetrapod shape is already largely implemented as an element for breakwaters and coastal protections, see Figure 2.4b.

**Propeller**
This concept is called the 'propeller'. The concept contains two crossing rectangular plates, that are perforated, which form a 3D cross, see Figure 2.4c.

**Open table**
The open table concept consists of a table shape where the legs protrude to both sides, allowing the table to be able to stand on two sides. The table is perforated in the middle, see Figure 2.4d.

**Anchor**
The anchor concept consists of three beams that are connected. Two outer beams have the same length and are attached to the inner centre beam. All beams differ in direction with an angle of 90 degrees. When the concept is settled at the bottom, one outer beam lays on the ground and the other outer beam penetrates upwards, see Figure 2.4e.

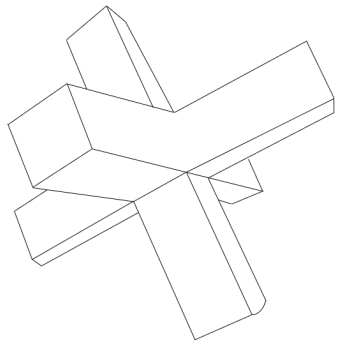

**(a)** Xblock concept

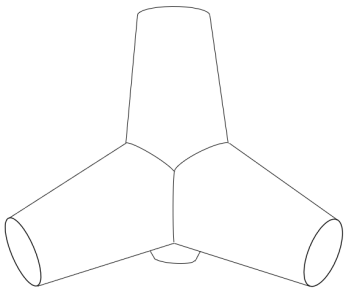

**(b)** Tetrapod concept

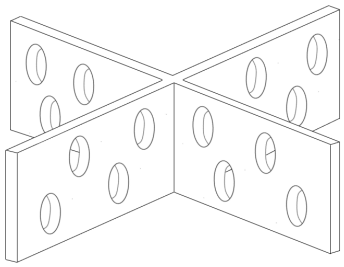

**(c)** Propeller concept

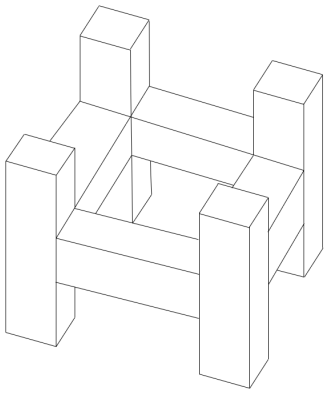

**(d)** Open table concept

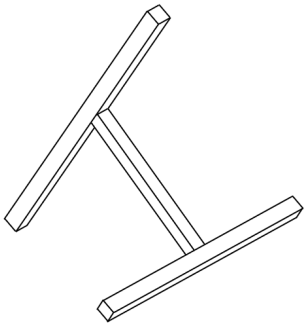

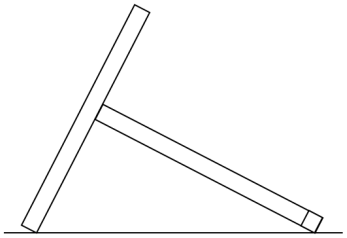

**(e)** Anchor concept

**Figure 2.4:** Basic concepts with arms

## 2.2.2. Open concepts

In this subsection, open and/or hollow concepts are discussed. These concepts allow flow to go through the structures and offer protection to the oysters. The oysters are attached to the inside of these concepts.

**Cube framework**
The cube framework concept consists of twelve beams, which form a cube framework, see Figure 2.5a. This shape has already been applied as a reef enhancement structure, see Figure 2.3c.

**Reef cube**
The reef cube concept is a hollow cube with round holes at four sides and open at the top and bottom, see Figure 2.5b. The reef cube concept is based on a design of 'Arc Marine' [Marine, 2020]. The original design of Arc Marine has a different purpose than the intention of this study, see Figure 2.3d.

**Tetrahedron**
This concept involves a framework of a tetrahedron shape. The frames consist of triangular shaped beams, see Figure 2.5c.

**Open tent**
This concept is called 'the open tent'. It is a 3D triangle, with is perforated, with one rectangular hole per side, see Figure 2.5d.

**Truncated cone**
This concept is a hollow truncated cone, which is perforated, see Figure 2.5e.

**Dodecahedron**
This concept consists of a dodecahedron-shaped framework, see Figure 2.5f.

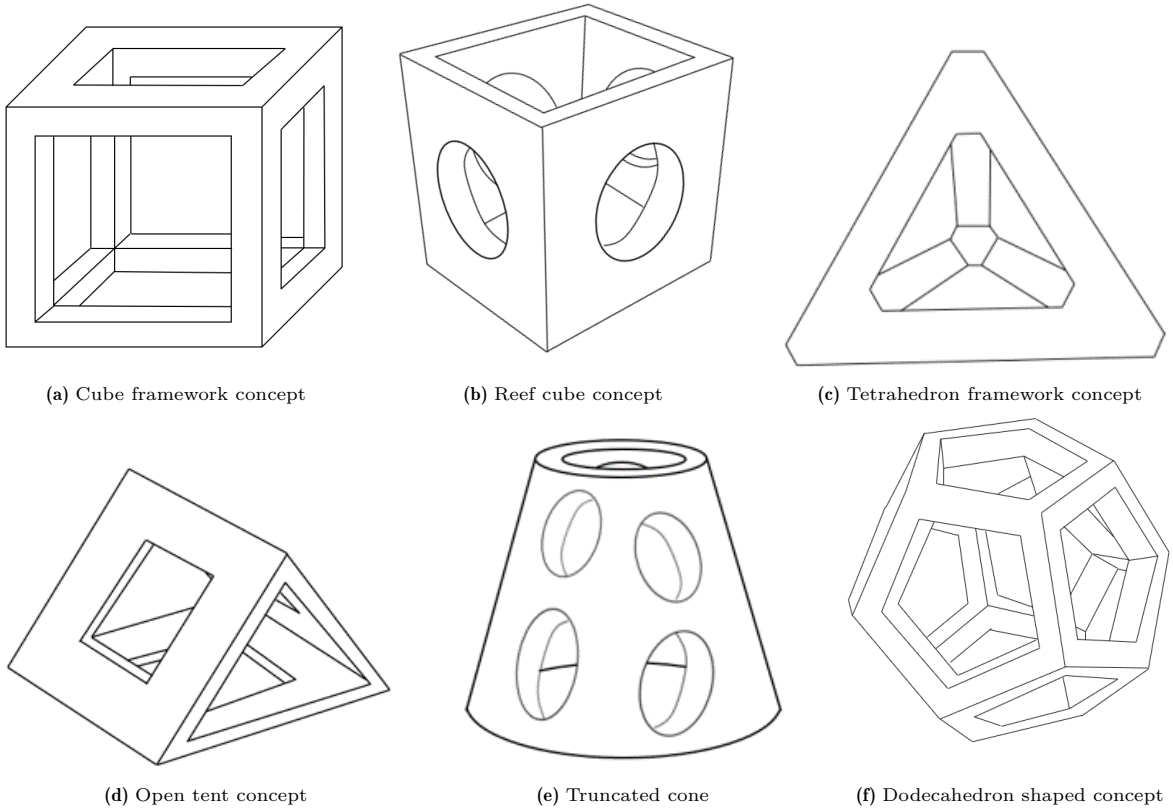

**(a)** Cube framework concept **(b)** Reef cube concept **(c)** Tetrahedron framework concept

**(d)** Open tent concept **(e)** Truncated cone **(f)** Dodecahedron shaped concept

**Figure 2.5:** Basic open concepts

### 2.2.3. Penetrating concepts

The concepts discussed below will try to penetrate the scour protection, with their cone shape. The concepts try to anchor themselves in the seabed to stabilise.

**Cone arrow**
This concept has two variants. The first one has one thicker cylinder attached to the cone, see Figure 2.6a. The second one has multiple thinner cylinders attached to the cone, see Figure 2.6b.

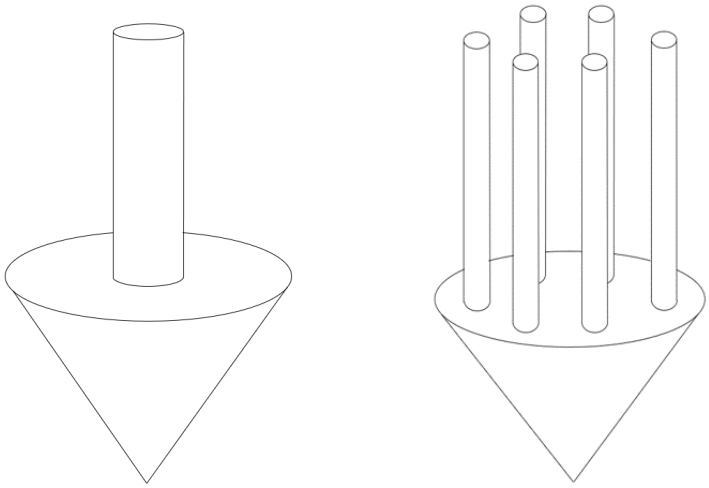

**(a)** Cone arrow, with one cylinder **(b)** Cone arrow, with multiple cylinders

**Figure 2.6:** Penetrating concepts

# 2.3. Design principles

The design criteria for the concepts are addressed in this section. Two requirements result from the design criteria. Design specifications that arise from these criteria are also elaborated.

## 2.3.1. Design criteria

The design criteria regarding the ecological and structural aspects of the design are discussed in this section. These criteria are partly based on the lessons learned from executed pilot projects for oyster restoration Table 1.1. Other design criteria are developed by consultations with experts and literature studies regarding oysters. An overview of the defined design criteria is presented in Table 2.5.

The ecological criteria relate to the way the structure interacts with the flat oysters attached to the structure and how the structure can best facilitate them. The structural criteria relate to the structural integrity of the design of the brood stock structure.

**Flow**

The oysters must experience sufficient flow. In Section B.0.1, it is explained that the optimal flow velocity along an individual oyster is in the range of 0.25 to 0.6 m/s. This requires that the oysters attached to the structure are placed in such a way that the individual oysters experience this flow. Near to the monopile, the flow pattern is affected by the presence of the slender structure. This induces accelerating flow velocities, which are not desired for the brood stock structure. The flow will allow them to extract sufficient nutrients and oxygen from the water. This also means that sedimentation on the structure should be avoided. Sedimentation can lead to burial of the oysters, which results in suffocation. The design should incorporate aspects that result in optimal flow and limited sedimentation. This could entail elevation from the seabed, oblique surfaces or oysters attached at vertical surfaces.

**Space**

The oysters will be attached to the structure using an adhesive. This prevents the oysters from being able to move. The oysters still need to be able to grow and feed. For this to be possible, an individual oyster needs enough space. However, flat oysters also prefer to be in the presence of other flat oysters. Therefore, the distance between them should not be too great. The structure should provide optimal surface availability to which the oysters can be attached to. Flat oysters are roughly round shaped and can get a maximum of 12 cm in diameter. Therefore for each oyster a minimal surface of 0.0113 $m^2$ ($= \pi 6^2$) should be reserved.

**Protection**

During the deployment of the structure, it will be dropped in the water from a vessel. The structure will likely be impacted by hitting the water and by hitting the scour protection. The oysters still need

to be intact after this impact is made. The oysters need to be protected from being damaged during the deployment.

**Predation**
Predators of the flat oyster are present in the North Sea bed. For the flat oysters to survive, predation should be reduced as much as possible. The design should entail measures to ensure that the oysters are harder to access for predators. This could include elevated structures, higher placed oysters and/or a barrier between the oysters and the predators (cages).

**Oyster settlement**
The structure must be suitable for the oysters to settle on. The material must therefore have the appropriate roughness for non-attached oysters and larvae to settle on the structure.

**Durability**
The structure remains on the scour protection of the offshore wind farm for approximately 30 years. Therefore, the structure must also remain intact for this period. It is important to take into account that the material used for the structure stays intact for this period, as the structure is located nearby sensitive equipment, which cannot be damaged because the structure is in decay.

**Stability**
The wind farm owners request stability of the structure during its lifetime. The structure should remain stable, due to the sensitive environment at and around the scour protection (wind turbine, energy cables, etc.). As stated, the lifetime of a structure is approximately 30 years. Therefore, the structures should remain stable for approximately 30 years. A storm with a return period of 10 years has a probability of occurrence of 96 percent (Table 2.2). Therefore the structures should at least be able to remain stable during this storm event, but is preferred if the structures can also remain stable during a storm event with a return period of 50 years, which has a probability of occurrence of 45 percent within 30 years. Previously installed (oyster brood stock) structures for nature enhancement at the scour protection are also designed to withstand storm conditions with a return period of 10 years ([Heijningen and Mungar, 2022]).

**Positioning**
The designed structure will be dropped from a vessel on the scour protection. The structure must be dropped at the scour protection, because the structure will likely sink into the sand when placed at the 'natural seabed' of the North Sea. This will lead to burial of the oysters. In the vicinity of the scour protection, at the offshore wind farms, a lot of sensitive material is present. This equipment may not be damaged due to large consequences. Especially the cables placed on the scour protection should be avoided. The structures cannot be placed within 10 meters of the cables.

The structure should also not be placed too near to the monopile, due to accelerating flow velocities. To avoid turbulence effects, the structure is desired to be placed 90 degrees from the incoming current.

Within the scour protection, it is preferred if the structure is placed on the armour layer of the scour protection, but not mandatory. The armour layer is more stable than the filter layer. These conditions necessitate a very specific positioning of the structure to ensure that it is in the right location. Therefore, the positioning of the structure during the deployment, should be as accurate as possible. The diameter of the averaged armour layer is approximately 24 m, with a pile diameter of 9 m (see Table 2.3, this implies a width of 8 meters of armour layer from the pile to the filter layer. This results in a positioning accuracy during deployment of a maximum horizontal displacement of approximately 4 meters. When considering that the structure can also land on the filter layer, the maximum horizontal displacement is larger and approximately equal to 5.5 meters.

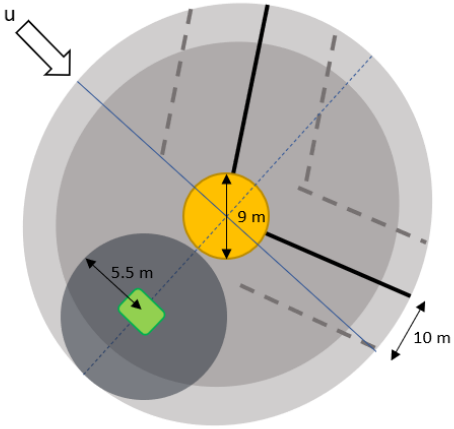


**Figure 2.7:** Positioning accuracy of structure

**Intact**
The designed structure will be dropped from a vessel on the scour protection. This means that the structure will approximately be dropped from a height of 30 meters (water depth and vessel height). The structure will be impacted by the hit of the waterline first and thereafter also by the hit on the scour protection, during the fall. The structure should be able to withstand these impacts and should not be damaged once it has been settled at the scour protection. This means that the structure should be rigid enough for these conditions.

**Installation**
The designed structure will be dropped from a vessel onto the scour protection. This installation method is what distinguishes this design of the brood stock structures compared to previous projects. The brood stock structure must be able to be dropped manually in the water. The weight is especially important considering this criterion, but also the shape. The design should also take this action of installation into account and ensure that the structure endures little to no damage.

**Manufacturing**
In a previously executed pilot project there appeared to be problems with the manufacturing of the concepts, once the design was finished. The manufacturability of the concepts should be checked beforehand. The structure should be easy to fabricate to prevent high costs. This involves the avoidance of complex structures. Manufacturers need to be consulted to gain better insight into the complexity of the fabrication of the concept designs.

**Transportation**
For the application of the structures to the scour protection, the structures must first be transported from the manufacturer to the harbour and from the harbour to the vessel. It is expected that one structure will not contain enough oysters required, since the structures must be simple to install (which will limit the weight and size). It is therefore expected that several structures need to be installed per scour protection. For this reason, the structures must be shaped such that they can easily be transported (i.e. stacked or small).

**Table 2.5:** Overview of ecological and structural design criteria for brood stock structure

| **Ecological criteria** | **Structural criteria** |
|---|---|
| Optimal *flow* | Sufficient *durability* |
| Sufficient *space* | Sufficient *stability* |
| *Protection* during deployment | Accurate *positioning* |
| Minimal *predation* | *Intact* after deployment |
| Suitable for *oyster settlement* | *Installation* without equipment |
| | Cheap *manufacturing* |
| | Easy *transportation* |

## 2.3.2. Design requirements

Two set requirements regarding the behaviour of the droppable oyster brood stock structure arose from the defined design criteria

**Positioning accuracy**

The positioning accuracy during deployment should have a maximum horizontal displacement of approximately 4 meters when the structure must land on the armour layer. When considering that the structure can also land on the filter layer, the maximum horizontal displacement is 5.5 meters.

**Stability**

The structures must at least be able to remain stable during a storm event with a return period of 10 years, and is preferred if the structures can also remain stable during a storm event with a return period of 50 years.

## 2.3.3. Design specifications

The design criteria for a droppable oyster brood stock structure induce some specifications for the design, regarding the material and weight.

**Material**

To select the material for the brood stock structure, both ecological and structural design criteria are taken into account. Based on the ecological design criteria, the material must have the optimal roughness for larvae and oysters to settle on. For structural reasons, the material must be durable enough to remain intact on the bottom of the North Sea for several decades. The material of the structure should also be rigid enough to withstand the impact during the deployment and should not be damaged once it has been settled at the scour protection. The structure must also be simple to manufacture (i.e. easily accessible and available in the desired shapes and sizes).

Several studies and experiments have been conducted and manufacturers are consulted to determine the best material for such a structure. Based on these investigations and the specific design criteria, concrete is considered to be the most suitable material for the structure [Belzen et al., 2021]. The use of fibre-reinforced concrete is recommended by consulted manufacturers. Concrete usually is not a very environmentally friendly material, due to the carbon emissions during production. There are new technologies that provide concrete types, which are more environmentally friendly with a smaller carbon footprint (e.g. ECOncrete, green concrete, AHScrete [Concrete, 2019]). These concrete types should be considered for fabrication, especially as this is a project to enhance nature.

**Weight**

In defining, the shape and dimensions of the structure, the required weight is an important boundary condition. Considering the stability of the structure after it has been installed at the scour protection, the structure should be as heavy as possible to withstand storm conditions and therefore ensure stability. Also, for the positioning of the structure during deployment, a heavy structure is expected to endure less horizontal displacement during the fall.

Given the deployability of the structure, it is desired that the application is easy. This entails that the structure should be able to be dropped manually into the sea, without the use of a crane or other installation equipment.

Assuming an average man, it is concluded that the maximum weight one individual can (dead)lift is approximately 70 kilograms. However, safety rules apply to all employees working for a company in the Netherlands, which is set up in the 'Working Conditions Act'. The Working Conditions Act lays down rules for employers and employees to promote the health and safety of employees. The 'Working Conditions Act' of the Netherlands specifies that the maximum weight an individual may carry during optimal conditions, entails a maximum weight of 23 kilograms. For multiple individuals, a maximum weight of 50 kg is defined [Oord, 2014]. The weight classes will be considered for each concept continuing the design process. Weight class 1, entails a structure with a weight of 23 kg and weight class 2, entails a structure of 50 kg.

## 2.4. Concept analysis

Each considered concept will be elaborated on and assessed shortly on two aspects. Thereafter a concept selection is made based on the design criteria.

### 2.4.1. Concept assessment

Per concept, two aspects are specifically elaborated. The first aspect discusses the influence of shape on the specified design criteria and the second aspect discusses the likely reaction of the oysters. These aspects are assessments based on hypothetical judgement and literature study and do not yet give any certainty of how the concepts will react in reality.

**Xblock**

- *Shape*

  The symmetrical shape of the Xblock concept allows it to land on each side. During the landing, the arms can land in between or around the scour protection stones, which results in the core of the concept also being impacted. The protruding shape of the concept makes it difficult to stack multiple structures on top of each other, without damaging the attached oysters. This will make it more difficult to transport multiple structures at once. The concept is not easy to carry (and therefore dropped), as it has no handles for grip.

- *Oysters*

  The oysters will be attached to the arms of the concept, this will likely cause a part of the oysters to be damaged during the hit with the scour protection. Considering the habitat requirements for the flat oyster, the shape of the concept ensures sufficient flow along the attached oysters. Sedimentation is not likely to occur, due to sloping surfaces. The oysters will (partly) be elevated, which will minimise predation.

**Tetrapod**

- *Shape*

  The concept has a symmetrical shape, such that it can land on each side. During the landing, the arms can land in between the stones, which would result in the core of the concept also being impacted. Depending on the dimensions, the concept could fall around a scour protection rock. The protruding shape of the concept makes it difficult to stack multiple structures on top of each other, without damaging the attached oysters. This will make it more difficult to transport multiple structures at once. Due to the round shape of the arms, it is relatively difficult to attach the oysters to the concept. The concept is difficult to carry (and therefore dropped manually).

- *Oysters*

  The oysters will be attached to the arms of the concept. It is expected that a large amount of oysters will get damaged during the landing. Considering the habitat requirements for the flat oyster, the concept shape ensures enough flow for the oysters. The occurrence of sedimentation is small, due to sloping surfaces. The oyster will (partly) be elevated, this will minimise predation.

**Propeller**

- *Shape*

The concept is intended to be able to fall on two sides (top and bottom in Figure 2.4c). The arms are exposed to high resistance from the waves and currents. The concept is not likely to settle 'in between' the scour protection rocks. Multiple structures can be fitted next to each other and with a plate on top, multiple can be stacked on top of each other. The transportability of multiple structures can be managed. The structure is relatively not easy to carry (and therefore dropped).

- *Oysters*

  The oysters will be attached to the vertical surfaces. If the concept hits the bottom during the landing, the oysters will not get hit. During the operational lifetime, it is expected that sedimentation will occur at the centre of the concept, in the corners of the arms, because there is minimal flow. The oyster will (partly) be elevated, this will minimise predation.

**Open table**

- *Shape*

  The concept could fall on each side, but is desired to stabilise on a side that has four legs (wide side). Multiple concepts can be fitted next to each other and on top of each other. Therefore the transportability of multiple structures can be managed. The shape of the concept is sufficient to be carried by individuals.

- *Oysters*

  The oysters will be attached to all the surfaces on the inside of the concept. These areas are protected during the fall and therefore will minimise the damage to the oysters, but damage will likely be significant. The oysters that are attached to the top of the horizontal plate are likely to endure sedimentation. The risk of predators is minimised, because the table is lifted from the bottom.

**Anchor**

- *Shape*

  The concept will always land on one long side of the outer beam and one short side of the other outer beam. Two out of the three beams are then elevated from the ground. The concept is very slender, therefore multiple structures can be fitted next to each other. The transportability of multiple structures can be managed. The shape of the concept is sufficient to be carried by individuals.

- *Oysters*

  The oysters will be attached to all four sides of the three beams. Two sides of one outer beam will get hit during the landing, these oysters will therefore be lost. The oysters that survive are attached to the settled outer beam and are likely to endure sedimentation. The risk of predators at the inner and other outer beam is minimised, because these beams are lifted from the seabed.

**Cube framework**

- *Shape*

  The concept can fall on each side due to its symmetrical shape. The concepts can easily be stacked on top and next to each other. The oysters are attached to the inside for protection. This allows easy transportation of multiple structures. The concept has an appropriate shape to be carried, which is convenient for the dropping of the structure into the water.

- *Oysters*

  The oysters will be attached to the inside of the concept. This will make sure that the oysters are protected during the fall and landing. The framework concept is very permeable, so the oysters will endure enough flow. Only the oysters attached to the bottom beams might endure sedimentation and/or damage during the landing. The other oysters are all elevated, so predation is reduced.

**Reef cube**

- *Shape*

  The concept can fall on each side, but is not the same on each side. The concepts can be stacked next to each other and also on top of each other. Therefore multiple structures can easily be transported. The concept can be carried by individuals due to its shape.

- *Oysters*

  The oysters will be attached to the inside of the concept. This will make sure that the oysters are protected during the fall and landing. The concept is not fully permeable and therefore sedimentation may arise on the inside, especially at the bottom. Clogging was encountered for this concept during similar use. Part of the oysters are elevated, to reduce predation.

**Tetrahedron**

- *Shape*

  Due to its symmetrical shape, the structure can fall on each side. The shape will also make sure that the bottom of the concept is always wider than the top. The oysters are attached to the inside of the concept. Multiple structures can be stacked, which makes it easy for multiple structures to be transported. The structure can be carried by individuals.

- *Oysters*

  The oysters will be attached to the inside of the triangular framework, such that they will be protected during the fall and landing. The oysters at the bottom three beams of the framework are likely to endure sedimentation and/or damage. The other three beams are elevated and permeable, therefore they endure optimal flow for the oysters.

**Open tent**

- *Shape*

  The concept is intended to fall on one of the perforated sides. The shape will make sure that the bottom of the structure is always wider than the top. As the oysters are attached to the inside of the concept, multiple structures can be stacked. This makes it easy for multiple structures to be transported. The shape of the concept is not optimal to be carried by individuals.

- *Oysters*

  Oysters will be attached to the inside of the concept, such that they are protected during the fall and landing. During the fall they will endure a strong flow. The oysters that are attached to the inside of the bottom plate are likely to be exposed to sedimentation, due to the horizontal bottom plate. The oysters that are attached to the other side will encounter enough flow and also be elevated.

**Truncated cone**

- *Shape*

  This concept is intended to fall lengthwise through the water column, such that flow runs through it. If the concept lands on another side, it is not fit for use anymore. The concept is not easy to carry. However, if the perforated holes are large enough, these can act as handles for grip. As the oysters are attached to the inside, this makes it possible for the structures to be stacked.

- *Oysters*

  Oysters will be attached to the inside of the concept, such that they are protected during the fall and landing. During the fall they will endure a strong flow. Sedimentation is not expected as the oysters are elevated from the seabed and also are attached to a vertical surface.

**Dodecahedron**

- *Shape*

  Due to its symmetrical shape, the concept can fall on each side. However, the round shape of the concept suggests that the concept can easily roll over. As the oysters are attached to the inside of the concept, multiple structures can be stacked, but the shape is not optimal for stacking. The concept has an appropriate shape to be carried, which is convenient for dropping the concept into the water. This is because the beams provide grip.

- *Oysters*

  The oysters will be attached on the inside, such that they will not be crushed when hitting the bottom. The concept is permeable, so it is expected that no oysters will endure enough flow. Sedimentation can occur at the bottom side, because it is close to the seabed, but is not likely to occur much.

**Cone arrow**

- *Shape*

  The cone of the concept should face downwards. This side is the only suited side for the structure to land on. It is only suited for use if it penetrates the substrate. The concepts are difficult to stack on top of each other or next to each other. This makes it difficult for multiple structures to be transported. The concept is difficult to be carried by individuals.

- *Oysters*

  The oysters will be attached to the top of the cone and to the cylinder, such that they will not be crushed when hitting the bottom. Sedimentation could occur on the top of the cone, because it is horizontal. The oysters attached to the cylinder will have enough flow along them and will also be elevated for predators.

## 2.4.2. Concept selection

In this section, the concepts are assessed on their suitability to act as an oyster brood stock structure, based on the defined design criteria in Section 2.3.1. This assessment results in a selection of the concepts that are considered further on in this research.

The cone arrow concepts are not suited for hard substrates. The goal of this research is to find a design that can be installed at the scour protection of offshore wind farms. Therefore, this concept is not considered anymore in this research.

As stated in Section 2.3.1, the manufacturability of a concept is important for the applicability of the final design. Certainty about the manufacturability of the concepts is required. This ensures minimal costs and this increases the probability of (frequent) application.

To gain a better understanding of the manufacturability of the concepts, three manufacturers (D&M Engineers, Waco B.V., Rutte Circulair) were consulted. Based on the knowledge of the manufacturers, the concepts were assessed as 'not manufacturable', 'manufacturable' or 'easily manufacturable'. The concepts that are 'not manufacturable' are; Propeller, Tetrahedron, Open tent and Dodecahedron. These concepts are not considered anymore in this study, as they do not appear to be feasible concepts.

The concepts are assessed on their suitability using a multi-criteria analysis, based on the defined design criteria in Section 2.3.1. However, some design criteria cannot be properly assessed in this stage of the research, because these assessments would be inadequately substantiated. These design criteria are 'stability' and 'positioning', which define the design requirements. For proper assessment, calculations and/or physical modelling is required on these aspects.

The design criteria, 'oyster settlement', 'durability' and 'intact' are addressed by the material used to create the concepts. Therefore these design criteria are considered to be met, based on the chosen material, concrete.

This leaves the following design criteria on which the concepts are assessed for suitability; 'flow', 'space', 'protection', 'predation', 'installation', 'manufacturing' and 'transportation'. A multi-criteria analysis is used to assess the remaining concepts, using the weighted objectives method.

*The weighted objectives method* is an evaluation method for comparing design concepts based on the overall value of each design concept. The method assigns scores to the degree to which a design alternative satisfies a criterion [van Boeijen et al., 2020]. Each criterion is assigned a weight between 0 and 100, which in total adds up to 100. The different concepts are rated on this criteria, with a score between 0 and 5. 0 indicates that the concept does not meet this design criterion and 5 indicates that this design criterion is fully met. These scores are multiplied by the weight and then divided by 100 (total score), which results in the final score between 0 and 5. The concepts that receive the highest scores, are most suited to act as a flat oyster brood stock structure.

The chosen weighting factors determined for each design criterion are elaborated. For the 'flow' and 'protection' criteria, a weighting factor of 25 is chosen. These two criteria are critical for the oyster survival and therefore indicate boundary conditions. The other criteria ('space', 'predation', 'installation', 'manufacturing' and 'transportation') are not critical for survival, but indicate preferred properties. For these criteria, a weighting factor of 10 is chosen.

The drawn up multi-criteria analysis is shown in Table 2.6, in which seven remaining concepts are assessed. The structures have great variation in shape. The total scores do not vary greatly. Some design criteria are not yet able to be assessed in this stage of the research. Based on these three aspects, it is chosen to continue the research with five concepts and eliminate only two concepts. The concepts with the top five scores are Cube framework, Xblock, Tetrapod, Anchor and Open table. Which results in eliminating the Truncated cone and Reef cube concepts.

A final concept is introduced in the continuation of this research, the Reference block. This is the solid cube. This concept is introduced to act as an observation concept for the next steps in this study.

**Table 2.6:** Multi-criteria analysis to assess the suitability of design concepts, using the weighted objective method

| **Design criteria** | Flow | Space | Protection | Pred-ation | Install-ation | Manu-facturing | Trans-portation | **Total** |
|---|---|---|---|---|---|---|---|---|
| *Weight* | *25* | *10* | *25* | *10* | *10* | *10* | *10* | *100* |
| Xblock | 5 | 3 | 2 | 4 | 3 | 3 | 2 | 3.3 |
| Tetrapod | 5 | 3 | 2 | 4 | 1 | 5 | 2 | 3.3 |
| Open table | 4 | 3 | 4 | 4 | 4 | 3 | 4 | 3.8 |
| Anchor | 4 | 2 | 2 | 2 | 5 | 5 | 4 | 3.3 |
| Truncated cone | 2 | 2 | 4 | 2 | 3 | 5 | 3 | 3.0 |
| Cube framework | 4 | 3 | 5 | 4 | 5 | 3 | 5 | 4.3 |
| Reef cube | 1 | 2 | 5 | 3 | 4 | 3 | 5 | 3.2 |

## 2.5. Conclusion

In this chapter, several concepts have been drawn up based on literature research and consultations with experts. These concepts have been analysed and assessed according to defined criteria. A multi-criteria analysis assessed on the design criteria selected the most suited concepts. These concepts are; the Xblock, tetrapod, open table, anchor and the cube framework concept. As a reference during the remaining of this research, one more concept is introduced, namely the Reference block. This leads to six concepts that are designed and considered in the continuation of this research, see Figure 2.8. The size and dimensions of the concepts are not yet identified. These will be addressed further in this research, taking their behaviour and design specifications into consideration.

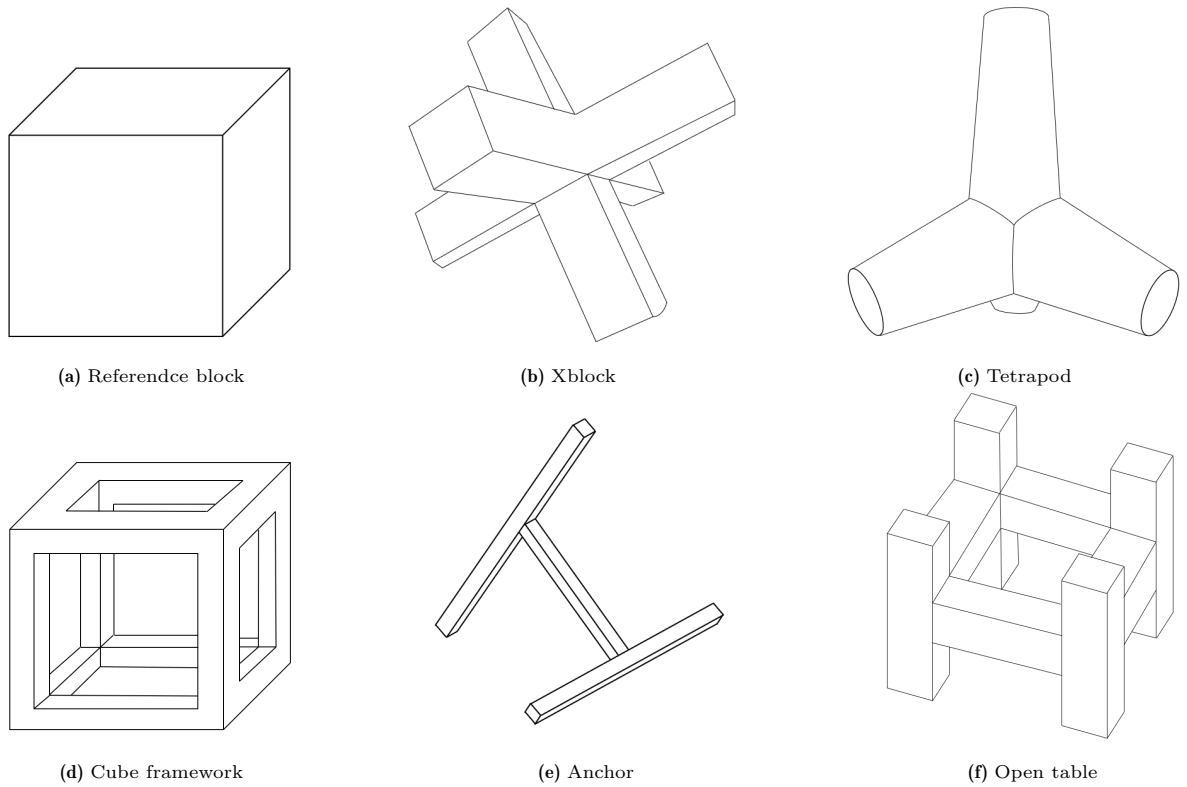

**(a)** Referendce block **(b)** Xblock **(c)** Tetrapod

**(d)** Cube framework **(e)** Anchor **(f)** Open table

**Figure 2.8:** Selected concepts, which are investigated further in research.

# 3

# Definition of concept parameters by behavioural prediction calculations

The basic designs of the concepts are defined in Chapter 2. However, nothing is said about the volume, size, ratio and dimensions of the concepts. These concept parameters define the designs of the concepts. In this chapter, the parameters are defined, based on behavioural predictions for the concepts. The concept parameters which result in the most suitable behaviour during relevant phases in their operational lifetime are selected. Behavioural predictions are made by identifying the relevant forces that act upon the concepts. Multiple concept parameter combinations per basic concept are considered using an iterative process.

*This chapter addresses Technical Readiness Level 2. TRL 2 entails that, the basic principles have been examined and the formulation of the technological concept and practical applications are now being considered. In this phase, experimental and/or analytical research is the main area of focus.*

## 3.1. Relevant information for behavioural predictions

All relevant information acquired to make predictions about the behaviour of the concepts is discussed in this section.

### 3.1.1. Concept parameters

The concepts have three relevant parameters which need to be determined to obtain the dimensions and therefore the final design of the concepts. The parameters are elaborated below; volume, beam thickness and dimension ratios. These parameters are used as input for the behavioural prediction calculations and changed iteratively, until a suited concept is found, which indicates

**Volume**

In Section 2.3.3, the weight requirements for the concepts are elaborated. Two weight classes are considered per concept. Weight class 1 implies that the structure is equal to 23 kg and weight class 2 implies that the structure is 50 kg. The chosen material for the structures is fibre-reinforced concrete, which has a specific weight of 2500 kg/m$^3$. This results in a volume of 0.0092 m$^3$ for structures with weight class 1 and a volume of 0.02 m$^3$ for structures with weight class 2.

**Beam thickness**

Each concept consists of beams or 'arms'. The thickness of these elements is an important variable for the final design of the concepts. Based on the consultations with concrete manufacturers, a minimal thickness of 5 cm is chosen, to guarantee the strength of the beams. A maximum beam thickness of 12 cm is chosen, based on the maximum diameter of a (round) flat oyster. This does not mean that

the beam thickness should be at least 12 cm, as the oysters are allowed to protrude to the sides. This should be considered when the amount of attached oysters to a structure is defined.

**Dimension ratio**
For the concepts presented in Section 2.3.1, certain dimension ratios are assumed. However, different ratios per concept can be considered to obtain the design. For the Cube framework concept, alternatives are considered. Instead of a cube, a shoe-box shaped framework and a piebox shaped framework are also considered. For the shoe-box framework, the height and the width are smaller than the length and for the piebox framework, only the height is smaller than the width and the length. For the Open Table, multiple length dimensions for the 'table legs' and connecting beams in the centre are considered. This results in lower and wider 'Open Table' concepts or more slender and higher 'Open Table' concepts. For the Anchor, the two outer beams keep the same dimensions. However, the length of the outer beams compared to the inner beam can be altered. This can result in a longer and lower 'Anchor' concept or a higher and more compact 'Anchor' concept. Ratio alterations for the Xblock and Tetrapod are not considered, all arms of these concepts have the same dimensions. The Reference block also keeps constant ratios, such that it is a cube.

### 3.1.2. Relevant situations during the lifetime of a droppable oyster brood-stock structure

To obtain the most sufficient concept parameters, the relevant situations during the lifetime of a droppable oyster brood stock structure are identified. When insight into these relevant situations is gained, the concept parameters can be substantially defined. Three situations are identified; fall, land and stability. These situations are elaborated below.

**Fall situation**
The first relevant situation that the droppable oyster brood stock structure encounters is the fall from the vessel onto the scour protection, during the deployment. The structure will be dropped manually from a vessel. The structure will then flow in the water column for a depth of approximately 30 meters (see Table 2.3) until it hits the scour protection. During this situation, it is important that the structure does not experience too much horizontal displacement during the fall. The positioning due to the dropping should be accurate (as defined in Section 2.3.1). The maximum horizontal displacement experienced during the drop is defined to be between 4 to 5.5 metres. The design parameters of the concept influence dropping accuracy during the fall.

**Land situation**
The second relevant situation that the droppable oyster brood stock structure encounter, is the landing on the scour protection. The landing is defined as the moment between the first hit of the structure on the scour protection until it has settled on the scour protection. It is important that minimal oysters get damaged during this situation. This is affected by the interaction between the structure and the scour protection, defined by the different sides of the concepts hit during the landing. The parameters of the concepts define, how the structures react to the scour protection rocks and therefore how much oysters get damaged.

**Stability situation**
The next relevant situation that a droppable oyster brood stock structure endures, is encountered during storm events. The structure is intended to have a lifetime of approximately 30 years. A criterion is that the structure should remain stable for this period, which resulted in a requirement that the structure should endure a storm event with a return period of 10 years. This is dominant during a storm event, because then extreme hydraulic conditions occur, which could trigger movement. The parameters of the concept influence the stability of the concepts and are therefore relevant for this situation (i.e. total height of structure).

### 3.1.3. Hydraulic conditions

The hydraulic conditions that prevail during the defined relevant situations are addressed.

**Fall situation**
For the fall situation, the hydraulic conditions which prevail during deployment are considered. These conditions are elaborated in Section 2.1.1. This results in a significant wave height ($H_s$) of 1 meter, a significant wave period ($T_s$) of 7 seconds and a depth-averaged current velocity ($\bar{u_c}$) of 0.3 m/s is considered (see Table 2.1).

**Land situation**
The land situation also takes place during deployment conditions, hence the same conditions that are defined for the fall situation apply here, see Table 2.1.

**Stability situation**
For the stability situation, extreme conditions are considered. For extreme conditions, multiple load combinations can be used. This entails a combination of tidal current and wind-driven waves. The structures should remain stable for a storm with a return period of 10 years (see Section 2.3.1). However, extreme current velocities and extreme wave conditions do (usually) not occur simultaneously [Bosboom and Stive, 2022]. Therefore a combination of the 5 and 10 year return period extremes is considered. The dominant combination is normative for the stability calculations, to obtain a safe result.

For the combinations, the three reference wind farms and the average of the three are investigated. The corresponding current and wave information for these locations is given in Table 2.3.

The load combinations (current and waves) are converted to a flow velocity to compare them with each other, which entails the current at 1.5 meters above the seabed ($u_{c-1.5m}$) and the orbital motion induced by waves at 1.5 meters above the seabed ($u_{w-1.5m}$). This is obtained by vectorially summing up the flow velocities. The orbital motion induced by the waves is obtained using Equation 3.1, in which $\theta$ is assumed at 90 degrees to obtain the maximum orbital velocity.

To compute the orbital motion induced by the waves, the mean wave period ($T_m$) and the wave height which is exceeded by 1 % of the waves ($H_{1\%}$) are used. These can be obtained using Equation 3.2 and Equation 3.3 [Schiereck, 2003].

$$u_w = \omega a \frac{cosh(k(h+z))}{sinh(kh)} sin(\theta) \tag{3.1}$$

$$T_m = \frac{T_p}{1.2} \tag{3.2}$$

$$H_{1\%} = 1.5 \cdot H_s \tag{3.3}$$

The resulting flow velocities for the two load combinations per location are given in Table 3.1. Load combination 1 represents the current velocities with a 10 year return period and the wave-induced orbital motion with a 5 year return period. Load combination 2 represents the current velocities with a 5 year return period and the wave-induced orbital motion with a 10 year return period. It can be concluded that the wave load is always dominant for these locations and the loads occurring at Gemini are the most extreme. The conditions at Gemini are therefore considered normative in the behavioural prediction calculations for the stability, to obtain safe concept design parameters. The significant wave height ($H_s$) is 9.1 m, the peak wave period ($T_p$) is 13.8 s, for a storm event with a return period of 10 years. The current velocity 1.5 meters above the seabed ($u_{c-1.5m}$) is 0.57 m/s, for a storm event with a return period of 5 years (see Table 3.2).

**Table 3.1:** Resulting velocities for load combinations for extreme conditions at different offshore wind farm locations, given in [m/s]. Load combination 1 represents a current velocity at 1.5 meters above seabed ($u_{c-1.5m}$) with 10 year return period and a wave-induced orbital motion at 1.5 meters above the seabed with a 5 year return period ($u_{w-1.5m}$), providing a combined flow velocity 1.5 meters above the bottom ($u_{r-1.5m}$). Load combination 2 represents a current velocity at 1.5 meters above the seabed with 5 year return period ($u_{c-1.5m}$) and a wave-induced orbital motion at 1.5 meters above the seabed with a 10 year return period ($u_{w-1.5m}$), providing a combined flow velocity 1.5 meters above the bottom ($u_{r-1.5m}$).

| **Location** | $u_{c-1.5m}$ [m/s] | | $u_{w-1.5m}$ [m/s] | | $u_{r-1.5m}$ [m/s] | |
|---|---|---|---|---|---|---|
| | *5 year RP* | *10 year RP* | *5 year RP* | *10 year RP* | *1* | *2* |
| HKW | 0.50 | 0.50 | 1.64 | 1.87 | 2.14 | 2.37 |
| Borssele | 0.83 | 0.85 | 1.03 | 1.18 | 1.88 | 2.01 |
| Gemini | 0.57 | 0.60 | 2.42 | 2.74 | 3.02 | **3.31** |
| Average | 0.60 | 0.61 | 1.69 | 1.93 | 2.30 | 2.53 |

The hydraulic conditions which are used for the behavioural prediction calculations are presented in Table 3.2, for each relevant situation.

**Table 3.2:** The hydraulic conditions used for the behavioural prediction calculations for each situation.

| **Situation** | $\bar{u_c}$ [m/s] | $u_{c-1.5m}$ [m/s] | $u_{r-1.5m}$ [m/s] | $H_s$ [m] | $T_m$ [s] | $T_p$ [s] |
|---|---|---|---|---|---|---|
| Fall | 0.3 | - | - | 1 | 7 | 8.4 |
| Land | 0.3 | - | - | 1 | 7 | 8.4 |
| Stability | - | 0.57 | 3.31 | 9.1 | 11.5 | 13.8 |

## 3.1.4. Relevant forces that act on droppable broodstock structures

There are five relevant forces that need to be considered when studying subsea structures. These forces are; gravitational, drag, lift, bottom friction and inertia force [Elger et al., 2020]. These forces are elaborated in this subsection.

**Gravitational force**

In Newton's Law of Universal Gravitation (NLUG), it states that two objects attract each other with a force, which is called the gravitational force. This applies to any two objects located anywhere in the universe, which is the weight of the gravitational force acting on an object. The magnitude of this force is given by Equation 3.4 [Elger et al., 2020].

$$F_G = (\rho_s - \rho_w)gV \tag{3.4}$$

In which,

$\rho_s$ : specific weight of object [kg/m$^3$]
V : volume of object [m$^3$]

**Drag force**

If an object moves through a fluid or if a fluid flows along an object, the fluid exerts a resultant force on this object. The component of this resultant force that is parallel to the velocity of the free stream is called the drag force. The drag force is limited to those forces produced by a flowing fluid Nakayama [2018]. The maximum drag force is used to investigate the response of the structure in a fluid. This is obtained by taking the maximum wave period. The equation used for the drag force in given in Equation 3.5 [Elger et al., 2020].

The drag coefficient is a parameter that characterises the drag force associated to the shape of a given body. Values for the drag coefficient are difficult to define and are usually found by experiment. Many experiments have been done, with several basic shapes to obtain better inside [Ghassemi et al., 2013].

The shapes of the structures considered in this research are complex as they consist of several elements. The drag coefficient used in the calculations of the behavioural predictions are based on

simplified shapes. For a 3D flat plate, a drag coefficient between 1.5 and 2 is found [Elger et al., 2020] [van Oord, 1996] [Nakayama, 2018]. In a study executed by G. Van Oord, using scale experiments, the drag coefficients for multiple shapes are defined (see Figure C.1) [van Oord, 1996]. Using this study, the drag coefficient for the different concepts are defined.

$$F_D = \frac{1}{2} C_D \rho_w S u^2 \tag{3.5}$$

In which,

| | | |
|---|---|---|
| $C_D$ | : drag coefficient | [-] |
| S | : projected area of object normal to the force direction | [$m^2$] |
| u | : velocity of object relative to the fluid | [m/s] |

**Lift force**
The perpendicular component to the velocity of the free stream of the resultant force is called the lift force [Elger et al., 2020]. The lift force can be obtained using Equation 3.6.

The lift coefficient is a parameter that characterises the lift that is associated with an object. The lift coefficient depends on the flow direction, the shape and on the angularity of the object. These dependencies bring a lot of discussion in literature about the value of the coefficient. A lot of research is carried out to determine the values for the coefficient, but still only rough estimations are defined. These estimations depend on many flow and particle parameters, so the estimations vary considerable [Elger et al., 2020]. Based on experiments performed on a rectangular flat plate, a lift coefficient of 0.2 is assumed [Ortiz et al., 2015] [Dessens, 2004] [Ghassemi et al., 2013]. This lift coefficient is considered for the behavioural prediction calculations.

$$F_L = \frac{1}{2} C_L \rho_w S u^2 \tag{3.6}$$

In which:

| | | |
|---|---|---|
| $C_L$ | : lift coefficient | [-] |

**Bottom friction force**
The substrate on which an object is placed, exerts a force on the object. This force provides resistance to movement of the object. This force is called the bottom friction force. The bottom friction force results from vertical force components, which are multiplied by a bottom friction coefficient $\mu$. The bottom friction coefficient is dependent on the interaction between the substrate and the object. The roughness of the substrate and the object are important for the definition of this coefficient. Values for the coefficient are difficult to determine and are usually found by experiment [Elger et al., 2020]. In a previous pilot project for oyster brood stock structures, executed at Luchterduinen offshore wind farm, a bottom friction coefficient of 0.6 is assumed [Heijningen and Mungar, 2022]. As these structures have similar purposes and the same type of substrate, this value is also considered for all the concept calculations. The bottom friction force can be obtained using Equation 3.7.

$$F_B = \mu(F_G - F_L) \tag{3.7}$$

In which:

| | | |
|---|---|---|
| $\mu$ | : bottom friction coefficient | [-] |

**Inertia force**
Inertia is the resistance of an object to a change in its velocity. It is a resisting force against movement of the object. The inertia force can be obtained using Equation 3.8 [Elger et al., 2020].

The added mass coefficient represents the force necessary for the acceleration of the fluid to go around the object [Dessens, 2004]. Inertia is therefore dependent on the mass of the object. Larger object have greater inertia and a greater tendency to resist changes in their motion than smaller and more slender bodies.

The concepts are all very slender (except reference block concept, which is not realistic for actual use). It is therefore assumed that inertia has minimal impact and (drag forces are dominant) on the behaviour of the brood stock structures and is therefore neglected in the calculations of the forces on the concepts ($KC > 45$) [Journée and Massie, 2001].

$$F_I = \rho_w(1 + C_A)V\dot{u} \tag{3.8}$$

In which:

| | | |
|---|---|---|
| $C_A$ | : added mass coefficient | [-] |
| $\dot{u}$ | : fluid particle acceleration amplitude (only for orbital motion) | [m/s$^2$] |

This results in four relevant forces which are considered for the behavioural prediction calculations to identify the dimensions of the concepts, which are gravitational force, drag force, lift force and bottom friction force.

# 3.2. Method for behavioural prediction calculations

The methodology to predict the behaviour during each situation is elaborated in this section.

## 3.2.1. Fall situation

The fall situation entails, the fall from the vessel until just before the first hit on the scour protection. To predict the horizontal displacement encountered during the fall and therefore the positioning accuracy, only the fall in the water column is considered. This excludes the fall above the water (in the air), from the vessel until the waterline.

Three relevant forces are identified which influence the movement of the structure during the fall; the gravitational force, the drag force in the vertical direction and the drag force in the horizontal direction (see Figure 3.1). The drag force in the horizontal direction is caused by the velocity of the current, therefore this force is called flow force ($F_u$) from now on.

The flow force ($F_u$), is effected by the depth-averaged current velocity ($\bar{u_c}$), present in the water column. The flow velocity induced by the waves (orbital motion) is not taken into account here. The waves induce a circular motion. It is assumed that this circular motion leads to a resulting horizontal displacement of zero [Bosboom and Stive, 2022].

The drag force is dependent on the velocity of the structure in the vertical direction, the fall velocity. During the fall of the structure, the structure accelerates more and more until it has reached its (constant) equilibrium velocity. When the equilibrium velocity is reached, a balance is found between the two vertical forces (drag and weight). The equilibrium fall velocity follows from the equalisation of the drag force and the gravity force, which leads to the equation given in Equation 3.9 [van Oord, 1996]. This constant equilibrium speed is reached after a short time. The depth after which the equilibrium velocity is reached is equal to approximately eight times the diameter of falling object ($d \approx 2.5m$) [Schiereck, 2003]. In the calculation for the behavioural predictions during the fall situation, it is assumed that the structure has reaches its equilibrium velocity instantly and that it remains constant for the entire fall in the water column.

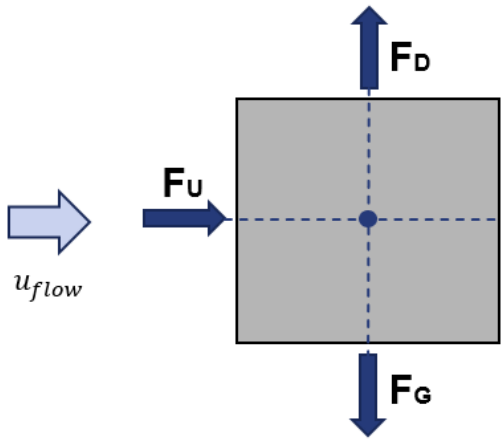


**Figure 3.1:** Relevant forces that act upon the structure, which influence the movement during the fall in flowing water.

When considering the design criteria for the brood stock structure during the fall situation defined in Section 2.3.1, it is mainly relevant to consider the horizontal displacement of the structure. As it is desired to have accurate positioning during the installation. The horizontal displacement during the fall is defined a maximum of 5.5 meters. The horizontal displacement ($x_h$) is determined using the equilibrium fall velocity and the current velocity, see Equation 3.10 and Equation 3.11. The horizontal displacement is based on the assumption that the flow comes from the same direction over the entire water depth, which results in a safe estimation (see Figure 3.2).

$$w = \sqrt{2\Delta \frac{Vg}{SC_D}} \tag{3.9}$$

$$tan(\varphi) = \frac{\bar{u}}{w} \tag{3.10}$$

$$x_h = tan(\varphi)d \tag{3.11}$$

In which,

| | | | |
|---|---|---|---|
| $w$ | : | equilibrium velocity | [m/s] |
| $\varphi$ | : | fall angle | [degree] |
| $d$ | : | water depth | [m] |
| $x_h$ | : | horizontal displacement | [m] |

For the considered concept, the drag coefficient ($C_D$) and the projected area on which the force acts ($S$) need to be determined.

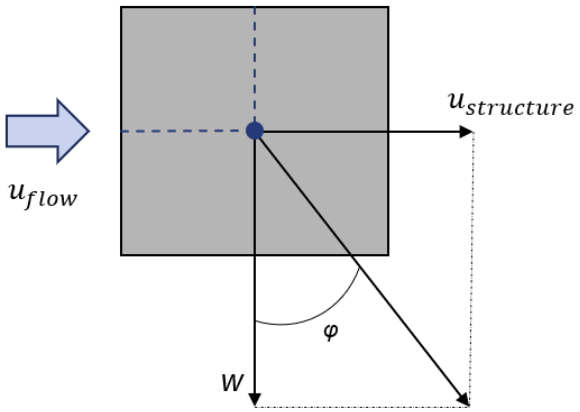


**Figure 3.2:** Relevant parameters which influence the horizontal displacement of the structure during fall in flowing water.

### 3.2.2. Land situation

For the land situation, the number of sides hit and bounces the structure will encounter during the landing are mainly relevant. These aspects are difficult to predict, due to an irregular bottom, many different substrate layers and complex shapes of the concepts. No behavioural prediction about the movement during the landing is made by using the relevant forces. However, an estimation of the surface that gets hit during the landing can be made. It can be said with certainty that one side per concept minimally will be hit during the landing, therefore an assumption is made that only one side per concept gets hit during the landing. The surface hit during the landing can be used to estimate the oyster loss, by defining the amount of oysters attached to the structure. This is used to determine the total amount of structures needed at one scour protection (based on the critical mass defined in Section 2.1.2).

### 3.2.3. Stability situation

The stability is checked for the most extreme combination of prevailing storm conditions, to obtain safe design results for the concepts. The stability of the structure during a storm can be examined using multiple methods. In this study, two methods are investigated, a force equilibria based method and a shear stress based method.

**Force equilibria**

The force equilibrium method is based on the sum and momentum of the relevant forces acting upon the structure during the stability situation. The relevant forces for this situation entail lift, gravitational, drag and bottom friction force (see Figure 3.3).

As the structure is intended to settle on the scour protection, which consists of large rocks, the structure is likely to settle at an angle ($\alpha$), such that it is tilted. The scour protection consists of rocks of different sizes and shapes, which are dumped at the bottom of the sea. It is inevitable that the scour protection has an irregular profile. This results in sloping surfaces on which the structure can settle. Based on the nominal diameter of the armour rock ($d_{n50} = 294mm$), an angle of inclination ($\alpha$) with the seabed of 5 degrees is assumed, based on previous research [Van Rie, 2020].

Considering the angle of inclination, the lift, drag and gravitational force are therefore divided into two components (parallel and perpendicular to the structure) for the calculations. The direction of the bottom friction force is only parallel.

Three force equilibria are examined to test the stability of the structure during extreme conditions. These are, the horizontal equilibrium, the vertical equilibrium and the moment equilibrium.

The horizontal equilibrium reviews the acting and resisting forces in the horizontal direction. The structure is considered stable when the resisting forces (bottom friction) are greater than the acting forces (drag force). However, as the structure is tilted, the gravitational and lift force also provide horizontal force component which needs to be taken into account. This criterion examines whether or not the structure will slide due to prevailing wave and current-induced forces. The calculation steps are addressed below, for which the drag coefficient ($C_D$) and the surfaces on which the forces act upon ($A_{side}$, $A_{top}$) per concept need to be determined.

$$F_{D-h} = \cos(\alpha) \cdot \frac{1}{2} \cdot C_D \cdot \rho_w \cdot A_{side} \cdot u^2_{r-1.5m} \tag{3.12}$$

$$F_{L-h} = \sin(\alpha) \cdot \frac{1}{2} \cdot C_L \cdot \rho_w \cdot A_{top} \cdot u^2_{r-1.5m} \tag{3.13}$$

$$F_{G-h} = \sin(\alpha) \cdot (\rho_s - \rho_w) \cdot g \cdot V \tag{3.14}$$

$$F_B = \mu \cdot (F_{D-h} - F_{G-h}) \tag{3.15}$$

$$\sum F_h = -F_{D-h} + -F_{L-h} - F_{G-h} + F_B \tag{3.16}$$

The vertical equilibrium reviews the acting and resisting forces in the vertical direction. The structure is considered stable when the resisting forces (weight) are greater than the acting forces (lift). However, as the structure is tilted, the drag force also provides a vertical force component which needs to be taken into account as well. This criterion examines whether or not the structure will start to float due to the prevailing wave and current forces. The calculation steps are addressed below, for which the drag coefficient ($C_D$) and the surfaces on which the forces act upon ($A_{side}$, $A_{top}$) per concept need to be determined.

$$F_{D-v} = \sin(\alpha) \cdot \frac{1}{2} \cdot C_D \cdot \rho_w \cdot A_{side} \cdot u^2_{r-1.5m} \tag{3.17}$$

$$F_{L-v} = \cos(\alpha) \cdot \frac{1}{2} \cdot C_L \cdot \rho_w \cdot A_{top} \cdot u^2_{r-1.5m} \tag{3.18}$$

$$F_{G-v} = \cos(\alpha) \cdot (\rho_s - \rho_w) \cdot g \cdot V \tag{3.19}$$

$$\sum F_v = -F_{D-v} - F_{L-v} + F_{G-v} \tag{3.20}$$

The last equilibrium is the moment equilibrium. The structure is considered stable if the momentum exerted by the resisting forces (weight) is greater than the momentum exerted by the acting forces (drag and lift). This criterion examines whether or not the structure will tilt (rotate) due to the prevailing wave and current forces. The moment equilibrium is considered with respect to the bottom back side relative to where the flow is coming from (see Figure 3.3). This presents the most likely position where the rotation will occur and therefore provides the safest calculations. It is assumed that the relevant forces act upon one point of the side they encounter, namely the defined centre of gravity per side of the concepts. The gravitational force acts upon the centre of gravity of the concepts. The bottom friction force goes through the momentum point and is, therefore not included in the moment equilibrium. To determine the moment equilibrium, the drag coefficient ($C_D$), the distances from (horizontal and vertical) distances ($a_n$) from the point they act upon and the centre of gravity per concept need to be determined. $a_1$ is defined as the vertical distance between the moment point and the centre of gravity. $a_2$ is defined as the horizontal distance between the point where the drag force acts upon the side surface of the concept and the moment point. $a_3$ is defined as the horizontal distance between the moment point and the centre of gravity. $a_4$ is defined as the vertical distance between the point where the lift force acts upon the side surface of the concept and the moment point. The calculation steps are addressed below;

$$M_D = -F_{D-h} \cdot a_1 - F_{D-v} \cdot a_2 \tag{3.21}$$

$$M_G = -F_{G-h} \cdot a_1 + F_{G-v} \cdot a_3 \tag{3.22}$$

$$M_L = -F_{L-h} \cdot a_4 + F_{L-v} \cdot a_3 \tag{3.23}$$

$$\sum M = M_D + M_W + M_L \tag{3.24}$$

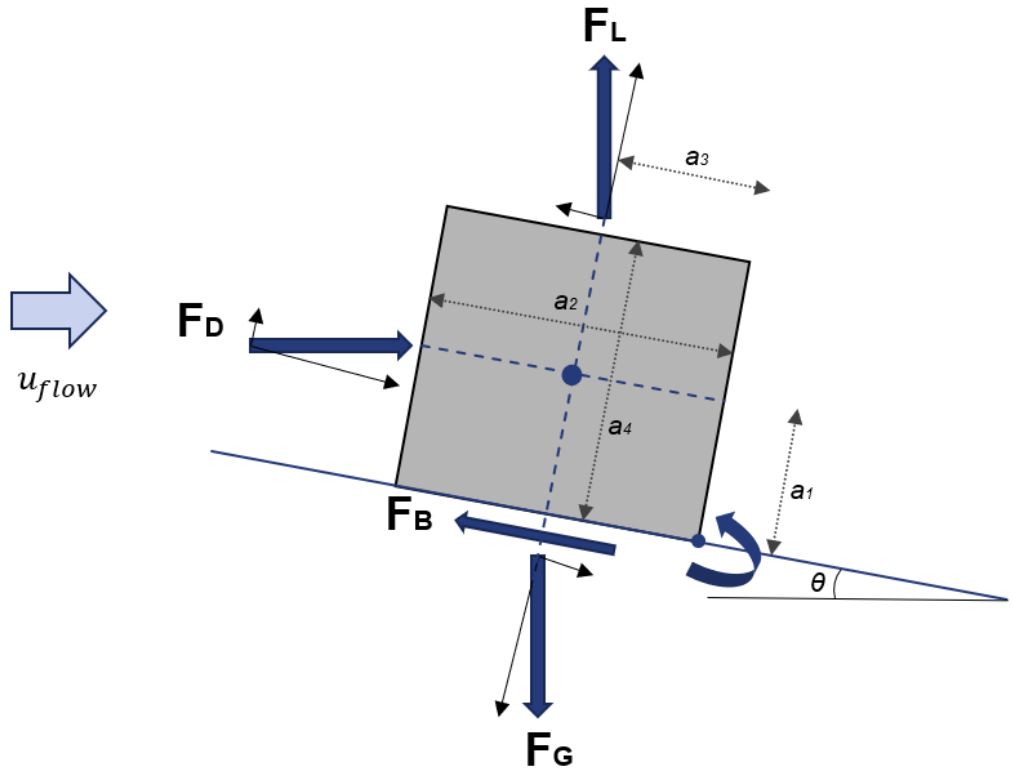


**Figure 3.3:** Forces on a structure at the seabed in flowing water

**Shear stresses**

A method that is broadly used to determine the stability of rocks at a bed protection is defined by Shield, using critical shear stress. The structure is assessed as stable if the critical stress of the structure is higher than the shear stress induced by currents and/or waves. The value for the Shields parameter ($\psi$) is a measure to assess the stability of a rock. As the threshold of motion is a subjective matter when judged in an experiment, multiple values for Shields parameter are defined [Schiereck, 2003]. In an investigation performed in 1971 in the Hydraulic Engineering Laboratory, seven stages of transport were defined. Based on this investigation, a value of 0.056 indicates stable rock with no significant movement, thus a stable design [ir. H.N.C Breusers and Schukking, 1971]. Therefore this value is used as the Shields parameter. Using this value, the critical shear stress can be determined with Equation 3.25 [Schiereck, 2003].

$$\tau_{cr} = (\rho_s - \rho_w) g D_{50} \psi_{cr} \tag{3.25}$$

In which,

| | | | |
|---|---|---|---|
| $\tau_{cr}$ | : | critical shear stress | [N/m$^2$] |
| $D_{50}$ | : | median grain size | [m] |
| $\psi_{cr}$ | : | Shields parameter | [-] |

The relevant shear stress is based on whether currents or waves are the dominant hydraulic condition.

When waves are dominant, it is recommended to use the wave-induced shear stress that occurs near the bottom. The shear stress induced by short waves can be much higher than in flow. The shear stress induced by waves can be calculated using the following equations.

$$\hat{\tau}_w = \frac{1}{2} \rho_w c_f \hat{u}_b^2 \tag{3.26}$$

$$\hat{u}_b = \omega a_b = \frac{\omega a}{sinh(kh)} \tag{3.27}$$

$$c_f = exp[-6 + 5.2(a_b/k_r)^{-0.19}] \tag{3.28}$$

In which,

| | | |
|---|---|---|
| $\tau_w$ | : wave-induced shear stress | [N/m$^2$] |
| $c_f$ | : friction coefficient | [-] |
| $\hat{u}_b$ | : wave-induced current at the bottom | [m/s] |
| a | : wave amplitude | [m] |
| $k_r$ | : bottom roughness | [m] |

When currents are dominant, a combination of waves and current-induced shear stress is used, by adding up shear stress velocities. The combination of those stresses is determined according to the method of Bijker-Shields formula, which appears to be a conservative method [Schiereck, 2003]. According to Bijker, the influence of waves can be taken into account by summing up the current and orbital velocity vectorially [Bijker, 1967]. This resulting flow velocity is used to determine the combined shear stress.

The maximum resulting shear stress occurs when the wave direction is parallel to the flow ($\phi = 90°$). This direction is assumed in the calculations for a safe outcome.

$$u_r = \sqrt{\frac{g}{\kappa^2 C^2}u_c^2 + \frac{c_f}{2\kappa^2}u_b^2 sin^2(\omega t) + 2\frac{\sqrt{g}}{\kappa C}u_c\frac{1}{\kappa}\sqrt{\frac{c_f}{2}}u_b sin(\omega t)sin(\phi)} \tag{3.29}$$

$$\tau_r = \rho_w \kappa^2 u_r^2 \tag{3.30}$$

In which,

| | | |
|---|---|---|
| $u_r$ | : resulting flow velocity | [m/s] |
| $\kappa$ | : coefficient | [-] |
| C | : Chezy value | [$\sqrt{m}/s$] |
| $u_c$ | : current velocity | [m/s] |
| $u_b$ | : maximum orbital velocity at the bottom | [m/s] |
| $\phi$ | : the angle between wave and current direction | [°] |

The force equilibria method indicates stability when $\sum F_h$, $\sum F_v$ and $\sum M$ are larger than zero, which are dependent on the height, width, drag coefficient, side surface, top surface and lift coefficient of the concepts.

The shear stress method indicates stability for a concept, when the critical shear stress of the concept is larger than the induced shear stress by the hydraulic conditions ($\tau_{cr} > \tau_w$). This method is widely applied to assess the stability of rock layers (for bed, bank and scour protections). The critical shear stress is mainly dependent on the $d_{50}$ of a rock (median grain size). To determine the stability of the concepts based on this method, the $d_{50}$ is defined by $\sqrt{A}$ of the concepts. However, the concepts are not 'rock' shaped, and therefore cannot be fully defined by their $d_{50}$.

Stability calculations using shear stresses are mainly intended to investigate the stability of stone layers and not for complex shapes and structures. It is difficult to define the relevant parameters for complex shapes. The force equilibrium method is dependent on more and more accurate concept parameters, than the shear stress method. This implies that the force equilibria method provides more precise stability results. Therefore the force equilibria method is selected to investigate the stability of the concepts.

## 3.3. Results of behavioural predictions calculations

The methods explained in Section 3.2, to predict the behaviour during relevant situations are executed. The calculations elaborated in Section 3.2 are performed by an iterative process, using a variety of concept parameters. The concept parameters (volume, beam thickness and ratios) are adjusted iteratively, to obtain the most favourable results for the behavioural predictions.

The results for the behavioural predictions for the three relevant situations are presented for ten considered concepts. The concepts are; Reference block, Xblock, Tetrapod, Cube framework, Piebox framework, Anchor long, Anchor short, Open Table 1, Open Table 2 and Open Table 3.

### 3.3.1. Fall situation

The horizontal displacement after a fall of 30 meters through the water column is determined, using the described method in Section 3.2. The flow velocity used is the depth-averaged current velocity ($\bar{u_c}$), defined to be 0.3 m/s, based on historic data. The volume ($V$) of the concepts depends on the weight classes, weight class 1 results in a volume of 0.0092 $m^2$ and weight class 2 results in a volume of 0.02 $m^2$. The drag coefficient ($C_D$) values are identified as described in Section 3.1.4 for each considered concept. The projected area of the concepts normal to the force direction ($S$) is defined for each concept, based on an assumption of the most likely position the concepts will take during the fall. $S$ is the area of the side that is facing upwards during the fall. For the five basic concepts defined in Chapter 2 (excluding the Reference block), these sides are presented in Figure 3.4 with a red line, to provide insight for each considered concept.

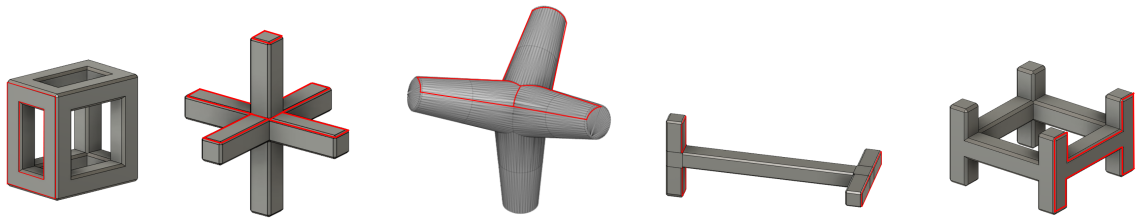

(a) (b) (c) (d) (e)

**Figure 3.4:** The projected area of the concepts normal to the force direction ($S$) indicated with a red line, defined for the basic concepts

The calculation steps for a reference block with weight class 1 are presented in Section C.1.1. The horizontal displacement ($x_h$) after the fall is defined per concept and is presented in Table 3.3. The parameters used and obtained which differ per concept ($V$, $S$, $C_D$, $w$) are presented in Table 3.7, in which $S$ is indicated as $A_{top}$. The parameters which are the same for each concept ($\rho_s$, $\rho_w$, $\Delta$, $d$, $\bar{u_c}$) are presented in Table 3.6.

According to the positioning accuracy requirement, the maximal horizontal displacement during the fall may be 4 meters if the structure should land on the armour layer and 5.5 metres if the structure can also land on the filter layer. In Table 3.3 it is seen that, two concepts (Tetrapod and Piebox framework) meet the 4 meter positioning criteria. The other eight concepts meet the 5.5 meter positioning criteria.

**Table 3.3:** Horizontal displacement per selected concept obtained by behavioural prediction calculations

| **Concept** | Horizontal displacement, $x_h$ [m] |
|---|---|
| Reference block | 4.4 |
| Xblock | 4.7 |
| Tetrapod | 3.7 |
| Cube framework | 4.5 |
| Piebox framework | 3.9 |
| Anchor long | 4.4 |
| Anchor short | 4.4 |
| Open Table 1 | 4.5 |
| Open Table 2 | 5.0 |
| Open Table 3 | 5.6 |

### 3.3.2. Land situation

To predict relevant information about the landing of the concepts, it is assumed that only one side of the concepts gets hit during the landing (described in Section 3.2). The surfaces hit are presented in

Figure 3.5 with a red line. The surfaces are only presented for six basic concepts defined in Chapter 2. The percentage of surface hit with respect to the total surface of the concepts during the landing ($A_{hit}$) is determined based on the defined concept parameters and presented in Table 3.4, per concept.

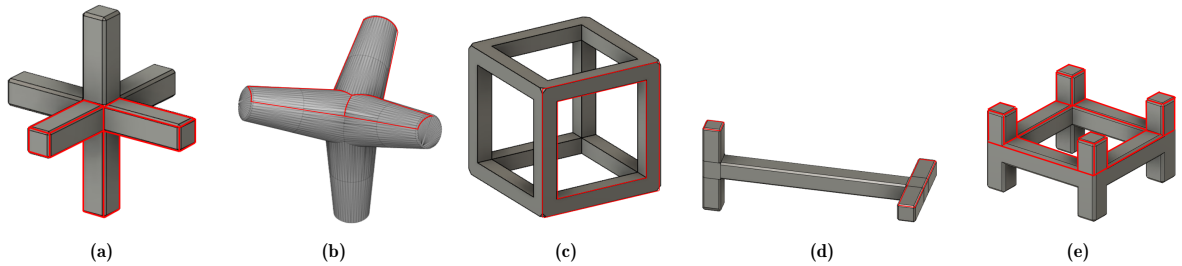


**Figure 3.5:** Surface hit during landing, marked with a red line. Used to define the percentage of surface hit ($A_{hit}$), with respect to total available surface per concept.

The dimensions and shape of the concept influence the amount of oysters that can be attached to one structure. The oysters will be attached to all the available surface for each concept. It is stated that the diameter of an oyster is equal to 12 cm (surface of 0.0144 $m^2$), which is used to determine the amount of oysters that can fit at one concept. Per concept a percentage of surface hit during the landing is determined, see Table 3.4. This percentage can identify the amount of oysters that get damaged during the landing. Taken this number of lost oysters into account, the number of intact oysters after the landing can be defined. This is used to determine the amount of structures required per scour protection. The defined critical mass is set at 500 intact oysters (see Section 2.1.2). The amount of structures per concept type at one scour protection are presented in Table 3.4. These values are not expected to be fully accurate, but do give insight in the order of magnitude.

**Table 3.4:** Behavioural prediction results for the land situation, including the surface hit per concept provided in percentage of the total surface, $A_{hit}$ and the amount of structures needed at one scour protection per concept.

| **Concept** | $A_{hit}$ [%] | Amount of structures [-] |
|---|---|---|
| Reference block | 0.17 | 18 |
| Xblock | 0.20 | 12 |
| Tetrapod | 0.33 | 17 |
| Cube framework | 0.17 | 13 |
| Piebox framework | 0.20 | 16 |
| Anchor long | 0.13 | 22 |
| Anchor short | 0.13 | 14 |
| Open Table 1 | 0.40 | 21 |
| Open Table 2 | 0.40 | 15 |
| Open Table 3 | 0.40 | 15 |

### 3.3.3. Stability situation

The behavioural predictions regarding the stability situation determined whether the concepts remained stable during a storm event, using the force equilibria method. The storm event conditions which are considered are presented in Table 3.1. This entails a storm event with a return period of 10 years for the wave conditions and a return period of 5 years for the current conditions at Gemini. This results in a near bottom flow velocity ($u_{r-1.5m}$) of 3.31 m/s, which includes the wave and current-induced flow velocity, 1.5 meters above the seabed.

The centre of gravity, the projected area normal to the force directions and the arm distances to the momentum point are relevant parameters for each concepts. These are determined for each considered concept. The centre of gravity is the centre of each concept is elaborated for each basic concept. For the Framework and Open Table concepts results in a centre of gravity in the middle where it does not 'touch' the concepts. For the Xblock, Tetrapod and Anchor concepts, the centre of gravity is also in the middle, where it does 'touch' the concepts. For the Frameworks, Xblock and Open Tables, the centre

of gravity is present at half the height ($H$) and half the width ($W$) of the concept dimensions. For the Tetrapod and Anchor, the centre of gravity is present at half the width ($W$) and at one third (1/3) of the height ($H$) of the concepts dimensions. The relevant arm distances are also presented in Figure 3.6 for each basic concept. For all the concepts, the arms are identified with the same arm symbols as used in Section 3.2 ($a_1$, $a_2$, $a_3$, $a_4$), but for the Anchor concepts, the arms are identified per force ($a_D$, $a_L$, $a_G$). See Figure 3.6 for the centre of gravity and the arm distances per concept.

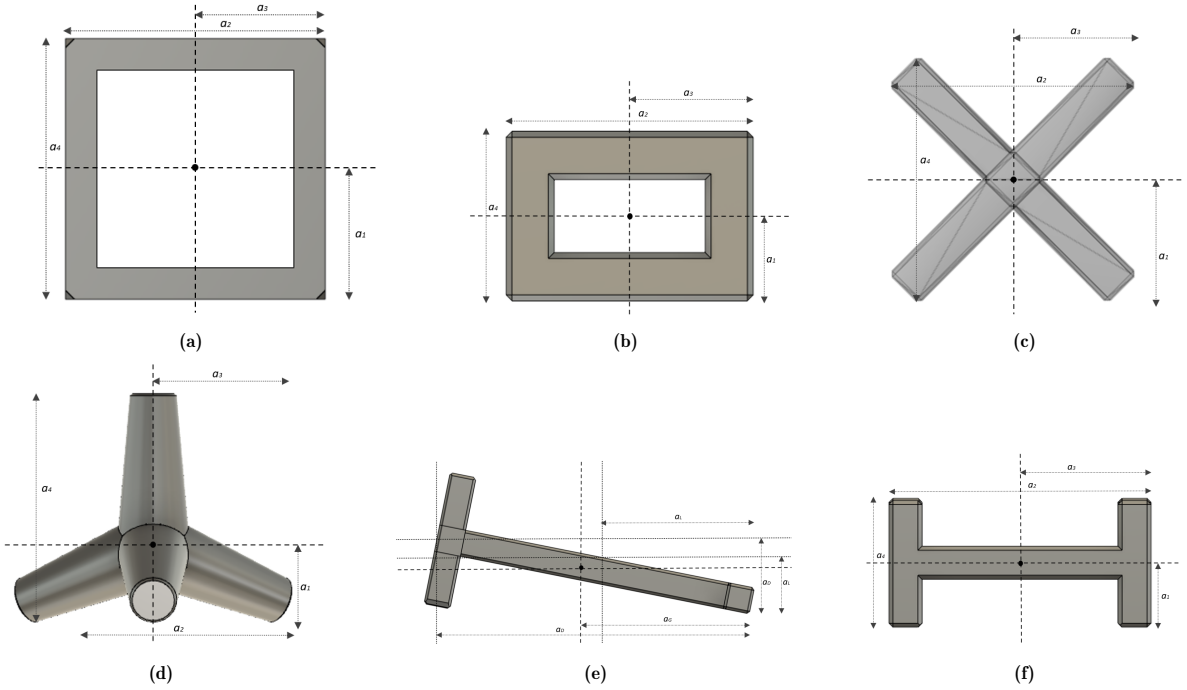


**Figure 3.6:** The centre of gravity and relevant arm distances per concept.

The projected areas normal to the force directions for each basic concept is presented in Figure 3.7, the yellow outlined areas represent the areas of the top sides ($A_{top}$) and the red outlined areas represent the areas of the sides ($A_{side}$), see Figure 3.7.

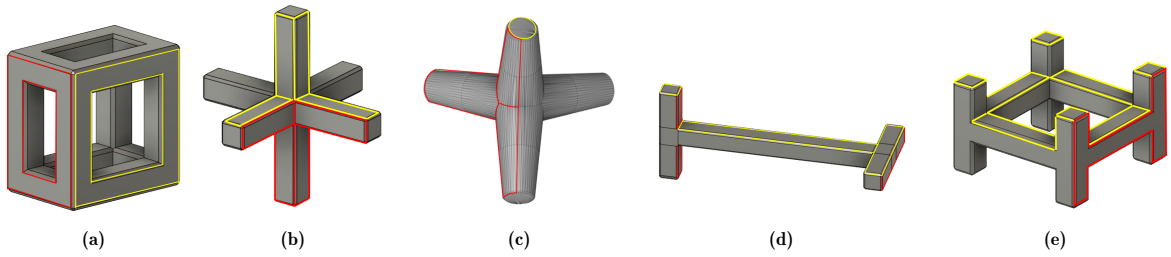


**Figure 3.7:** The projected areas for each basic concept. The yellow outlined areas represent the areas of the top sides ($A_{top}$) and the red outlined areas represent the areas of the sides ($A_{side}$).

The parameters used and obtained which differ per considered concept ($A_{top}$, $A_{side}$, $H$, $W$) are presented in Table 3.7. The parameters which are the same for each concept ($\rho_s$, $\rho_w$, $\alpha$, $u_{r-1.5m}$, $C_L$, $\mu$) are presented in Table 3.6.

A concept is considered stable when it complies with the three defined equilibria, the horizontal forces, vertical forces and the momentum. When the acting forces exceed the resisting forces, the equilibria are negative. The calculation steps for each method for a reference block with weight class 1 are presented in Section C.1.1.

When the horizontal force equilibrium is negative, this means that the structure is likely to slide. None of the considered concepts have a positive horizontal force equilibrium. However, when the inside

of the structure is larger than an armour rock it is likely that they will nestle around a stone and therefore are less likely to slide, only the dimensions of the Piebox framework does not allow the inside of the concept to settle around an armour rock with a nominal diameter. When the vertical force equilibrium is negative, the structure floats in the water. All the considered concept have a positive vertical force equilibrium and therefore meet this criterion. If the momentum equilibrium is negative, the structure is likely to rotate and roll over. Only one considered concept meets this criterion; Anchor long.

Based on the three force equilibria, only the Anchor long concept will remain stable during a storm event with a return period of 10 years at Gemini, assuming that the concepts will not slide due to the resistance of the armour rock, see Table 3.5.

**Table 3.5:** Force equilibria results based on calculations to define stability during a storm event with a return period of 10 years

| **Concept** | $\sum F_v$ [N] | $\sum F_h$ [N] | $\sum M$ [Nm] |
|---|---|---|---|
| Reference block | 234 | -473 | -56 |
| Xblock | 213 | -714 | -175 |
| Tetrapod | 241 | -396 | -51 |
| Cube framework | 220 | -635 | -176 |
| Piebox framework | 235 | -328 | -20 |
| Anchor long | 222 | -607 | 5 |
| Anchor short | 222 | -607 | -25 |
| Open Table 1 | 181 | -356 | -38 |
| Open Table 2 | 202 | -342 | -35 |
| Open Table 3 | 220 | -300 | -28 |

**Table 3.6:** Parameters used for behavioural prediction calculations, which remain the same for each concept

| **Parameter** | Value | Unit |
|---|---|---|
| $\rho_s$ | 2500 | $kg/m^3$ |
| $\rho_w$ | 1025 | $kg/m^3$ |
| $\Delta$ | 1.44 | - |
| $d$ | 29.5 | $m$ |
| $\bar{u_c}$ | 0.3 | $m/s$ |
| $\alpha$ | 5 | $^\circ$ |
| $u_{r-1.5m}$ | 3.31 | $m/s$ |
| $C_L$ | 0.2 | - |
| $\mu$ | 0.6 | - |

**Table 3.7:** Parameters per concept used for calculations for behavioural predictions, which differ for each concept

| **Concept** | $V$ | $C_D$ | $w$ | $A_{top}$ | $A_{side}$ | $H$ | $W$ |
|---|---|---|---|---|---|---|---|
| Reference block | 0.02 | 1.5 | 2.06 | 0.07 | 0.07 | 0.27 | 0.27 |
| Xblock | 0.02 | 1.1 | 1.91 | 0.14 | 0.14 | 0.50 | 0.50 |
| Tetrapod | 0.02 | 0.9 | 2.41 | 0.11 | 0.11 | 0.58 | 0.57 |
| Cube framework | 0.02 | 1 | 2.01 | 0.14 | 0.14 | 0.58 | 0.58 |
| Piebox framework | 0.02 | 1 | 2.29 | 0.11 | 0.09 | 0.26 | 0.42 |
| Anchor long | 0.02 | 0.9 | 2.05 | 0.15 | 0.15 | 0.40 | 1.10 |
| Anchor short | 0.02 | 0.9 | 2.05 | 0.15 | 0.15 | 0.47 | 0.97 |
| Open Table 1 | 0.02 | 1 | 1.60 | 0.22 | 0.09 | 0.29 | 0.87 |
| Open Table 2 | 0.02 | 1 | 1.79 | 0.18 | 0.09 | 0.31 | 0.63 |
| Open Table 3 | 0.02 | 1 | 2.01 | 0.14 | 0.08 | 0.31 | 0.49 |

## 3.4. Conclusion of concept parameters

Behavioural prediction of the droppable oyster broodstock structure are made. The concept parameters (volume, beam thickness and ratios) are adjusted iteratively, to obtain the most favourable results for the behavioural predictions. This iterative process has resulted in a total of ten suitable concepts. These ten concepts are based on the six defined concepts, defined in Section 2.3.1.

In Figure 3.8, the selected concepts are presented and in Table 3.8 the corresponding dimensions are provided. All concepts have a weight of 50 kg (weight class 2), as it appeared that the concepts with a weight of 23 kg were not suitable. The concept encountered too much displacement during the fall and showed to be even less stable. Therefore no concept with a weight of 23 kg is selected.

Based on the behavioural prediction calculations, all the concepts meet the design criteria of a positioning accuracy of 5.5 metres during a fall over a depth of 30 metres. Two concepts have a maximum horizontal displacement which is less than 4 metres.

For the landing situation, it can be concluded that the Open Table concepts encounter the most damage during the landing and the Anchor long and Open Table 1 requires the most structures.

For the stability situation only one concept remains stable, based on the calculations, which is the Anchor long concept. Many parameter alternatives have been tested and these concepts provided relatively the most stable results. Further investigation into the stability of the concepts is required.

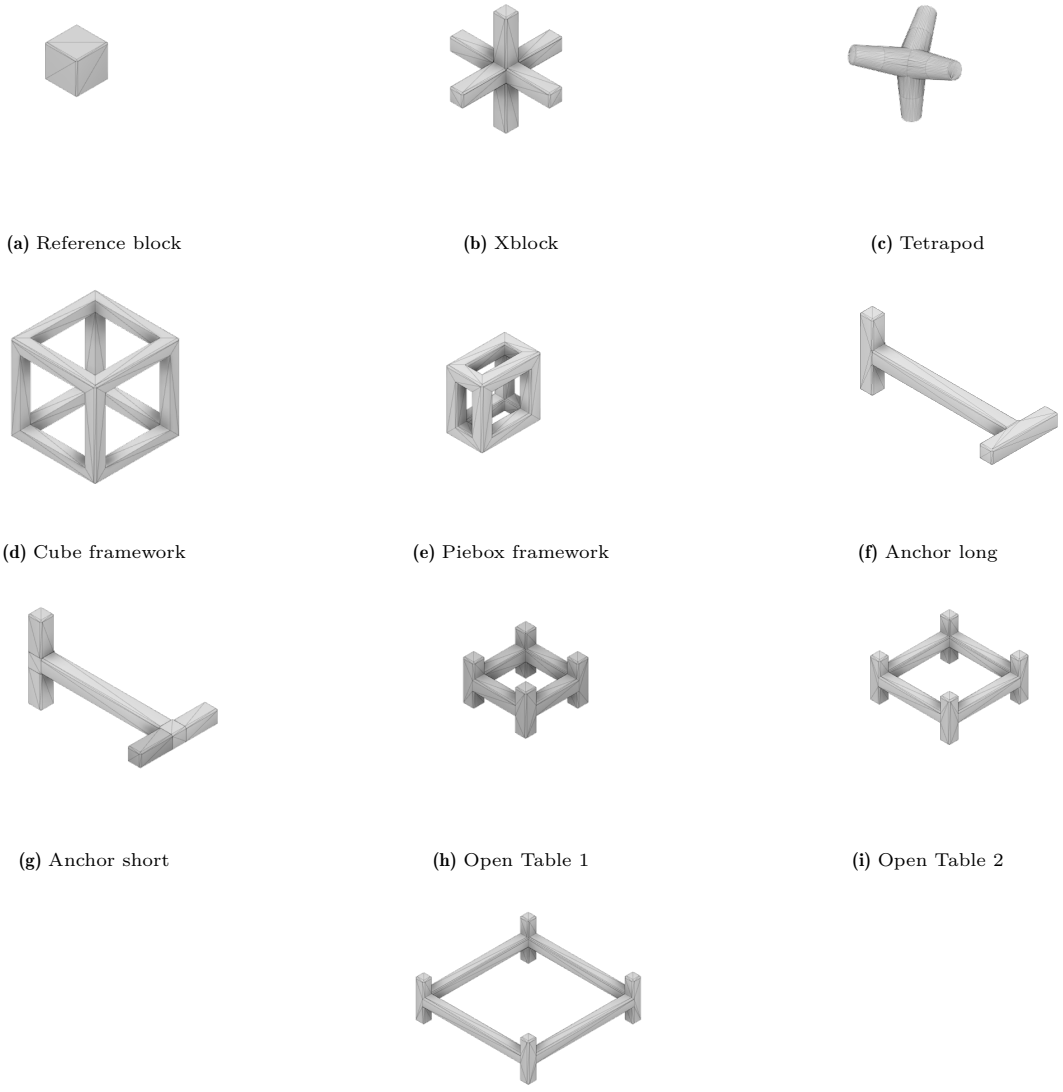

**(a)** Reference block **(b)** Xblock **(c)** Tetrapod

**(d)** Cube framework **(e)** Piebox framework **(f)** Anchor long

**(g)** Anchor short **(h)** Open Table 1 **(i)** Open Table 2

**(j)** Open Table 3

**Figure 3.8:** Concepts considered most suited, based on behavioural prediction calculations

**Table 3.8:** Concept dimensions provided in mm. The Tetrapod has an arm radius growth rate of 5°.

| **Concept** | Width | Length | Height | Thickness beam | Length 1 arm |
|---|---|---|---|---|---|
| Reference block | 270 | 270 | 270 | - | - |
| Xblock | 740 | 740 | 740 | 100 | 320 |
| Tetrapod | - | - | - | 100 | 300 |
| Cube framework | 580 | 580 | 580 | 70 | - |
| Piebox framework | 420 | 420 | 260 | 80 | - |
| Anchor long | 1200 | 500 | 500 | 100 | - |
| Anchor short | 1060 | 570 | 570 | 100 | - |
| Open Table 1 | 490 | 490 | 310 | 90 | - |
| Open Table 2 | 630 | 630 | 310 | 80 | - |
| Open Table 3 | 870 | 870 | 290 | 70 | - |

# 4

# Physical model set-up

The design of ten concepts is selected using the results of Chapter 2 and Chapter 3. To assess the performance of the concepts to function as a droppable oyster brood stock structure, behavioural predictions are made in Chapter 3. This presents a simplification of reality, based on many assumptions. To obtain more accurate insight intothe behaviour of the ten selected concepts, physical modelling is required.

In this chapter the experimental setup, used instruments and test program of the physical model are discussed. Three types of tests (fall, land and stability) were performed in the wave flume at the hydraulic engineering laboratory at the faculty of Civil Engineering, to mimic the relevant situations of a droppable oyster brood stock structure.

*This chapter addresses Technical Readiness Level 3. TRL 3 entails that, research is carried out into the applicability of the concept on an experimental basis (experimental proof of concept). Hypotheses about different parts of the concept are tested and validated.*

## 4.1. Scaling

A model study is a study that takes place according to a simplified and reduced representation of reality (the prototype). Generally, scale models are used because they are cheaper and more manageable to carry out than full-scale tests. When executing scale tests, the starting point is that the same processes occur in both the model and in reality. There must be a (geometric, kinematic and dynamic) similarity between the model and reality. To guarantee the similarity in behaviour in the model and the real world, scale rules apply [Kirkegaard et al., 2011] [Hughes, 1993].

A requirement for the correct application of scaling in model testing is that the relevant key numbers in the model and the prototype are constant. For the tests, two scales were applied, scale 1:10 and scale 1:15. This indicates that the tested situation is reduced 10 and 15 times in the model, relative to reality. The relevant scaling rules are elaborated below.

**Froude**

The Froude number presents the ratio between inertia and gravitation. The Froude number should be kept constant, using Equation 4.1.

$$Fr = \frac{u}{\sqrt{gd}} \tag{4.1}$$

Using the Froude number, the ratio between the model and the reality can be scaled. The length scales in the model are $n$ times smaller than their sizes in reality. Time scales, for instance wave periods, are $\sqrt{n}$ times smaller in the model [ir. G.J. Schiereck, 2007]. Flow velocities and orbital motions [m/s] are also $\sqrt{n}$ times smaller in the model.

**Reynolds**
The Reynolds number indicates whether the flow in the model is turbulent (inertia dominates viscosity). This determines many flow properties. When the Reynolds number is larger than 2000, the flow is considered turbulent. The Reynolds number in the model should be turbulent to avoid scale effects [ir. G.J. Schiereck, 2007]. This affects the minimal characteristic length of the prototypes (see Equation 4.2). Based on practical physical modelling experience the minimal characteristic length of a prototype is approximately 3 to 5 mm [Wolters and Gent].

$$Re = \frac{uL}{\upsilon} \tag{4.2}$$

In which,

$\upsilon$ : viscosity ($= 10^{-6}$) $[m^2/s]$
L : wave length [m]

**Density**
The density of the seawater ($\rho \approx 1025\ kg/m^3$) differs from the density of fresh water ($\rho \approx 1000\ kg/m^3$) in which the tests are performed. This difference in the density of the water affects the required density of the prototype to keep the correct interaction. There are two methods to define the scaling of the densities, based on waves or flow velocity. For both methods, the scaling factor ($N$) should be kept constant (see Equation 4.3 and Equation 4.4). Both methods provide the same result, when all parameters are scaled geometrically.

$$N_1 = \frac{H_s}{\Delta D_{n50}} \tag{4.3}$$

$$N_2 = \frac{u^2}{\Delta g d} \tag{4.4}$$

In which,

$D_{n50}$ : nominal diameter of concept [m]

For the tests performed in this research, the wave flume dimensions in correspondence with the chosen scales, it is not possible to geometrically scale all parameters. The flume height is too limited to represent a scaled water depth of 30 meters. To represent the scaled water depth correctly, a distorted scaling model is applied [Peakall et al., 1996]. This entails scaling the wave conditions with this distorted model for two tests. The orbital motion induced by the waves (see Equation 3.1) near the seabed is scaled using Froude instead of scaling the wave height and wave period directly with Froude. The scaling method based on the flow velocity (Equation 4.4) is therefore more appropriate. This scaling method defined a required density of 2440 $kg/m^3$ for the prototypes. This complies with a real-life density of 2500 $kg/m^3$ (fibre-reinforced concrete) for the broodstock structures.

# 4.2. Model set-up

In this section, the general layout of the wave flume and the model set-up per performed test is presented. Three scenarios were investigated in the tests, to obtain insight into the suitability of the concepts to act as an oyster broodstock structure; fall, landing and stability.

## 4.2.1. Wave flume

The tests were performed in the wave flume of the hydraulic engineering laboratory at the faculty of Civil Engineering at Technical University Delft (see Figure 4.1). The dimensions of the wave flume are 39 x 0.8 x 1 m, indicating the length, width and height subsequently. The length of the wave flume that can be used for practice, excluding the area in which the wave generator operates and the sinkage basins at the begin and end of the flume, is approximately 36 meters. The wave generator is an electrical piston-type generator, with a stroke of 2 meters. The generator can generate regular

and irregular shallow water waves. The maximum significant wave height which can be generated is approximately 0.2 meters. The waves can be combined with flow. The pump capacity of the flow generator is approximately 220 l/s.

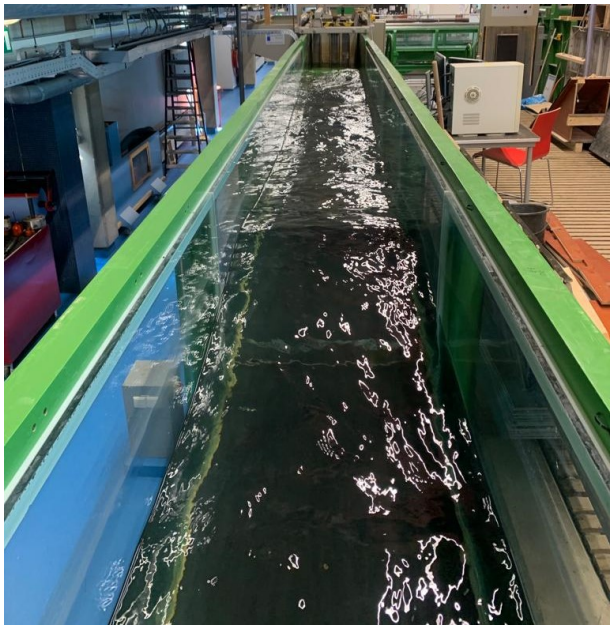

**Figure 4.1:** Wave Flume at Hydraulic Engineering Laboratory

During the tests, the monopile located at a scour protection (in reality) is not included in the set-up. In Chapter 1, it is stated that the flow pattern around a monopile changes, due to the presence of slender structures. This changing flow velocity is not incorporated in the set-up, because the brood stock structure should be positioned away from these accelerating flow velocities around the monopile. The oysters would not be able to survive in the presence of these accelerating flow velocities. Further away from the monopile, where the brood stock structures are intended to be positioned, the flow pattern is minimally affected, due to the presence of the monopile and therefore not incorporated [Schiereck, 2003].

### 4.2.2. Fall test

The first test that was performed in the fall test. The goal of this test was to obtain insight into the positioning accuracy during the fall of the concepts when dropped from the vessel until the first hit with the scour protection, which is approximately a fall of 30 meters. To test this behaviour, the concepts were dropped at a random moment in the wave flume several times.

As the water depth in the wave flume is limited, the tests cannot be scaled such that the drop over the full depth ($d \approx 30m$) is tested. This would result in unwanted scale effects. The test was therefore executed on two scales (1:10 and 1:15). In these two scale tests, the top 7 and 13 meters of the water column in which the concepts are dropped, are mimicked. These two tests were used to obtain the movement behaviour of the concepts over these two water depths (at the top of the water column). These results were used to predict the horizontal displacement over the full depth using extrapolation.

The model set-up for the fall test is presented in Figure 4.2. For a model detailed overview of the model set-up, see Section E.1.

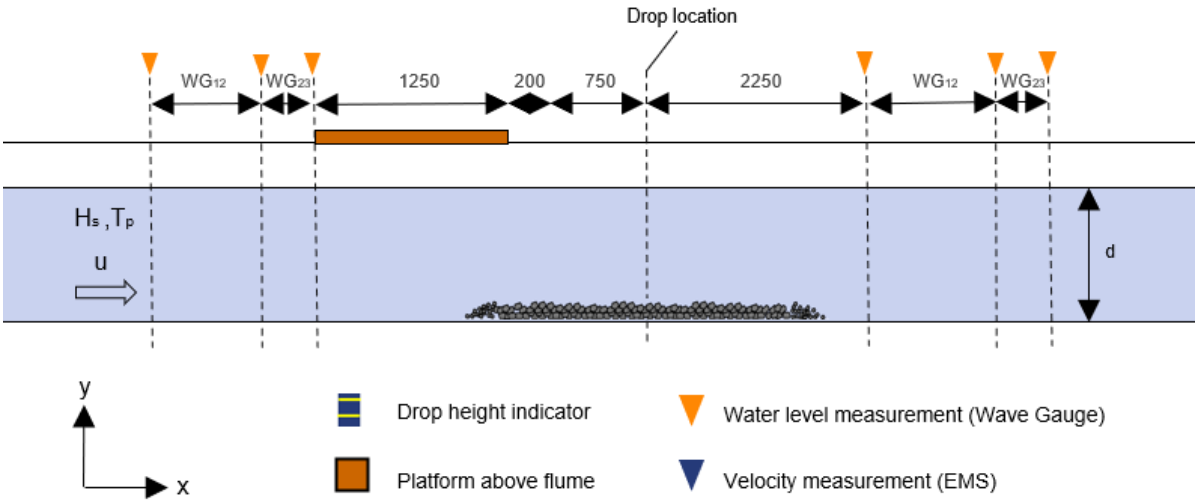


**Figure 4.2:** The wave flume set-up for the fall test, including relevant parameters

### 4.2.3. Land test

The second test that was performed, was the land test. The goal of this test was to obtain insight intothe behaviour of the concepts during the landing, after being dropped from a vessel and falling for approximately 30 meters in the water column. To test this behaviour the concepts were dropped at a random moment in the wave flume on a layer of stones. This test is performed using scale 1:15. In this test, the full water depth cannot be mimicked, due to the limited wave flume height. The landing is assessed based on the number of sides of the concepts that are hit during the landing on the stone layer and assessed based on the number of bounces the concepts make during the landing on the stone layer.

The flume set-up for the land test is given in Figure 4.3. For a model detailed overview of the model set-up, see Section E.1. A stone layer was placed at the bottom of the flume, to mimic the scour protection. Calculations were performed beforehand to check the stability of the stones for prevailing hydraulic conditions (see, Section 4.4.5).

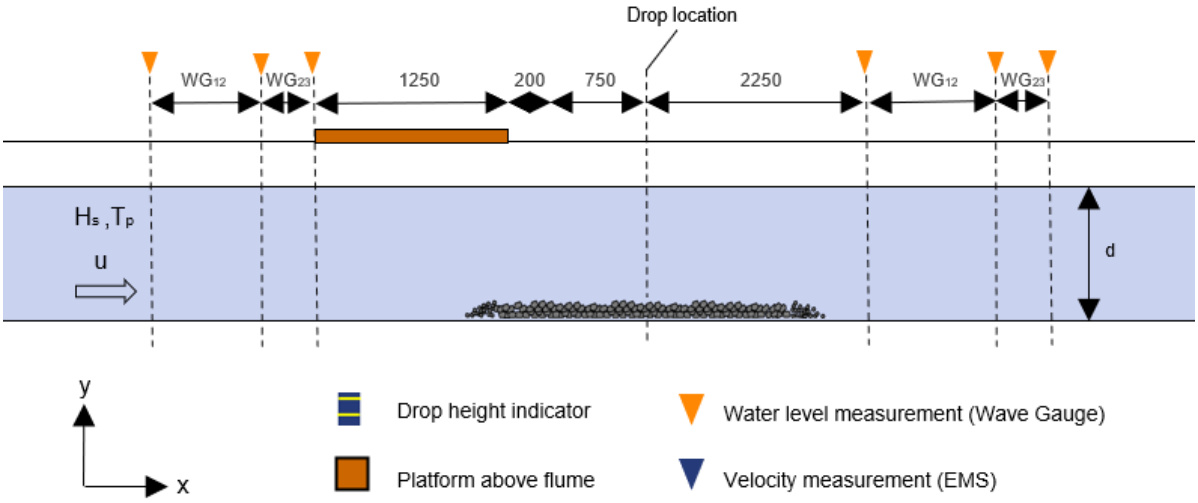


**Figure 4.3:** The wave flume set-up for the land test, including relevant parameters

### 4.2.4. Stability test

The third test that was executed was the stability test. The goal of this test was to assess the stability of the concepts when they have settled on the scour protection, during storm conditions. To determine

whether the concepts would remain stable during the operational lifetime of the offshore wind farms.

To test the stability, the concepts were placed on the stone layer. After which scaled storm conditions were generated in the wave flume to observe if the concepts remain stable or start to move. The concepts were assessed on their behaviour and categorised on it; stable (no movement), minimal movement (toggled around 1 time) or unstable (toggled around more than 1 time).

The flume set-up for the stability test is presented in Figure 4.4. The same stone layer was used as in the land test. For a model detailed overview of the model set-up, see Section E.1.

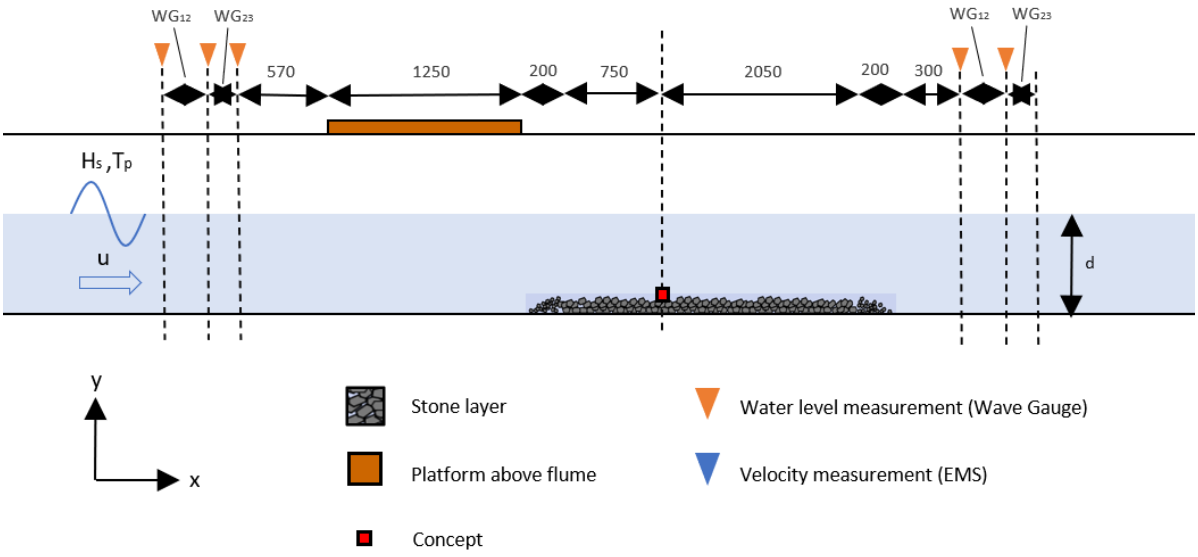


**Figure 4.4:** The wave flume set-up for the stability test, including relevant parameters

# 4.3. Test conditions

This section elaborates on the hydraulic conditions used in the physical model tests performed.

The design conditions are chosen based on the hydraulic conditions present at offshore wind farms in the Dutch North Sea. In Section 2.1.1, the three considered offshore wind farms are selected; 'Hollandse Kust West' (HKW), 'Borssele' and 'Gemini'. The hydraulic conditions selected for the tests are based on the averaged conditions at the three offshore wind farms (see Table 2.3).

## 4.3.1. Fall test

For the deployment of the oyster brood stock structures, appropriate weather conditions are necessary. Maximum 'deployment conditions' are defined for vessels going out for installation. These maximum deployment conditions were selected to be suitable conditions for the fall test, as the fall test represents the deployment of the brood stock structures. The fall is assessed based on the horizontal displacement of the concepts during the fall and the influence of the drop height on the horizontal displacement during the fall.

The hydraulic conditions during deployment entail a significant wave height, $H_s$ of 1 m, a significant wave period, $T_s$ of 7 s and a depth-averaged current $\bar{u_c}$ of 0.3 m/s, see Table 2.1. $H_s$, $T_s$ and $\bar{u_c}$ are scaled to scale 1:10 and scale 1:15 using Froude. The hydraulic conditions for scale 1:10 and scale 1:15 are presented in Table 4.3. The direction of the flow induced by the waves and the current are the same, this results in maximum horizontal displacement during the fall for the concepts to obtain safe results.

For the installation of brood stock structures multiple types of vessels can be used, see Figure 4.5. These vessels all have different sizes, which results in different drop heights for the broodstock structures. Three drop heights were investigated in the tests. The first drop height corresponds to 5 meters above the waterline, which relates to a drop from a 'Side Stone Dumping Vessel'. The second drop height corresponds to 1 meter above the waterline, which relates to a drop from a 'Multicat Vessel'. The third

drop height corresponds to 1 meter below the waterline. This drop height is applied when the other two drop heights above the waterline result in undesired behaviour and or damage to the broodstock structures (due to the impact when hitting the waterline). The scaled drop heights are presented in Table 4.1.

**(a)** Side Stone Dumping Vessel **(b)** Multicat vessel

**Figure 4.5:** Installation vessels used by marine contractors

**Table 4.1:** Drop heights from the waterline for the fall test for scale 1:10 and scale 1:15, given in mm.

| **Drop height** | scale 1:10 | scale 1:15 |
|---|---|---|
| $dh_1$ [mm] | +500 | +333 |
| $dh_2$[mm] | +150 | +100 |
| $dh_3$ [mm] | -100 | -67 |

### 4.3.2. Land test

The land test represents the second part of the deployment of the brood stock structures, therefore the deployment conditions also apply to the land test, see Table 2.1. The same hydraulic conditions prevail as in the fall test, namely the deployment conditions. However, the wave conditions in the fall test are scaled directly using Froude, which results in corresponding wave conditions to the top of the water column. In the land test, the landing of the concepts was only of importance, this means that the hydraulic conditions should comply with the near-the-bottom situation. The wave conditions therefore cannot be scaled directly using the Froude number. To mimic the near bottom conditions, the wave characteristics are altered such that the orbital motion velocity ($u_{w-1.5m}$) near the bottom induced by the waves comply. This is done using the distorted scaling model, by defining the orbital motion velocity near the bottom ($u_{w-1.5m}$) during deployment conditions, created by the deployment waves ($H_s = 1m$, $Ts = 7s$). This orbital motion velocity ($u_{w-1.5m}$) is scaled using Froude, which is converted back to input conditions represented by a significant wave height ($H_s$) and a peak wave period ($T_p$), which induce this scaled orbital motion. The peak wave period ($T_p$) is selected such that it induced shallow water waves, which is desired in the wave flume. The hydraulic conditions for the land test on scale 1:15 are presented in Table 4.3.

The stone layer placed on the bottom of the wave flume represents the scour protection. The average scour protection nominal diameter ($d_{n50}$) at offshore wind farms in the North Sea is 300 mm. This results in a scaled stone nominal diameter ($d_{n50}$) of 20 mm, with a grading width of 16-25 mm. More details about the size distribution of the stones in the layer is presented in Section 4.4.5. The dimensions of the stone layer used in the wave flume is presented in Table 4.2

**Table 4.2:** Stone layer parameters for the land test at scale 1:15

| **Parameter** | Unit | Value |
|---|---|---|
| $w_a$ | mm | 2000 |
| $w_f$ | mm | 200 |
| $d_{50_a}$ | mm | 20 |
| $d_{50_f}$ | mm | 5 |
| $t_a$ | mm | 67 |
| Grading armour stones | mm | 16-25 |

The concepts were dropped above the waterline at a random moment, to make sure the equilibrium velocity of the concepts was reached before hitting the bottom. The equilibrium fall velocity is approximately reached after 8 times the diameter of the concept [van Oord, 1996]. The largest prototype has a diameter of 7 cm on scale 1:15, which results in a minimal flume water depth of 0.56 m. The water depth ($d = 0.866m$) is sufficient for the concepts to reach their equilibrium velocity.

### 4.3.3. Stability test

In Section 2.3.1, it is stated that the concepts should at least remain stable during a storm with a return period of 10 years and are preferred to remain stable during a storm event with a return period of 50 years. In the stability test, it was investigated, whether the concepts remain stable during multiple storm events. Five different storm conditions are generated, boosted from mild to rough storm conditions. This results in five stability tests. The first storm condition combination is based on a storm event with a return period of 10 years averaged over the three offshore wind farms. The fifth storm condition combination is based on conditions that are rougher than a storm with a return period of 50 years at Gemini offshore wind farm. For the duration of the tests, 1000 waves were considered [Schiereck, 2003], which resulted in a duration of 33 minutes per test. A real storm duration can contain much more waves, but the peak of a storm usually contains fewer waves. For all tests, the same averaged extreme current velocity is used, which is a current of 1.5 m above the bottom with a return period of 5 years ($u_{c-1.5m} = 0.6m/s$), see Table 2.3. The current velocity is scaled using the Froude number.

The wave conditions are scaled based on the orbital motion velocity 1.5 meters above the bottom ($u_{w-1.5}$) generated by the storm waves. As the wave flume has a limited water depth, the wave conditions for the test were altered such that the orbital motion velocity 1.5 meters above the bottom corresponded. The same stone layer was used as for the land test (see Table 4.2). The hydraulic conditions per test are presented in Table 4.3.

**Table 4.3:** Input hydraulic conditions per test, including water depth ($d$) in the wave flume, generated depth-averaged flow velocity in the wave flume ($\bar{u}$), significant wave height ($H_s$) with 13 % exceeding change and peak wave period ($T_p$) generated by the wave generator using Jonswap spectrum

| **Test** | | d [m] | $\bar{u}$ [m/s] | Hs [m] | Tp [s] |
|---|---|---|---|---|---|
| Fall test 1 | scale 1:10 | 0.7 | 0.095 | 0.1 | 2.66 |
| Fall test 2 | scale 1:15 | 0.87 | 0.077 | 0.067 | 2.17 |
| Land test | scale 1:15 | 0.87 | 0.077 | 0.02 | 5 |
| Stability test SC 1 | scale 1:15 | 0.5 | 0.15 | 0.15 | 2 |
| Stability test SC 2 | scale 1:15 | 0.5 | 0.15 | 0.2 | 2 |
| Stability test SC 3 | scale 1:15 | 0.4 | 0.15 | 0.19 | 2 |
| Stability test SC 4 | scale 1:15 | 0.4 | 0.11 | 0.15 | 2 |
| Stability test SC 5 | scale 1:15 | 0.4 | 0.11 | 0.17 | 2 |

### 4.3.4. Wave generation

The wave spectrum chosen for the tests is a Jonswap wave spectrum, as it indicates not fully developed sea states, which are common coastal sea states used in physical model testing [Bosboom and Stive, 2022]. The waves in reality represent intermediate water waves.

**Type of wave**
The waves generated in the wave flume are shallow water waves, because this is preferred in the wave flume. The hydraulic conditions for the waves should therefore have shallow water wave characteristics. A wave is shallow when $h/L_0$ is smaller than 0.05. A wave is a deep water wave when $h/L_0$ is larger than 0.5. In between these values, a wave is in transitional waters [Bosboom and Stive, 2022].

**Wave breaking**
The waves generated in the wave flume should not break, because the waves do not break in reality. A wave must meet two requirements in order not to break, $H_s/d$ should be smaller than 0.8 and the steepness of the wave ($H_s/L_0$) should be smaller than 10 percent. For the maximal wave height in the flume, the still water level in the wave flume is summed with two times the wave height to avoid overtopping the flume height.

**Ursell**
The Ursell number classifies the non-linearity of a wave. The Ursell number provides the wave theory that is applicable for the prevailing conditions. If $N_{Ursell} > 26$, the cnoidal theory is best applicable and for $N_{Ursel} < 10$, the theory of Stokes is best applicable (Holthuijsen, 2007). In this report, the theory of stokes is used and therefore the conditions of the waves that are generated by the wave generator should have an Ursell number that is smaller than 10 [Kirkegaard et al., 2011].

$$U_{Ursell} = \frac{HL^2}{h^3} \tag{4.5}$$

**KC number**
The Keulegan and Carpenter number (KC) indicates the relative importance of drag forces versus inertia forces. It compares the wave length scale to the characteristic length scale of the object (concept). Small KC numbers indicate dominating inertia and large KC numbers indicate dominating drag. Drag dominates in turbulent water. The critical value lies around 15, indicating that the generated waves should provide a KC value larger than 15 [Keulegan and Carpenter, 1958]. The KC number can be obtained using Equation 4.6 [Keulegan and Carpenter, 1958], in which $u_o$ represents the amplitude of the orbital motion, T the wave period and L the characteristic length.

$$KC = \frac{u_o T}{L} \tag{4.6}$$

# 4.4. Instrumentation & equipment

The instrumentation and equipment used for each executed test are elaborated in this section.

## 4.4.1. Camera set-up

To analyse and process the test results, cameras were used. For the recording of the tests, two GoPro 10 cameras and two GoPro 7 cameras were used. A different set-up is used for the three types of tests.

- *Fall test*

  One GoPro cameras was installed outside the flume from the side at a distance of 42 cm from the flume and a height of 50 cm (see Figure E.1). The GoPro recorded the fall of each concept dropped. One GoPro was used to take photos from above after the fall to obtain the exact location of the concepts directly after the fall.
- *Land test*

  One camera was used to record the landing from the side of the flume. The camera was placed at a distance of 42 cm from the flume and a height of 50 cm from the bottom (see Figure E.2). The GoPro recorded the fall and landing of each concept dropped.
- *Stability test*

  One cameras was used to record the concepts from the side of the flume. The camera was placed nearby the flume at a distance of 35 cm of the flume and a height of 30 cm from the bottom (see Figure E.3). The GoPro recorded the concepts during the entire test duration (t=33 min.).

### 4.4.2. Wave Gauge

A wave gauge is a water level measuring equipment. The spacings between the wave gauges need to be optimal to obtain accurate wave data.

There are multiple methods defined in studies, using different quantities of wave gauges to indicate the appropriate spacing. In this study, the Mansard and Funke (MF(3b)) [Mansard and Funke, 1980] method is applied for spacing the wave gauges, using sets of three wave gauges [Hofland and Wenneker, 2014]. Two sets were used, one set before and one set after the location where the concepts were tested.

The spacing is dependent on the wave length ranges of the generated waves. The wave length in shallow water is dependent on the wave period and wave depth ($L = T\sqrt{gh}$). The minimal wave length is defined by the significant wave period ($T_m$) multiplied by 0.9 and the maximal wave height by the peak wave period ($T_p$). Using the MF(3b) method, the ratio between the distance between the first and the second wave gauge ($x_{12}$) and the maximal wave length should be 0.05 ($x_{12}/L_{max} = 0.05$) and the ratio between the distance between the first and the second wave gauge ($x_{12}$) and the minimal wave length should be 2.96 ($x_{12}/L_{min} = 2.96$). To define the distance between the second and the third wave gauge, the following ratio is defined ($x_{23}/x_{12} = 0.15$) [Hofland and Wenneker, 2014]. These ratios are used to define the position of the wave gauges. The spacings of the wave gauges are shown in Table 4.4, per test.

**Table 4.4:** Distances in between wave gauges (WG $x_n$) per executed test, given in meters

| **Test** | WG $x_{12}$ [m] | WG $x_{23}$ [m] |
|---|---|---|
| Fall test 1 | 0.35 | 0.092 |
| Fall test 2 | 0.32 | 0.047 |
| Land test | 0.05 | 0.079 |
| Stability test SC1 | 0.20 | 0.030 |
| Stability test SC2 | 0.20 | 0.030 |
| Stability test SC3 | 0.40 | 0.060 |
| Stability test SC4 | 0.40 | 0.060 |
| Stability test SC5 | 0.40 | 0.060 |

**Wave Gauge calibration**

The wave gauges measure in voltage, this had to be converted to an elevation. To compute the conversion formula, the wave gauges were calibrated 20 times by lowering the wave gauges from the still water level in steps from a couple of centimeters at a time. For each height, the voltage was noted, per wave gauge. This provided voltage to water height graphs per wave gauge (see Figure E.6), which are used to define the conversion rate per wave gauge, see Table 4.5.

| **WG** | G07 | G15 | G12 | G21 | G22 | G18 |
|---|---|---|---|---|---|---|
| Conversion rate | 2.0886 | 2.1337 | 2.0504 | 2.4568 | 2.4652 | 2.4486 |

**Table 4.5:** Conversion rates from voltage to elevation [cm] for each wave gauge (WG)

### 4.4.3. Electromagnetic Flow Meter

To measure the flow velocity of the water in the flume, three Electromagnetic Flow Meters (EFM) were installed for each test. EFMs measure the flow velocity in voltage, therefore this needed to be converted to m/s. This is done using the following formula; $|V| = -0.000188U^2 + 0.1023|U| + 0.002m/s$, defined by Deltares [EMS]. Two EFMs were installed at a height of 35 cm and one was installed at a height of 29 cm from the bottom. The three EFMs were installed before flow reached where the concepts were tested.

### 4.4.4. Parabolic damper

The function of the parabolic damper is to absorb the waves such that they reflect minimally. The top of the parabolic damper had to be approximately 10 cm above the waterline with an angle parallel to the water line (0 °). The angle of the damper had to correspond to the wave steepness. This position

ensures maximum absorption of the waves (see Figure 4.6). The damper is elevated from the bottom, for the flowing water to pass the damper, which makes the installation complex. The damper only functions near the water surface.

**Figure 4.6:** Parabolic damper in the wave flume

### 4.4.5. Stone layer

The same stones layer was used for the land test and the stability test.

The armour stones have a nominal diameter of 20 mm. The grading curve of the stones is presented in Figure 4.7. For the filter layer, stones with a nominal diameter of 5 mm are used.

To examine the stability of the stones in the wave flume for the different hydraulic conditions, Shields method is used. The stones were tested for the shear stress induced by waves ($\tau_w$) and shear stress induced by waves and currents ($\tau_r$). The critical stress (Equation 3.25) must be higher than the combined shear stress induced by currents (Equation 4.10) and wave action (Equation 4.7). Shear stresses result from wave- and current action (Equation 4.11), which can be calculated according to the approach of Bijker-Shields formula [CETMEF, 2007], [CETME, 2007].

Using a shields critical value of 0.056 (no significant movement Section C.1.2) and for the hydraulic roughness a value of 2 times the nominal diameter ($k_s = 2d_{n50}$), the critical shields shear stress (=27.2 $N/m^2$) is larger than the shear stresses induced by waves and or current for the hydraulic conditions combinations (waves and currents) used for the land and stability test (Table 4.6).

$$\tau_w = \frac{1}{2}\rho_w f_w u_o^2 \tag{4.7}$$

$$f_w = 0.237(\frac{a_o}{k_s})^{-0.52} \tag{4.8}$$

$$z_0 = 0.033k_s \tag{4.9}$$

$$\tau_c = \rho_w g \frac{\bar{u}^2}{C^2} \tag{4.10}$$

$$\tau_{cw} = \tau_c + \frac{1}{2}\tau_w \tag{4.11}$$

In which,

$f_w$ : friction factor [-]
$k_s$ : hydraulic roughness [m]

**Table 4.6:** Calculated shear stresses for the conditions which prevail during the tests.

| **Parameter** | Land test | Stability test |
|---|---|---|
| $\tau_w$ | 1.42 | 25.4 |
| $\tau_{cw}$ | 0.764 | 12.7 |
| Stable: $\tau_{cr} > \tau$ | Yes | Yes |

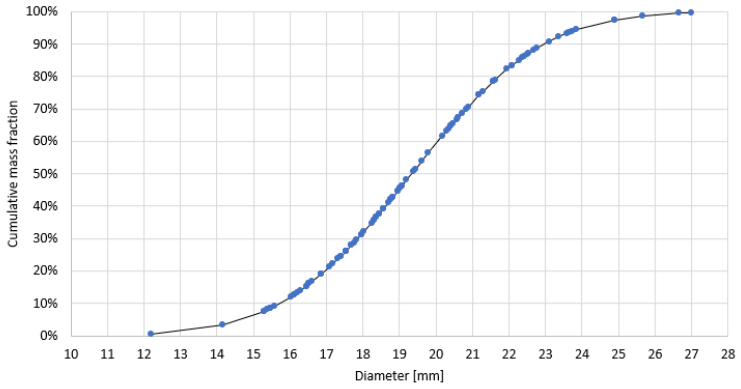


**Figure 4.7:** Grading curve of the armour layer material

# 5

# Physical model results

This chapter provides an overview of the results obtained during the performed tests in the wave flume at the Hydraulic Engineering Laboratory.

*This chapter addresses Technical Readiness Level 4. TRL 4 entails that, the proof-of-concept of the innovation is tested on a laboratory scale. The design, development and testing of the technological components take place in a laboratory environment. The basic technical components are integrated to ensure operation. A prototype developed in this phase costs relatively little money and time to develop and is therefore still far from a final product, process or service.*

## 5.1. Fall test

The fall test was executed on two scales, 1:10 and 1:15. In both tests, all concepts were dropped approximately thirty times from the same (x,z) location and three different heights (y). The fall test was recorded from two different perspectives, from above with a photo camera and from the side with a video camera. The photo camera from above observed the location of the concepts directly after the fall (x,z). The video camera from the side observed the movement during the fall (x,y). The results are analysed from these two perspectives (x,z and x,y). The hydraulic conditions that were generated in the wave flume during the fall tests are presented in Table 5.3.

### 5.1.1. Locations of the concepts at the end of the fall (in x-z plane)

The locations of the concepts where they hit the bottom first after the fall, are presented in graphs for the three drop heights per concept in Section F.1.2. This provides three location graphs (x,z) per tested concept containing each ten data points. These three location graphs per concept are merged into one graph. This provides two location graphs per concept, each for the test performed at scale 1:10 and 1:15. In Figure 5.1, the location graphs per test performed for the reference block are presented. The graph includes a dashed line. This line indicates the thickness of the boundary layer from the wall to this line. The boundary layer thickness for the tests performed at scale 1:10 was 7.7 cm and 11.4 cm for the tests performed at scale 1:15. The boundary layers are determined using the definition by [Jensen et al., 1989]. No concept had landed within the boundary layer during the tests. The location graphs (x,z) for all the other concepts are presented in Section F.1.2.

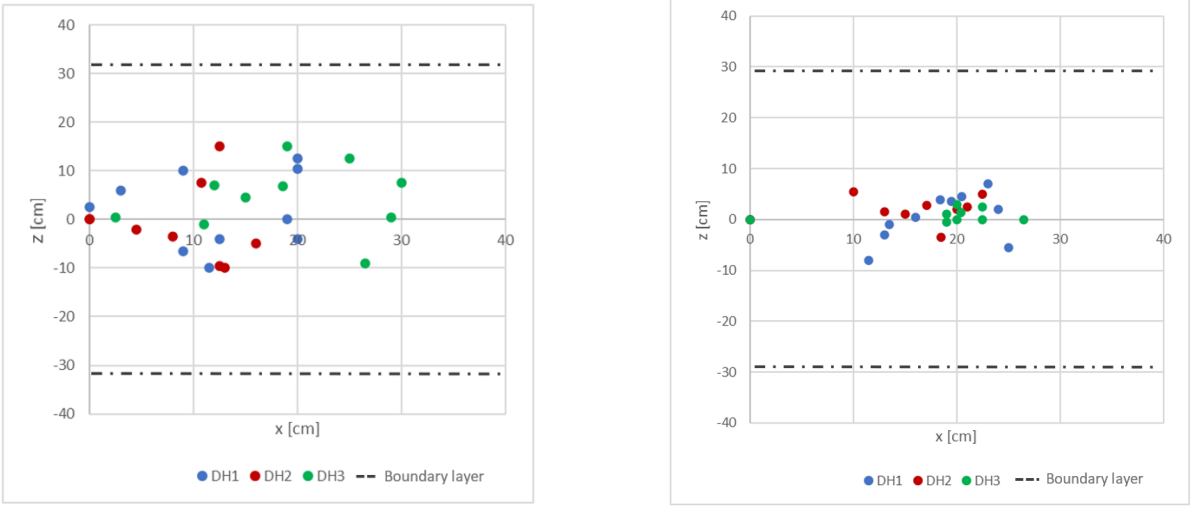


**(a)** Fall test scale 1:10

**(b)** Fall test scale 1:15

**Figure 5.1:** Locations (x,z) of Reference block directly after fall, given in cm. Including the thickness of the boundary layer, using the definition by [Jensen et al., 1989].

**Distinction between different drop heights during fall test**

The connection between the drop heights and the land locations was investigated. Only for the test performed on scale 1:10 for the Piebox framework (see Figure F.16), a clear pattern is observed. For all the other tests, no clear pattern is observed. Therefore, it is assumed that the difference in drop heights have a minimal effect on the land locations of the concepts. In the rest of the result analysis, no distinction is made between the drop heights. This results in that each concept is dropped thirty times (N=30) per test (scale 1:10 and scale 1:15), which gives a total of sixty drops (N=60) per concept.

**Horizontal distance between drop and land location per concept**

The distance in the horizontal direction (x,z), between the drop location and the land location, is determined per test. The thirty measured distances per test are averaged per concept. This is presented in Figure 5.2. The concepts are sorted from smallest to largest averaged distances. For scale 1:10, the Open table 1 and 3 (when the Reference block is not included) shows the least distance and the Cube framework shows the most distance. For scale 1:15, the Tetrapod and Open table 1 show the smallest distance and the Cube framework the largest distance.

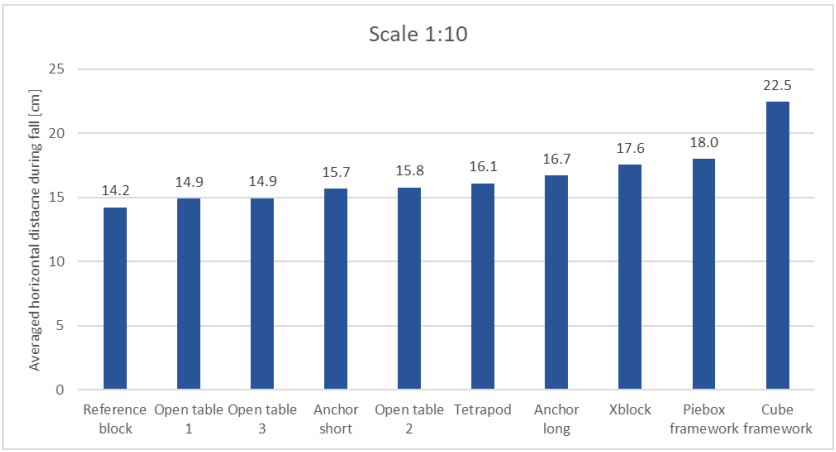


**(a)** Fall test scale 1:10

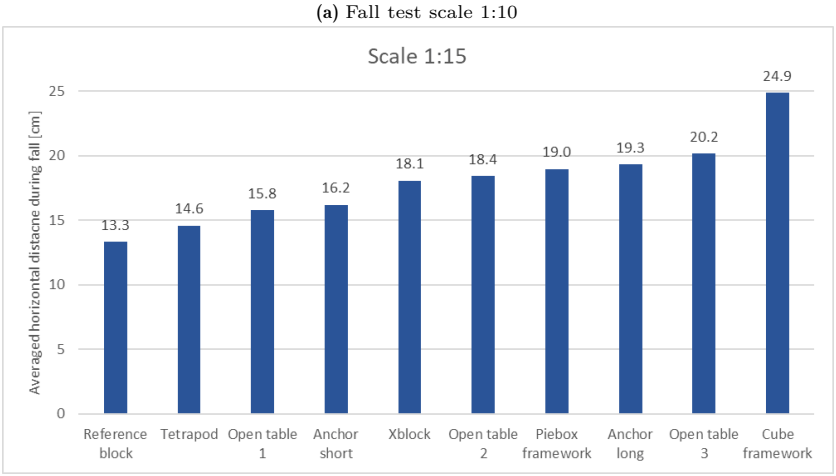


**(b)** Fall test scale 1:15

**Figure 5.2:** Averaged distances after fall (N=30) for each concept given in cm.

## 5.1.2. Movement of the concepts during the fall (in x-y plane)

The fall of the concepts was video recorded from the side to observe the movement behaviour over the depth (x,y). In Figure 5.3, the movement of the Reference block is shown for the Reference block for the two performed experiments. For the other concepts, the graphs are shown in Figure F.1.3. In Section F.1, it is explained how the movement data is obtained.

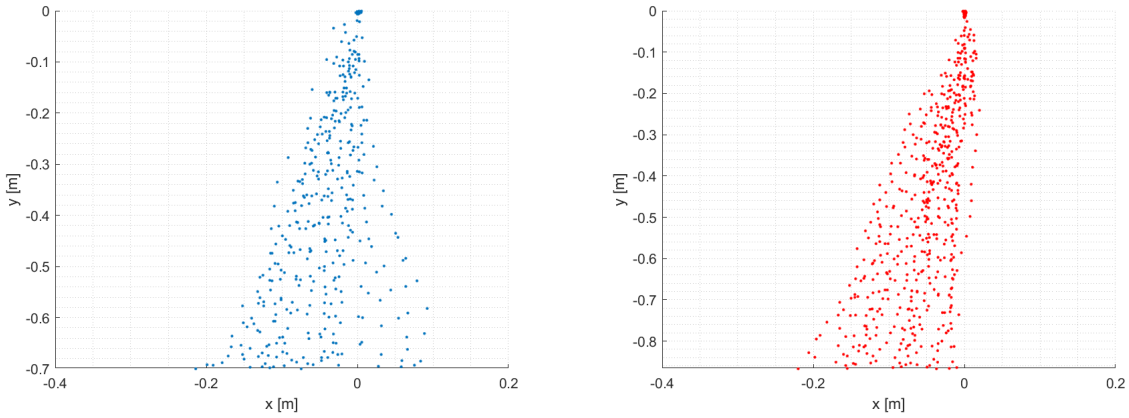


**(a)** Fall test scale 1:10

**(b)** Fall test scale 1:15

**Figure 5.3:** Track positions of the Reference block during Fall tests

## 5.2. Land test

In the land test, the ten concepts were tested on their behaviour during the landing on the stone layer. Two aspects were specifically investigated; the number of sides hit during the landing and the number of bounces. The test was recorded with a video camera from the side (x,y). The hydraulic conditions that were generated in the wave flume are presented in Table 5.3

The video recordings from the side of the tests, show the landing behaviour. During all the tests, no concept has 'bounced off' during the landing. The concepts all landed directly and toggled around a maximum of three times before settling.

The amount of sides hit during this toggling were counted per executed test per concept and are presented in Table 5.1. It can be seen that not every concept was tested the same amount of times. The tests per concept were repeated a minimum of five times.

The Open table concepts 1 and 2, fell with their small side pointing down and their wide side pointing in the horizontal direction. During all the tests, the Open table 1 and 2 landed on their small side first. During most of the tests, the Open tables 1 and 2 would subsequently roll over to the wide side and settle. In some cases the Open table concepts settled on the small side. It is expected that they will later on (during a storm) toggle over to their wide side and therefore would still hit two sides in total. The Open table 3 could also land directly on its 'wide' side.

**Table 5.1:** Number of sides of the concepts hit during the landing test per test.

| **Test** | 1 | 2 | 3 | 4 | 5 | 6 | 7 | 8 | 9 | 10 | 11 | 12 |
|---|---|---|---|---|---|---|---|---|---|---|---|---|
| Ref. Block | 1 | 2 | 2 | 2 | 1 | 3 | 2 | | | | | |
| Xblock | 2 | 2 | 1 | 1 | 2 | 1 | | | | | | |
| Tetrapod | 1 | 1 | 1 | 1 | 1 | 1 | | | | | | |
| Piebox fr. | 1 | 2 | 1 | 2 | 1 | 1 | 1 | | | | | |
| Cube fr. | 1 | 1 | 1 | 1 | 1 | 1 | 1 | 2 | 1 | 1 | | |
| Anchor long | 2 | 1 | 1 | 1 | 1 | 2 | 2 | 3 | | | | |
| Anchor short | 2 | 1 | 2 | 1 | 1 | | | | | | | |
| Open table 1 | 2 | 2 | 1 | 1 | 2 | 1 | 2 | 2 | 1 | 1 | 2 | 2 |
| Open table 2 | 2 | 2 | 1 | 1 | 2 | 1 | 2 | 2 | 1 | 1 | | |
| Open table 3 | 2 | 1 | 2 | 2 | 2 | 1 | 2 | 2 | 1 | 2 | 1 | |

## 5.3. Stability test

During the stability tests, the concepts were tested on their stability in storm conditions and the conditions at which the concepts started to move were investigated, using five (increased) storm conditions. The concepts were placed on the stone layer in the wave flume followed by generating the storm conditions (see Figure 5.4). If a concept appeared to be unstable twice for the same conditions, it was assumed that the threshold of motion of that concept was reached. When the concepts did not show the same behaviour for the first two times the test was performed, the test was repeated an extra time. In case the concepts were not stable, they were not tested further in the increased storm conditions (assuming they would also be unstable in these conditions). The hydraulic storm conditions per storm that were generated in the wave flume are presented in Table 5.3. The behaviour of the concepts is elaborated per tested storm condition. The behaviour shown per executed tests is presented in Section F.3.

**(a)** Cube framework

**(b)** Tetrapod

**Figure 5.4:** Concepts on the stone layer in wave flume during the stability test

During storm condition 1, only the Cube framework concept did not remain stable. The Cube framework concept was not tested further on in the stability tests. The dimensions of the Cube framework reached highest, compared to the other concepts. Therefore it was expected, that this concept would become unstable first. The storm conditions in the following tests were increased compared to storm conditions 1. When storm conditions 2 were prevailing, the Xblock concept and the Piebox framework concept did not remain stable. The storm conditions in the following tests were increased compared to storm conditions 2. During storm condition 3, the Anchor short concept became unstable twice when. The Open table 1 concept did also not remain fully stable for any test, it was assumed the threshold of motion for this concept was reached. The duration of the tests in the wave flume was limited. The Reference block was not tested further on in the stability tests as this is not a realistic design of a brood stock structure. During storm condition 4, the Tetrapod and the Anchor long concepts were unstable twice. The Open table 2 and 3 concepts were the only concepts that did not reach their threshold of motion until storm conditions 5. The Open table 2 concept had reached its threshold of motion during these conditions. The Open table 3 concept had diverse results during these conditions.

In Table 5.2, an overview at which storm conditions the concepts became unstable is displayed.

**Table 5.2:** Overview of the storm conditions tested in the wave flume at which the concepts started to move.

| **Concept** | Storm condition |
|---|---|
| Reference block | 3 |
| Xblock | 2 |
| Tetrapod | 4 |
| Cube framework | 1 |
| Piebox framework | 2 |
| Anchor long | 4 |
| Anchor short | 3 |
| Open table 1 | 3 |
| Open table 2 | 5 |
| Open table 3 | 5 |

## 5.4. Output hydraulic conditions wave flume

The input hydraulic conditions for the wave flume were selected per test, based on the hydraulic conditions during the deployment of the brood stock structure and during storm conditions in the North Sea (Table 4.3). These conditions were scaled for the tests performed in the wave flume (fall, land and stability tests) and generated by a pump and a wave generator. The input hydraulic conditions per test are presented in Table 5.3.

The hydraulic conditions in the wave flume were measured using EFM, for the flow velocity, and wave gauges, for the wave height. The output is processed in DASYlab, which provided data files with the output of all six wave gauges and three EFMs. The output of the wave gauges is processed using Matlab, to provide the significant wave height and peak wave period per test. The output of the DASYlab file

containing the EFM data is processed using Excel. The output of the hydraulic conditions averaged per type of test is presented in Table 5.3. The output per performed test is presented in Section F.3.1.

The output conditions differ (slightly) from the input conditions. The generated peak wave period ($T_p$) and flow velocity ($u$) output substantially correspond and have minimal deviations from the input conditions. The generated significant wave height ($H_s$) output is consistently lower than input conditions for the fall tests and the stability tests. Only the land test output wave height matches the input wave height. The Reynolds, Ursell and KC numbers were considered for each test condition, to investigate whether scale effects were experienced (see Table F.16). For all test conditions, the numbers complied.

**Table 5.3:** Input and output of hydraulic conditions per test performed in the wave flume. SC stands for storm combination

| **Test** | *Input* | | | *Output* | | |
|---|---|---|---|---|---|---|
| | $\bar{u}$ [m/s] | $H_s$ [m] | $T_p$ [s] | $\bar{u}$ [m/s] | $H_s$ [m] | $T_p$ [s] |
| Fall *scale 1:10* | 0.10 | 0.10 | 2.66 | 0.10 | 0.09 | 2.54 |
| Fall *scale 1:15* | 0.08 | 0.07 | 2.17 | 0.07 | 0.06 | 2.22 |
| Land | 0.08 | 0.02 | 5.00 | 0.08 | 0.02 | 4.78 |
| Stability *SC 1* | 0.15 | 0.15 | 2.00 | 0.15 | 0.13 | 1.98 |
| Stability *SC 2* | 0.15 | 0.20 | 2.00 | 0.16 | 0.17 | 1.99 |
| Stability *SC 3* | 0.15 | 0.19 | 2.00 | 0.16 | 0.15 | 2.00 |
| Stability *SC 4* | 0.11 | 0.15 | 2.00 | 0.13 | 0.13 | 2.00 |
| Stability *SC 5* | 0.11 | 0.17 | 2.00 | 0.13 | 0.15 | 2.00 |

The wave field generated in the wave flume consists of a combination of incident and reflected waves. The incident wave is of importance as this wave exerts a load on the concepts. The reflected wave disrupts the desired wave field. The waves that were measured by the wave gauges are a combination of the two waves. To minimise the reflected waves, the parabolic damper was installed. As the parabolic damper was lifted from the bottom of the flume, to allow flow to pass underneath the damper, the reflection coefficient of the waves was difficult to define using literature. Due to the accurate positioning of the parabolic damper, it is assumed that the reflection coefficient had a maximum of 30 % [Hofland and Wenneker, 2014], resulting in $H_{s-r} = 0.3 \cdot H_{s-i}$. Resulting from the total wave energy equation [Bosboom and Stive, 2022], which is proportional to $Hsi^2 + Hsr^2$, the total wave height can be written accordingly;

$$H_t = \sqrt{H_{s-i}^2 + H_{s-r}^2} = \sqrt{H_{s-i}^2 + 0.3H_{s-i}^2} = H_{s-i} + \sqrt{1 + 0.3^2} = 1.044H_{s-i} \tag{5.1}$$

This results in a maximum effect of approximately 4% on the incident wave height, which is small. It is therefore assumed that the reflecting wave has minimal impact on the behaviour of the concepts tested in the wave flume and is therefore not considered in the rest of the research.

# 6

# Physical model result interpretation

In Chapter 2, the design criteria and requirements for an oyster broodstock structure are defined. The results of the tests performed are analysed and processed to the extent that they can be linked to the defined design criteria.

*This chapter addresses a part of Technical Readiness Level 5. TRL 5 entails that, research is carried out into the operation of the technological concept in a relevant environment. This is the first step in demonstrating the technology. A prototype developed in this phase costs a relatively large amount of time and money and is not far removed from the final product or system.*

## 6.1. Fall test

In Section 2.3.1, the positioning accuracy during deployment for the brood stock structures is defined. The maximum position accuracy is indicated to be between 4 and 5.5 meters over a depth of 30 meters. This section processes the results of the fall test to provide inside in the horizontal displacement of the concepts during the deployment and compare them to this positioning accuracy requirement.

To investigate whether the concept exceeds the maximum allowed horizontal displacement during the fall, the results from the fall tests performed at scale 1:10 and 1:15 are converted to scale 1:1. The direction of the generated flow and waves is the same, which is unlikely to occur in reality. This results in maximum horizontal displacement values for the concepts, and could also lead to an overestimation of the horizontal displacement.

The results of the converted displacement data (at scale 1:1) represent the horizontal displacement encountered over a depth of 7 meters (for the test at scale 1:10) and a depth of 13 meters (for the test at scale 1:15). This data is merged, which contains information from sixty drops per concept. The horizontal displacement during the fall was observed from two points of view. The first point of view is from above, which gives insight into the locations of the concepts directly after the fall in the x-z plane. The second point of view is from the side, which provides insight into the movement of the concepts during the fall in the x-y plane.

### 6.1.1. Locations of the concepts after the fall (x-z plane)

The locations after the fall tests per concept are presented in graphs in Section F.1.2 on scale. These graphs are converted to one graph at 'real' scale 1:1 per concept, to compare the results for different depths with each other. In Figure 6.1(a), the converted graph on scale 1:1 is presented for the Reference block. For the other concepts the graphs are presented in Section F.5.1. The averaged distance of all the fall locations from the centre (0,0) per concept is determined and is presented in Figure 6.1(b). The histogram is sorted from smallest to largest distance (based on the fall test performed at scale 1:15). It is seen, that for all concepts the horizontal displacement is larger at a depth of 13 meters than at a depth of 7 meters, which was expected.

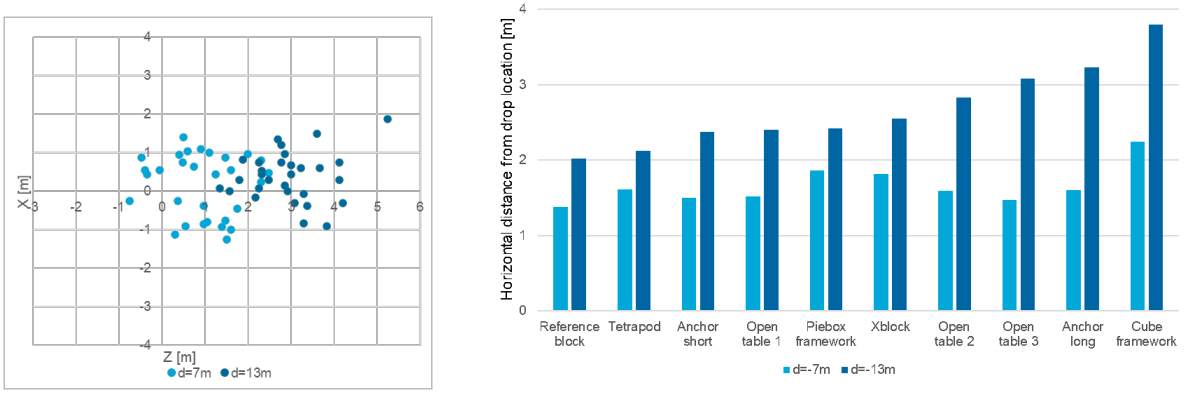


(a) Reference block

(b) All concepts

**Figure 6.1:** (a) The locations after the fall test for the Reference block, converted to scale 1:1. (b) Histogram with averaged distances from (0,0) per concept per test, sorted from small to large distance (based on the test performed at scale 1:15).

The averaged distances are defined based on the x and z location. For all concepts, the x values (absolute) of the locations are larger than the z values (absolute). This was expected as the flow and waves are generated in x direction, which enhances the movement in this direction. The horizontal displacement in the x direction is therefore assumed to be dominant in defining the maximum horizontal displacement during the fall per concept.

### 6.1.2. Movement of the concepts during the fall (x-y plane)

In Figure 5.3, the tracked positions during the drops of the Reference block are presented on scale 1:10 and 1:15. These two graphs are converted to scale 1:1 and merged into one graph per concept. In Figure 6.2, the merged graph for the Reference block at scale 1:1 is presented. The merged graphs for the other concepts are presented in Section F.5.2. The horizontal displacement during the fall of the Reference block is presented until a depth of 13 meters, because the tests were conducted until this (scaled) depth.

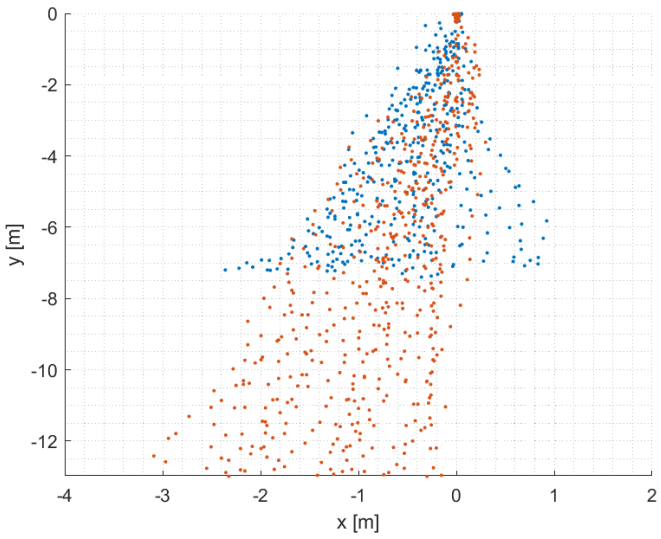


**Figure 6.2:** Reference block horizontal displacement in x-y plane (N=60), converted to 'real' scale 1:1, presented until a depth of 13 meters

At offshore wind farms in the North Sea, the average depth is approximately 30 meters (see Table 2.3). The horizontal displacement of the concepts until a depth of 30 meters is required, to assess whether

the concepts comply with the positioning design requirement. To predict the horizontal displacement at a depth of 30 meters, the data needs to be extrapolated. Extrapolation is a method of using existing trends to make statistical forecasts to find new data points, which are outside the range of the known data points. Extrapolation assumes that recent and historical trends will continue, in the future [Glantz and Mun, 2011]. Outlier drops were disregarded for the extrapolation. Two extrapolation methods are investigated; linear and second order polynomial.

**Linear extrapolation**
To predict the horizontal displacement at a depth of 30 meters, the data points are linearly extrapolated. Linear extrapolation needs a minimum of two data points to form a line, to find a new data point. This is a very simple extrapolation method. Linear extrapolation is used to define the maximum horizontal displacement during the fall, starting from the drop location. The extrapolation is also used to define the expected landing location of the concepts after the fall. The results of the linear extrapolation per concept are presented in Figure F.33. For the Reference block, it is presented in Figure 6.3.

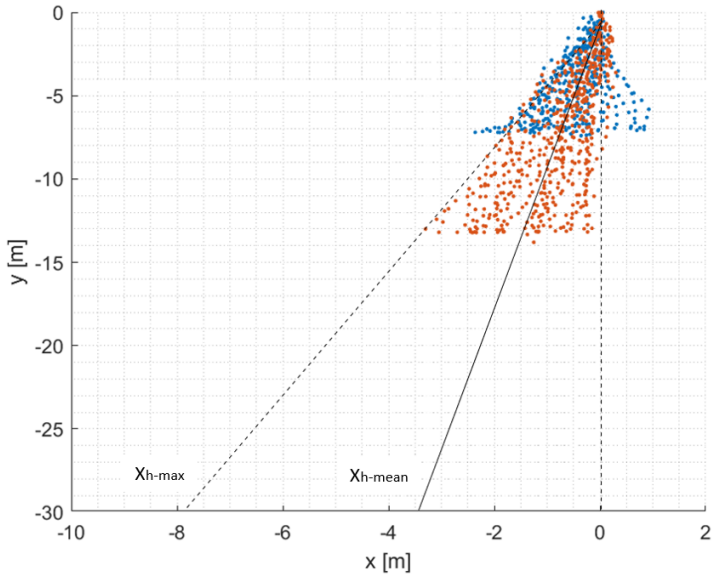


**Figure 6.3:** Linear extrapolating tracking points of Reference block during fall, to obtain horizontal displacement after fall. $x_{h-mean}$ indicates the most likely location after the fall and the corresponding displacement from the drop location of the concept after the fall and $x_{h-max}$ is the maximum horizontal displacement encountered during the fall per concept.

**Second order polynomial extrapolation**
The second order polynomial method creates a line with the coefficients for a polynomial $p(x)$ of degree n that is the best fit for the data. The length of p is $n + 1$ [pol, 2022]. The second order polynomial method is therefore based on three data points. The curve has to start at (0,0), because this is the drop location for the concepts, therefore a zero-intercept is used and is this the first data point, for both the mean and the maximal displacement prediction. The second and third data points are visually determined, neglecting outliers.

The second order polynomial extrapolation method is used to define the maximum horizontal displacement during the fall, starting from the drop location (0,0). The extrapolation is also used to define the expected landing location of the concepts after the fall, which provides the mean horizontal displacement during the fall. For the Reference block, the extrapolation is presented in Figure 6.4(b). For the other concepts, the extrapolation is presented in Section F.5.2.

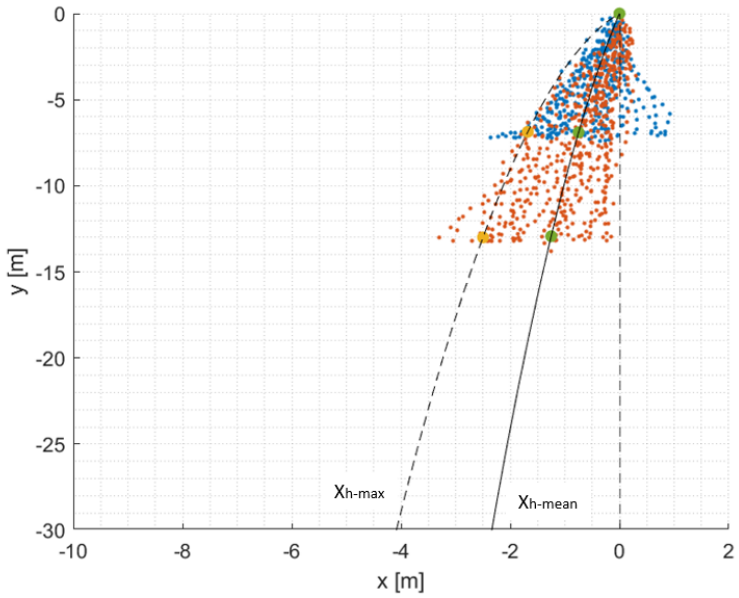


**Figure 6.4:** Second order polynomial extrapolating tracking points of Reference block during fall, to obtain horizontal displacement after fall. $x_{h-mean}$ indicates the most likely location after the fall and the corresponding displacement from the drop location of the concept after the fall and $x_{h-max}$ the maximum horizontal displacement encountered during the fall per concept.

When the concepts are dropped in the water column, many (hydraulic) aspects, affect the movement of the concepts during fall, which influences the horizontal displacement. Three hydraulic factors are considered, the tidal current, the orbital motion velocity created by the waves and the turbulence.

The velocity profile of tide waves, the current velocity ($u_c$), follows a logarithmic profile. The largest velocities are found at the water surface and near the bottom the current velocities decrease rapidly. The general vertical velocity distribution of the current velocity is presented in Figure 6.5a [Schiereck, 2003].

Underneath the wave surface, there is a fluid motion associated with the motion of the water surface. The fluid particles describe an orbital path, which is called the orbital motion. According to the linear wave theory, the horizontal orbital velocity generated by the waves, varies harmonically with an amplitude $\hat{u}$ (see Equation 3.1). The flow velocity is in the direction of the propagating wave. Using approximations for kh values (kh «1, kh ≈ 1, kh » 1), the horizontal velocity profiles over the depth can be drawn schematically for shallow, transitional and deep water [Bosboom and Stive, 2022]. The considered offshore wind farms in this research are located in transitional waters (kh ≈ 1) in the Dutch North Sea. The vertical velocity distribution of the maximum velocity amplitude generated by the orbital motion of the waves in transitional waters is presented in Figure 6.5b [Bosboom and Stive, 2022].

The linear wave theory (and other wave theories) are valid from the water surface until a small distance above the bottom. Closer to the bottom, a turbulent boundary layer is present, because of the presence of a rough bottom. The flow velocity in the boundary layer is larger than the free stream velocity (according to the linear wave theory). The thickness of the boundary layer ($\delta$) is generally between 1 cm and 10 cm for wind-generated waves (T < 10 s), which is very small. This is because, there is no sufficient time for the layer to grow out in the vertical direction, because the current regularly reverses [Bosboom and Stive, 2022]. As the thickness of this layer is so small, it is assumed that this velocity profile does not have a significant effect on the total horizontal displacement of the concept during the fall (d=30m).

The current velocity profile and the orbital motion velocity profile are considered for the horizontal displacement of the concepts during the fall. These velocity profiles are combined by linear summation to obtain a combined maximum velocity profile. This is a simplification, as in reality the average current mainly adapts to the waves, see Figure 6.5c. The orbital motion induced by the waves is circular, so the velocity profile can be induced to two sides. To obtain a safe result, the maximum velocity profile is considered and it is therefore assumed that the velocity profiles for the waves and the current are

towards the same direction. This velocity profile indicates the maximum movement of an object in the water column. This movement profile (x,y) is shown in Figure 6.5(d).

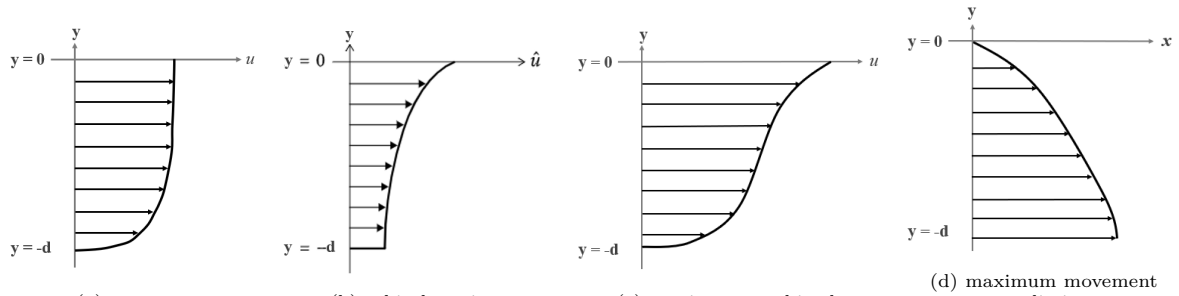


(a) current (b) orbital motion (c) maximum combined (d) maximum movement prediction

**Figure 6.5:** Velocity profiles over depth induces by (a) current [Schiereck, 2003], (b) orbital motion and (c) current and orbital motion combined (in the same direction) [Bosboom and Stive, 2022]. Movement profile over depth based on combined velocity profile (d).

Based on this movement pattern, the second order polynomial extrapolation method is selected as the best fit due to its correspondence to the defined movement pattern. This method is therefore assumed to be more accurate for a prediction of the concept movement in the water column than the (simpler) linear extrapolation method.

The mean and maximum horizontal displacement at a depth of 30 meters obtained using the second order extrapolation are presented in Table 6.1. In Figure 6.6, the results from Table 6.1 are presented in a histogram. The orange lines indicate the values for the positioning accuracy requirement with a maximum horizontal displacement of the concept after the fall, with values 4 and 5.5 meters.

The maximum horizontal displacement for the Reference block, Tetrapod, Open table 1, Piebox framework do not exceed the 4 and 5.5 meter lines. The Open table 2, Anchor short and Xblock, just slightly exceed the 5.5 meter value. For the mean horizontal displacement obtained, all concepts comply with the design criteria.

**Table 6.1:** The mean and maximum horizontal displacement at a depth of 30 meters, obtained using second order polynomial extrapolation.

| **Concept** | $x_{h-max}$ [m] | $x_{h-mean}$ [m] |
|---|---|---|
| Reference block | 4.1 | 2.4 |
| Xblock | 5.75 | 3.1 |
| Tetrapod | 4.9 | 2.9 |
| Cube framework | 7.5 | 4.75 |
| Piebox framework | 5.25 | 3.85 |
| Anchor long | 7.55 | 4.6 |
| Anchor short | 5.7 | 4.1 |
| Open table 1 | 5.2 | 3.8 |
| Open table 2 | 5.6 | 4.65 |
| Open table 3 | 6.4 | 4.45 |

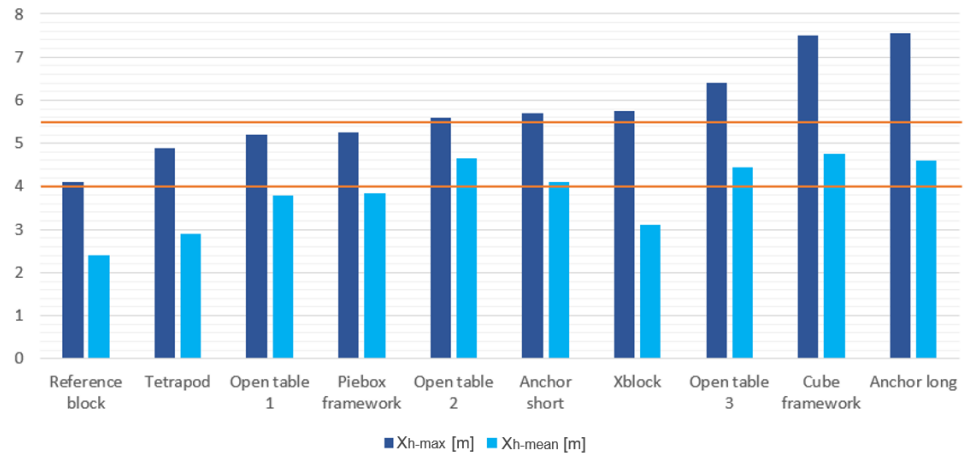


**Figure 6.6:** Horizontal displacement results obtained using second order polynomial extrapolating. The orange lines indicate the values for positioning accuracy.

## 6.2. Land test

In the land test, the landing of the concept is investigated and the amount of sides hit is counted. In Chapter 2, it is stressed that the oysters need to be protected from being damaged during the deployment.

### 6.2.1. Surface of concepts hit during landing

The amount of sides that are hit during the landing in the land test are presented in Table 5.1. The values in this table are converted to a percentage of surface hit per concept ($A_{hit}$). This is based on the surface, a side of the concept represents. The surface of each side for each concept is different and therefore needs to be defined per concept. For example, if for the Reference block (solid cube), only one side is hit during the landing, 1/6 of the surface is touched during the landing, which equals 0.167 percent of the total outside surface of the Reference block. The definition of 'one side' for the Reference block is straightforward, however the shapes of the other concepts are more complex and the definition of 'one side' is not as outspoken. In Figure 6.7, the definitions of the minimal surface touched when 'one side' and 'two sides' are hit, are clarified for each concept. The concept sides of frameworks, Anchors and Open tables are defined the same. The surfaces marked with a red line, indicate the first side that gets hit by the bottom. The surfaces marked with a yellow line, indicate the second side that gets hit by the bottom. Open table 1 and 2 always hit two sides, as they always fall on their slender side first and thereafter roll over to their wider side. For Open table 3 it is also possible to fall on the wide side directly. For the Open table concepts the 'legs' are fully hit, as the scour protection has an irregular subsurface and therefore it is expected that they will nestle between the stones.

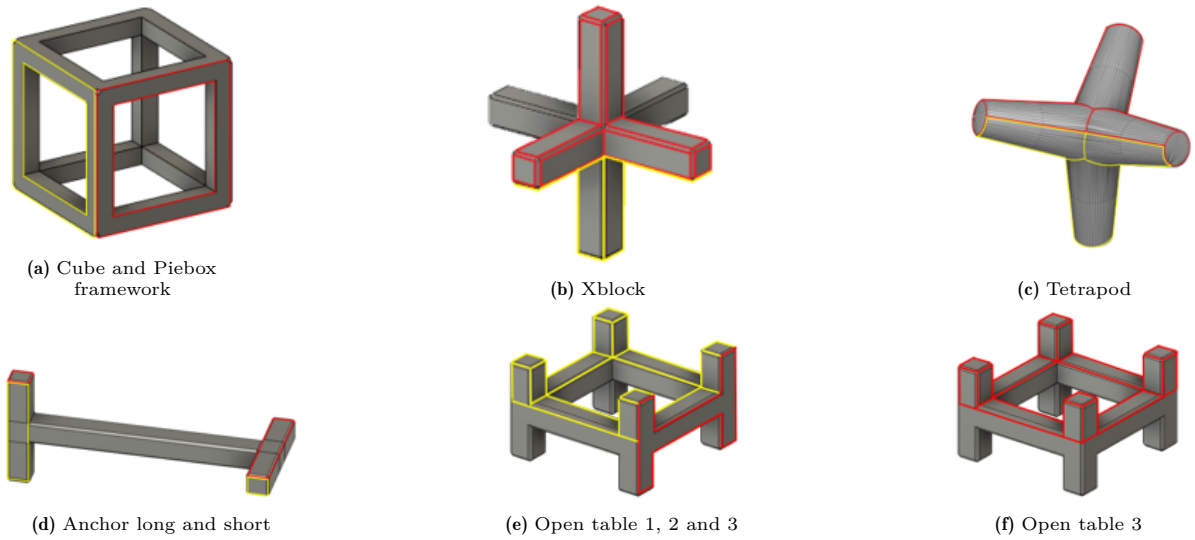

**(a)** Cube and Piebox framework

**(b)** Xblock

**(c)** Tetrapod

**(d)** Anchor long and short

**(e)** Open table 1, 2 and 3

**(f)** Open table 3

**Figure 6.7:** Surface hit during landing on one side (red) or two sides (yellow) per concept

The sides hit, defined in Table 5.1, are converted to surface hit as a percentage of the total outside surface ($A_{hit}$), using the definitions from Figure 6.7. The results are presented in Table F.18. The values per test per concept are averaged per concept and presented in a histogram, sorted from smallest to largest value, see Figure 6.8. From the histogram, it is observed that the Open table concepts get hit the most during the landing. The Framework and Anchor concepts get hit the least during the landing.

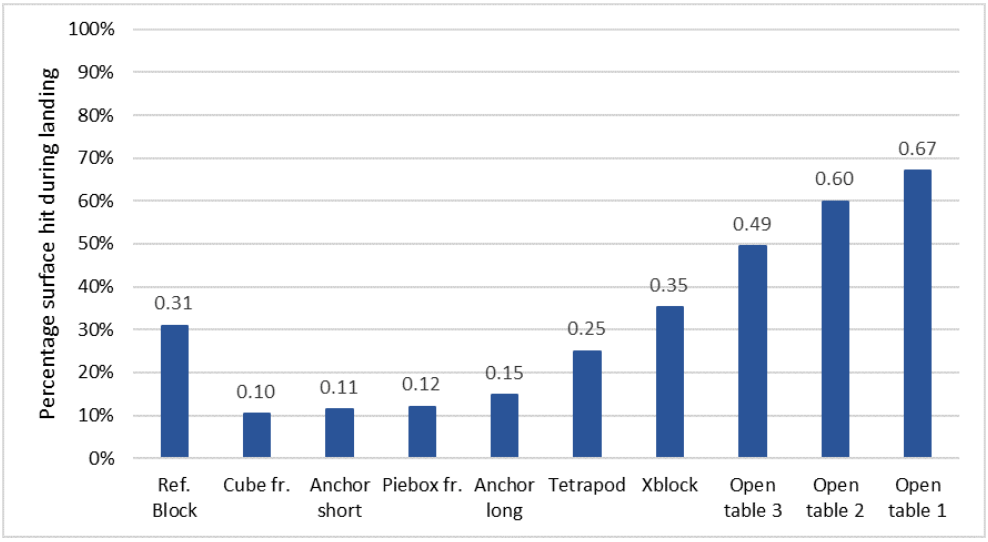


**Figure 6.8:** Averaged surface hit during landing per concept during landing test, given in percentage from total surface

## 6.2.2. Oyster attachment to concepts

The indication about surface hit during the landing, can be used to define on which sides of the concepts the oyster will be attached to. Protected areas are desired, because this will minimise oyster loss. When a large part of the concept is likely to get hit (based on Figure 6.8), a smaller part of the surface of the concept is left to attach the oysters to. This results in more concepts required for the same amount of oysters. The surface to which the oysters are assumed to be attached to, is elaborated per concept. This assumption is subjectively selected and could differ when applied in reality. For the Reference block, all available surface is used to attach oysters. For the Xblock, Tetrapod, Anchor long and Anchor short only the bottom of the end of the legs is not used to attach oysters, the rest of the surface is used to attach oysters. For the Cube framework and Piebox framework, only the inside is used to attach oysters. For the Open tables, the bottom at the end of the legs is not used and the outside surface of

the concept is not used. In Figure 6.9, the oyster attach sides are displayed. The orange sides indicate the sides to which the oysters are attached.

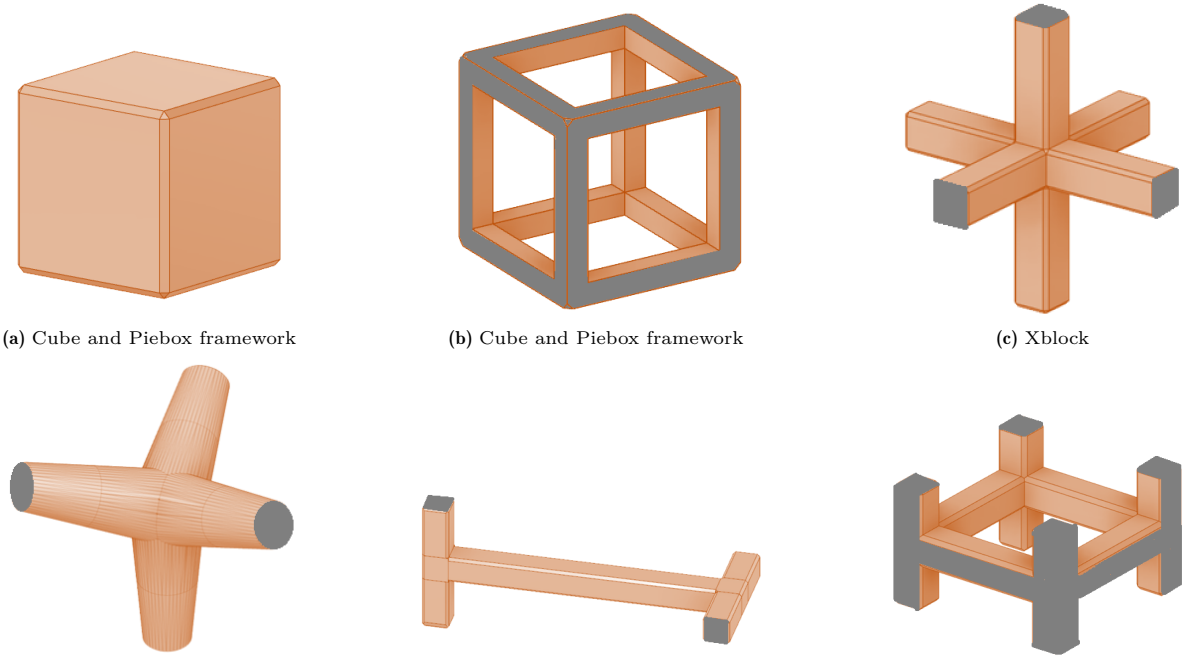

**(a)** Cube and Piebox framework **(b)** Cube and Piebox framework **(c)** Xblock

**(d)** Tetrapod **(e)** Anchor long and short **(f)** Open table 1, 2 and 3

**Figure 6.9:** Surface on which oysters are attached to, presented in orange

### 6.2.3. Amount of oysters and concepts required

Based on the surface per concept to which the oysters will be attached is determined subjectively in Section 6.2.2 and the surface an oyster will occupy ($r_{oyster} = 60mm$), the amount of oysters that can be attached to one concept is defined, see Table 6.2, column 2. The amount of oysters lost during the fall can be identified based on the surface hit, presented in Table F.18 and the surface to which the oysters are attached to, presented in Figure 6.9, see Table 6.2, column 3. This results in a total amount of intact oysters per structure after the landing, by multiplying the amount of oysters attached by one minus the percentage of oysters lost, see Table 6.2, column 4. In Section 2.1.2, the amount of oysters placed on one scour protection for restoration is defined to be 500. The amount of structures at one scour protection needed to reach this number of oysters is defined, by dividing 500 by the amount of intact oysters, see Table 6.2 column 5. This relates to the design criteria; installation and transportation, because fewer structures make these aspects easier. Three concepts only require up to 10 structures for one scour protection; Cube framework, Anchor long and Anchor short. Five concepts require 11 to 20 structures per scour protection; Reference block, Xblock, Piebox framework and Open table 3. The Open table 1 and Tetrapod require 27 and 37 structures subsequently, for one scour protection.

**Table 6.2:** Amount of oysters attached to the available surface, percentage of oysters lost during the landing, amount of intact oysters after the landing and amount of structures per scour protection, given per concept.

| | Oysters attached | Percentage lost | Intact oysters | Structures |
|---|---|---|---|---|
| Reference block | 39 | 0.31 | 27 | 19 |
| Xblock | 51 | 0.35 | 33 | 15 |
| Tetrapod | 18 | 0.25 | 14 | 37 |
| Cube framework | 70 | 0.00 | 70 | 7 |
| Piebox framework | 33 | 0.00 | 33 | 15 |
| Anchor long | 57 | 0.15 | 49 | 10 |
| Anchor short | 57 | 0.11 | 51 | 10 |
| Open table 1 | 37 | 0.50 | 18 | 27 |
| Open table 2 | 50 | 0.50 | 25 | 20 |
| Open table 3 | 70 | 0.50 | 35 | 14 |

The land test addresses three design criteria, which were defined in Section 2.3.1; protection, installation and manufacturing. The protection criterion can be assessed subjectively by the percentage of oysters lost (see Table 6.2, column 3), because this identifies the amount of oysters that get damaged during landing based on the assumed amount of oysters attached to structures. The protection criterion is also assessed objectively by the percentage surface hit, shown in Figure 6.8. These results are objective, because they are directly based on test results.

The installation and manufacturing can be approached by the amount of structures required for one scour protection (see Table 6.2, column 5), because fewer required structures result in easier transportation and installation. These results are based on subjective assumptions.

# 6.3. Stability test

The brood stock structures must be able to resist at least the storms with a return period of 10 years, as they are very likely to occur within 30 years. The stability tests provided insight into the thresholds of motion per test storm conditions.

## 6.3.1. Output hydraulic conditions interpretation

In Table 5.3, it is seen that the output conditions in the wave flume did not fully correspond to the defined input conditions. The significant wave height generated was consistently lower than the input. To relate the test results to the storm events, in reality, the output conditions generated in the wave flume are interpreted. The generated flow velocity is converted directly using Froude scaling, to obtain the current velocity near the bottom ($u_{c-1.5m}$). The wave conditions are related to the reality based on the induced orbital motion near the bottom. The orbital motion velocity, generated by the waves in the wave flume is based on the significant wave height ($H_s$) and peak wave period ($T_p$) generated in the flume. This induced orbital motion velocity is converted to reality using Froude, to obtain the orbital motion velocity induced by the waves near the bottom ($u_{w-1.5m}$). The converted hydraulic conditions are presented in Table 6.3, together with a brief elaboration on which storm events these conditions represent. Further elaboration about the generated hydraulic conditions translated to reality is provided in Section F.7.1.

**Table 6.3:** Output of hydraulic storm conditions (SC) generated in the wave flume, converted to depth-averaged current velocity and orbital motion velocity induced by the waves 1.5 meters above the seabed, it corresponds to in reality and to which storm conditions per offshore wind farm (OWF) it relates.

| **Test** | Parameter | Value [m/s] | Corresponds to storm event ; |
|---|---|---|---|
| Stability SC 1 | $u_{c-1.5m}$ | 0.57 | 5 year RP for Gemini OWF |
| | $u_{w-1.5m}$ | 1.12 | 10 year RP for Borssele OWF |
| Stability SC 2 | $u_{c-1.5m}$ | 0.62 | 10 year RP for average 3 OWF |
| | $u_{w-1.5m}$ | 1.46 | 10 year RP for HKW OWF |
| Stability SC 3 | $u_{c-1.5m}$ | 0.62 | 10 year RP for average 3 OWF |
| | $u_{w-1.5m}$ | 1.44 | 50 year RP for Borssele OWF |
| Stability SC 4 | $u_{c-1.5m}$ | 0.66 | 50 year RP for average 3 OWF |
| | $u_{w-1.5m}$ | 2.30 | 50 year RP for Gemini OWF |
| Stability SC 5 | $u_{c-1.5m}$ | 0.66 | 50 year RP for average 3 OWF |
| | $u_{w-1.5m}$ | 2.69 | >50 year RP for 3 OWF |

The wave generator in the wave flume reached its maximum capacity during generating storm conditions combination 3. To still be able to test the concepts in heavier wave conditions, it was decided to decrease the density of the concepts [Shields, 1936]. If the concepts have a smaller density, the same (or less extreme) hydraulic conditions, exert a relatively greater force on the concepts, see Equation 4.3. The new prototypes had a density of 1170 $kg/m^3$ (the prototypes that were previously tested had a density of 2440 $kg/m^3$).

This significant weight difference in the prototypes, resulted in a relatively large increase in hydraulic conditions between storm condition combination 3 and 4 for the concepts, see Table 6.3 $u_{w-1.5m}$ values. Storm condition combination 3 represented conditions just below a storm event with a return period of 10 years. The storm condition combination 4, represented conditions that exceeded a storm event with a return period of 50 years.

### 6.3.2. Thresholds of motion of concepts

In Table 6.4, the near bed orbital motion velocities ($u_{w-1.5m}$) range induced by the waves at which the concepts start to move based on the test results are presented. In Figure 6.10, the thresholds of motion are displayed. The dashed lines indicate the orbital motion velocity corresponding to the conditions for an averaged storm event with a return period of 10 and 50 years, representing a near bed orbital motion velocity of 1.56 and 1.82 m/s subsequently. It is seen that the concepts, Anchor short, Open table 1, Xblock, Piebox framework, Cube framework and Reference block, do not remain stable during conditions that corresponds to averaged storm event with a return period of 10 years. The concepts, Open table 2 and 3, Tetrapod and Anchor long, remain stable during conditions that corresponds to averaged storm event with a return period of 10 years. The Open table 2 and 3 also remain stable during conditions that corresponds to an averaged storm event with a return period of 50 years. See Table 6.4 for the results, expressed in the near bed orbital motion velocity conditions for which the concepts became unstable.

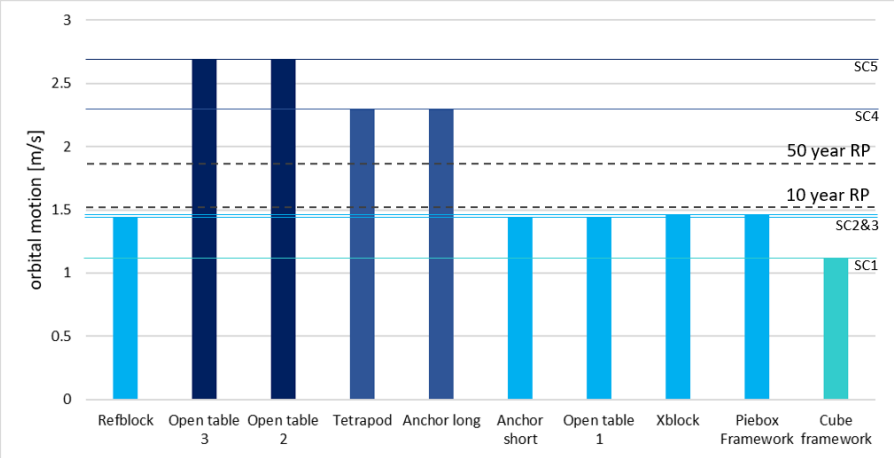


**Figure 6.10:** Orbital motion velocity induced by the waves in the wave flume converted to reality near bed orbital motion velocity induced by the waves with a 13 percent exceeding change, for which the concepts fail to remain stable during stability test. Sorted from most to least stable. Including the orbital motion velocities corresponding to the storm conditions averaged over the three considered offshore wind farms for a return period of 10 and 50 years, shown with dashed lines. Including the tested storm conditions (SC) indicated with lines

The Tetrapod and Anchor long became unstable during storm condition combination 4, which indicates a large range for the defined threshold of motion, namely somewhere between storm conditions combination 3 and 4. It can not be said with certainty that the concepts remains stable for a storm event with a return period of 50 years, but it can be said with certainty that they remain stable during a storm event with a return period of 10 years (see Figure 6.10). The Open table 2 and 3, do remain stable during a storm event with a return period of 50 years, because they remain stable during storm conditions combination 4. The Open table 2 and 3 are therefore assessed most suitable based on the stability criterion.

**Table 6.4:** The conditions range in which the concepts start to move, expressed in $u_{w-1.5m}$.

| | $u_{w-1.5m}$ range $[m/s]$ |
|---|---|
| Reference block | 1.12-1.44 |
| Xblock | 1.44-1.46 |
| Tetrapod | 1.46-2.30 |
| Cube framework | 0.57-1.12 |
| Piebox Framework | 1.44-1.46 |
| Anchor long | 1.46-2.30 |
| Anchor short | 1.12-1.44 |
| Open table 1 | 1.12-1.44 |
| Open table 2 | 2.30-2.69 |
| Open table 3 | 2.30-2.69 |

# 7

# Comparison of physical model results and behavioural predictions

The results obtained in the physical model tests are used to determine the accuracy of the results obtained in Chapter 3 by the behavioural prediction calculations. The physical model results are used to improve the behavioural predictions of the concepts made with calculations to make more accurate predictions in the future without the need for physical modelling.

## 7.1. Comparison of results

The results obtained with both methods are compared to each other, for the three relevant situations.

### 7.1.1. Fall situation

The horizontal displacement ($x_h$) during the fall obtained using calculations and the maximum and mean horizontal displacement ($x_{h-max}$, $x_{h-mean}$) obtained in physical modelling per concept are presented in Table 7.1. The results are in the same order of magnitude. The Anchor long is undervalued in the calculations compared to the physical model, which could be due to an undervalued drag coefficient estimation. The other concepts show similar results. The calculation results especially comply with the mean horizontal displacement predictions ($x_{h-mean}$) obtained using physical modelling. The horizontal displacement predictions ($x_h$) obtained using calculations are therefore an adequate initial assessment.

**Table 7.1:** Horizontal displacement ($x_h$) results obtained with calculations (Calc.) and physical model (PM), given in meters

| **Concept** | **Calc.** | **PM** | |
|---|---|---|---|
| | $x_h$ [m] | $x_{h-mean}$ [m] | $x_{h-max}$ [m] |
| Reference block | 4.3 | 2.4 | 4.1 |
| Xblock | 4.6 | 3.1 | 5.8 |
| Tetrapod | 3.7 | 2.9 | 4.9 |
| Cube framework | 4.4 | 4.8 | 7.5 |
| Piebox framework | 3.9 | 3.9 | 5.3 |
| Anchor long | 4.3 | 4.6 | 7.6 |
| Anchor short | 4.3 | 4.1 | 5.7 |
| Open table 1 | 5.5 | 3.8 | 5.2 |
| Open table 2 | 4.9 | 4.7 | 5.6 |
| Open table 3 | 4.4 | 4.5 | 6.4 |

## 7.1.2. Land situation

The results obtained using the calculations and the physical model are presented in Table 7.2. The results are in the same order of magnitude and therefore provide an adequate first estimation. However, the results obtained using the calculations are frequently lower than the physical model results. This is because only one side hit per concept is assumed for the calculation and during physical modelling, some concepts showed to hit multiple sides during the landing. Especially, the amount of structure defined for the Tetrapod is significantly less obtained with the calculations. This is because, different assumptions have been made about the oyster attachment surfaces.

**Table 7.2:** Behavioural prediction results for the land situation based on calculations obtained in Chapter 3 and physical modelling (Section F.7.1), including the surface hit per concept provided in the percentage of the total surface, $A_{hit}$ and the amount of structures needed at one scour protection per concept.

| **Concept** | **Calc.** | | **PM** | |
|---|---|---|---|---|
| | $A_{hit}$ [%] | Amount of structures [-] | $A_{hit}$ [%] | Amount of structures [-] |
| Reference block | 0.17 | 18 | 0.31 | 19 |
| Xblock | 0.20 | 12 | 0.35 | 15 |
| Tetrapod | 0.33 | 17 | 0.25 | 37 |
| Cube framework | 0.17 | 13 | 0.10 | 7 |
| Piebox framework | 0.20 | 16 | 0.12 | 15 |
| Anchor long | 0.13 | 22 | 0.15 | 10 |
| Anchor short | 0.13 | 14 | 0.11 | 10 |
| Open Table 1 | 0.40 | 21 | 0.67 | 27 |
| Open Table 2 | 0.40 | 15 | 0.60 | 20 |
| Open Table 3 | 0.40 | 15 | 0.49 | 14 |

## 7.1.3. Stability situation

In the stability calculations performed in Chapter 3, the results provided by the moment equilibrium method were dominant, over the horizontal and vertical force equilibria. In this comparison, only the moment equilibria are considered.

To compare the stability results obtained using both methods, the near-bed orbital motion velocity ($u_{w-1.5m}$) for which the moment equilibria ($\sum M$) is exactly equal to 0 Nm and therefore becomes unstable is determined for each concept. These values can be compared to the near-bed orbital motion velocity range ($u_{w-1.5m}$) for which the concepts became unstable during physical modelling. The results are presented in Table 7.3. The third column provides a sign ($<$,$>$,$=$,$\approx$). This sign indicates whether the calculated $u_{w-1.5m}$ value (column 1) is smaller ($<$), larger ($>$), in between ($=$) or almost in between ($\approx$), the $u_{w-1.5m}$ range for which the concepts became unstable during physical modelling (provided in column 2).

The physical model tests for the Reference block were stopped early due to time constraints and therefore do not give accurate results. The results for the Reference block are not considered for comparison.

The stability results obtained during physical modelling are compared to the results obtained by calculations. Two concept fall (approximately) within the range of the physical model results (Tetrapod and Open table 3). Two concepts have a smaller $u_{w-1.5m}$ in the calculations than the physical model range, Xblock and Open table 2. The other six concepts are overvalued and therefore provide larger $u_{w-1.5m}$ values in the calculations. These six concepts provide safe results. The results obtained by the calculations require improvements, because they differ from the physical modelling results.

**Table 7.3:** Stability situation results obtained with calculations (Calc.) provided in the near-bed orbital motion velocity ($u_{w-1.5m}$) [m/s] for which the moment equilibria ($\sum M$) is exactly equal to 0 Nm and the near-bed orbital motion velocity range ($u_{w-1.5m}$) [m/s] for which the concepts became unstable during physical modelling. Compared using signs (<,>,=,≈).

| **Concept** | **Calc.** | **PM** | **Comparison** |
|---|---|---|---|
| | $u_{w-1.5m}$ [m/s] | $u_{w-1.5m}$ range [m/s] | |
| Xblock | 1.24 | 1.44-1.46 | < |
| Tetrapod | 1.78 | 1.46-2.30 | = |
| Cube framework | 1.33 | 0.57-1.12 | > |
| Piebox framework | 2.28 | 1.44-1.46 | > |
| Anchor long | 2.79 | 1.46-2.30 | > |
| Anchor short | 2.34 | 1.12-1.44 | > |
| Open table 1 | 2.21 | 1.12-1.44 | > |
| Open table 2 | 2.22 | 2.30-2.69 | < |
| Open table 3 | 2.31 | 2.30-2.69 | = |

# 7.2. Calibration of behavioural prediction calculations

For the behavioural prediction calculation methods to be used in the future, they should provide accurate results. In Chapter 3, the method and input parameters used for the calculations are defined, based on literature study and estimations. In the physical model, some of these input parameters are addressed. The physical model results can therefore be used to improve the calculation accuracy. The adjusted calculation results are compared to the physical model results to obtain insight into whether these changes provide more accurate results.

In the concept observation test results (see Appendix D), the equilibrium fall velocity ($w$) and the drag coefficient ($C_D$) for each concept are determined. These parameters are adjusted from the previously estimated values in Chapter 3 used in the calculations.

## 7.2.1. Fall situation

For the calculations to determine the horizontal displacement defined in the (original) calculation method, the orbital motion induced by the waves was not incorporated, because it was assumed that these would lead to a net horizontal displacement of zero due to the circular motion of waves. However, Figure 6.5d presents that the orbital motion induced by waves does have an influence on the movement of the concepts during the fall.

In the calibrated calculation method, the depth-averaged orbital motion velocity induced by the (deployment condition) waves is incorporated into the depth-averaged current velocity, resulting in a depth-averaged flow velocity ($\bar{u}$) of 0.44 m/s (instead of 0.3 m/s). Using this depth-averaged flow velocity ($\bar{u}$) provides insights that correspond to the maximum horizontal displacement, The previously used depth-averaged current velocity ($\bar{u_c}$) provided insights that correspond to the mean horizontal displacement.

This leads to three input values ($w$, $C_D$ and $\bar{u}$) which are adjusted in the calculations, resulting in new horizontal displacement predictions ($x_h$), see Table 7.4.

These new horizontal displacement predictions ($x_h$) are compared to the maximum horizontal displacement ($x_{h-max}$) obtained in the physical model (and extrapolation). It is observed in Table 7.4, that $x_{h-max}$ in the physical model, results in larger values than $x_h$, for each concept. This indicates that the calculation method provides undervalued results for the maximum horizontal displacement.

**Table 7.4:** Comparison output calibrated calculations (Calibrated calc.) with physical model parameters with output physical model (PM)

| **Concept** | **Calibrated calc.** | **PM** |
|---|---|---|
| | $x_h$ [m] | $x_{h-max}$ [m] |
| Ref. block | 3.1 | 4.1 |
| Xblock | 4.4 | 5.8 |
| Tetrapod | 3.9 | 4.9 |
| Cube framework | 5.9 | 7.5 |
| Piebox framework | 4.7 | 5.3 |
| Anchor long | 4.3 | 7.6 |
| Anchor short | 4.8 | 5.7 |
| Open table 1 | 4.2 | 5.2 |
| Open table 2 | 4.4 | 5.6 |
| Open table 3 | 4.9 | 6.4 |

### 7.2.2. Land situation

The results obtained with the calculations are based on estimations for the number of sides hit and not based on calculation methods that can be improved. Therefore the physical model results are dominant and should be considered in future applications of oyster brood stock structures.

### 7.2.3. Stability situation

For the stability calculations, two parameters are adjusted, the drag coefficient ($C_D$), obtained with the concept observation test, and the bottom friction coefficient ($\mu$). The bottom friction coefficient is assumed to be 0.6. This value is determined based on calculations performed for an oyster brood stock structure installed using a crane on the same type of scour protection [Heijningen and Mungar, 2022]. This brood stock structure is approximately 3-5 times larger than the considered droppable oyster brood stock structures in this research (depending on the concept). The bottom friction coefficient is dependent on the interaction between the substrate and the object [Elger et al., 2020]. The roughness of the substrate compared to the object is important for the definition of this coefficient. The bottom friction coefficient considered in the calculations is therefore undervalued, because the substrate is rougher relative to a smaller structure than to a larger structure. Therefore the bottom friction coefficient value should be larger, which will lead to more stable results for the horizontal force equilibrium in the behavioural prediction calculations. In the calibrated calculation model, an bottom friction coefficient ($\mu$) of 2.5 is used (approximately 4 times larger than 0.6).

To compare the results, the same method as elaborated in Section 7.1 for the stability situation is used.

It can be seen that the calculations provide more similarity than those in Section 7.1 to the physical model results. The same two concepts as in Section 7.1 provide undervalued results in the calculations, Xblock and Open table 2. The other seven concepts provide accurate results compared to the physical model results. Based on the findings, it can be said that the calibrated calculation method provides an adequate indication of the stability of the concepts.

**Table 7.5:** Stability situation results obtained with calibrated calculations (Calibrated calc.) provided in the near-bed orbital motion velocity ($u_{w-1.5m}$) [m/s] for which the moment equilibria ($\sum M$) is exactly equal to 0 Nm and the near-bed orbital motion velocity range ($u_{w-1.5m}$) [m/s] for which the concepts became unstable during physical modelling. Compared using signs (<,>,=,≈).

| **Concept** | **Calibrated calc.** | **PM** | **Comparison** |
|---|---|---|---|
| | $u_{w-1.5m}$ [m/s] | $u_{w-1.5m}$ range [m/s] | |
| Xblock | 1.14 | 1.44-1.46 | $<$ |
| Tetrapod | 1.46 | 1.46-2.30 | $=$ |
| Cube framework | 0.73 | 0.57-1.12 | $=$ |
| Piebox framework | 1.39 | 1.44-1.46 | $\approx$ |
| Anchor long | 1.75 | 1.46-2.30 | $=$ |
| Anchor short | 1.45 | 1.12-1.44 | $\approx$ |
| Open table 1 | 1.32 | 1.12-1.44 | $=$ |
| Open table 2 | 1.88 | 2.30-2.69 | $<$ |
| Open table 3 | 2.27 | 2.30-2.69 | $\approx$ |

# 8

# Final concept selection

The results obtained during the performed tests in the wave flume were analysed and fed back to the design criteria for the broodstock structure in Chapter 6. In this chapter, these results are used to select the most suited concept for application to function as a droppable oyster brood stock structure.

## 8.1. Overview results

The objective results per executed test, which are relevant to consider for the assessment are presented in Table 8.1. The maximum horizontal displacement at a depth of 30 meters during deployment conditions is presented by $x_{h-max}$. The surface hit per concept during the landing of the total surface is presented by $A_{hit}$. The range in between the conditions for which the concepts start to move is presented by $u_{w-1.5m}$ range. These results can also be used in future research, as they are directly obtained from the test results. The findings are shortly summarised per test.

The horizontal displacement during the fall in the x direction over the depth is more relevant than the horizontal displacement during the fall in the z direction, because the tests are performed using flow and waves generated in x direction. The maximum horizontal displacement considered is therefore in the x direction. The observed movement in the tests is translated to a horizontal displacement at a depth of 30 meters in reality using second order polynomial extrapolation.

These test results are used to assess the suitability of the concepts based on the positioning accuracy requirement, which defined that the maximum horizontal displacement during the fall is 5.5 meters, see Table 8.1. The Reference block, Tetrapod, Open table 1 and Piebox concepts comply with the positioning accuracy requirement. The Open table 2, Anchor short and Xblock slightly exceed this maximum value. The Open table 3, Cube framework and Anchor long show too much displacement during a fall in the water column.

The surface hit during the landing, indicates the percentage of surface hit based on the amount of sides hit. This percentage is desired to be minimal for the protection design criteria. Based on the results presented in Table 8.1, the Cube framework, Piebox framework, Anchor Short and Anchor long encounter minimal surface hit during the landing. The Tetrapod, Reference block and Xblock encounter moderate surface hit. The Open Table 1,2 and 3 encounter large surfaces hit during the landing. The amount of structures needed for each concept is also determined, by assuming a certain amount of oysters that can be attached per concept and the percentage of oyster loss, see Table 3.4. This amount is desired to be minimal, relating to the installation and transportation design criteria. The Cube framework requires the least amount of structures and the Tetrapod requires the most structures.

Considering the stability requirement, the concepts must remain stable during storm events with a return period of 10 years (averaged conditions of three considered offshore wind farms). This storm event corresponds to near-bed orbital motion velocity of 1.56 m/s. A storm event with a return period of 50 years (averaged conditions of three considered offshore wind farms) corresponds to a near-bed orbital motion velocity of 1.82 m/s. The Open table 3, Open table 2, Tetrapod and Anchor long,

comply with the design criteria that the concepts should at least remain stable during a storm event with a return period of 10 years. For the Open table 3 and Open table 2 it can be said with certainty that the concepts also remain stable for storm conditions with a return period of 50 years. For the Tetrapod and Anchor long, this cannot be said with certainty.

**Table 8.1:** The objective results per executed test. The maximum horizontal displacement at a depth of 30 meters during deployment conditions ($x_{h-max}$). The surface hit per concept during the landing of the total surface ($A_{hit}$). The range in between the conditions for which the concepts start to move $u_{w-1.5m}$ range.

| | $x_{h-max}$ $[m]$ | $A_{hit}$ $[m^2]$ | $u_{w-1.5m}$ range $[m/s]$ |
|---|---|---|---|
| Reference block | 4.10 | 0.31 | 1.12-1.44 |
| Xblock | 5.58 | 0.35 | 1.44-1.46 |
| Tetrapod | 4.90 | 0.25 | 1.46-2.30 |
| Cube framework | 7.50 | 0.10 | 0.57-1.12 |
| Piebox Framework | 5.25 | 0.12 | 1.44-1.46 |
| Anchor long | 7.55 | 0.15 | 1.46-2.30 |
| Anchor short | 5.70 | 0.11 | 1.12-1.44 |
| Open table 1 | 5.20 | 0.49 | 1.12-1.44 |
| Open table 2 | 5.60 | 0.60 | 2.30-2.69 |
| Open table 3 | 6.40 | 0.67 | 2.30-2.69 |

## 8.2. Concept selection

To obtain the most suited design, two selection methods are applied to assess the results; requirement analysis and multi-criteria analysis. To assess the suitability of the considered concepts a requirement analysis is performed. The requirement analysis only considers, the concepts that meet the set requirements. When multiple concepts comply with the set requirements, a multi-criteria analysis is performed to assess the remaining concepts on their suitability based on the design criteria (which indicate desired properties as opposed to requirements).

### 8.2.1. Requirement analysis

The design criteria 'positioning' and 'stability' identify requirements. The other design criteria indicate desired properties.

The concepts that meet the positioning accuracy requirement, namely a maximum horizontal displacement of 5.5 meters during the fall, are Reference block, Tetrapod, Open table 1 and Piebox framework. Six concepts do not comply with this requirement, namely Open table 2, Anchor short, Xblock, Open table 3, Cube framework and Anchor long.

The concepts that meet the stability requirement, namely remain at least stable during a storm event with a return period of 10 years, are Open table 3, Open table 2, Tetrapod and Anchor long. Six concepts do not comply with this requirement, namely the Reference block, Anchor short, Open table 1, Xblock, Piebox framework and Cube framework.

The only concept that complies with both requirements is the Tetrapod and therefore results in the only suited concept to act as a droppable brood stock structure. The Open table 2 concept exceeds the positioning requirement with only 0.1 meters and does meet the stability requirement. It can therefore be said that the Open table 2 can also be considered for application.

### 8.2.2. Multi-Criteria Analysis

The specific requirements which arose from the design criteria drafted in Section 2.3.1, define the suitability of the concepts for the conditions chosen for this research. In the situation that multiple concepts appeared to be suited based on the requirement analysis, a multi-criteria analysis can be used to determine which of these concepts is best suited based on the other design criteria.

A multi-criteria analysis is drawn up for the two remaining concepts, Tetrapod and Open table 2. The design criteria set in Section 2.3.1 are assessed per concept, based on the results in Chapter 2 and the results obtained with the tests in Chapter 6. The design criteria; 'positioning' and 'stability' are not assessed as it is assumed that these are met based on the requirement analysis. The design

criteria 'flow', 'space', 'predation', 'installation', 'manufacturing', 'transportation' were assessed based on literature study and understandings. The design criteria 'protection', 'installation', 'transportation' are assessed based on the land test results. The design criteria 'installation', 'transportation' are therefore assessed on their shape (literature study) and amount of structure required (land test). All the design criteria are assigned a weighting factor. These weighting factors are now considered for the preferences of this specific research. These weighting factors can change per application to select the most suited concept for each situation.

The weighting factors considered for each design criteria in this research are elaborated. For the 'flow' criteria, a weighting factor of 20 is chosen, because this criterion is critical for the oyster survival. The 'protection' criterion is also critical for oyster survival and is substantiated by test results. Therefore a weighting factor of 25 is chosen. The criteria 'space' and 'predation' are not critical for survival, but indicate preferred properties and are not substantiated with tests. For these criteria, a weighting factor of 5 is chosen. The design criteria 'installation', 'manufacturing' and 'transportation' are not critical for survival, but indicate preferred properties and are substantiated with tests. For these criteria, a weighting factor of 15 is chosen. The multi-criteria analysis is presented in Table 8.2.

**Table 8.2:** Multi-criteria analysis which assesses all remaining concepts based on set design criteria (see Section 2.3.1), with subjectively selected weighting factors.

| | Flow | Space | Predation | Manufact. | Protect. | Install. | Transport. | **Total** |
|---|---|---|---|---|---|---|---|---|
| *Weight* | *20* | *5* | *5* | *15* | *25* | *15* | *15* | ***100*** |
| Tetrapod | 5 | 1 | 3 | 5 | 2 | 2 | 1 | **2.0** |
| Piebox fr. | 3 | 3 | 3 | 3 | 5 | 4 | 4 | **3.6** |

From this multi-criteria analysis, presented in Table 8.2, the Open table 2 is more suitable than the Tetrapod to act as a droppable oyster brood stock structure.

## 8.3. Conclusion

The requirement analysis assesses that the Tetrapod is the only suited concept to act as a droppable oyster brood stock structure for the requirements set in this research, see Figure 8.1a. When looking closely into the results presented in Table 8.1, the Open table 2 concept just slightly exceeds the positioning requirement and is therefore also considered to assess with the multi-criteria analysis. The multi-criteria analysis assesses the Open table 2 to be more suited to act as a droppable brood stock structure, see Figure 8.1b.

**(a)** Tetrapod

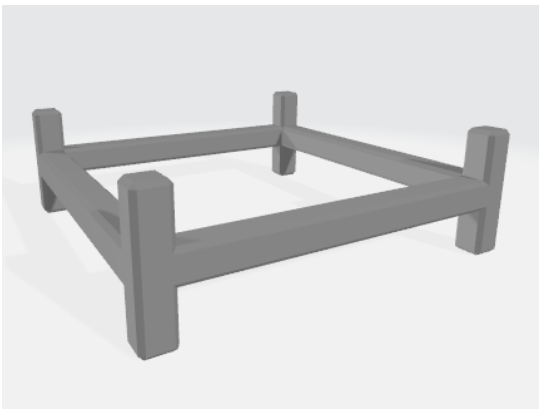

**(b)** Open table 2

**Figure 8.1:** Best-suited concepts to act as a droppable oyster brood stock structure, based on results in this research

The selection methods are based on the specific criteria and conditions that are applied in this research. When a droppable brood stock structure is implemented in the future, the specific preferences and conditions for this specific purpose should be fed back to the concept selection process to apply the most suited concept for this situation.

# 9

# Discussion

In the discussion, the validity of the results is argued and limitations are discussed. Expectations are linked to the results, to find new insights and draw (new) conclusions from them. Finally, possible implications of the study are also elaborated.

## 9.1. Design of basic concepts

The design of the concepts is based on the set design criteria, which define desired properties for the concepts. These design criteria have led to two design specifications of the structure, the material used is fibre-reinforced concrete ($\rho = 2500kg/m^3$) and the maximum weight is 50 kg. The design criteria have also led to two requirements regarding the behaviour of the concepts, the maximum positioning accuracy during deployment is equal to 5.5 metres and the structure should remain stable during a storm event with a return period of 10 years.

Twelve basic concepts were drawn up by performing literature studies on existing subsea structures (armour units, reef enhancement structures) and consultations with ecological and hydraulic experts. A multi-criteria analysis is set up which selects the most suited concepts, based on the set design criteria. The design criteria 'stability' and 'positioning' could not be properly assessed at this stage of the research and were therefore not taken into account in the multi-criteria analysis. The Reference block, Xblock, Tetrapod, Cube framework, Anchor and Open table were selected.

The Xblock and Tetrapod concepts are already widely applied as coastal protection elements. The Cube framework has already been applied for use in coral reef restoration projects by organisations such as 'Coral Reef Care' [Voorhuis, 2021]. The Anchor and Open table concept originated from existing breakwater elements but are simplified to better suit the purpose of this research [CETME, 2007]. The basic principle of the selected concepts are thus already being applied as subsea structures, but are now adjusted to serve as (droppable) oyster brood stock structures.

The multi-criteria analysis drawn up to select the basic concepts and the final concept design, uses the weighing objective method. This includes assigning a weighting factor to each design criterion based on its given importance. The weighting factors are based on aspects considered most important for the application of the concepts, to ensure that the specific preferences of an application are properly represented in the concept design. The weighting factors can therefore be adjusted per application to properly account for these preferences. This is therefore a subjective method as the weighting factors have been instinctively determined based on the preferences of this study.

The selection of the concepts is based on the order of the total scores. The total scores obtained from the multi-criteria analyses have little differences between the values. The weighting factors therefore have a large influence, because little change in total scores results in the order of the total scores to change. They could therefore affect the results of the multi-criteria analysis greatly, which can lead to a different concept selection.

In this research, the maximum weight requirement was dominant and led to a large influence on the design of the structure. This weight restriction (< 50 kg) resulted from a combination of the design criteria (stability, easy installation). Stability increases with increasing weight, maximum weight is therefore desired. Easy installation is defined for the structure to be dropped manually, which results in a maximum weight of 50 kg by the Dutch labour law. If these criteria would deviate from other application situations, this could result in fewer restrictions regarding this weight. These weighting factors in the multi-criteria analysis should therefore be considered and adjusted based on the specific preferences of the initiative when a droppable oyster brood stock structure is applied in to select the best-suited concepts for the specific situation.

## 9.2. Definition of concept parameters by behavioural prediction calculations

Behavioural predictions during relevant situations are made for the concepts, to identify the most suited parameters for the basic concepts. The predictions are made based on defined relevant forces that act upon the concept during these situations. For the stability situation, the moment equilibrium method was dominant in the selection of the concept parameters to obtain safe concepts. The hydraulic conditions used for the stability situation are extreme. The hydraulic wave loads occurring at Gemini are the most extreme and are therefore considered normative in the calculations, to obtain safe results. These extreme conditions were used instead of the averaged conditions that are used in physical modelling.

An iterative process with testing alternative concept parameters resulted in ten suited concepts, Reference block, Xblock, Tetrapod, Cube framework, Piebox framework, Anchor long, Anchor short, Open table 1, Open table 2 and Open table 3.

When the force equilibria result in positive values, the concepts are defined as stable. Noticeable results are obtained for the horizontal force equilibria. All values were found to be negative for the tested concepts. A negative horizontal force equilibrium suggests sliding behaviour occurs. However, the rough substrate (scour protection) indicates that sliding can hardly occur. The negative values for the horizontal equilibrium force may have been the result of an undervalued bottom friction coefficient. The coefficient is assumed to be 0.6. This value is determined based on calculations performed for an oyster brood stock structure installed using a crane on the same type of scour protection [Heijningen and Mungar, 2022]. This brood stock structure is approximately 3-5 times larger than the considered droppable oyster brood stock structures in this research. The bottom friction coefficient is dependent on the interaction between the substrate and the object [Elger et al., 2020]. The roughness of the substrate compared to the object is important for the definition of this coefficient. The bottom friction coefficient considered in the calculations is therefore undervalued, because the substrate is rougher relative to a smaller structure than to a larger structure. Therefore the bottom friction coefficient value should be larger, which will lead to more stable results for the horizontal force equilibrium in the behavioural prediction calculations.

## 9.3. Environmental conditions

Three offshore wind farm locations were selected to represent the environmental conditions; Hollandse Kust West (HKW) (not yet constructed), Borssele and Gemini. The storm and scour protection conditions for the three locations are averaged, to obtain representative conditions for the Dutch North Sea.

The fall situation is assessed based on the maximum positioning accuracy which is based on the scour protection conditions. The scour protection dimensions are significantly greater at HKW than the dimensions at Gemini and Borssele. By taking the average dimensions of these three locations as normative for the design of the structure, the design of the concepts is under-dimensioned for HKW and over-dimensioned for the Gemini and Borssele sites, for the positioning requirement.

The positioning accuracy for each site based on the scour protection data (from Table 2.4) and the percentage deviation from the averaged value is presented in Table 9.1. The percentage deviation is significant for each considered site, especially for Gemini, which deviates more than 50 %.

**Table 9.1:** Positioning accuracy per site and percentage deviation from average defined maximum positioning accuracy of 5.5 meters, which is used in the report.

| | Positioning accuracy [m] | Deviation[%] |
|---|---|---|
| HKW | 7.7 | +29 |
| Borssele | 4.4 | -26 |
| Gemini | 3.6 | -54 |

The stability situation is assessed based on the storm conditions. The hydraulic conditions at Gemini are significantly rougher than the storm wave conditions that occur at HKW and Borssele. By taking the average conditions of these three locations as normative for the design of the structure, the design of the concepts is under-dimensioned for Gemini and over-dimensioned for the HKW and Borssele sites, for the stability requirement.

The wave conditions were dominant for the storm conditions for each site (see Chapter 3). In Table 9.2, the percentage deviation from the average significant wave height with a return period of 10 years, which is considered in the stability tests, are determined for each site. For HKW, only a 6 % deviation is observed which is minimal. However, for Borssele and Gemini, almost 20 percent deviation is observed, which is significant.

**Table 9.2:** Significant wave height with a return period of 10 years per site and percentage deviation from average significant wave height ($H_s = 7.4m/s$), which is used in the report.

| | Wave height, $H_s$ [m] | Deviation [%] |
|---|---|---|
| HKW | 7 | +6 |
| Borssele | 6.2 | +19 |
| Gemini | 9.1 | -19 |

When a droppable broodstock is decided for application at a specific location, the conditions that are present, should be re-evaluated and compared to the used conditions in this research to determine whether the deviation is significant such that it causes under- or over-dimensioning of the concepts. In that case, new conditions should be considered.

## 9.4. Physical model interpretation of test results

The results obtained during physical modelling, provide insight into the concept behaviour during relevant situations; fall, landing and stability. The tests were executed in the wave flume in the hydraulic engineering laboratory at TU Delft.

The wave field generated in the wave flume consists of a combination of incident and reflected waves. The incident wave is of importance as this wave exerts a load on the concepts. The reflected wave disrupts the desired wave field. It was concluded that the reflected wave had a maximum effect of approximately 4% on the incident wave height and therefore was neglected.

The output wave data used in the results to indicate the behaviour of the concepts could therefore entail small overestimations of the wave height, because the reflected wave coefficient is neglected. This would indicate that the results obtained in physical modelling are less safe, than interpreted.

To execute the tests, prototypes of the concepts were created. To create the concept prototypes, liquid Poly-Pur was mixed with leaden balls (with a mixing ratio of 1:1 by weight) and then poured into the moulds. The moulds were kept in movement for equal distribution, but this method does not guarantee equal distribution. However, it is mainly important that the centre of mass is at the correct location [Gueron and Tessler, 2002]. The leaden balls were positioned such, to guarantee the centre of mass as best as possible (by placing the leaden balls at the ends of the arms equally), but this can also not be guaranteed. When the centre of gravity is dislocated, this could result in deviating behaviour of the concepts in the tests. The dislocation of the centre of gravity is assumed to be minimal.

### 9.4.1. Fall test

In the fall test, the horizontal displacement of the concepts during the fall was investigated. Each concept was dropped sixty times, to ensure that outliers were identified. The concepts were only tested until a depth that represents 13 meters (on real scale) due to limited wave flume height, however the depth at offshore wind farms in the North Sea is approximately 30 meters. To obtain insight into the maximum horizontal displacement at the seabed, the fall data is extrapolated. The second order polynomial extrapolation method mimics the movement profile which is induced by the current and waves velocity profiles. However, the shape of a second order polynomial extrapolation line is not the same as the shape of the movement profile line. Close to the bottom, the object movement line, deflects inwards (indicating less displacement), due to decreasing velocities near the bottom, caused by the current. This phenomenon is not incorporated in the second order polynomial line. The horizontal displacements using the second order polynomial extrapolation method may be overestimated and therefore provides safer results.

The fall test defines the maximum and mean horizontal displacement for each concept. The determined maximum horizontal displacement is dominant over the mean horizontal displacement to secure a safe outcome. Three concepts exceed the requirement; Open table 3, Cube framework and Anchor long. These three concepts are the three 'widest' concepts (together with the Anchor short). The results indicate that wider (and less streamlined) structures result in more displacement during the fall, which can be the result of more induced drag force (due to larger drag coefficients) [van Oord, 1996].

**Comparison to concept observation test**

The fall results obtained with physical modelling are compared to the results obtained in the concept observation test (see Appendix D). The concept observation test is executed in still water. The results per concept were compared relatively to each other (not value), to obtain insight into the difference between the concepts compared to the other concepts. Both methods indicate minimal horizontal displacement for Open table 1 and Open table 2, medium horizontal displacement for Anchor short and Xblock and maximum horizontal displacement for Anchor long. The results obtained for the Cube framework and Tetrapod are contradicting. In still water, the Cube framework showed minimal horizontal displacement and in the wave flume, maximum horizontal displacement was observed. For the Tetrapod the opposite behaviour is observed.

A possible explanation for this contradicting result can be addressed by the equilibrium fall velocity. The equilibrium fall velocity for the Cube framework is determined to be 0.35 m/s (see Table 9.3), which is the smallest velocity compared to the other concepts. A small fall velocity results in a longer fall time. The prevailing flow in the wave flume has more time to induce force upon the concept, which could have led to more horizontal displacement. The equilibrium fall velocity for the Tetrapod is defined to be 0.55 m/s (see Table 9.3), which is the largest velocity compared to the other concepts (excluding the Reference block). A large fall velocity results in a shorter fall time. The prevailing flow in the wave flume in the fall test has less time to induce force upon the concept, which could have led to less horizontal displacement.

The other fall velocities $\bar{w}$ and horizontal displacement are also provided in Table 9.3. In Figure 9.1, a correlation between the equilibrium fall velocity is observed, indicated by the dotted trendline. This trendline supports the assumption made that smaller falling velocities ($\bar{w}$) result in larger displacements ($x_h$) and larger falling velocities ($\bar{w}$) result in smaller displacements ($x_h$).

**Table 9.3:** Averaged equilibrium velocity $\bar{w}$ [m/s] per concept and horizontal displacements $x_{h-mean}$ [m] and $x_{h-max}$ [m].

| | $\bar{w}$ [m/s] | $x_{h-mean}$ [m] | $x_{h-max}$ [m] |
|---|---|---|---|
| Reference block | 0.66 | 2.4 | 4.1 |
| Xblock | 0.47 | 3.1 | 5.75 |
| Tetrapod | 0.55 | 2.9 | 4.9 |
| Piebox framework | 0.45 | 4.75 | 7.5 |
| Cube framework | 0.35 | 3.85 | 5.25 |
| Anchor long | 0.49 | 4.6 | 7.55 |
| Anchor short | 0.48 | 4.1 | 5.7 |
| Open table 1 | 0.42 | 3.8 | 5.2 |
| Open table 2 | 0.49 | 4.65 | 5.6 |
| Open table 3 | 0.44 | 4.45 | 6.4 |

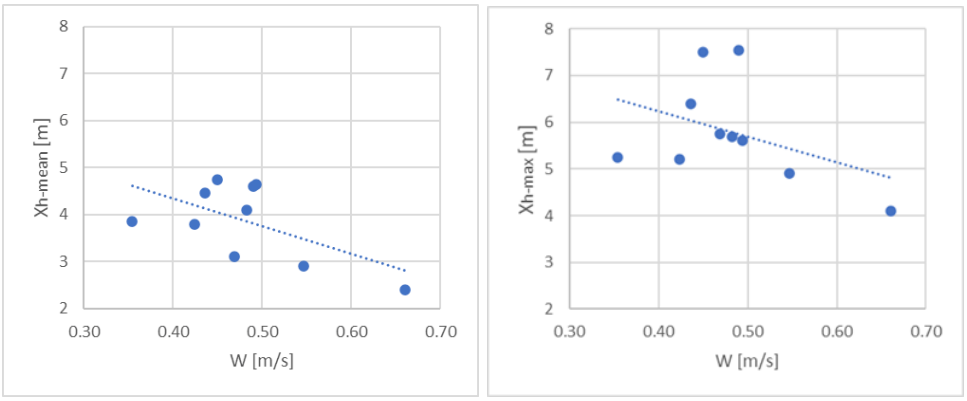


(a) (b)

**Figure 9.1:** Correlation graphs for equilibrium fall velocity $\bar{w}$ and horizontal displacements (a) $x_{h-mean}$ [m] and (b) $x_{h-max}$

## 9.4.2. Land test

In the land test, the surface hit during the landing on the scour protection is investigated. Each concept is dropped a minimum of five times in the wave flume on a stone layer. This repeating number is low, which makes the results less accurate, because outliers cannot be defined with such a small data set and are therefore included in the results.

The results obtained during the land test provide insight into the protection, installation and transportation design criteria.

The protection criterion states that minimal oysters should get damaged during the installation, to secure oyster survival. Four concepts indicate minimal oysters damaged during the landing; Cube framework, Piebox framework, Anchor long and Anchor short. The three Open table concepts are certain to damage half of the attached oysters For the Open table concepts is could be considered to attach fewer oysters to the structure, which would result in fewer oysters getting damaged during the landing. However, this would lead to more structures necessary to obtain the desired amount of intact oysters, which would increase the involved costs.

An explanation for the fact that the Framework and Anchor concepts experience minimal surface to be hit during the landing can be addressed by the sides hit definitions, presented in Figure 6.7. For the Cube and Piebox framework and the Anchor long and short, the sides hit are minimal estimations. These results therefore might be undervalued for the framework and Anchor concepts and have led to these four concepts being damaged the least. For the Open tables, four legs are defined to get fully hit during the landing by the sides definitions. This might be an overestimation, because it cannot be said with certainty that these sides are fully damaged during the landing.

It is expected that the land results do not differ significantly for different hydraulic conditions, because the concepts tend to land in the same manner for different conditions and in both performed tests, the concepts have reached their equilibrium fall velocity. In Appendix D, the executed concept observation test is discussed. These experiments were performed in still water. The results regarding the landing of the concepts were similar to the results obtained in the land test executed in the wave flume (with generated flow and waves). The results are therefore assumed to be directly usable for applications of the droppable oyster brood stock, regardless of the selected location where different conditions might occur.

### 9.4.3. Stability test

In the stability test, the conditions at which the concepts become unstable are defined, by mimicking five increased storm events. The concepts were dropped (from a small height) onto the stone layer in the wave flume after which the scaled storm conditions were generated. If a concept was assessed unstable twice in the same conditions, it was assumed that the threshold of motion was reached. The threshold of motion is defined in a range of near-bed orbital motion velocity induced by the waves between the (extremest) conditions it did remain stable and the conditions it started to move.

The results of the stability test provide insight into whether concepts comply with the stability design criterion. This stability criterion indicates a requirement that the concepts should at least remain stable during a storm event with a return period of 10 years. Four concepts comply with this requirement; Open table 3, Open table 2, Tetrapod and Anchor long. The Open table 2 and 3 and the Anchor long are relatively wide and low structures which imply stability, because rotation is more difficult to occur. The Tetrapod does not have a small height (relative to the other concepts), but does entail a small impact surface and round surfaces, which results in less flow force acting upon the structure (see Chapter 3). The results indicate that the Cube framework is the least stable. The Cube framework has the largest height, which can cause rotation to occur sooner relatively to other concepts. The Cube framework also has a relative large (side) surface, this provides a relatively large surface for the flow force (see Chapter 3) to act upon, to cause movement.

The wave generator in the wave flume reached its maximum capacity during generating storm conditions combination 3. To still be able to test the concepts in heavier wave conditions, it was decided to decrease the density of the concepts. The new prototypes also have a deviating shape relative to the original shape. Due to lack of time, the prototypes were created by using the 3D printed concepts (used to make the moulds) and attaching leaden balls at the outside to them to make them heavier (for the desired density), see Figure 9.2. The shape deviations could result in a greater force acting upon the structures due to larger outside surfaces relative to the original concepts. This would result in safer results obtained during tests executed for storm conditions 4 and 5, because more surface indicates a larger surface to which the flow forces can act and cause movement.

**Figure 9.2:** Adjusted concepts used for stability test, with storm condition combination 4 and 5

The stability test is repeated per storm conditions per concept a minimum of two times. This repeating number is low, which makes the results less accurate, because outliers cannot be defined with such a small data set and are therefore included in the results. The concepts were all located on different spots on the stone layer, because they were dropped to mimic reality. This could have led

to different settle positions for the same concept, for example in between stones or on top of a stone, which could lead to less or more stable settle positions. As a concept could have settled differently, the concept could have been assessed incorrectly with regard to their threshold of motion. The hydraulic output conditions per test are the same or differ minimally (see Section F.3.1), which does minimise the difference in results per test.

During the application of a droppable oyster brood stock structure, the specific conditions should be considered to conclude which concepts remain stable in these results. Also, the preferences for the application can deviate from the stability requirement in this research, for example that it is allowed for the structure to move during its lifetime. This can also lead to other suitable concepts and should be considered with care per situation.

# 9.5. Calibration of the calculation method

The results obtained in the physical model were used to improve the behavioural prediction calculations of the concepts in Chapter 7. There are still deviations between the results obtained with the calibrated calculations in Chapter 7 and the physical model.

For the fall situation, the calibrated calculations provided undervalued results for the maximum horizontal displacement. For these calculations, it was assumed that the equilibrium velocity is reached immediately. In reality, the equilibrium velocity is reached after the object has already been falling for approximately eight times its object's diameter (in water). The fall velocity ($\bar{u}$), used in the calculations for the fall situation is therefore larger than in reality (physical model). When the accelerating fall velocity starting from zero is included in the calculations, the displacement during the fall is likely to become larger due to longer falling time. The flow force ($F_u$) has more time to act upon the structure, which results in more displacement. This would lead to safer results, leading to more correspondence to the maximum displacements obtained in physical modelling.

For the stability situation, two concepts provide undervalued results in the calibrated calculations, namely Xblock and Open table 2. However, when the results provided in Section 5.3 are reviewed, it can be seen that the Xblock already showed minimal movement during storm conditions 1 ($u_{w-1.5m} = 0.57 - 1.12m/s$) . The Open table 2, already showed to be unstable storm condition 4 ($u_{w-1.5m} = 1.46 - 2.30m/s$). These conditions do comply with the results provided in the numerical model and therefore it could also be that the concepts are assessed stable for overvalued conditions at the physical modelling, due to limited test repeats.

# 9.6. Application

When an oyster brood stock structure is considered to be applied, two considerations need to be made; the type of installation method and the type of brood stock structure.

## 9.6.1. Installation method

The impetus for this research arose from the difficulties encountered during the installation of a structure using a crane and especially the high costs involved in this installation. This installation method however did ensure high ecological value as the number of damaged oysters arising from this installation method is minimal. The alternative installation method, considered in this research, the drop method, ensures easy deployment and minimal involved costs. However, the ecological value is lower compared to the crane installation method, because part of the oysters will be lost during the installation due to damage encountered during the landing.

The choice of installation method and therefore type of brood stock structure installed, is dependent on the preferences and requirements of the specific application. When costs and required resources allow it, a crane installation is preferred to maximise ecological value. If costs and/or resources form a constraint for application, a droppable oyster brood stock structure is chosen, to enable application. The financial versus ecological value consideration is a trade-off for each situation where an oyster brood stock structure is desired. To make a substantiated decision about which installation method and corresponding structure should be applied per situation, cost indications are needed. The following aspects should be considered;

- *Amount of structures* - Amount of structures is larger for the drop method than for the crane installation method. In previously executed pilot projects, where brood stock structures were installed, approximately two structures were needed to introduce 500 oysters [Van Rie, 2020]. In Table 6.2, the amount of droppable oyster brood stock structures needed to introduce 500 intact oysters at the scour protection, is defined for each considered concept. The average order of magnitude is between 10-20 structures.
- *Cost per structure* - The costs for one structure will be less for the droppable broodstock structure, because they require less material. The exact costs are not determined for the droppable brood stock structure. For the crane installation method, the costs per structure are determined for previously executed pilot projects. The costs depend on the type of brood stock structure installed.
- *Amount of oysters* - A certain percentage of oysters is lost during the drop method, which is not encountered for the crane installation method. Therefore more oysters are required for the drop method to reach the desired amount of 500 intact oysters. The exact amount is dependent on the selected concept. For the crane installation method 500 oysters are necessary.
- *Cost per oyster* - The costs per oyster needs to be considered, because more oysters are needed for the droppable oyster brood stock structure.
- *Cost of installation* - The installation costs for the crane method are higher, because special equipment is necessary for this method, such as a crane. This is not necessary for the drop method. Both methods require a vessel for installation.

### 9.6.2. Concept selection

The application of the research is now discussed. When the drop method is selected, a concept to function as a droppable oyster brood stock structure needs to be selected for implementation. Some steps need to be taken, based on the executed research to obtain the most suited concept. The steps are discussed below;

1. *Design criteria* - The drafted design criteria should be compared with the specific preferences of the application. It should be considered if design criteria need to be added or removed. It should be examined whether any considered design criteria result in new requirements (e.g. a minimum dimension or that structures should be stackable). It should also be considered whether the requirements relating to stability and positioning still apply (e.g. whether the structure should land on the scour protection, or whether the structure should remain stable for the lifetime of the offshore wind farm).
2. *Environmental conditions* - The scour protection conditions and water depth must be considered to determine the maximum horizontal displacement during the fall for the positioning criterion. These can be compared to the displacements ($x_h$) determined for the concepts obtained in physical modelling, see Table 6.1. The hydraulic storm conditions which the structure should be able to resist at the specific site need to be defined. These conditions should be compared with the conditions where the concepts were found to be unstable, see Figure 6.10.
3. *Final concept selection* - The requirement analysis can now be used to determine which concepts meet the set requirements. If multiple suitable concepts emerge from the requirement analysis, the multi-criteria analysis can be used. Appropriate weighting factors have to be selected for each defined criterion, based on the application purpose. The most suitable concept (out of the ten considered concepts studied) can be selected.
4. *New concept design* - If no suitable concept can be selected, there are three options to determine new concepts; 1) select other concept parameters for the existing concepts defined in by behavioural prediction calculations, leading to a new concept, 2) revisit the eliminated concepts considered in Chapter 2, 3) design a new concept.
5. *Behavioural prediction calculations assessment* - These new concepts need to be reassessed for suitability based on behavioural prediction calculations. This does require improvements to be made to the calculation methods.
6. Repeat from step 2.

# 10

# Conclusion & Recommendations

This chapter presents the conclusion of this research by addressing all research questions discussed in the introduction. Subsequently, recommendations for future research are given.

## 10.1. Conclusion

With increasing interest in finding alternatives for fossil fuels by wind energy in the Netherlands, the construction of offshore wind farms in the North Sea is in full swing. Wind turbines n these offshore wind farms are generally surrounded by scour protections. These consist of hard substrate, which could serve as a habitat for European flat oysters, as opposed to the original seabed, which merely consists of sand. Using scour protection as a location to kick-start oyster reefs, is investigated in multiple studies. The existing method, to install oyster brood stock structures at scour protections of offshore wind farms, uses cranes. This crane installation method has shown to involve difficulties, due to their size and weight, and high involved costs. This study considers an alternative installation method for the oyster brood stock structure, by manual dropping. With an alternative installation method, the need to find a corresponding appropriate design, for the brood stock structure, arises. The objective of this research was therefore to investigate;

***What is the design for a flat oyster brood stock structure, that can be installed at the scour protection at offshore wind farms, via dropping from a vessel, such that it will be stable and integer during deployment and operational lifetime?***

This research question was subdivided into four sub-questions to aid in answering the main research question. The conclusions for each individual sub-question are given below.

1. *Which design criteria apply for a droppable oyster brood stock structure?*

The design criteria are divided into two subjects, ecological and structural. The ecological design criteria relate to the way the structure interacts with the oysters attached to the structure and how the structure can best facilitate them. The structural criteria relate to the structural integrity of the design of the brood stock structure. The ecological and structural design criteria are; 'flow', 'space', 'protection', 'predation', 'oyster settlement', 'durability', 'stability', 'positioning', 'installation', 'manufacturing' and 'transportation'. The design criteria are elaborated below;

- Flow - The oysters attached need to experience sufficient flow, for the oysters to abstract enough nutrients from the water and not suffocate.
- Space - The oysters attached to the structure require sufficient space to grow and reproduce.
- Protection - The oysters need to be protected from being damaged during the deployment, to optimise survival and reproduction.

- Predation - The predation of the oysters should be reduced as much as possible, to optimise survival and reproduction.
- Oyster settlement - The material used for the structure must be suitable for the settlement of oysters and larvae for the oysters to start reef formation.
- Durability - The structures must remain intact for a period of approximately 30 years, including deployment and storm events.
- Stability - The structure must remain stable on the scour protection during the operational lifetime, for protection of the sensitive surroundings.
- Positioning - The dropping accuracy during deployment should be minimal to ensure sufficient positioning at the scour protection.
- Installation - For easy installation, the structure should be able to be manually dropped in the water.
- Manufacturing - The structure should be easy to fabricate to prevent complications in this construction phase and high costs.
- Transportation - The structures should be easily transportable (in large quantities), to avoid logistic complications.

From these design criteria, two specific design requirements have arisen. The first requirement entails that the horizontal displacement encountered during the fall for deployment has a maximum value between 4 meters (armour layer) to 5.5 meters (filter layer), based on the positioning criterion. The second requirement entails that the structure should remain stable during a storm event with a return period of 10 years, based on the stability criterion.

Also, two specifications regarding the design of the structure resulted from the set design criteria, that the material chosen for the structure is (fibre-reinforced) concrete and that the maximum weight of the structure is 50 kg.

2. *Which concepts can be designed for a droppable oyster brood stock structure, considering the design criteria?*

Based on literature studies on existing subsea structures and expert consultation sessions, twelve concept designs were drafted. These concepts were assessed based on the set design criteria by the use of a multi-criteria analysis. Five basic concepts were selected as suitable; Xblock, Tetrapod, Cube framework, Anchor and Open table. One extra concept was introduced to act as an observation concept, the Reference block.

The parameters (volume, size, dimensions) of these basic concepts were not yet considered. The design specifications lead to a maximum volume of 20 liters for the structures. To define the other parameters, behavioural predictions of the concepts during relevant situations were made based on calculations. The most suited parameters for each concept were determined using an iterative process for the calculations. This led to a total of ten concepts. These ten concepts involve multiple versions of the same basic concept, including the Cube framework, Anchor and Open table. The ten resulting concepts are; Reference block, Xblock, Tetrapod, Cube framework, Piebox framework, Anchor long, Anchor short, Open table 1, Open table 2 and Open table 3 (see Figure 10.1).

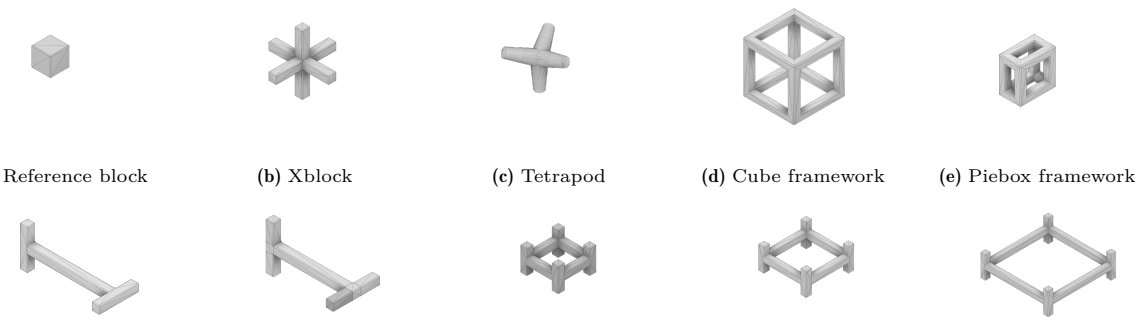

**(a)** Reference block **(b)** Xblock **(c)** Tetrapod **(d)** Cube framework **(e)** Piebox framework

**(f)** Anchor long **(g)** Anchor short **(h)** Open Table 1 **(i)** Open Table 2 **(j)** Open Table 3

**Figure 10.1:** Selected concepts

3. *What is the performance of the concepts to function as a droppable oyster brood stock structure?*

To obtain more accurate insight into the behaviour of the concepts and to assess their performance, physical modelling is required. Three relevant situations during the lifetime of an oyster broodstock structure are investigated by three types of tests (fall, landing and stability). These were performed in the wave flume at Hydraulic Engineering Laboratory at the faculty of Civil Engineering (TU Delft).

The goal of the fall test was to obtain insight into the dropping accuracy of the concepts during the fall from the vessel until the first hit with the scour protection. In the test, the concepts were dropped in the flume to obtain insight into the falling behaviour and subsequent horizontal displacement during deployment conditions. Deployment conditions are defined as the maximum hydraulic conditions for which the installation can be performed. These entail $H_s = 1m$, $T_p = 7s$ and $\bar{u_c} = 0.3m/s$. From extrapolation of the test results, the maximum horizontal displacement during the fall of the dropped concepts was determined. The maximum horizontal displacement should not exceed a value of 5.5 meters, based on the positioning criterion. The Tetrapod, Open table 1 and Piebox framework concepts meet this criterion. The Open table 2, Anchor short and Xblock concepts slightly exceed this maximum value. The Open table 3, Cube framework and Anchor long, do not meet this criterion. See Table 10.1 for the maximum horizontal displacement encountered during fall per concept.

The goal of the land test was to obtain insight into the behaviour of the concepts during the landing, after being dropped from a vessel and falling in the water column. The landing was assessed based on concept interaction with a stone layer present at the bottom of the flume after it was dropped. The test results were used to indicate the amount of oysters lost during the landing and the amount of structures required at one scour protection to reach the critical mass of oysters to start reef formation. It is desired to obtain minimal oyster loss, for the protection criterion. The Open table concepts encounter a minimum of 50 percent oyster loss. The Xblock and Tetrapod encounter moderate (20-30%) oyster loss and the Cube framework, Piebox framework, Anchor long and Anchor short encounter minimal (<20%) oyster loss due to the landing. It is also desired to have a minimal amount of structures, for the installation and transportation criteria. The Cube framework only needs 7 structures, the Tetrapod requires 37 structures and the Open table 1, requires 27 structures. The other structures require between 10 to 20 structures, at one scour protection. See Table 10.1 for results per concept.

The goal of the stability test was to assess the stability of the concepts when they have settled on the scour protection, during storm conditions. Storm events were generated in the wave flume to obtain insight into the threshold of motion. The concepts should at least remain stable during a storm event with a return period of 10 years (corresponds to $u_{w-1.5m}$ of 1.56 m/s), and is desired to remain stable during a storm with a return period of 50 years (corresponds to $u_{w-1.5m}$ of 1.82 m/s). Based on the test results, the Open table 2 and 3, Tetrapod and Anchor long, remain stable during a storm event with a return period of 10 years. Open table 2 and 3 also remain stable during a storm that corresponds to averaged conditions with a return period of 50 years. Anchor short, Open table 1, Xblock, Piebox framework, Cube framework and Reference block, do not remain stable during a storm event with a return period of 10 years. See Table 10.1 for the near bed orbital motion velocity range in which the concepts became unstable during the tests, translated to reality.

**Table 10.1:** Overview of relevant results obtained in research, in concept observation test ( $C_D$, $\bar{w}$), fall test ($x_h$), land test ($A_{hit}$, structures) and stability test ($u_{w-1.5m}$ *range*).

| | $C_D$ [-] | $\bar{w}$ [m/s] | $x_h$ [m] | $A_{hit}$ [m$^2$] | *structures* | $u_{w-1.5m}$ *range* [m/s] |
|---|---|---|---|---|---|---|
| Reference block | 1.2 | 0.66 | 4.1 | 0.31 | 19 | 1.12-1.44 |
| Xblock | 1.2 | 0.47 | 5.75 | 0.35 | 15 | 1.44-1.46 |
| Tetrapod | 1.2 | 0.55 | 4.9 | 0.25 | 37 | 1.46-2.30 |
| Cube framework | 2.1 | 0.45 | 7.5 | 0.1 | 7 | 0.57-1.12 |
| Piebox framework | 2.1 | 0.35 | 5.25 | 0.12 | 15 | 1.44-1.46 |
| Anchor long | 1.9 | 0.49 | 7.55 | 0.15 | 10 | 1.46-2.30 |
| Anchor short | 1.9 | 0.48 | 5.7 | 0.11 | 10 | 1.12-1.44 |
| Open table 1 | 2.3 | 0.42 | 5.2 | 0.67 | 27 | 1.12-1.44 |
| Open table 2 | 1.3 | 0.49 | 5.6 | 0.6 | 20 | 2.30-2.69 |
| Open table 3 | 1.0 | 0.44 | 6.4 | 0.49 | 14 | 2.30-2.69 |

4. *Which concepts best meet the proposed design criteria of the droppable oyster brood stock structure, according to their performance?*

Physical modelling provides insight into the behaviour of the different concepts in three relevant situations that they encounter during deployment and operational lifetime. Based on the results, the concepts were assessed. First, a requirement analysis is performed to check which concepts comply with the two set requirements, regarding maximum positioning accuracy and stability. Only the Tetrapod complies with both these requirements and is therefore the only suited concept to act as a droppable oyster brood stock structure. The Open table 2 concept, exceeds the positioning accuracy only by 0.1 meters and complies with the stability requirement. Therefore, a multi-criteria analysis is performed for these two concepts (Tetrapod and Open table 2), which assesses the concepts based on the other set design criteria. The multi-criteria analysis assesses the Open table 2 concept to be better suited to act as a droppable oyster brood stock structure.

## 10.2. Recommendations

Based on the discussions addressed in Chapter 9, several recommendations for future research have been established. This section addresses these recommendations for possible future research.

**Alternative dimensions of basic concepts**
For the five basic concepts that were defined in Chapter 2, multiple versions with different ratios were considered in behavioural prediction calculations in Chapter 3. However, no alternative ratio versions were considered for the Xblock and the Tetrapod. Different 'arm' thicknesses and lengths were considered, but asymmetric versions were not. The Tetrapod is assessed to be a suitable concept. In future research, different versions of the Tetrapod can be investigated, for example where one 'arm' is longer and thinner and the other three 'arms' are thicker and shorter. This would enable more space and elevation for the oysters on the longer arm.

**Improve behavioural prediction calculations**
The results obtained with the physical model are used to improve the behavioural prediction calculations, but more improvements can be made. If the behavioural prediction calculations would provide more accurate results, physical modelling is not necessary for the future. Physical modelling is time-consuming and more expensive than performing calculations. Three known aspects that can be improved have already been defined in Chapter 9 and Chapter 3;

- Include inertia force in the behavioural prediction calculations. This force is now neglected.
- Include the accelerating fall velocity of the objects. The concepts are now assumed to have reached their equilibrium fall velocity directly.
- Improve the bottom friction coefficient value estimation. This coefficient is now determined based on a previously executed brood stock structure installation, which had greater dimensions.

**Prototype material**
The creation of the prototypes involved some complications regarding the material. The material should possess the correct density to avoid scale effects. The prototypes entailed relatively small details, which resulted in some complications to mimic. Eventually, a mixture of Poly-Pur with leaden balls is used. However, equal distribution of the leaden balls in the mixture cannot be guaranteed. Filling the moulds with this mixture, was also labour intensive. In future research (especially when many prototypes are required), the use of an alternative material should be investigated to simplify the development of the prototypes.

**Include wave reflection**
The wave reflection coefficient could not be determined, due to complications, regarding the data processing of the DASYlab files which contained the wave gauge information, in the 'Decomp' Matlab script. It is recommended to make improvements to the 'Decomp' Matlab script to increase usability to obtain the wave reflection coefficients (more easily). The DASYlab files should be tested beforehand to observe whether they obtain the correct data. This would provide more accurate information regarding the generated waves in the wave flume.

**Test repeats**
The fall test is repeated sixty times. The land experiment is repeated a minimum of five times and the stability test is repeated per storm conditions a minimum of two times. The accuracy of the results increases with the amount of repeating of an experiment, because the error percentage decreases. To obtain more accurate results, the land and stability test should be repeated more in future research in order to better indicate the outliers of the data.

**Fall test on full depth**
Due to limitations regarding the flume height, the fall test was performed on two scales, which represent a real-life depth of 7 and 13 meters. To indicate the horizontal displacement over a depth of 30 meters, extrapolation is applied. Extrapolation methods use 'historic' data to predict 'future' data and therefore assume previous trends to continue. To obtain more substantiated indications about the movement during the fall of the structures, the fall test should be performed where the fall over the entire depth can be mimicked (on scale).

**Smaller storm conditions steps**
To define accurate stability data for which conditions the concepts fail to remain stable, the steps between the test conditions should be small. The threshold of motion is defined as a range. In the stability test, the increase from storm condition combination 3 to storm condition combination 4 is large. The threshold of motion of the concepts Tetrapod and Anchor long, which became unstable during storm conditions combination 4, entails a large range and is therefore not defined accurately. In future research, the jump between the storm conditions should be small to obtain more accurate results.

**Associate equilibrium fall velocity to the strength of the structure**
The equilibrium fall velocity for each concept is different (as defined in Appendix D). The fall velocities for which the concepts hit the bottom influence the required strength of the material of the structures. In future research, when application is considered, the required strength based on the fall velocities should be determined. This defines the necessity of reinforcement of the concrete.

**Costs versus ecological value for the considered installation method**
To determine the appropriate installation method and the corresponding type of brood stock structure for application, an inventory of the costs involved for each installation of a brood stock structure should be made. This inventory should incorporate the ecological value and corresponding costs per installation method and type of structure. Based on the requirements and preferences for a situation, a substantiated decision can be made about which installation method and therefore type of brood stock structure are most suited.

**Real-scale test for ecological value**
It is recommended to carry out a pilot project to observe the ecological value after using the drop method. The ecological value is not thoroughly examined in this research. In projects carried out with crane installation structures, losses (due to external factors) were already encountered. Since the drop method guarantees oyster losses, it is worthwhile to investigate whether the oyster loss becomes too significant. The effect of marine fouling, which is not considered in the research can also be observed. Marine fouling can cause the structure dimensions and weight to change over time, which can lead to a change in behaviour.

# References


Airoldi, L., & Beck, M. W. (2007). Loss, status and trends for coastal marine habitats of europe. *Oceanography and Marine Biology*, *45*, 345–405. https://doi.org/10.1201/9781420050943.ch7

Beck, M. W., Brumbaugh, R. D., Airoldi, L., Carranza, A., Coen, L. D., Crawford, C., Defeo, O., Edgar, G. J., Hancock, B., Kay, M. C., Lenihan, H. S., Luckenbach, M. W., Toropova, C. L., Zhang, G., & Guo, X. (2011). Oyster reefs at risk and recommendations for conservation, restoration, and management. *BioScience*, *61*, 107–116. https://doi.org/10.1525/bio.2011.61.2.5

Belzen, J. V., Poppel, J. V., & Bouma, T. (2021). How to deploy adult european flat oysters to establish an initial source population for reef recovery: Methods and bottlenecks suitability of using adults for outplacement deliverable 1.4. *Two Towers B.V., Van Oord Offshore Wind B.V. Investri Offshore, and Green Giraffe*.

Bijker, E. (1967). *Some considerations about scales for coastal models with movable bed* (tech. rep.). Delft Hydraulics Laboratory. http://resolver.tudelft.nl/uuid:cdf2f061-3fe6-4361-a0e7-636fc69c9eca

Blankenweg, J., & Elleswijk, A. J. (2017). *Scour protection van oord dredging and marine contractors b.v. borssele wind farm zone (bwfs iii &iv)* (tech. rep.). Van Oord Marine contractors.

Blankenweg, J. (2017). Scour protection. borsselewindfarmzone (bwfs iii andiv). *Van Oord Dredging and Marine ContractorsB.V.*

Bosboom, J., & Stive, M. J. (2022). *Coastal dynamics* (Third Edition). TU Delft OPEN. https://doi.org/https://doi.org/10.5074/T.2021.001

Bouma, T., der Heide, T. V., Christianen, M., Koningsveld, M. V., & Murk, A. (2017). North sea reef vitalization for ecosystem services (north sea revifes). *Applied and Engineering Sciences*.

Breusers, H., & Schukking, W. (1971). *Begin van beweging van bodemmateriaal speurvverkverslag waterloopkundig laboratorium delft • s159-i* (tech. rep.). Deltares. http://resolver.tudelft.nl/uuid:5917d19a-e14e-4b39-8ccc-bef0976d232c

Breusers, H. N. C., Nicollet, G., & Shen, H. (1977). Local scour around cylindrical piers. *Journal of Hydraulic Research*, *15*(3), 211–252. https://doi.org/10.1080/00221687709499645

CETME, C. C. (2007). Chapter 5 physical processes and design tools. In J. Simm (Ed.). C683, CIRIA, London. https://www.kennisbank-waterbouw.nl/DesignCodes/rockmanual/chapter205.pdf

CETMEF, C. C. (2007). Chapter 4 physical site conditions and data collection. In J. Simm (Ed.). C683, CIRIA, London. https://www.kennisbank-waterbouw.nl/DesignCodes/rockmanual/chapter204.pdf#page=119&zoom=100,0,0

Child, A. R., & Laing, I. (1998). Comparative low temperature tolerance of small juvenile european, ostrea edulis l., and pacific oysters, crassostrea

gigas thunberg. *Aquaculture Research*, *29*(2), 103–113. https://doi.org/10.1046/j.1365-2109.1998.00934.x

Christianen, M., Lengkeek, W., Bergsma, J. H., Coolen, J. W., Didderen, K., Dorenbosch, M., Driessen, F. M., Kamermans, P., Reuchlin-Hugenholtz, E., Sas, H., Smaal, A., van den Wijngaard, K. A., & van der Have, T. M. (2018). Return of the native facilitated by the invasive? population composition, substrate preferences and epibenthic species richness of a recently discovered shellfish reef with native european flat oysters (ostrea edulis) in the north sea. *Marine Biology Research*, *14*, 590–597. https://doi.org/10.1080/17451000.2018.1498520

Concrete, S. (2019). Eco-friendly alternatives to traditional concrete [[Online; accessed 17-October-2022]]. https://www.specifyconcrete.org/blog/eco-friendly-alternatives-to-traditional-concrete

Cozzi, L., & Wanner, B. (2019). Offshore wind outlook 2019: World energy outlook special article. *World Energy Outlook*. www.iea.org/tandc/

Culloty, S. C., Cronin, M. A., & Mulcahy, M. F. (2001). An investigation into the relative resistance of irish flat oysters ostrea edulis l. to the parasite bonamia ostreae (pichot et al., 1980). *Aquaculture*, *199*, 229–244. https://doi.org/https://doi.org/10.1016/S0044-8486(01)00569-5

Davis, H., & Ansell, A. (1962). Survival and growth of larvae of the european oyster, o. edulis, at lowered salinities. *The Biological Bulletin*, *122*(1), 33–39.

Dessens, M. (2004). *The influence of flow acceleration on stone stability* (Doctoral dissertation). TU Delft. http://resolver.tudelft.nl/uuid:17f63722-b650-4207-b71d-1ef657f75a0b

Desyani, R., & Mungar, S. (2022). Monopile scour protection design hollandse kust west. *Van Oord Dredging and Marine Contractors*.

DHL. (1969). *Begin van beweging van bodemmateriaal* (tech. rep.).

Didderen, K., Bergsma, J. H., & Kamermans, P. (2019). Offshore flat oyster pilot luchterduinen wind farm results campaign 2 (july 2019) and lessons learned status: Draft. *Bureau Waardenburg*. www.buwa.nl

Didderen, K., Lengkeek, W., Bergsma, J. H., Dongen, U. V., Driessen, F. M. F., & Kamermans, P. (2020). Active restoration of native oysters in the north sea-monitoring. *Bureau Waardenburg*. www.buwa.nl

Didderen, K., Lengkeek, W., Kamermans, P., Deden, B., & Reuchlin-Hugenholtz, E. (2018). Pilot to actively restore native oyster reefs in the north sea comprehensive article to share lessons learned in 2018.

Didderen, K., Lengkeek, W., Kamermans, P., Deden, B., & Reuchlin-Hugenholtz, E. (2019). Pilot to actively restore native oyster reefs in the north sea comprehensive article to share lessons learned in 2018. *Bureau Waardenburg*. https://www.ark.eu/sites/default/files/media/Schelpdierbanken/article_Borkumse_Stenen.pdf

Drinkwaard, A. (1961). Current velocity as an ecological factor in shell growth of ostrea edulis. *ICES Shellfish Committee*, *47*, 1–3.

Duren, L. V., Gittenberger, A., Smaal, A., Koningsveld, M. V., Osinga, R., der Lelij, J. C. V., & Vries, M. D. (2016). Rijke riffen in de noordzee. *Deltares*. https://publications.deltares.nl/1221293_000.pdf

Elger, D. F., LeBret, B. A., Crowe, C. T., & Roberson, J. A. (2020). *Engineering fluid mechanics*. John Wiley & Sons.

Engelsma, M., Culloty, S., Lynch, S., Arzul, I., & Carnegie, R. (2014). Bonamia parasites: A rapidly changing perspective on a genus of important mollusc pathogens. *Diseases of Aquatic Organisms*, *110*(1-2), 5–23. https://doi.org/10.3354/dao02741

Foighil, D. O., & Taylor, D. J. (2000). Evolution of parental care and ovulation behavior in oysters. *Molecular Phylogenetics and Evolution*, *15*(2), 301–313. https://doi.org/https://doi.org/10.1006/mpev.1999.0755

Gercken, J., & Schmidt, A. (2014). Current status of the european oyster (ostrea edulis) and possibilities for restoration in the german north sea. *Bundesamt für Naturschutz*.

Ghassemi, H., Noshadi, E., & Rezaei, A. (2013). Determination of the lift and drag of 2d planing flat plate riding on the free surface. *Journal of Ocean, Mechanical and Aerospace-Science and Engineering*, *1*. https://www.researchgate.net/publication/304158077

Glantz, M., & Mun, J. (2011). Chapter 8 - projections and risk assessment. In M. Glantz & J. Mun (Eds.), *Credit engineering for bankers (second edition)* (Second Edition, pp. 185–236). Academic Press. https://doi.org/https://doi.org/10.1016/B978-0-12-378585-5.10008-9

Gueron, S., & Tessler, R. (2002). The fermat-steiner problem. *The American Mathematical Monthly*, *109*(5), 443–451. https://doi.org/10.1080/00029890.2002.11919871

Haelters, J., & Kerckhof, F. (2009a). Background document for ostrea edulis and ostrea edulis beds. *OSPAR commision*.

Haelters, J., & Kerckhof, F. (2009b). Background document for ostrea edulis and ostrea edulis beds.

Haure, J., Penisson, C., Bougrier, S., & Baud, J. (1998). Influence of temperature on clearance and oxygen consumption rates of the flat oyster ostrea edulis: Determination of allometric coefficients. *Aquaculture*, *169*(3), 211–224. https://doi.org/https://doi.org/10.1016/S0044-8486(98)00383-4

Hayward, P. J., & Ryland, J. S. (2017). *Handbook of the marine fauna of north-west europe*. Oxford University Press. https://doi.org/10.1108/RR-06-2017-0153

Heijningen, B. V., & Mungar, S. (2022). *Stability calculations oyster structure luchterduinen 2.0* (tech. rep.). Van Oord.

Hofland, B., & Wenneker, I. (2014). *Optimal wave gauge spacings for separation of incoming and reflected waves* (tech. rep.). Deltares. https://www.researchgate.net/publication/342927356

Hofstede, R. T., Williams, G., & Koningsveld, M. V. (2022). *The potential impact of human interventions at different scales in offshore wind farms* (Doctoral dissertation).

HUBS. (2019). *Injection molding: The definitive engineering guide* (tech. rep.). HUBS. https://www.hubs.com/nl/handleiding/spuitgieten/

Hughes, S. (1993). *Physical models and laboratory techniques in coastal engineering* (Vol. 7). World Scientific.

Ices ecosystem overviews baltic sea ecoregion 4.1 baltic sea ecoregion-ecosystem overview. (2019). https://doi.org/10.17895/ices.advice.5752

Jensen, B., Sumer, B., & Fredsoe, J. (1989). Turbulent oscillatory boundary layers at high reynolds numbers. *Journal of Fluid Mechanics*, *206*, 265–297. https://doi.org/https://doi.org/10.1017/S0022112089002302

Jonkman, S. N., Steenbergen, R. D. J. M., Morales-Nápoles, O., Vrouwenvelder, A. C. W. M., & Vrijling, J. K. (2017). *Probabilistic design: Risk and reliability analysis in civil engineering lecture notes cie4130*.

Journée, J., & Massie, W. (2001). *Chapter 12 wave forces on slender cylinders* (1st ed., Vol. 570). Delft University of Technology. https://ocw.tudelft.nl/wp-content/uploads/Part_4.pdf

Kamermans, P. (2018). Restoration of european flat oyster reefs in the north sea and wadden sea. *Nature conservation*.

Kamermans, P., van Duren, L., & Kleissen, F. (2018). European flat oysters on offshore wind farms: Additional locations : Opportunities for the development of european flat oyster (ostrea edulis) populations on planned wind farms and additional locations in the dutch section of the north sea. *Wageningen University and Research*. https://doi.org/10.18174/456358

Kamermans, P., Walles, B., Kraan, M., van Duren, L. A., Kleissen, F., van der Have, T. M., Smaal, A. C., & Poelman, M. (2018). Offshore wind farms as potential locations for flat oyster (ostrea edulis) restoration in the dutch north sea. *Sustainability (Switzerland)*, *10*. https://doi.org/10.3390/su10113942

Kardinaal, W. E. A., Bergsma, J. H., Dongen, L. G. J. M. V., & Driessen, F. M. F. (2021). Active restoration of native oysters in the north sea. *Bureau Waardenburg*. www.buwa.nl

Kennedy, R., & Roberts, D. (2006). Commercial oyster stocks as a potential source of larvae in the regeneration of ostrea edulis in strangford lough, northern ireland. *Journal of the Marine Biological Association of the United Kingdom*, *86*, 153–159. https://doi.org/10.1017/S0025315406012963

Keulegan, G. H., & Carpenter, L. H. (1958). Forces on cylinders and plates in an oscillating fluid. *Journal of research of the National Bureau of Standards*, *60*(5), 423–440.

Kirkegaard, J., Wolters, G., & Sutherland, R. (2011). *Users guide to physical modelling and experimentation*. CRC Press Taylor & Francis group Leiden.

Kuijper, W. (2013). Schelpdieren van het nederlandse noordzeegebied-ecologische atlas van de mariene weekdieren (mollusca). *De Strandloper*, *45*(3), 23–23.

Lallias, D., Arzul, I., Heurtebise, S., Ferrand, S., Chollet, B., Robert, M., Beaumont, A. R., Boudry, P., Morga, B., & Lapègue, S. (2008). Bonamia ostreae-induced mortalities in one-year old european flat oysters ostrea edulis: Experimental infection by cohabitation challenge. *Aquatic Living Resources*, *21*, 423–439. https://doi.org/10.1051/alr:2008053

Lengkeek, W., Didderen, K., Teunis, M., & Driessen, F. (2017). *Eco-friendly design of scour protection: Potential enhancement of ecological functioning in offshore wind farms* (17-001, Vol. 98). Bureau Waardenburg. https://edepot.wur.nl/411374

Lindeboom, H., Dijkman, E., Bos, O., Meesters, H., Cremer, J., de Raad, I., van Hal, R., & Bosma, A. (2008). *Ecologische atlas noordzee ten behoeve van gebiedsbescherming*.

Maar, M., Møller, E. F., Larsen, J., Madsen, K. S., Wan, Z., She, J., Jonasson, L., & Neumann, T. (2011). Ecosystem modelling across a salinity gradient from the north sea to the baltic sea. *Ecological Modelling*, *222*, 1696–1711. https://doi.org/https://doi.org/10.1016/j.ecolmodel.2011.03.006

Mankins, J. (1995). Technology readiness levels a white paper. *NASA*. https://aiaa.kavi.com/apps/group_public/download.php/2212/TRLs_MankinsPaper_1995.pdf

Mansard, E. P. D., & Funke, E. R. (1980). The measurement of incident and reflected spectra using a least squares method. https://doi.org/https://doi.org/10.9753/icce.v17.8

Marine, A. (2020). Reef cubes. Retrieved March 14, 2022, from https://www.arcmarine.co.uk/homepage/technology/#

Martens, J. (2019). Oyster cage stability at borssele owf. borssele wind farm zone (bwfs iii and iv). *Van Oord*.

Millican, P., & Helm, M. (1994). Effects of nutrition on larvae production in the european flat oyster, ostrea edulis. *Aquaculture*, *123*(1), 83–94. https://doi.org/https://doi.org/10.1016/0044-8486(94)90121-X

Molines, J., & Medina, J. R. (2015). Calibration of overtopping roughness factors for concrete armor units in non-breaking conditions using the clash database. *Coastal Engineering*, *96*, 62–70. https://doi.org/https://doi.org/10.1016/j.coastaleng.2014.11.008

Muus, B. J., Dahlström, P., & Terofal, F. (1973). *Meeresfische der ostsee, der nordsee, des atlantiks: In farben abgebildet u. beschrieben; biologie, fang, wirtschaftliche bedeutung*. BLV-Verlag-Ges.

Nakayama, Y. (2018). *Drag and lift*. Elsevier. https://doi.org/10.1016/b978-0-08-102437-9.00009-7

Noordzee-atlas : Voor het nederlands beleid en beheer. (1992). *Rijkswaterstaat*. https://puc.overheid.nl/doc/PUC_7854_31

NORA. (2017). Native oyster restoration alliance projects [[Online; accessed 26-October-2022]]. https://noraeurope.eu/restoration-projects/projects-overview/

ODNM. (2021). Mariene voorspellingen, operationele oceanografische voorspelling voor de noordzee [[Online; accessed 17-October-2022]]. https://odnature.naturalsciences.be/marine-forecasting-centre/nl/forecasts

of Encyclopaedia Britannica, T. E. (2021). Refraction. *Encyclopedia Britannica*. https://www.britannica.com/science/refraction

of South Hampton, U. (2022). Marineff – marine infrastructure effects initiative. https://noraeurope.eu/england-marineff-marine-infrastructure-effects-initiative/

Olsen, O. (1883). *The piscatorial atlas of the north sea, english channel, and st. george's channels.* Creative commons. https://wellcomecollection.org/works/up4zvcsn

Oord, V. (2014). Safe work practice manual handling, 5.

Ortiz, X., Rival, D., & Wood, D. (2015). Forces and moments on flat plates of small aspect ratio with application to pv wind loads and small wind turbine blades. *Energies*, *8*, 2438–2453. https://doi.org/10.3390/en8042438

Peakall, J., Ashworth, P., & Best, J. (1996). Physical modelling in fluvial geomorphology: Principles, applications and unresolved issues. *The scientific nature of geomorphology*, 221–253.

Perry, F., & Jackson, A. (2017). Native oyster (ostrea edulis. *Marine Information Network*. https://doi.org/10.17031/marlinsp.1146.2

Pogoda, B. (2019a). Current status of european oyster decline and restoration in germany. *Humanities*, *8*(1). https://doi.org/10.3390/h8010009

Pogoda, B. (2019b). Current status of european oyster decline and restoration in germany. *Humanities*, *8*, 9. https://doi.org/10.3390/h8010009

Polynomial curve fitting matlab polyfit mathworks benelux 2022. (2022). https://nl.mathworks.com/help/matlab/ref/polyfit.html

Programmable electromagnetic liquid velocity meter. (n.d.). https://www.deltares.nl/app/uploads/2016/04/Programmable-electromagnetic-liquid-velocity-meter.pdf

Raaijmakers, T., Roetert, T., & Steijn, P. V. (2017). Scour and scour mitigation hollandse kust (zuid) wind farm zone. *Deltares*.

Raspoort, A. (2022). *The design of a reef tile for the restoration of flat oyster reefs in the dutch north sea* (tech. rep.). Technical University Delft. http://resolver.tudelft.nl/uuid:666727e3-30dd-4734-9ee2-b0dbfc7b9afb

Raudkivi, A., Ettema, R., & Asce, A. (1985). *Scour at cylindrical bridge piers in armored beds* (tech. rep.). https://doi.org/https://doi.org/10.1061/(ASCE)0733-9429(1985)111:4(713)

Rijkswaterstaat. (2022). Waterinfo. https://waterinfo.rws.nl/#!/nav/index/

RVO. (2021a). Nieuwe routekaart windenergie op zee. https://www.rvo.nl/onderwerpen/windenergie-op-zee/routekaart (accessed: 16.10.2022)

RVO. (2021b). Windparken op de noordzee. https://www.rvo.nl/sites/default/files/2022-06/Routekaart-windenergieopzee-juni-2022.pdf

Sas, H., Kamermans, P., Have, T. V. D., Lengkeek, W., & Smaal, A. (2016). Shellfish reef restoration pilots voordelta the netherlands. *Bureau Waardenburg*. https://library.wur.nl/WebQuery/wurpubs/fulltext/405730

Schiereck, G. (2003). *Introduction to bed, bank and shore protection* (Vol. 399). Delft University Press.

Schiereck, G. (2007). *Concise overview of scale rules in coastal engineering* (tech. rep.). Technical University Delft.

Schupp, M. F., Kafas, A., Buck, B., K., G., Onyango, V., Stelzenmüller, V., Davies, I., & Scott, B. E. (2021). Fishing within offshore wind farms in the north sea: Stakeholder perspectives for multi-use from scotland and germany. *Journal of Environmental Management*, *279*. https://doi.org/10.1016/j.jenvman.2020.111762

Schutter, M. (2021). Ecoscour project borssele v. *Bureau Waardenburg*. www.buwa.nl

Schutter, M., Tonk, L., Kamermans, P., Kardinaal, E., & Hofstede, R. T. (2021). Ecoscour project borssele v. *Bureau Waardenburg*. www.buwa.nl

Sea, W., Fey, F., Brink, A. M. V. D., Wijsman, J. W. M., & Bos, O. G. (2010). Risk assessment on the possible introduction of three predatory snails (ocinebrellus inornatus, urosalpinxcinerea , rapana venosa) in the dutch wadden sea. *Ligthart*. http://www.exoticsguide.org/species_pages/u_cinerea.html%20http://upload.wikimedia.org/wikipedia/commons/f/fb/Rapana_Black_Sea_2008_G1.jpg

Shields, A. (1936). Application of similarity principles and turbulence research to bed-load movement.

Smaal, A., Kamermans, P., Kleissen, F., van Duren, L., & van der Have, T. (2017a). Flat oysters on offshore wind farms : Opportunities for the development of flat oyster populations on existing and planned wind farms in the dutch section of the north sea. *Wageningen University and Research*. https://doi.org/10.18174/418092

Smaal, A., Kamermans, P., Kleissen, F., van Duren, L., & van der Have, T. (2017b). Platte oesters in offshorewindparken (pop). *Wageningen Marine Research, Deltares, Bureau Waardenburg*. https://doi.org/10.18174/412950

Smaal, A. C., Kamermans, P., Have, T. M. V. D., Engelsma, M., & Sas, H. J. W. (2015). Feasibility of flat oyster (ostrea edulis l.) restoration in the dutch part of the north sea. *Wageningen University*. www.imares.wur.nl

Tönis, I., Stam, C.-J., & der Sar, R. V. (2013). Scour protection design basis gemini. *Van Oord Dredging and Marine Contractors*.

Uitvoeringsprogramma natuur. (2020). https://www.aanpakstikstof.nl/de-stikstofaanpak/documenten/kamerstukken/2020/12/8/bijlage-uitvoeringsprogramma-natuur

Van Rie, V. (2020). *Oyster broodstock structures in offshore wind farms* (tech. rep.). Delft, Delft University of Technology. http://resolver.tudelft.nl/uuid:652c435c-f01a-4077-b322-81da5a102488

van Boeijen, A., Daalhuizen, J., & Zijlstra, J. (2020). *Delft design guide: Perspectives, models, approaches, methods* (2nd). BIS Publishers.

van Oord, G. (1996). *Spreiding van steen in het stortproces van schuifstorters* (Doctoral dissertation). http://resolver.tudelft.nl/uuid:87326f1e-6524-43b7-81eb-95832e29fd2a

van Verkeer en Waterstaat, M., (RWS), R., & (WL), W. L. (1985). Harmonisatie noordzeebeleid waterkwaliteitsplan noordzee achtergronddocument 2a. *Rijkswaterstaat*. https://puc.overheid.nl/doc/PUC_81064_31

Voorhuis, R. (2021). REEF PROTECTION & RESTORATION, BUKTI (BALI) [[Online; accessed 12-October-2022]].

Walne, P. R. (1970). Seasonal variation of meat and glycogen content of seven populations of oysters ostrea edulis l. and a review of the literature.

Walne, P. (1958). Growth of oysters (ostrea edulis l.) *Journal of the Marine Biological Association of the United Kingdom*, *37*(3), 591–602.

Wolters, G., & Gent, M. V. (n.d.). *Hydralab iii: Guidelines for physical model testing of rubble mound breakwaters* (tech. rep.). Deltares. http://www.hydralab.eu/

Yildiz, H., Berber, S., Acarli, S., & Vural, P. (2011). Seasonal variation in the condition index, meat yield and biochemical composition of the flat oyster ostrea edulis (linnaeus, 1758) from the dardanelles, turkey. *Italian Journal of Animal Science*, *10*, 22–26. https://doi.org/10.4081/ijas.2011.e5

# List of Figures

# List of Tables

# A

# Introduction

## A.1. Relevant feasibility studies

**Table A.1:** Relevant feasibility studies for flat oyster restoration in Dutch offshore wind farms.

| Feasibility study | Content |
|---|---|
| *Feasibility of Flat Oyster (Ostrea edulis L.) restoration in the Dutch part of the North Sea* [Smaal et al., 2015] | – Fate of the North Sea flat oysters and the possible causes of extinction.<br>– Environmental conditions and restoration sites.<br>– Identification of the legal framework for restoration.<br>– Identification of stakeholder requirements.<br>– Program for pilot experiments. |
| *European flat oysters on offshore wind farms: additional locations* [Kamermans et al., 2018a] | – Potential areas for offshore wind farms in the Dutch Exclusive Economic Zone were analysed.<br>– Biotic and abiotic factors of importance for flat oyster survival, growth, reproduction and recruitment, were compared.<br>– Recommendations for best locations that are suitable for flat oyster restoration. |
| *Flat oysters on offshore wind farms* [Smaal et al., 2017a] | – The requirements that flat oysters make on their environment have been identified.<br>– Identification of crucial preconditions for the development of flat oyster beds on wind farms.<br>– Recommendations for best locations that are suitable for flat oyster restoration. |
| H*ow to deploy adult European flat oysters to establish an initial source population for reef recovery: methods and bottlenecks* [Belzen et al., 2021] | – The experiments and measurements performed aim to better understand the species-specific tolerance to sediment dynamics and hydrodynamics that can be encountered.<br>– Provide input for the development of the outplacement methodology (Which adhesives and substrates to use, logistics).<br>– Investigation to various possibilities for deployment of the adult oysters (loose, fixed). |
| *Offshore Wind Farms as Potential Locations for Flat Oyster (Ostrea edulis) Restoration in the Dutch North Sea* [Kamermans et al., 2018b] | – Presents results to determine suitability of wind farms for flat oyster restoration.<br>– Provides recommendations for pilot studies. |
| *Platte oesters in offshore windparken (POP)* [Smaal et al., 2017b] | – Possible developments regarding flat oyster restoration in existing and planned offshore wind farms in the Netherlands.<br>– Environmental requirements for flat oysters. |

## A.2. Pilot projects

The first pilot project for oyster restoration started in 2016 in the Voordelta, a coastal area of the North Sea. The pilot project consisted of three elements for restoration of oysters. The three elements were placed at two locations with different environmental conditions. The first element consists of cages of different mesh sizes with oysters inside. These cages are placed in larger racks to ensure stability and protection. The second element consists of empty mussel shells and settling plates, which are distributed along the racks. These empty shells serve as settlement substrate for oyster spat. The oyster racks and reef domes have been installed using cranes on the seabed, which consists of soft sandy material. Since 2016, several monitoring and maintenance visits have been made to the pilot project [Sas et al., 2016]. During these monitoring visits, the main observation was that the cage structures had largely sunk into the soft sandy sediment. This resulted in high mortality rates of oysters due to suffocation. However, the oysters did seem to be disease free, which was promising.

In 2018 three pilot projects have started; Luchterduinen and Borkum Reef Ground. In Luchterduinen, three elements were used in the pilot project. The first element are three oyster racks in which flat oysters are placed. The second element consists of six substrate racks in which different substrate materials are placed. Finally, two reef domes are included in the design to facilitate the placement of the oyster racks and to serve as additional protection. For the installation a heavy deck crane was used [Didderen et al., 2019a]. During the monitoring visits, some time after installation, the main observations were that the oyster racks had largely sunk into the soft sandy sediment. This resulted in high mortality rates of oysters due to suffocation. However, these oysters did seem to be disease free as well, which was promising.

The pilot at Borkum Reef Ground consisted of four elements. First approximately 80 thousand live flat oysters were deployed. Second, four research racks, with each four cages filled with flat oyster attached to them were installed at the seabed. Third, nine artificial 3D reef structures with flat oysters attached to them were also installed at the seabed. Lastly, approximately twelve square meters of empty mussels shells were deployed. The seabed in both the pilot site and the reference area generally consisted of a mixture of sand and small patches of gravel and shell fragments. The oyster racks and the reef structures were placed on the seabed using cranes. During monitoring visits at the site, some time after the installation, the main observations were that the racks partly got clogged, which can lead to suffocation of the oysters, but the research racks did remain stable a the hard substrate [Didderen et al., 2020], [Didderen et al., 2018], [Kardinaal et al., 2021].

At Borssele offshore wind farm also two pilot projects have been executed. At Borssele III & IV and at Borssele V. At Borssele III & IV, the 'Blauwwind' concept has been tested. The Blauwwind concept consist of a large and heavy concrete plate on which were 8 cages filled with oyster placed. Four of these structures were placed on the scour protection (hard substrate) from monopiles using cranes [Martens, 2019]. No report with the results of this project has been made available yet.

In October 2020, four oyster brood stock structures are placed at Borssele V. These structures have a terraced shape, composed of horizontal concrete plates separated by steel spacers. 250 live adult flat oysters were attached to the each structure with glue. Two of the four structures have large holes in the horizontal plates, which means that they are perforated. The other two structures have no holes in the horizontal plates, so they were solid. The four structures were placed using cranes, at the scour protection of the innovation site Borssele V (hard substrate) [Schutter et al., 2021]. The main observation, during monitoring visits appears to be that the horizontal plates of the structure attract sedimentation, which leads to suffocation of the oysters.

Currently, several new restoration projects are already being planned and prepared for implementation. In Luchterduinen, a number of parties are working together to implement a second pilot project. Also a new restoration project is also in progress at Gemini.

## A.3. Technical Readiness Levels

**Table A.2:** TRL's explained [Mankins, 1995]

| TRL | Description |
|---|---|
| 1 | Research is carried out into the innovative idea and the basic principles of the innovation. This involves fundamental research and desk research. |
| 2 | The basic principles have been examined and the formulation of the technological concept and practical applications are now being considered. In this phase, experimental and/or analytical research is the main area of focus. |
| 3 | Research is carried out into the applicability of the concept on an experimental basis (experimental proof of concept). Hypotheses about different parts of the concept are tested and validated. |
| 4 | The proof-of-concept of the innovation is tested on a laboratory scale. The design, development and testing of the technological components take place in a laboratory environment. The basic technical components are integrated with each other to ensure operation. A prototype developed in this phase costs relatively little money and time to develop and is therefore still far from a final product, process or service. |
| 5 | Research is carried out into the operation of the technological concept in a relevant environment. This is the first step in demonstrating the technology. A prototype developed in this phase costs a relatively large amount of time and money and is not far removed from the final product or system. |
| 6 | The concept is extensively tested and demonstrated in a relevant test environment. This test environment is comparable to an operational environment, for example in a pilot plant. Testing takes place after technical validation in a relevant (test) environment. The concept provides insight into the operation of all components together. |
| 7 | The concept is tested and demonstrated in a user environment to prove its operation in an operational environment. The demonstration of the concept in a practical environment provides new insights for the eventual market application of the innovation. |
| 8 | In this phase, the innovation takes on its final design. The technological operation is tested and it is demonstrated that it meets the expectations, qualifications and standards. In addition, the financial frameworks for (mass) production and launch are determined. |
| 9 | The innovation is technically and commercially ready; production-ready and ready for launch in the desired market environment. Now that the overall development process is complete, the next step is to commercially introduce the product to the desired target group in the right market. |

## A.4. Assumptions

- Critical mass for oyster restoration is assumed to be 500 intact oysters per scour protection.
- Reinforced concrete is assumed to stay intact by the impact it endures due to the hit by the waterline and the scour protection.
- Flow induces by waves and current is assumed to act upon exactly the same direction.
- Lift coefficient value of 0.2 is assumed for behavioural prediction calculations.
- Bottom friction coefficient value of 0.6 is assumed for behavioural prediction calculations.
- Inertia force is neglected in behavioural prediction calculations
- Waves are assumed not to have an effect on the horizontal displacement of the concept during the fall, predicted in the behavioural prediction calculations.
- It is assumed that the concepts reach their equilibrium velocity instantly and remains constant for the entire fall, in the behavioural prediction calculations.
- It is assumed that only one side per concept gets hit during the landing in the behavioural prediction calculations.
- An angle of inclination of the seabed is 5 degrees is assumed in the behavioural prediction calculations

- The horizontal force equilibrium is overruled, because it is assumed that the concepts will not slide due to resistance of the armour rock.
- It is assumed that the considered difference in drop heights in the fall test have a minimal effect on the land locations of the concepts, based on physical model results.
- If a concept appeared to be unstable twice for the same conditions in the stability test in physical modelling, it was assumed that the threshold of motion of that concept was reached.
- The horizontal displacement in the x direction during the fall test in physical modelling is assumed to be dominant over the horizontal displacement in the z direction, for the definition of the maximum positioning accuracy during the fall per concept.
- It is assumed that the change in velocity near the bed caused by the boundary layer does not have an effect on the total horizontal displacement of the concept during the fall, in the result analysis of the fall test.
- The second order polynomial extrapolation method is assumed to be more accurate for a prediction of the concept movement in the water column than the linear extrapolation method, in the result analysis of the fall test.
- Per concept a certain amount of surface is assumed to be suited for the oysters to be attached to, in the result analysis of the land test.
- During physical modelling, it is assumed that the parabolic damper allowed minimal reflection, resulting in neglecting the reflection coefficient of the generated waves.

# B

# Concept design

## B.0.1. Environmental conditions

European flat oysters exist within certain limits of abiotic factors and biotic factors. Based on the environmental conditions for a flat oyster habitat, design criteria and design requirements concerning the ecological aspects, can be defined [Smaal et al., 2017b]. These specific environmental conditions for flat oysters are addressed further in this section and are linked to (offshore wind farms in) the Dutch North Sea conditions. The environmental conditions include; substrate, water depth, water temperature, flow velocity, oxygen content, salinity, food concentration, and predation.

**Substrate**

Research has shown that coarse sand is unsuitable for the growth of the flat oyster. Fine sand is only moderately suitable. Firm silty sand, silty gravel with shells and rocks are suitable to act as substrate for the growth of flat oysters [Smaal et al., 2017a] [Kamermans et al., 2018a].

The natural substrate of the North Sea consists almost solely of fine sand. The substrate around monopiles of wind turbines is covered with scour protection (rocks), which consists of large rocks (stones). Therefore the substrate at offshore wind farms is suitable for flat oysters to grow on.

**Water depth**

The offshore and near shore areas of the Dutch North Sea have a water depth of between 10 to 40 meters deep [Lindeboom et al., 2008]. Flat oysters optimal living conditions occur in areas with a depth range between 0 until 40 meters deep [Lengkeek et al., 2017]. Flat oysters can survive at a maximum depth of 80 meters [Hayward and Ryland, 2017].

**Water temperature**

Adult oysters can survive at temperatures varying between 3 °and 30 °C [Child and Laing, 1998], [Haure et al., 1998]. The water temperature is mainly relevant for the reproduction phase of a flat oyster. Research has shown that larvae can survive within a range between 12.5 °and 27.5 °C, but show optimal growth at temperatures between 20 °and 27.5 °C. Spat can grow at temperatures varying between 12.5 °and 27.5 °C [Davis and Ansell, 1962]. In the offshore and near shore areas of the Dutch North Sea, the average minimum temperature is 3 °C and the maximum temperature is 18 °C [NZa, 1992]. The conditions in the Dutch North Sea therefore are suitable for the survival and growth of the adult oyster, but can cause limitations for the reproduction.

**Flow velocity**

The type of substrate on which the flat oyster is found is dependent on the flow velocity. Oysters are less able to attach themselves to soft substrate than to hard substrate [Perry and Jackson, 2017]. The allowed flow velocities for oysters on soft substrates are considerably lower than those for hard substrates. On soft substrates, oysters live at flow rates between 0 and 0.25 m/s, with the optimum flow velocity of 0.03 m/s. This is based on research studies covering the Eastern Scheldt in 1961 [Drinkwaard, 1961].

Historical data show that flat oysters also occur at much higher flow velocities [Gercken and Schmidt, 2014]. Based on these historical data and information from nautical maps, an optimal flow velocity is estimated between 0.25 and 0.6 m/s for the flat oyster [Smaal et al., 2017a]. Higher flow velocities may cause difficulties for larvae to settle on the substrate. Lower flow velocities may result in sedimentation, which will lead to buried oysters. Oysters can excavate themselves up to a certain level, but too high a sedimentation rate will lead to mortality of the oysters [Belzen et al., 2021]. The flow velocities near the bed at the Dutch North Sea comply lay within the range of 0.25 and 0.6 m/s. Only during storm conditions the flow velocities may exceed a value of 0.6 m/s [Tönis et al., 2013].

**Oxygen content**
The oxygen contents in water are essential for the survival of the flat oyster. Flat oysters can survive for some time without oxygen, because they are adapted to temporary dry periods at low tide in which they cannot filter oxygen from the water [Smaal et al., 2017a]. The oxygen consumption rates of flat oysters increase with temperature [Haure et al., 1998]. Consequently, the oysters can survive without oxygen for longer periods of time at low temperatures than at warmer temperatures. This ensures that the oysters can be stored dry for a while, depending on the temperature. In the North Sea there, there is a sufficient level of oxygen in the water [van Verkeer en Waterstaat et al., 1985]. However, if an oyster is buried due to sedimentation, this can cause the oyster to suffocate from a lack of oxygen.

**Salinity**
Salinities between 22.5 and 30 ppt (parts per thousand) are considered optimal for larval growth. At a salinity of 20 ppt, larval growth slows down significantly compared to higher salinities, and the setting intensity is reduced. Environments with a salinity of less than 17.5 ppt are no longer suitable for the growth of flat oysters [Davis and Ansell, 1962] Salinity levels in the North Sea are approximately 30 ppt and therefore suitable for flat oyster growth [Maar et al., 2011].

**Food concentration**
The suspended matter content in water is essential for the growth of the flat oyster. Oysters filter suspended matter from the sea, from which they obtain their nutrients. Nutrient availability is expressed as the amount of chlorophyll per litre. The amount of nutrients should be at least 0.5 $\mu$g/l for optimum conditions for the flat oyster [Millican and Helm, 1994].

In the Dutch North Sea, the availability of nutrients is in the range of 0.5 $\mu$g/l. The availability increases closer to the coast. The conditions are therefore suitable for the growth of flat oysters [Smaal et al., 2017b].

**Predation**
For oysters to survive, predation must be kept to a minimum. Larvae and young oysters can be particularly vulnerable to predation as their shells are not yet fully developed [Gercken and Schmidt, 2014].

Predators that can pose a threat to the flat oyster in this early stage of its life are; starfish, whelk, dogwhelk, shore crab, edible crab, the European sting winkle, the Atlantic oyster drill and Japanese oyster drill. From those predators, starfish and crabs are generally most common and most mobile in the Dutch North Sea. These predators are also found near offshore wind farms. Therefore it is necessary to incorporate measures to avoid these predators in the design of the brood stock structures as much as possible [Sea et al., 2010].

# C

# Behavioural prediction calculations

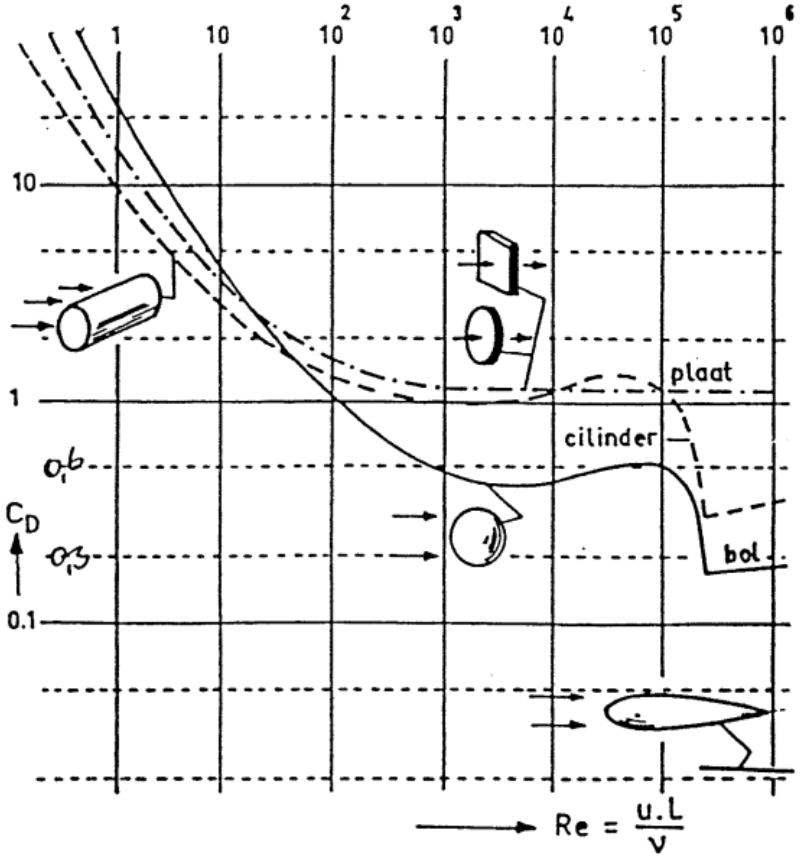


**Figure C.1:** $C_D$ values as function of Reynolds number for multiple shapes [van Oord, 1996]

## C.1. Calculation sheets

The calculations for the reference block concept with weight class 1 with corresponding input parameters are presented below;

## C.1.1. Fall situation

$$\Delta = \frac{\rho_s - \rho_w}{\rho_w} = \frac{2500 - 1025}{1025} = 1.44 \tag{C.1}$$

$$w = \sqrt{2\Delta \frac{Vg}{SC_D}} = \sqrt{2 \cdot 1.44 \cdot \frac{0.0092 \cdot 9.81}{0.044 \cdot 1.8}} = 1.81 m/s \tag{C.2}$$

$$tan(\varphi) = \frac{\bar{u}}{w} = \frac{0.40}{1.81} = 0.22 \tag{C.3}$$

$$x_h = tan(\varphi) d = 0.22 \cdot 29.5 = 6.51 m \tag{C.4}$$

$$F_G = (\rho_s - \rho_w) g V = (2500 - 1025) \cdot 9.81 \cdot 0.0092 = 133 N \tag{C.5}$$

$$F_D = \frac{1}{2} C_D \rho_w S w^2 = \frac{1}{2} \cdot 1.8 \cdot 1025 \cdot 0.044 \cdot 1.81^2 = 133 N \tag{C.6}$$

$$F_U = \frac{1}{2} C_D \rho_w S \bar{u}^2 = \frac{1}{2} \cdot 1.8 \cdot 1025 \cdot 0.044 \cdot 0.30^2 = 6.48 N \tag{C.7}$$

## C.1.2. Stability situation

**Force equilibria method**

$$F_{D-1} = \cos(5) \cdot \frac{1}{2} \cdot 1.5 \cdot 1025 \cdot 0.044 \cdot 3.31^2 = 368 N \tag{C.8}$$

$$F_{D-2} = \sin(5) \cdot \frac{1}{2} \cdot 1.5 \cdot 1025 \cdot 0.044 \cdot 3.31^2 = 32 N \tag{C.9}$$

$$F_{W-h} = \sin(5) \cdot (2500 - 1025) \cdot 9.81 \cdot 0.0092 = 12 N \tag{C.10}$$

$$F_{W-v} = \cos(5) \cdot (2500 - 1025) \cdot 9.81 \cdot 0.0092 = 133 N \tag{C.11}$$

$$F_{B-h} = 0.6 \cdot 133 = 80 N \tag{C.12}$$

$$\sum F_h = -F_{D-1} - F_{G-1} + F_B = -300 N \tag{C.13}$$

$$\sum F_v = -F_{D-2} + F_{G-2} = 100 N \tag{C.14}$$

$$M_D = -F_{D-h} \cdot \frac{1}{2} \cdot 0.21 - F_{D-v} \cdot 0.21 = -45 Nm \tag{C.15}$$

$$M_W = -F_{W-h} \cdot \frac{1}{2} \cdot 0.21 + F_{W-v} \cdot 0.21 = 15 Nm \tag{C.16}$$

$$\sum M = M_D + M_W = -30 Nm \tag{C.17}$$

**Table C.1:** Input parameter values for reference solid cube concept of weight class 1 for extreme hydraulic load conditions.

| Parameter | Value | Unit |
|---|---|---|
| $\rho_s$ | 1025 | kg/m$^3$ |
| $\rho_w$ | 2500 | kg/m$^3$ |
| $\bar{u_c}$ | 0.57 | m/s |
| $u_{w-1.5m}$ | 2.74 | m/s |
| $u_{r-1.5m}$ | 3.31 | m/s |
| V | 0.0092 | $m^2$ |
| S | 0.044 | $m^2$ |
| $H_{structure}$ | 0.21 | m |
| $W_{structure}$ | 0.21 | m |
| $C_D$ | 1.5 | - |
| $\mu$ | 0.6 | - |
| $z_0$ | 3 | m |

**Shields transport stages**
By performing experiments for the threshold of motion of stones in bed protections, seven transport stages were discerned [DHL, 1969].

0. No movement at all ($\psi_{cr} = 0.03$)
1. Occasional movement at some locations
2. Frequent movement at some locations
3. Frequent movement at several locations
4. Frequent movement at many locations
5. Frequent movement at all locations
6. Continuous movement at all locations ($\psi_{cr} = 0.056$)
7. General transport of grains

# D

# Concept observation test

In the Van Oord Yard in Moerdijk a modular water tank was used to perform the first test, the concept observation test. This test was intended to obtain better insight in the behaviour of the concepts during the fall in the water column and landing on the scour protection.

## D.1. Model set-up

In the water basin, no flow and waves were able to be generated, which results in that the tests were performed in still fresh water. The water tank is modular, which means that the tank can change in size. For the test the water tank had a size of 5 meters long, 2.5 meters wide and 2 meters high. Half of the long sides consisted of glass, allowing to see through the basin from one side.

**Figure D.1:** Modular water tank

This test is performed using a scale parameter of n=15. The basin was filled to a height of 1.9 meters. Which corresponds to a water depth of 28.5 meters in reality. At the bottom a layer of stones, with a $d_{50}$ of 20 mm (corresponding to a $d_{50}$ of 300 mm in reality) was placed. The scaled concepts were dropped multiple times from a height of 1.9 meters into the water column, to observe their behaviour during the fall and the landing.

On top of the water tank, a drop location was indicated, such that all the concepts were dropped from the same position. This location was set using a wooden board with a hole, of 6 cm in diameter, in it. This wooden board was placed on two iron beams, which were adjusted over the width on top of the water tank, see Figure D.2.

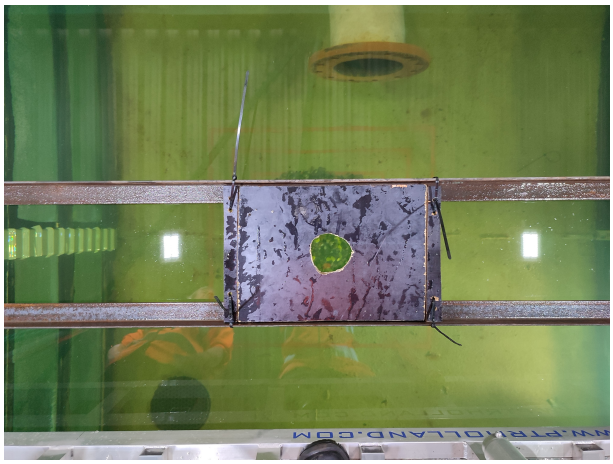

**Figure D.2:** Wooden board as drop location indicator

At the bottom a square calibration target of tape was created directly underneath the drop location, to indicate the horizontal movement during the fall, see Figure D.3(a). On top of this target, a layer of stones was placed. A part of the stones was painted yellow, to also create the square calibration target on the stones, see Figure D.3(b).

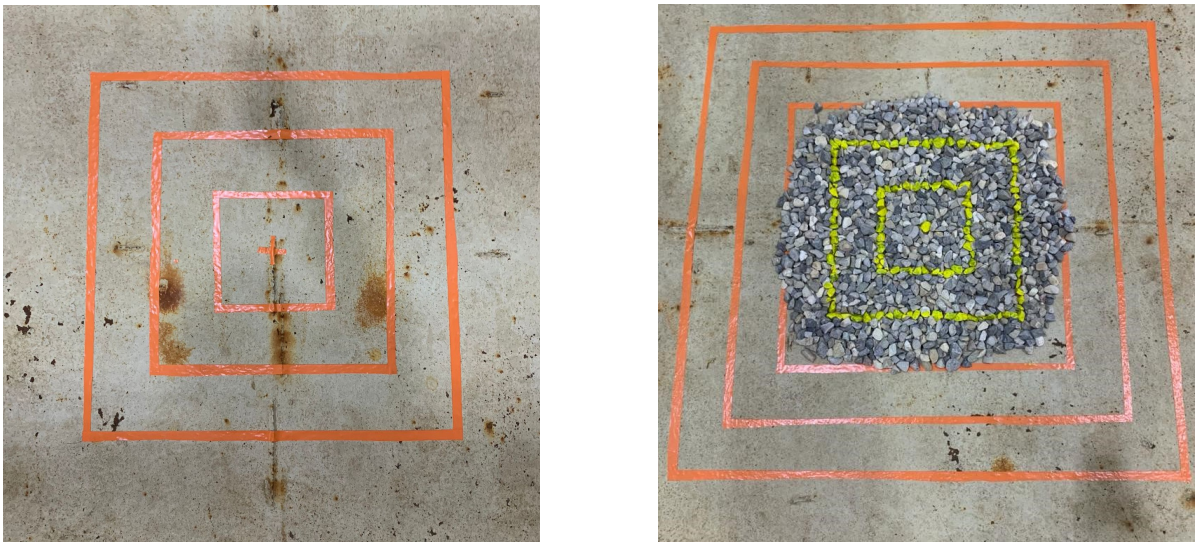

**(a)** **(b)**

**Figure D.3:** Calibration target on the bottom of the water tank, (a) without stones and (b) with (painted) stones on top.

## D.1.1. Instrumentation

**Video camera set-up**

To analyse the behaviour of the concepts during fall and landing, two camera's are used to capture it on video. The type of camera that was used to video tape the movement is GoPro Hero 7.

One GoPro was used to video the fall and landing from the side, near the bottom. The GoPro was adjusted to a aluminium beam, at a distance of 5 cm from the bottom (see Figure D.4a). This beam was placed in the water on the side of the tank.

The other GoPro recorded the behaviour of the concept during the entire fall from above. The camera's was installed next the drop hole on the backside of the wooden board (see Figure D.4b). This GoPro was therefore also placed in the water.

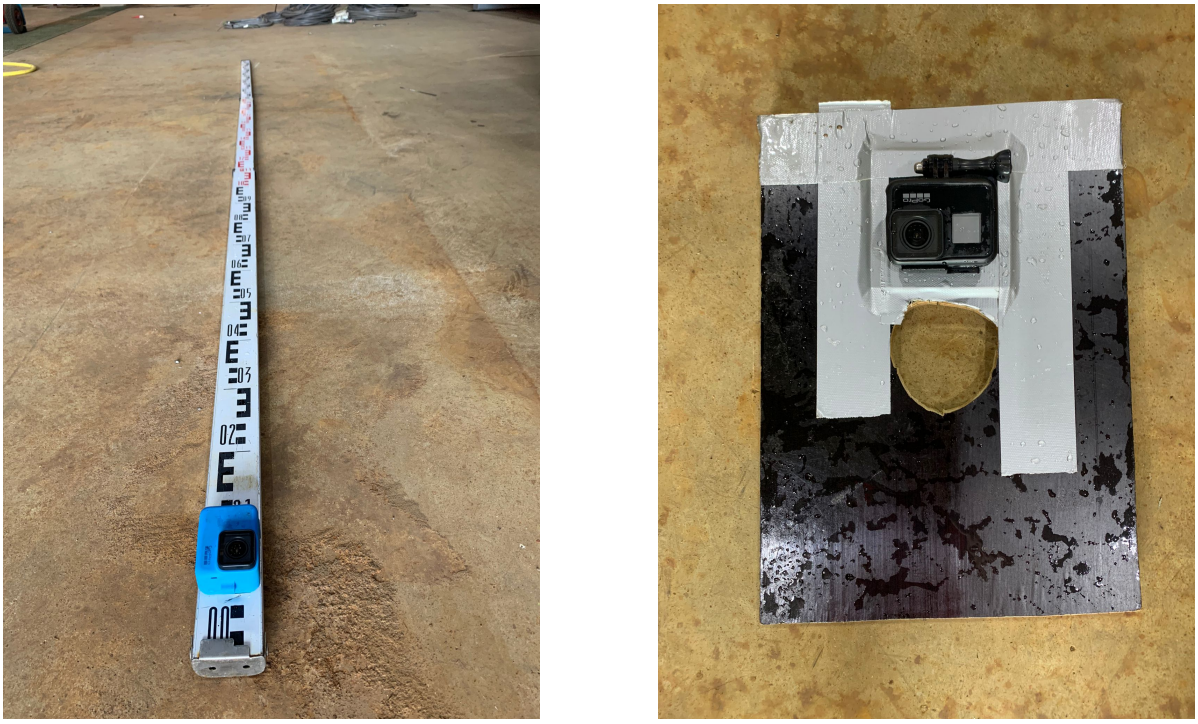

(a) (b)

**Figure D.4:** GoPro's used to record the falling concept, (a) from the side and (b) from above.

**Measuring bar**

To indicate the dimensions on the video recording, a measuring bar is placed at the other side of the side GoPro, inside the water tank, such that the measuring bar was visible behind the falling concepts. The measuring bar was made from a wooden beam and indicated 5 cm distances.

**Gangway**

To reach the drop location in the middle of the water tank at 2 metres high, a gangway was placed on top of the water tank. The gangway made it possible to move above the water tank. To reach the gangway, a ladder was installed next to the water tank.

**Fishing equipment**

When all the concepts were dropped in the water tank, the structures needed to be removed from the bottom again to allow the tests to be repeated. As the water depth was 1.9 meters, there was equipment needed to obtain the structures. Three types of material were used namely, a rake, a homemade grabber and a fishing net (see Figure D.5. It was important to be very careful when using this equipment, as the stones should not be moved to keep the calibration target intact.

(a)

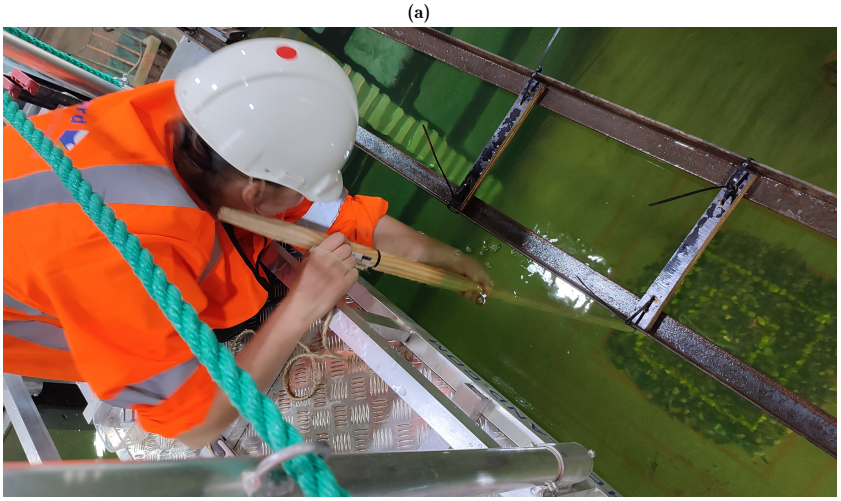

(b)

**Figure D.5:** (a) A rake, a homemade grabber and a fishing net, (b) used to retrieve the concepts from the bottom of the filled water tank

## D.1.2. Assessment method

1. The behaviour of the concepts during the fall.

   Based on the video recording from above and from the side, the behaviour during the fall will be assessed. The behaviour will be assessed on four different types of behaviour they can display, namely straight, spiral, swirling and irregular.

2. The total horizontal displacement of the concepts relative to each other during the fall.

   The total horizontal displacement during the fall for each concept will be determined using the video recording taken from above. The average total horizontal displacement per concept will be compared to each other, to obtain insight in which concepts show least horizontal displacement in still water during the fall relative to the other concepts.

3. The drag coefficient of the concepts.

   To determine the horizontal displacement during the fall more accurately in the behavioural prediction calculations and for future research on the concepts, the test was used to determine the drag coefficient per concept shape. The drag coefficient can be obtained by rewriting Equation 3.9. Therefor the equilibrium fall velocity is needed to determine the drag coefficient. This can be obtained using the camera recording from the GoPro from the side and the measuring bar.

4. The behaviour of the concepts during the landing.

   During the landing of the concepts on the scour protection, the concepts give a response. This response if of importance for the oysters that are attached to the structures, as they can get

damaged if too many sides are hit during the landing. Therefore, the jumping and bouncing of the concepts during the landing are observed and described.

## D.2. Test program

A description of how the test was carried out is outlined here.

**Preparation**

1. Prepare prototypes.
2. Make calibration target on bottom of tank with tape.
3. Lay stones on top of the calibration target.
4. Paint calibration target on stones.
5. Make modular water tank correct size
6. Install calibration stick.
7. Install side camera position.
8. Fill up tank with water.
9. Install gangway above tank.
10. Install drop location indicator.
11. Install top camera position.
12. Prepare concept grabber.

**Test run**

1. Lay out prototypes on gangway.
2. Turn on side camera.
3. Turn on top camera.
4. Drop first prototype through drop location.
5. Wait until concept has settled on the bottom.
6. Repeat from step 4 for all concepts.
7. Turn off top camera.
8. Turn off side camera.
9. Pick the concepts from the bottom of the tank with the grabber.
10. Repeat from step 1, until desired number of repeats is reached.

## D.3. Results & interpretation

The concept observation test was performed eleven times. The GoPro recording from above was used to analyse the fall and landing behaviour and horizontal displacement during the fall. The GoPro recording from the side was used to determine the equilibrium fall velocity per concept. Due to technical issues only ten recording could be used from the side camera.

### D.3.1. The behaviour of the concepts during the fall

Based on the video recordings from the side and from above made during the test, the behaviour of the concepts during the fall are described. The concepts were evaluated according to the behaviour they displayed during the fall in the modular water tank. Four categories have been defined, namely straight, spiral, swirl and irregular. A concept is classified as straight if it displays minimal to no rotation around its own horizontal and vertical axis during the fall and therefore falls relatively straight. A concept is classified as spiral if it rotates around its own horizontal axis during the fall. A concept is classified as swirling if it moves from side to side in horizontal direction during a fall. A concept is classified as irregular if it moves in an irregular pattern during the fall and therefore does not show an clear behaviour type. This indicates that it is difficult to predict how the concept moves during the fall in the water column and therefore difficult to predict the landing location.

Concepts are assessed on all categories using ++, +, 0. + is used when the behaviour is observed. - is used when the behaviour has not been observed. ++ is used when the behaviour concerned is highly

applicable. The results are shown in Table D.1. The cube framework shows only a straight falling behaviour, which indicates that the land location is relatively predictable. The Open tables show a straight and swirl falling behaviour, which also makes their land location relatively predictable. The Anchor short only displays a spiral falling behaviour. The Xblock, Tetrapod, Piebox framework and Anchor long show a irregular fall behaviour, which makes their land location more difficult to predict.

**Table D.1:** Falling behaviour of tested concepts in concept observation test

| | Straight | Spiral | Swirl | Irregular |
|---|---|---|---|---|
| Reference block | + | 0 | ++ | 0 |
| Xblock | 0 | 0 | + | + |
| Tetrapod | 0 | 0 | ++ | + |
| Cube framework | ++ | 0 | 0 | 0 |
| Piebox framework | 0 | 0 | ++ | ++ |
| Anchor long | 0 | + | + | ++ |
| Anchor short | 0 | ++ | 0 | 0 |
| Open table 1 | ++ | 0 | ++ | 0 |
| Open table 2 | + | 0 | ++ | 0 |
| Open table 3 | + | 0 | + | 0 |

## D.3.2. The total horizontal displacement of the concepts during the fall

Based on the video recordings made from above and the calibration target on the bottom, the horizontal distances between the drop location and the location where the concepts hit the bottom was determined. This distance is defined by determining the centre of mass of each concept after they landed per test. All the eleven images of which the distances for each test are determined are presented in Figure D.7. The results are presented in Table D.2 .

The test was repeated eleven times. The median distance of these eleven tests is determined (see Table D.2 and presented in a histogram, which is sorted from smallest to largest distance, in Figure D.6. From this histogram it is easily seen that the Anchor long displays the most horizontal displacement after the fall, followed by the tetrapod and the reference block. The Open Table 1 displays the least horizontal displacement after the fall, followed by the Open Table 2 and the Anchor short. In Figure D.6, the standard deviation per concept is also presented, which provides a (simplified) representation of the distribution of the data. The standard deviation shows that the Open Table 1 also has the smallest variation in the horizontal displacement distances obtained per test, in contrast with the reference block, which shows largest variations in horizontal displacement distances obtained per test.

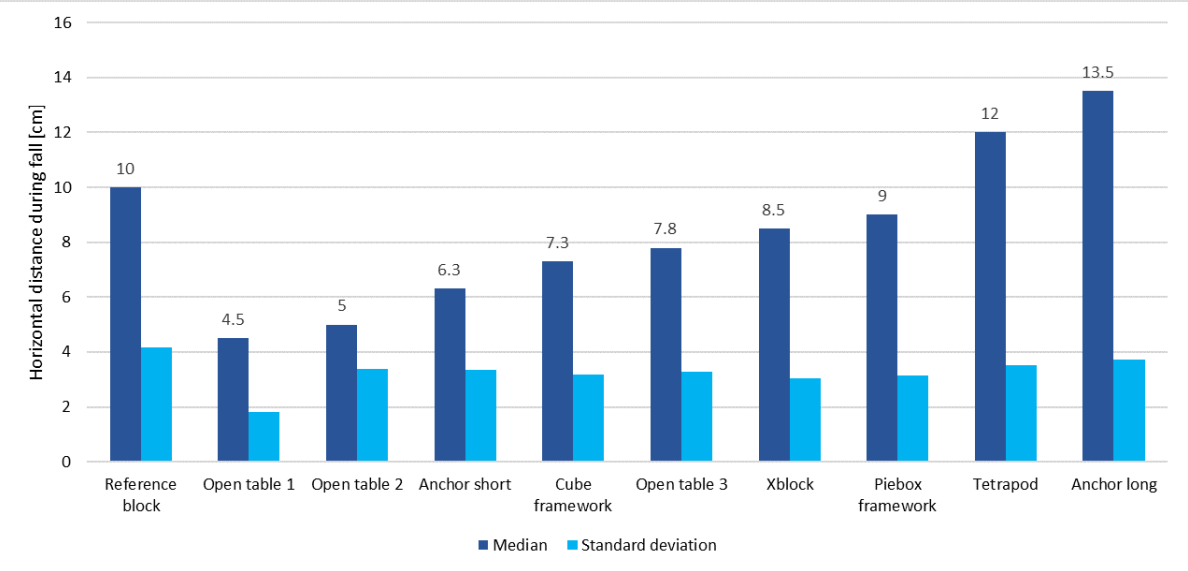


**Figure D.6:** Average distances from centre of target per concept (dark blue) and standard deviation of the distances measured in the different tests per concept (light blue), both given in cm

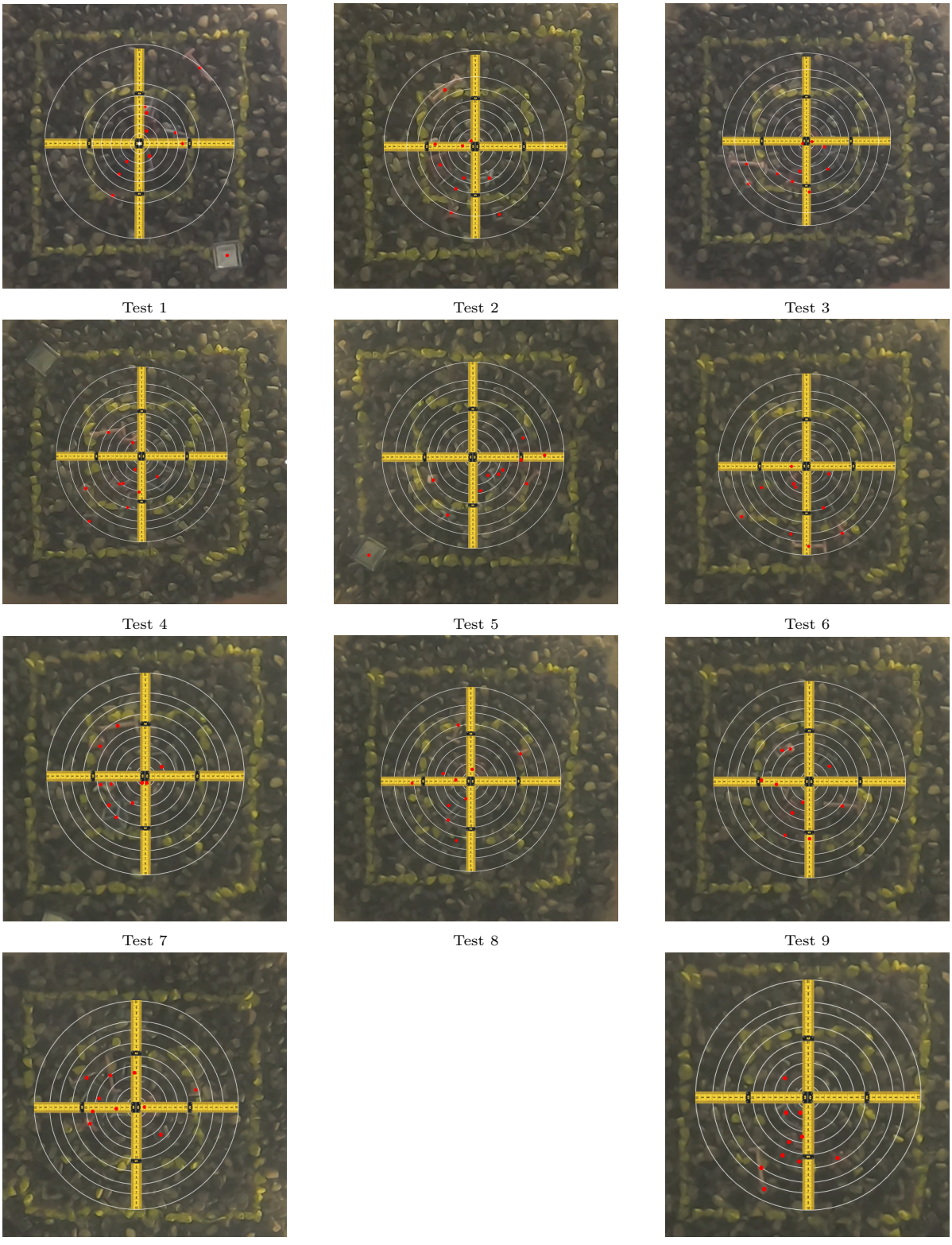

Test 1 Test 2 Test 3

Test 4 Test 5 Test 6

Test 7 Test 8 Test 9

Test 10 Test 11

**Figure D.7:** Movement during the fall in concept observation tests, defining the distance from target centre per concept, per test

**Table D.2:** Distances from centre of target per concept per test and averaged, given in centimetres

| **Test** | 1 | 2 | 3 | 4 | 5 | 6 | 7 | 8 | 9 | 10 | 11 | **Mean** |
|---|---|---|---|---|---|---|---|---|---|---|---|---|
| Reference block | 7.0 | 8.7 | 7.0 | 15.0 | 10.0 | 17.5 | 7.0 | 10.0 | 7.8 | 12.0 | 18.0 | 10.9 |
| Xblock | 7.8 | 7.0 | 7.3 | 13.0 | 13.5 | 5.3 | 9.0 | 3.5 | 10.0 | 8.5 | 11.0 | 8.7 |
| Tetrapod | 12.5 | 15.1 | 10.0 | 4.0 | 16.0 | 17.0 | 11.0 | 12.5 | 12.0 | 10.0 | 12.0 | 12.0 |
| Cube fr. | 8.0 | 3.0 | 4.5 | 3.5 | 12.0 | 10.0 | 10.0 | 7.3 | 5.0 | 7.0 | 11.5 | 7.4 |
| Piebox fr. | 9.0 | 5.5 | 12.0 | 9.7 | 5.0 | 15.5 | 9.5 | 13.0 | 8.5 | 7.0 | 8.5 | 9.4 |
| Anchor long | 20.0 | 14.0 | 15.0 | 10.0 | 13.5 | 18.0 | 12.0 | 13.0 | 8.3 | 8.0 | 15.0 | 13.3 |
| Anchor short | 3.5 | 1.5 | 10.0 | 8.3 | 7.0 | 3.5 | 1.0 | 6.3 | 7.0 | 11.5 | 5.5 | 5.9 |
| Open table 1 | 4.5 | 7.0 | 1.0 | 8.0 | 4.5 | 5.0 | 6.0 | 4.0 | 4.5 | 4.0 | 5.0 | 4.9 |
| Open table 2 | 3.0 | 8.5 | 1.0 | 8.0 | 11.0 | 5.0 | 1.0 | 3.0 | 7.0 | 2.0 | 7.0 | 5.1 |
| Open table 3 | 7.8 | 10.0 | 8.0 | 6.0 | 7.5 | 11.5 | 4.0 | 13.5 | 12.0 | 7.5 | 3.0 | 8.3 |

**Comparison location after fall with and without current and waves present**
The results from Figure D.6 were obtained during the test in the modular water tank, which contained still water. This test was performed at a scale 1:15. These results are compared to the averaged distances after the fall for each concept obtained in fall test at scale 1:15, presented in Figure 5.2(b). In the wave flume, current and waves were generated. When these two graphs are compared, it is observed that for all concepts the averaged horizontal displacement is larger in the tests performed in the wave flume, with moving water.

## D.3.3. The equilibrium velocity of the concepts

The equilibrium velocity (w) during the fall was determined, by using the side camera recordings. The equilibrium velocity is approximately reached after falling eight times the nominal diameter of the concept. As the water depth is 2 meters and the largest concept has a nominal diameter of approximately 10 centimetres, the equilibrium velocity is reached at 1.2 meter above the bottom. The last 40 centimetres in height of the fall of each concept was used to determine the falling velocity. The falling velocity was calculated using four locations points (every ten centimetres) of the concept in the water (read from the measuring bar) and the corresponding time in milliseconds. As the measuring bar was placed to the side of the water tank, the heights of the concepts in the water are not equal to the heights of the measuring bar as displayed in Figure D.8. To restore this perspective distortion, the heights per location point were converted. The actual heights of the concepts are 24.6 cm, 19 cm, 13.4 cm and 7.8 cm. The averaged velocity of the four measure points was defined per test. These velocities per test per concept were also averaged over the ten performed tests, to obtain an average falling velocity for each concept (see Table D.4). All the used location points, with corresponding times are given in Table D.3.

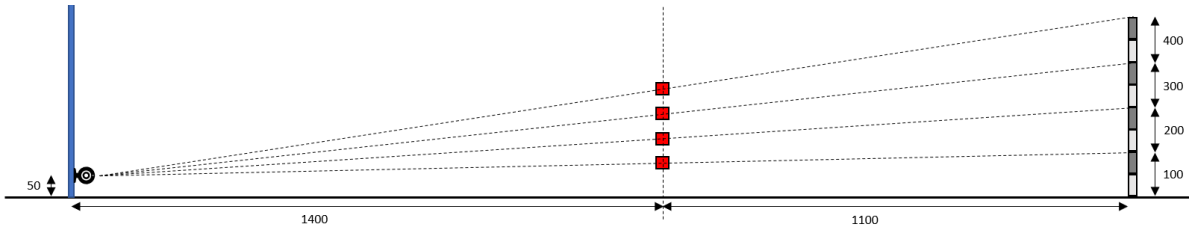


**Figure D.8:** Determining fall velocity. Distances given in mm

**Table D.3:** Equilibrium velocity per concept for each test and average, given in m/s

| **Test** | 1 | 2 | 3 | 4 | 6 | 7 | 8 | 9 | 10 | 11 | **Average** |
|---|---|---|---|---|---|---|---|---|---|---|---|
| Ref. block | - | 0.63 | 0.61 | 0.73 | 0.65 | 0.66 | 0.62 | 0.74 | 0.70 | 0.60 | 0.66 |
| Xblock | - | 0.44 | 0.46 | 0.51 | 0.47 | 0.49 | 0.48 | 0.47 | 0.46 | 0.44 | 0.47 |
| Tetrapod | - | 0.52 | 0.53 | 0.54 | 0.54 | 0.61 | 0.58 | 0.52 | 0.55 | 0.53 | 0.55 |
| Piebox fr. | - | 0.40 | 0.41 | 0.44 | 0.39 | 0.45 | 0.58 | 0.43 | 0.46 | 0.50 | 0.45 |
| Cube fr. | - | 0.35 | 0.36 | 0.34 | 0.35 | 0.35 | 0.35 | 0.38 | 0.35 | 0.35 | 0.35 |
| Anchor long | - | 0.51 | 0.49 | 0.49 | 0.50 | 0.50 | 0.49 | 0.48 | 0.48 | 0.47 | 0.49 |
| Anchor short | - | 0.51 | 0.46 | 0.46 | 0.51 | 0.51 | 0.47 | 0.47 | 0.48 | 0.47 | 0.48 |
| Open table 1 | - | 0.38 | 0.44 | 0.43 | 0.46 | 0.46 | 0.40 | 0.43 | 0.40 | 0.41 | 0.42 |
| Open table 2 | - | 0.54 | 0.39 | 0.58 | 0.42 | 0.58 | 0.64 | 0.38 | 0.42 | 0.48 | 0.49 |
| Open table 3 | - | 0.43 | 0.42 | 0.43 | 0.45 | 0.48 | 0.43 | 0.44 | 0.43 | 0.43 | 0.44 |

**Table D.4:** Averaged equilibrium velocity per concept, given in m/s

| | $\bar{w}$ [m/s] |
|---|---|
| Reference block | 0.66 |
| Xblock | 0.47 |
| Tetrapod | 0.55 |
| Piebox framework | 0.45 |
| Cube framework | 0.35 |
| Anchor long | 0.49 |
| Anchor short | 0.48 |
| Open table 1 | 0.42 |
| Open table 2 | 0.49 |
| Open table 3 | 0.44 |

**Drag coefficient of the concepts**

In Chapter 3, the drag coefficients per concept were estimated based on related literature. As further research into the design of the concepts might be necessary, it is useful to have a more accurate estimate of the drag coefficient. In the concept observation test, the equilibrium velocity per concept was determined (see Section D.3.3. The drag coefficient can be determined using Equation D.1.

$$C_D = \frac{2\Delta V g}{S w^2} \tag{D.1}$$

Based on the defined averaged equilibrium velocities per concept, the drag coefficient for each concept is determined using Equation D.1. For delta ($\Delta$) a value of 1.44 is used, for the volume (V) a value of $5.93 * 10^{-6}$ $m^3$ is used and the values used for the projected area of concept (S) are presented in Table D.6. In Table D.5, the determined drag coefficient per concept is shown, together with the estimated drag coefficient based on literature. The drag coefficient is dependent on shape and not size. Therefore the coefficients do not have to be scaled.

**Table D.5:** The calculated drag coefficient per concept, based on measured equilibrium velocity and estimated based on literature.

| **Drag coefficient,** $C_D$ [-] | Calculated | Estimated |
|---|---|---|
| Reference block | 1.2 | 1.8 |
| Xblock | 1.2 | 1.2 |
| Tetrapod | 1.2 | 0.9 |
| Piebox framework | 2.1 | 1 |
| Cube framework | 2.1 | 1 |
| Anchor long | 1.9 | 0.9 |
| Anchor short | 1.9 | 0.9 |
| Open table 1 | 2.3 | 1 |
| Open table 2 | 1.0 | 1 |
| Open table 3 | 1.3 | 1 |

**Table D.6:** The projected area of the concepts (S) for n=15

| | Projected area, S $[m^3]$ |
|---|---|
| Reference block | 0.000324 |
| Xblock | 0.000616 |
| Tetrapod | 0.000469 |
| Piebox framework | 0.000392 |
| Cube framework | 0.000635 |
| Anchor long | 0.000372 |
| Anchor short | 0.000387 |
| Open table 1 | 0.000408 |
| Open table 2 | 0.000711 |
| Open table 3 | 0.000680 |

## D.3.4. The behaviour of the concepts during the landing

All concepts showed similar behaviour during the landing. All the concepts, except the Open Tables, settled directly after landing, unless they land on an unstable side. If they land on an unstable side (i.e. a corner), the concept falls directly onto the stable side. The Open tables fall with their long side down. When this side touches the bottom, they directly flip a quarter turn, see Figure D.9.

(a) (b) (c) (d)

**Figure D.9:** Landing behaviour of Open tables concepts

# E

# Physical model set-up

## E.1. Model set-up

### E.1.1. Fall test

The model set-up for the fall test is presented in Figure E.1(a) from the side and Figure E.1(b) from above.

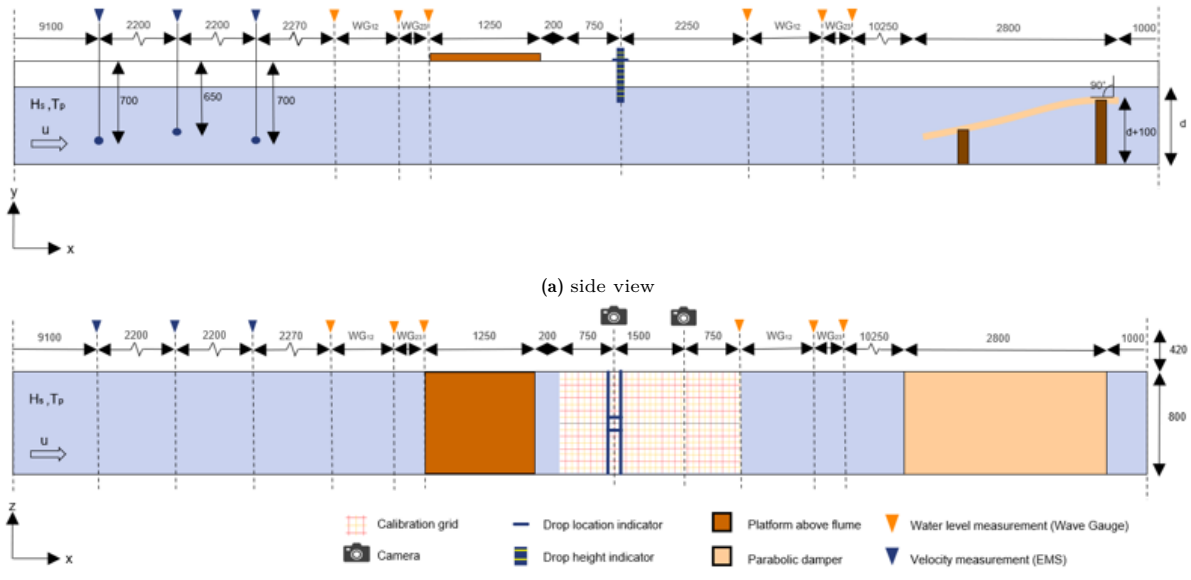


**(a)** side view

**(b)** top view

**Figure E.1:** Wave flume set-up for fall experiment including relevant parameters, with (a) side view, (b) top view.

### E.1.2. Land test

The model set-up for the fall test is presented in Figure E.2(a) from the side and Figure E.2(b) from above.

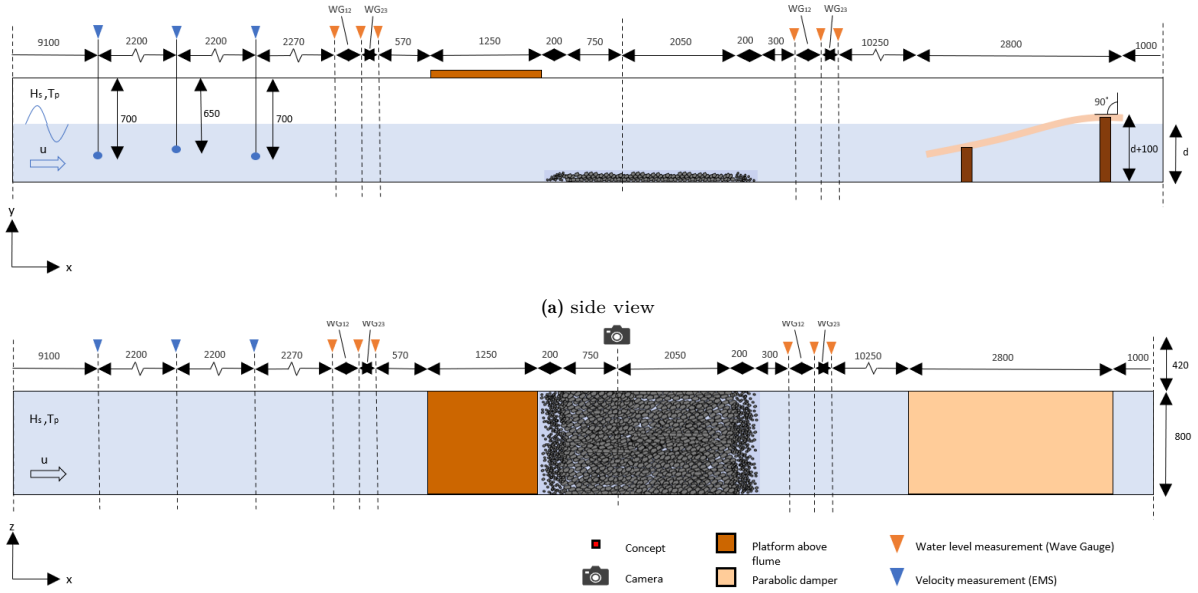


**(a)** side view

**(b)** top view

**Figure E.2:** Wave flume set-up for land experiment including relevant parameters, with (a) side view, (b) top view.

# E.2. Stability test

The flume set-up for the stability test is presented in Figure E.3. The same stone layer was used as in the land test.

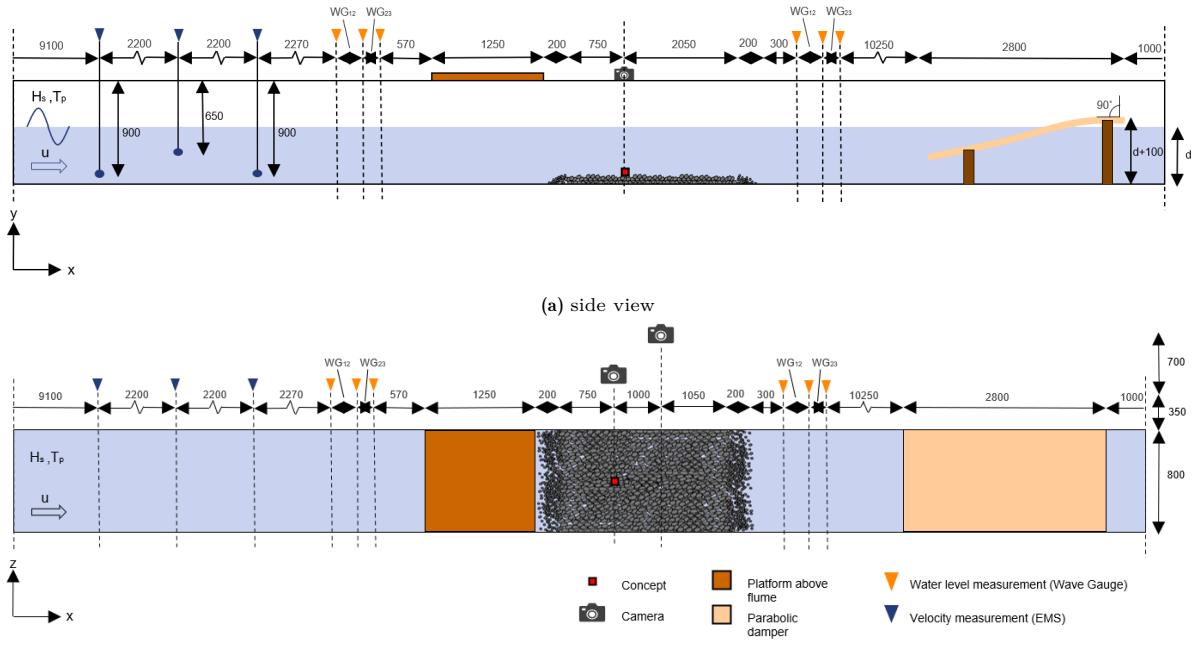


**(a)** side view

**(b)** top view

**Figure E.3:** Wave flume set-up for land experiment including relevant parameters, with (a) side view, (b) top view.

# E.3. Test runs

A description of how each test was carried out is outlined here. The order of the test was; fall test (scale 1:10), fall test (1:15), land test, stability test.

### E.3.1. General actions

For each new type of test is started, the parabolic damper and the wave gauges needed to be placed at the correct height. The top of parabolic damper had to be above the still water level by 10 cm. The wave gauges needed to be under water always, therefore the maximum and minimum water level were taken into account.

In order for the wave generator, to create the desired waves, a text file was prepared for each wave condition. This text file included the type of wave, reflection compensation, water depth, significant wave height, peak wave period, sigma and gamma of Jonswap spectrum and the duration of the generation. This text file was input for the matlab script created for the wave generator, which gave as output, the input files for the wave generator. These input files were imported in the wave generator programme, to create the desired waves by the generator.

It was an iterative process to obtain the correct flow velocity, with the corresponding water level. The intensity of the pumps, the drainage intensity and the height of the bulkhead just before the outlet, were the factors to take into account. This right combination was obtained per type of desired flow velocity by trial and error. The height of the bulkheads per test is provided in Table E.3.

DASYlab is the computer programme, which records and stores the Wave Gauge and EFM measurements. It stores the measurements per installed time step (0.005 seconds) in an ASC file. The DASYlab programme needed to start before each run was executed and turned off after each run.

### E.3.2. Fall test

The process of the fall tests is described in steps below. These steps are followed for the fall test performed at a scale of 1:10 and 1:15.

1. Install parabolic damper on the right position.
2. Install Wave Gauges on the right position.
3. Install EFM equipment on the right position.
4. Install side video camera and put photo camera on platform.
5. Place concepts and gripper on platform.
6. Turn on the pumps, open the outlet and install the bulkhead to create the correct water level and flow velocity.
7. Turn on wave generator.
8. Start the wave gauge and EFM measurements in DASYlab.
9. Start the recording of the video camera from the side.
10. Drop concept in the water from drop height 1.
11. Make a picture of the land location of the concept.
12. Grap the concept from the bottom with the gripper.
13. Repeat from step 10, until concept is dropped 10 times.
14. Stop the recording of the video camera from the side.
15. Stop the wave gauge and EFM measurements in DASYlab.
16. Repeat from step 8 for drop height 2 and 3.
17. Repeat from step 8 for other nine concepts.
18. Turn off wave generator.
19. Turn off pumps.
20. Close the outlet.

### E.3.3. Land test

The process of the Land test is described in steps below.

1. Install parabolic damper on the right position.
2. Install Wave Gauges on the right position.
3. Install stone layer on the bottom of the wave flume
4. Install side video camera.
5. Place concepts and gripper on platform.
6. Turn on the pumps, open the outlet and install the bulkhead to create the correct water level and flow velocity.
7. Turn on wave generator.
8. Start the wave gauge and EFM measurements in DASYlab.
9. Start the recording of the video camera from the side.
10. Drop concept in the water from above the waterline.
11. Grap the concept from the bottom with the gripper.
12. Repeat from step 10, until concept is dropped 10 times.
13. Stop the recording of the video camera from the side.
14. Stop the wave gauge and EFM measurements in DASYlab.
15. Repeat from step 8 for other nine concepts.
16. Turn off wave generator.
17. Turn off pumps.
18. Close the outlet.

### E.3.4. Stability test

The process of the stability test is described in steps below. The stone layer is still placed on the bottom of the flume.

1. Install parabolic damper on the right position.
2. Install Wave Gauges on the right position.
3. Install side video camera.
4. Place concepts and gripper on platform.
5. Turn on the pumps, open the outlet and install the bulkhead to create the correct water level and flow velocity.
6. Place concept on the stone layer, by dropping it from a small height above the bottom.
7. Start the recording of the video camera from the side.
8. Turn on wave generator for waves with storm conditions 1.
9. Start the wave gauge and EFM measurements in DASYlab.
10. Stop the recording of the video camera from the side.
11. Stop the wave gauge and EFM measurements in DASYlab.
12. Turn off wave generator.
13. Grap the concept from the bottom with the gripper.
14. Assess the concept on its behaviour.
15. Repeat from step 6, until all concepts are tested twice.
16. Assess which concepts showed contradicting behaviour during the two tests.
17. Repeat from step 6 for all concepts that showed contradicting behaviour.
18. Assess which concepts showed unstable behaviour and have reached their threshold of motion.
19. Set aside the concepts that showed unstable behaviour, these concepts will not be tested anymore.
20. Repeat from step 6 for other four storm conditions.
21. Turn off pumps.
22. Close the outlet.

# E.4. Prototypes

To use the chosen concepts on scale for the experiments, prototypes were made, for which some steps were taken. First the concepts were constructed in a 3D drawing program (software platform 360 Fusion). The concept designs in 360 Fusion were prepared for printing in 3D-printsoftware, Cura Ultimaker. This software prepares the designs for the 3D printer and also sets the scale for the designs, which enables the design to enlarge or reduce in total size. After the concepts were printed by the 3D printer, the printed concepts were used to make moulds of the shapes of the concepts. This entails collecting plastic cups, where a concept can fit in. A concept was placed in this cup and was then filled with liquid silicon until the concept is no longer visible. In which position the concept was placed in the cup was considered carefully per concept, as this defines how the mould was later filled. For the silicon, casting rubber with shore 25 was used. This type of silicone consists of two components, namely the base and the hardener. These two components have a mixing ratio of 1000:75 (by weight). The shore value determines the hardness of your silicone, so its flexibility and firmness. A shore of 25 indicates a rather firm silicone in order for the silicon not to tear when concepts were removed, but still flexible to get the shapes out. After approximately eight hours, the silicon has hardened and the printed concepts were removed from the silicon. To obtain the final concepts on scale, the moulds were filled with a filling material. This filling material had to correspond with the scaled density for the concepts.

The filling material that was used is Poly-Pur casting resin. Poly-Pur consists of two fluid components, which have have mixing ratio of 1:1 (by weight) and when it is mixed and dried it has a density of approximately 1170 $kg/m^3$. The desired density for the filling material should correspond to the density defined using scale rules (which is 2440 $kg/m^3$. This results in a weight of 48.8 grams for a concept with weight class 2 (50 kg) for scale n=10 and a weight of 14.5 grams for a concept with weight class 2 (50 kg) for scale n=15. The density of Poly-Pur is much lower than the desired density and therefore small leaden balls were added to the mixture in the moulds to increase the density. The ratio of Poly-Pur mixture and the leaden balls was approximately 1:1. The concepts were weighted after the Poly-Pur had hardened (after approximately 10 minutes). In case the concepts were still too light, extra leaden balls were added by making a small hole, adding the leaden ball in this hole and closing the hole using mouldable epoxy. This process is displayed in Figure E.4 for the reference block.

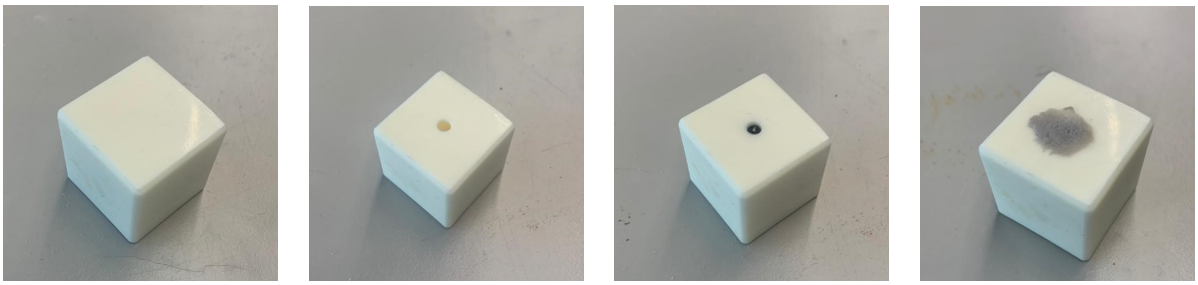

(a) (b) (c) (d)

**Figure E.4:** Steps to achieve the desired weight of the prototype

Not every concept can directly be used to make a mould. The cube framework, piebox framework and the xblock were concepts which cannot be made using one mould, because they cannot be removed from the silicon material as they will be closed in by the material. Therefore, the moulds for these concepts consist of two identical components. The 3D printed concepts for these shapes also consist of two identical components (see Figure E.5). When the parts of the concepts were made using moulds and the filling material, the two components of the concepts were combined together using superglue.

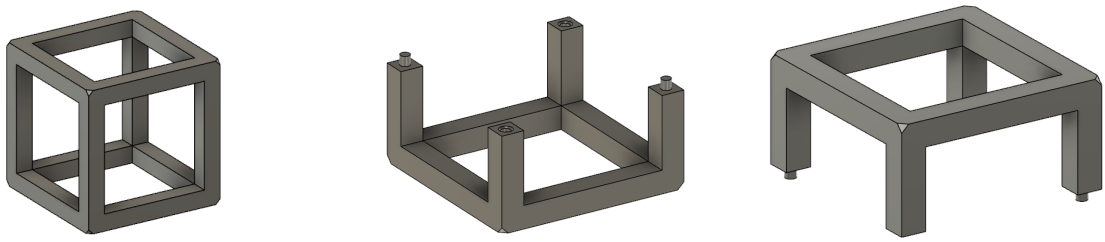

(a) (b) (c)

**Figure E.5:** Cube framework concept (a), composed of two components (b) and (c), allowing the concept to be constructed by using a mould

In the figures of the concepts created in 360 Fusion (Figure 3.8 and Figure E.5), it can be seen that the edges and corners are smoothed. This is done to minimize the stress at the corners to prevent crack formation [HUBS, 2019].

**Table E.1:** Dimensions of concepts that were tested in mm. Dimensions of Tetrapod concept are not given, because cannot be defined using the thickness, width, length, height.

| **Concept** | WC | Scale | Thickness | Width | Length | Height |
|---|---|---|---|---|---|---|
| Reference block | 2 | n=1 | | 270 | 270 | 270 |
| | | n=10 | | 27 | 27 | 27 |
| | | n=15 | | 13.5 | 13.5 | 13.5 |
| Cube framework | 2 | n=1 | 70 | 580 | 580 | 580 |
| | | n=10 | 7 | 58 | 58 | 58 |
| | | n=15 | 4.67 | 38.67 | 38.67 | 38.67 |
| Piebox framework | 2 | n=1 | 80 | 420 | 420 | 260 |
| | | n=10 | 8 | 42 | 42 | 26 |
| | | n=15 | 5.33 | 28 | 28 | 17.33 |
| Open table 1 | 2 | n=1 | 90 | 490 | 310 | 490 |
| | | n=10 | 9 | 49 | 31 | 49 |
| | | n=15 | 6 | 32.67 | 20.67 | 32.67 |
| Open table 2 | 2 | n=1 | 80 | 630 | 310 | 630 |
| | | n=10 | 8 | 63 | 31 | 63 |
| | | n=15 | 5.33 | 42 | 20.67 | 42 |
| Open table 3 | 2 | n=1 | 70 | 870 | 290 | 870 |
| | | n=10 | 7 | 87 | 29 | 87 |
| | | n=15 | 4.67 | 58 | 19.33 | 58 |
| Xblock | 2 | n=1 | 100 | 730 | 730 | 730 |
| | | n=10 | 10 | 73 | 73 | 73 |
| | | n=15 | 6.67 | 48.67 | 48.67 | 48.67 |
| Anchor short | 2 | n=1 | 100 | 570 | 1060 | 570 |
| | | n=10 | 10 | 57 | 106 | 57 |
| | | n=15 | 6.67 | 38 | 70.67 | 38 |
| Anchor long | 2 | n=1 | 100 | 500 | 1200 | 500 |
| | | n=10 | 10 | 50 | 120 | 50 |
| | | n=15 | 6.67 | 33.33 | 80 | 33.33 |

**Table E.2:** Dimensions of Tetrapod concept, given in mm

| **Concept** | WC | Scale | Length 1 arm | Diameter end of arm | slendering degree of arm |
|---|---|---|---|---|---|
| Tetrapod | 2 | n=1 | 300 | 100 | 5 |
| | | n-10 | 30 | 10 | 5 |
| | | n=15 | 20 | 6.67 | 5 |

# E.5. Flow generation

**Table E.3:** Bulkhead height per test, given in cm

| | Bulkhead height [cm] |
|---|---|
| Fall test 1 | 59 |
| Fall test 2 | 77 |
| Land test | 77 |
| Stability test SC1 | 35 |
| Stability test SC2 | 35 |
| Stability test SC3 | 25 |
| Stability test SC4 | 28 |
| Stability test SC5 | 28 |

# E.6. Wave generation

## E.6.1. Wave Gauge calibration

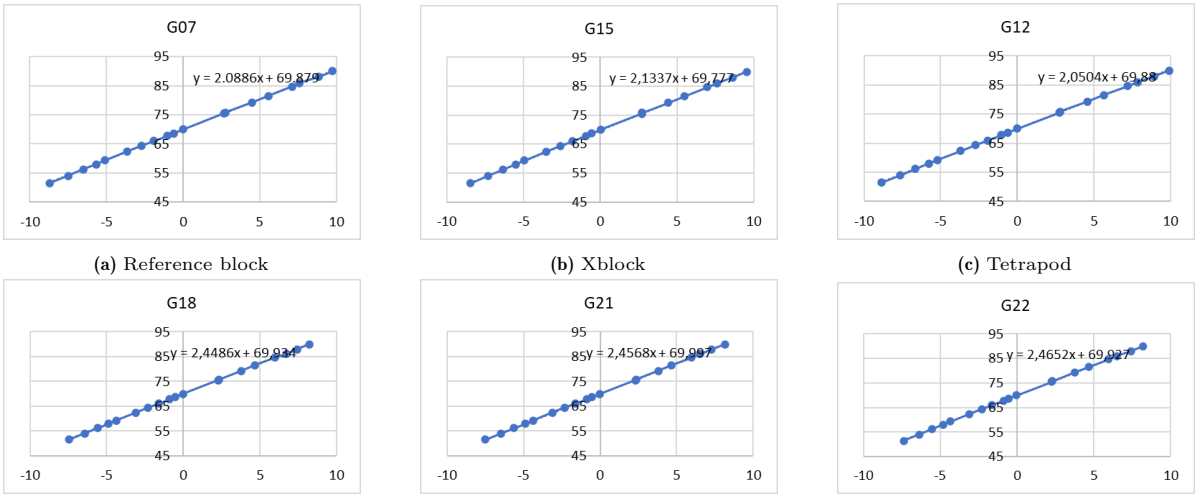


**(a)** Reference block **(b)** Xblock **(c)** Tetrapod

**(d)** Cube framework **(e)** Piebox framework **(f)** Anchor long

**Figure E.6:** Wave gauge calibration, voltage vs. elevation [cm]

# F

# Physical model results

## F.1. Fall experiment

### F.1.1. Test conditions

**Fall test scale 1:10**

**Table F.1:** Test conditions measured by DASYlab for fall experiment on scale 1:10

| **Fall test 1:10** | | $H_s$ *[m]* | $T_p$ *[s]* | $\bar{u}$ [m/s] |
|---|---|---|---|---|
| ***Drop height 1*** | Reference block | 0.093 | 2.6 | 0.096 |
| | Xblock | 0.093 | 2.6 | 0.097 |
| | Tetrapod | 0.095 | 2.6 | 0.097 |
| | Cube framework | 0.092 | 2.6 | 0.096 |
| | Piebox framework | 0.094 | 2.6 | 0.095 |
| | Anchor short | 0.093 | 2.7 | 0.096 |
| | anchor long | 0.094 | 2.6 | 0.096 |
| | Open table 1 | 0.095 | 2.6 | 0.097 |
| | Open table 2 | 0.096 | 2.6 | 0.097 |
| | Open table 3 | 0.095 | 2.6 | 0.096 |
| ***Drop height 2*** | Reference block | 0.094 | 2.6 | 0.097 |
| | Xblock | 0.094 | 2.6 | 0.097 |
| | Tetrapod | 0.094 | 2.6 | 0.097 |
| | Cube framework | 0.096 | 2.6 | 0.095 |
| | Piebox framework | 0.092 | 2.6 | 0.093 |
| | Anchor short | 0.096 | 2.6 | 0.095 |
| | anchor long | 0.092 | 2.7 | 0.096 |
| | Open table 1 | 0.095 | 2.6 | 0.096 |
| | Open table 2 | 0.093 | 2.6 | 0.097 |
| | Open table 3 | 0.093 | 2.6 | 0.096 |
| ***Drop height 3*** | Reference block | 0.094 | 2.6 | 0.097 |
| | Xblock | 0.093 | 2.7 | 0.096 |
| | Tetrapod | 0.094 | 2.7 | 0.098 |
| | Cube framework | 0.092 | 2.6 | 0.093 |
| | Piebox framework | 0.094 | 2.6 | 0.093 |
| | Anchor short | 0.094 | 2.7 | 0.097 |
| | anchor long | 0.093 | 2.7 | 0.096 |
| | Open table 1 | 0.095 | 2.6 | 0.096 |
| | Open table 2 | 0.095 | 2.6 | 0.096 |
| | Open table 3 | 0.094 | 2.6 | 0.096 |

**Fall test scale 1:15**

**Table F.2:** Test conditions measured by DASYlab for fall experiment on scale 1:15

| **Fall 1:15** | | $H_s$ *[m]* | $T_p$ *[s]* | $\bar{u}$ [m/s] |
|---|---|---|---|---|
| ***Drop height 1*** | Reference block | 0.062 | 2.3 | 0.073 |
| | Xblock | 0.063 | 2.2 | 0.072 |
| | Tetrapod | 0.062 | 2.3 | 0.072 |
| | Cube framework | 0.063 | 2.2 | 0.071 |
| | Piebox framework | 0.062 | 2.2 | 0.071 |
| | Anchor short | 0.060 | 2.2 | 0.073 |
| | anchor long | 0.062 | 2.2 | 0.071 |
| | Open table 1 | 0.061 | 2.1 | 0.072 |
| | Open table 2 | 0.062 | 2.2 | 0.072 |
| | Open table 3 | 0.060 | 2.2 | 0.073 |
| ***Drop height 2*** | Reference block | 0.063 | 2.2 | 0.073 |
| | Xblock | 0.063 | 2.2 | 0.072 |
| | Tetrapod | 0.062 | 2.1 | 0.072 |
| | Cube framework | 0.062 | 2.1 | 0.072 |
| | Piebox framework | 0.062 | 2.3 | 0.071 |
| | Anchor short | 0.058 | 2.3 | 0.072 |
| | anchor long | 0.063 | 2.2 | 0.072 |
| | Open table 1 | 0.061 | 2.2 | 0.072 |
| | Open table 2 | 0.062 | 2.3 | 0.073 |
| | Open table 3 | 0.061 | 2.1 | 0.071 |
| ***Drop height 3*** | Reference block | 0.063 | 2.3 | 0.071 |
| | Xblock | 0.062 | 2.3 | 0.072 |
| | Tetrapod | 0.061 | 2.2 | 0.072 |
| | Cube framework | 0.063 | 2.2 | 0.072 |
| | Piebox framework | 0.063 | 2.2 | 0.073 |
| | Anchor short | 0.063 | 2.3 | 0.071 |
| | anchor long | 0.063 | 2.2 | 0.073 |
| | Open table 1 | 0.060 | 2.2 | 0.073 |
| | Open table 2 | 0.062 | 2.3 | 0.071 |
| | Open table 3 | 0.061 | 2.2 | 0.071 |

## F.1.2. Location after drop

### Reference block

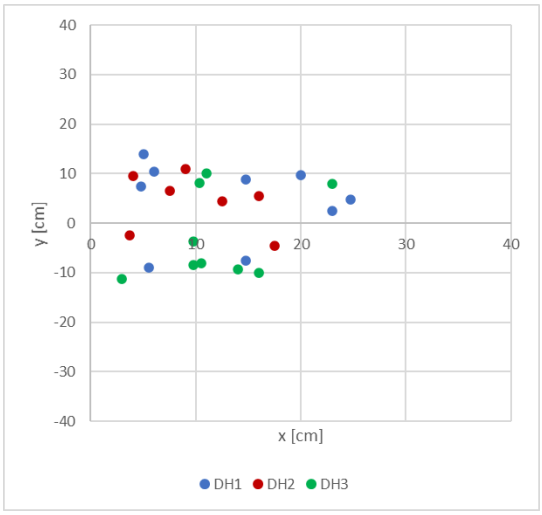


**(a)** Fall experiment scale 1:10

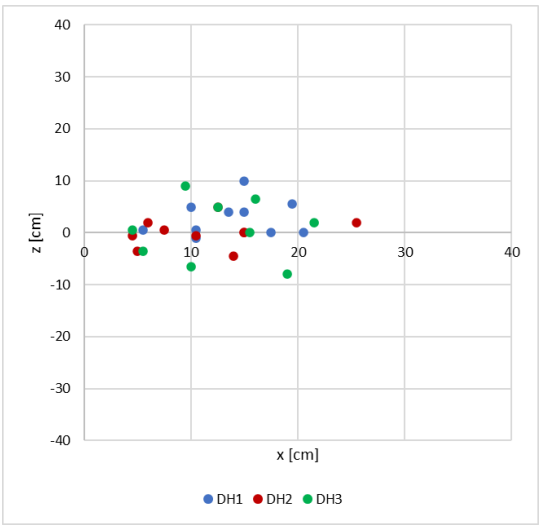


**(b)** Fall experiment scale 1:15

**Figure F.1:** Locations (x,z) of Reference block directly after fall, given in cm.

### Xblock

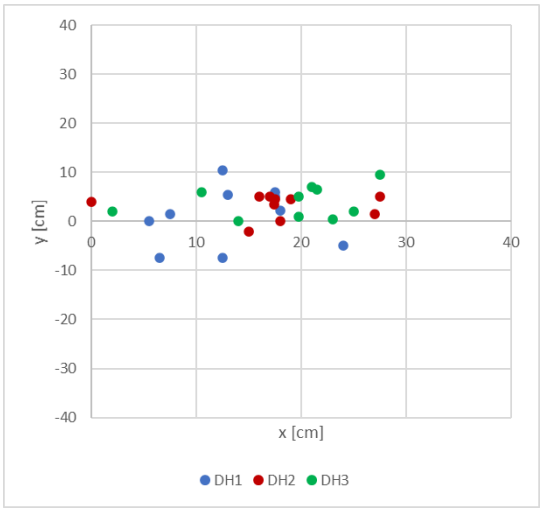


**(a)** Fall experiment scale 1:10

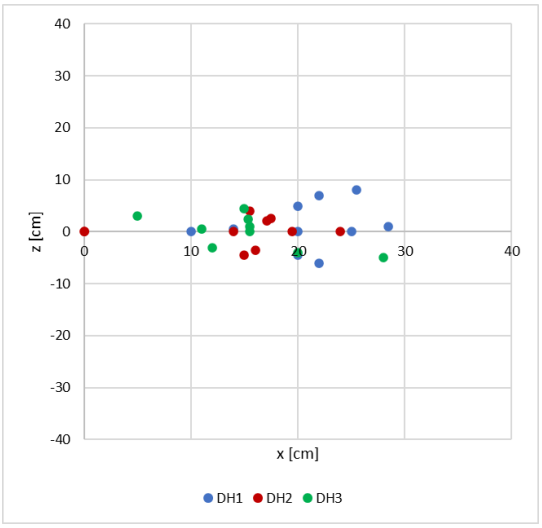


**(b)** Fall experiment scale 1:15

**Figure F.2:** Locations (x,z) of Xblock directly after fall, given in cm.

### Tetrapod

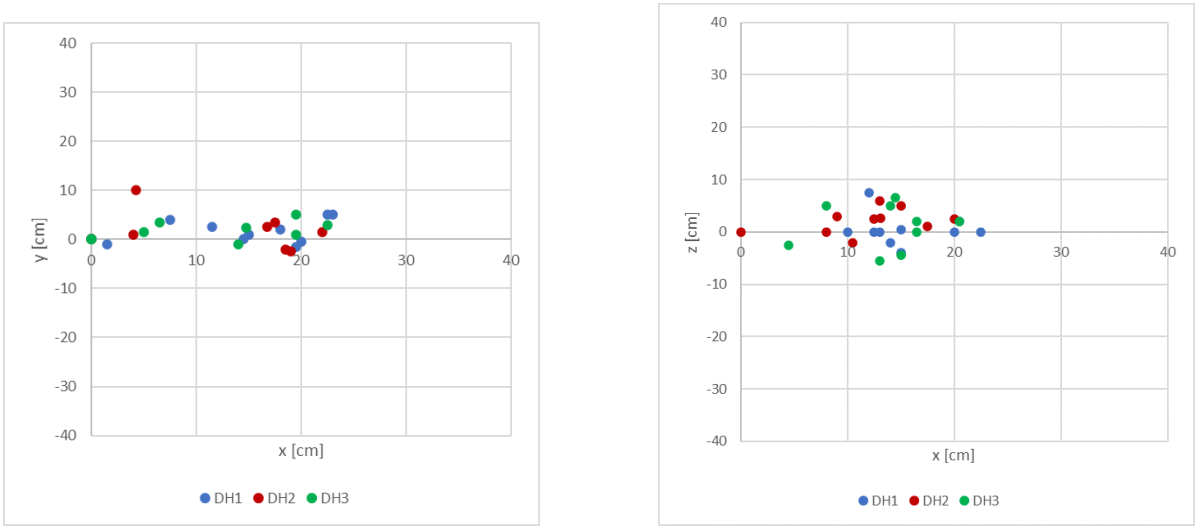


**(a)** Fall experiment scale 1:10

**(b)** Fall experiment scale 1:15

**Figure F.3:** Locations (x,z) of Tetrapod directly after fall, given in cm.

### Cube framework

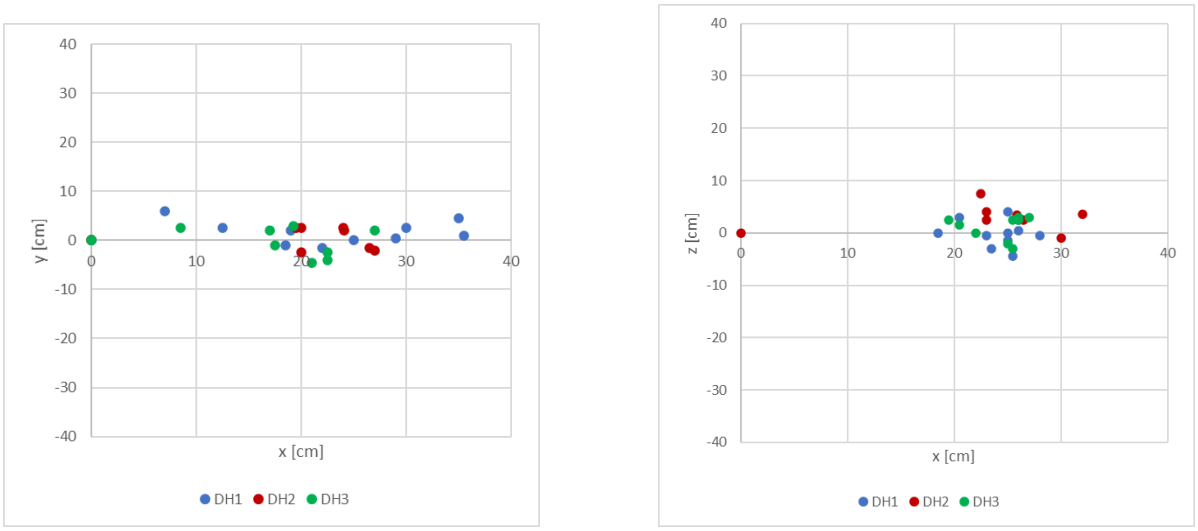


**(a)** Fall experiment scale 1:10

**(b)** Fall experiment scale 1:15

**Figure F.4:** Locations (x,z) of Cube framework directly after fall, given in cm.

### Piebox framework

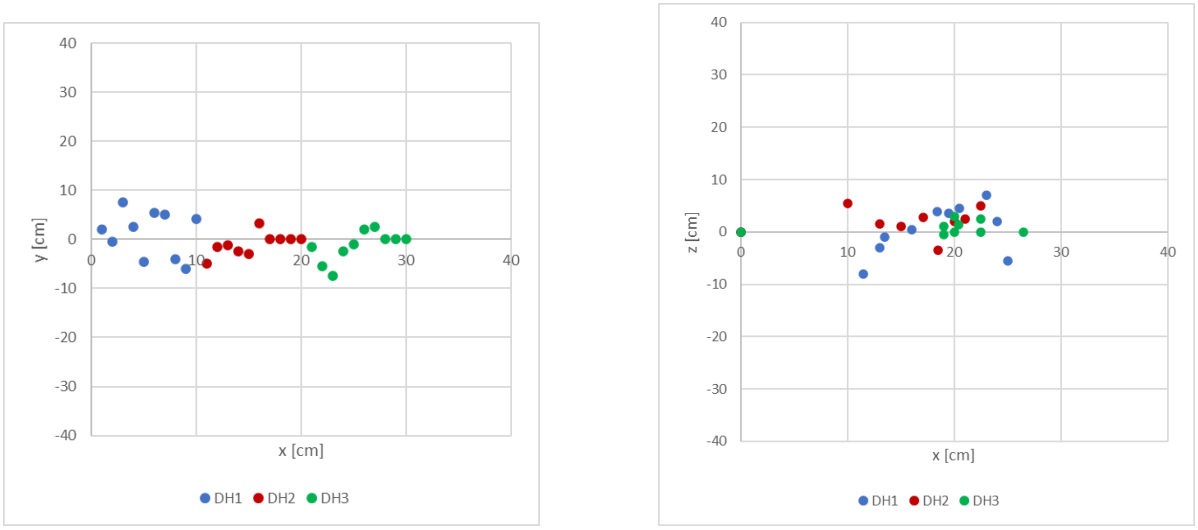


**(a)** Fall experiment scale 1:10

**(b)** Fall experiment scale 1:15

**Figure F.5:** Locations (x,z) of Piebox framework directly after fall, given in cm.

### Anchor long

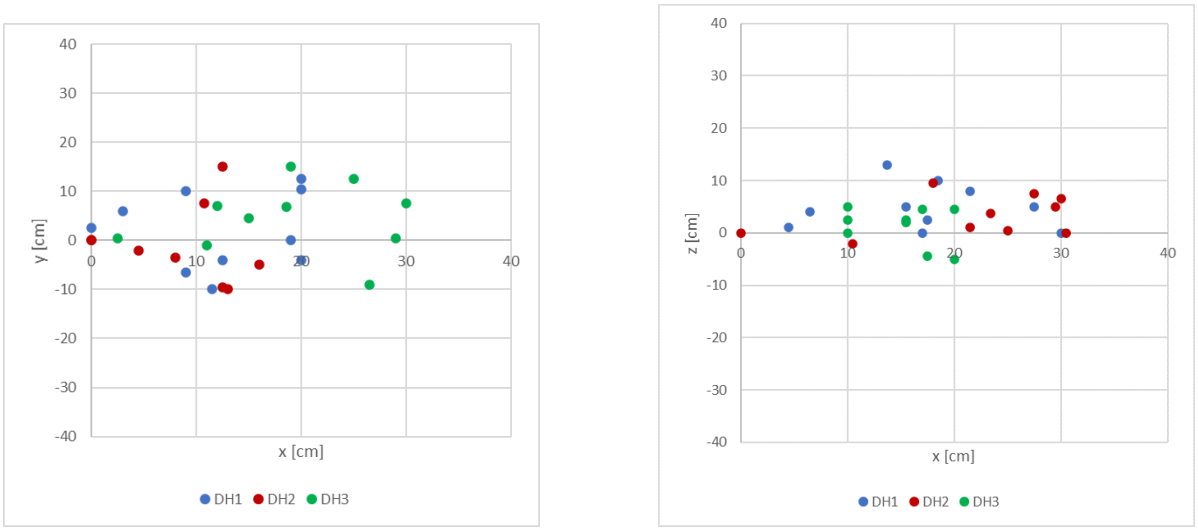


**(a)** Fall experiment scale 1:10

**(b)** Fall experiment scale 1:15

**Figure F.6:** Locations (x,z) of Anchor long directly after fall, given in cm.

### Anchor short

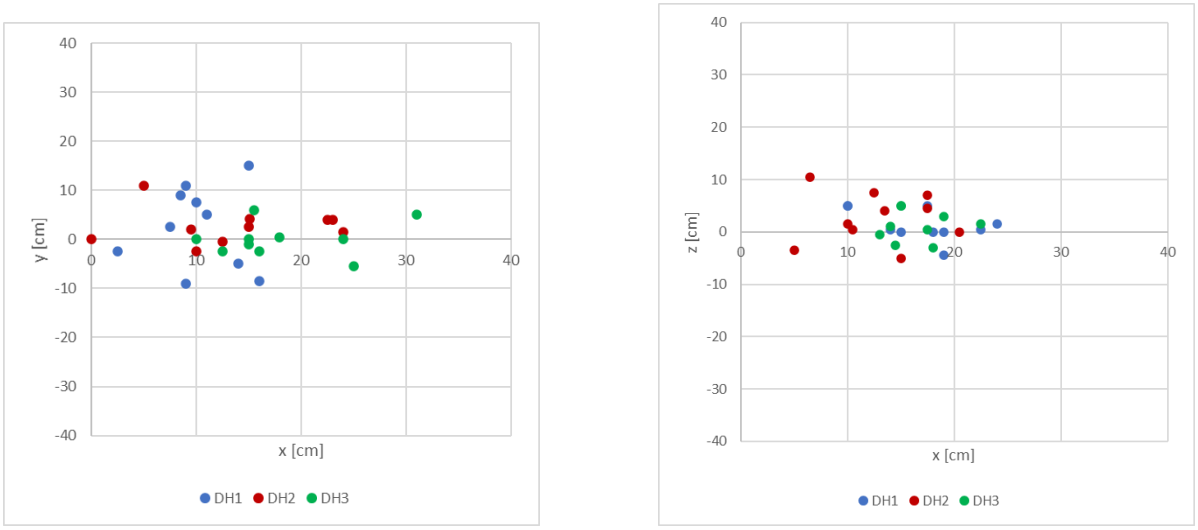


**(a)** Fall experiment scale 1:10

**(b)** Fall experiment scale 1:15

**Figure F.7:** Locations (x,z) of Anchor short directly after fall, given in cm.

### Open table 1

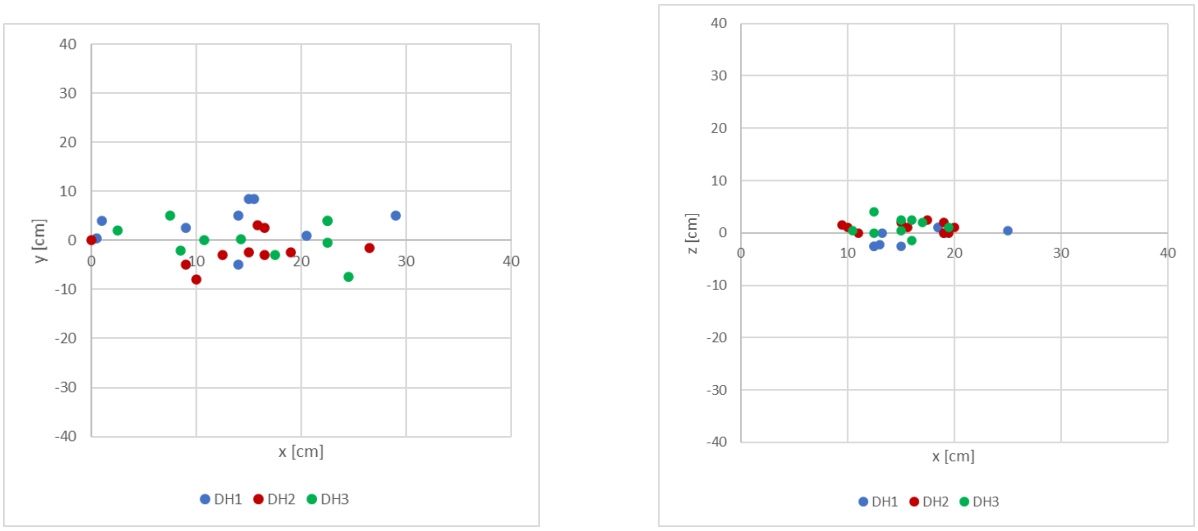


**(a)** Fall experiment scale 1:10

**(b)** Fall experiment scale 1:15

**Figure F.8:** Locations (x,z) of Open table 1 directly after fall, given in cm.

### Open table 2

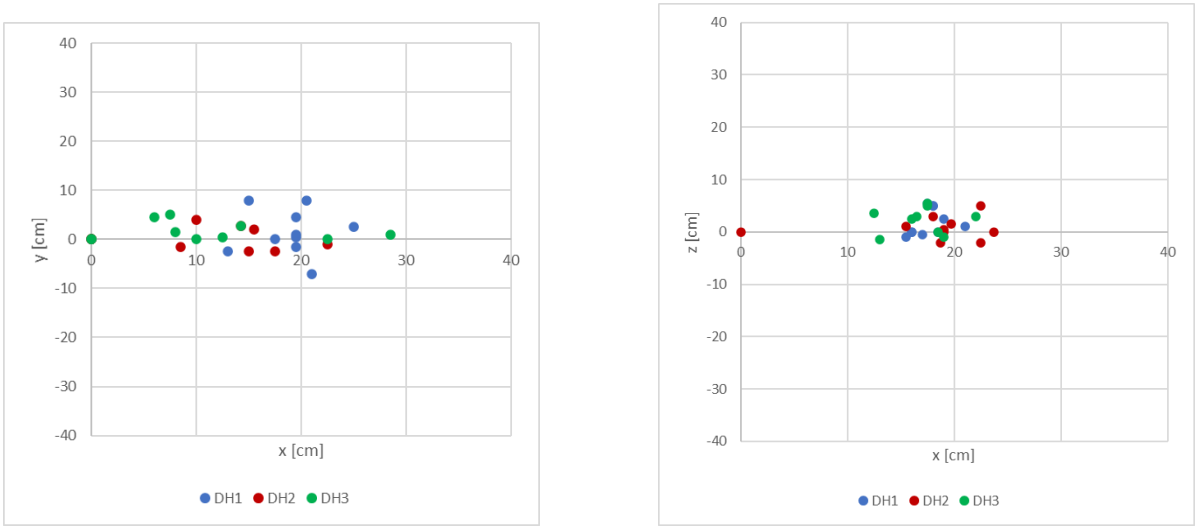


**(a)** Fall experiment scale 1:10

**(b)** Fall experiment scale 1:15

**Figure F.9:** Locations (x,z) of Open table 2 directly after fall, given in cm.

### Open table 3

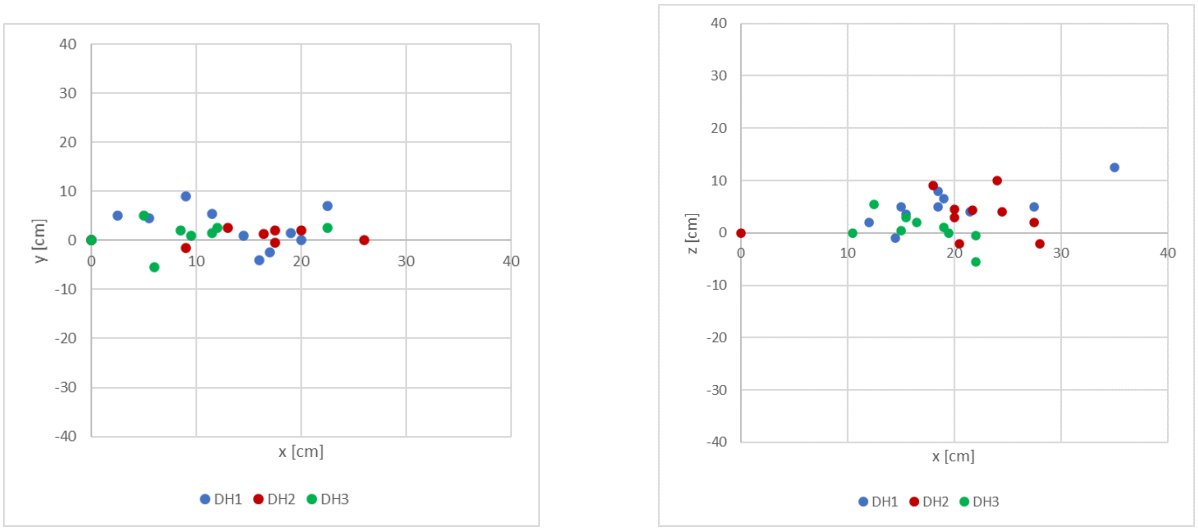


**(a)** Fall experiment scale 1:10

**(b)** Fall experiment scale 1:15

**Figure F.10:** Locations (x,z) of Open table 3 directly after fall, given in cm.

**Difference in drop heights**

**Table F.3:** The horizontal distances during fall experiment scale 1:10 per concept averaged per drop height and summed up per drop height and per concept, given in cm.

| | Drop height 1 | Drop height 2 | Drop height 3 | Total |
|---|---|---|---|---|
| Reference block | 16.9 | 11.0 | 14.3 | 42.2 |
| Open table 3 | 14.9 | 16.5 | 13.4 | 44.8 |
| Open table 1 | 13.8 | 16.4 | 14.7 | 44.9 |
| Anchor short | 12.8 | 16.2 | 18.2 | 47.3 |
| Tetrapod | 15.6 | 17.6 | 15.1 | 48.2 |
| Open table 2 | 19.6 | 14.6 | 14.6 | 48.8 |
| Anchor long | 14.8 | 14.5 | 20.6 | 49.9 |
| Xblock | 16.0 | 18.2 | 19.1 | 53.4 |
| Piebox framework | 17.3 | 16.7 | 19.9 | 53.9 |
| Cube framework | 23.7 | 24.2 | 19.5 | 67.4 |
| Total | 165.3 | 165.9 | 169.6 | |

**Table F.4:** The horizontal distances during fall experiment scale 1:15 per concept averaged per drop height and summed up per drop height and per concept, given in cm.

| | Drop height 1 | Drop height 2 | Drop height 3 | Total |
|---|---|---|---|---|
| Reference block | 14.4 | 11.9 | 13.8 | 40.1 |
| Tetrapod | 15.7 | 13.5 | 14.5 | 43.8 |
| Open table 1 | 16.7 | 15.7 | 14.8 | 47.3 |
| Anchor short | 17.3 | 14.7 | 16.7 | 48.6 |
| Xblock | 21.1 | 17.4 | 15.7 | 54.2 |
| Piebox framework | 19.0 | 17.4 | 20.6 | 57.1 |
| Open table 2 | 17.9 | 19.8 | 19.8 | 57.5 |
| Anchor long | 18.4 | 23.9 | 15.7 | 58.0 |
| Open table 3 | 20.5 | 22.3 | 17.7 | 60.5 |
| Cube framework | 24.1 | 26.2 | 24.4 | 74.7 |
| | 185.2 | 182.8 | 173.7 | |

## F.1.3. The movement during the fall

The fall of the concepts was video recorded from the side to observe the movement over the depth (x,y). The recordings were analysed using "Tracker Video Analysing and Modelling Tool" (see Figure F.11). The concepts were tracked manually in position per fall, meaning that for each video frame, the location (x,y) of the concept at that moment was tracked by clicking on the centre of mass of the concept. All the track positions per concept are merged in one graph per test (scale 1:10 and scale 1:15). This provides insight in their horizontal displacement during the fall.

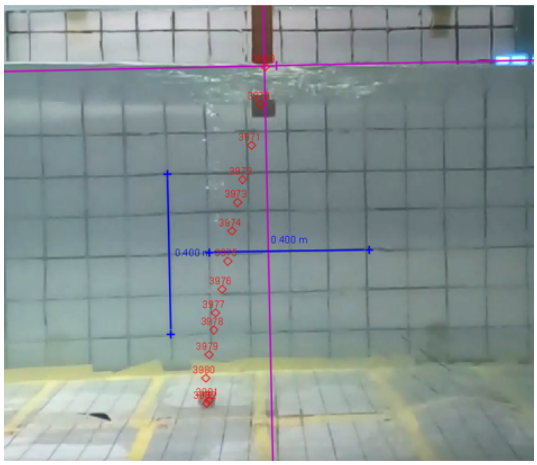


**Figure F.11:** Video analysing Fall tests in "Tracker Video Analysing and Modelling Tool"

## Reference block

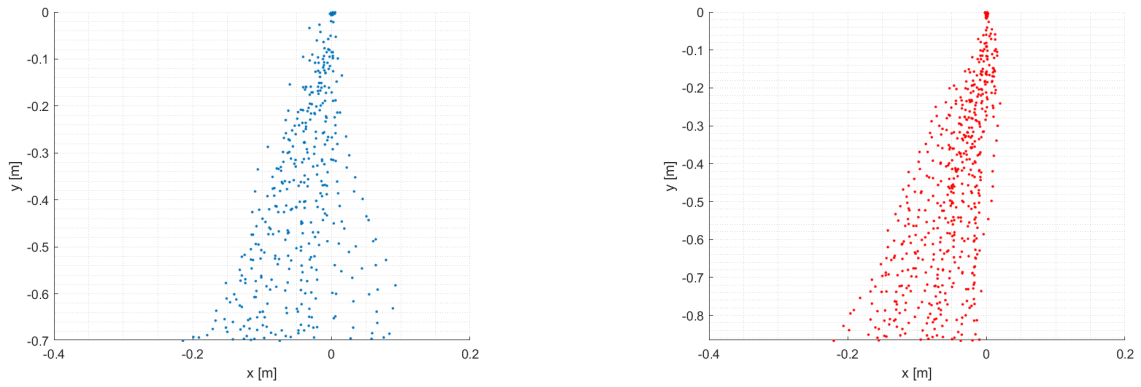


**(a)** Fall experiment scale 1:10

**(b)** Fall experiment scale 1:15

**Figure F.12:** Track positions of Reference block in fall experiment

## Xblock

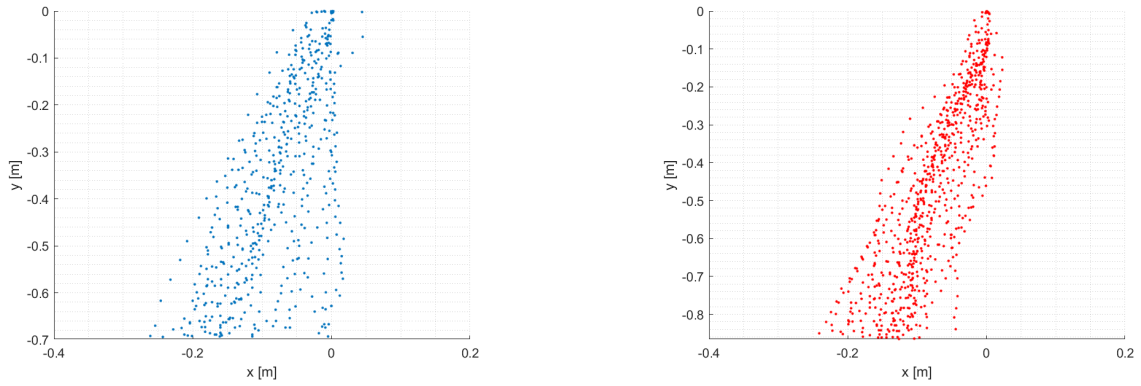


**(a)** Fall experiment scale 1:10

**(b)** Fall experiment scale 1:15

**Figure F.13:** Track positions of Xblock in fall experiment

### Tetrapod

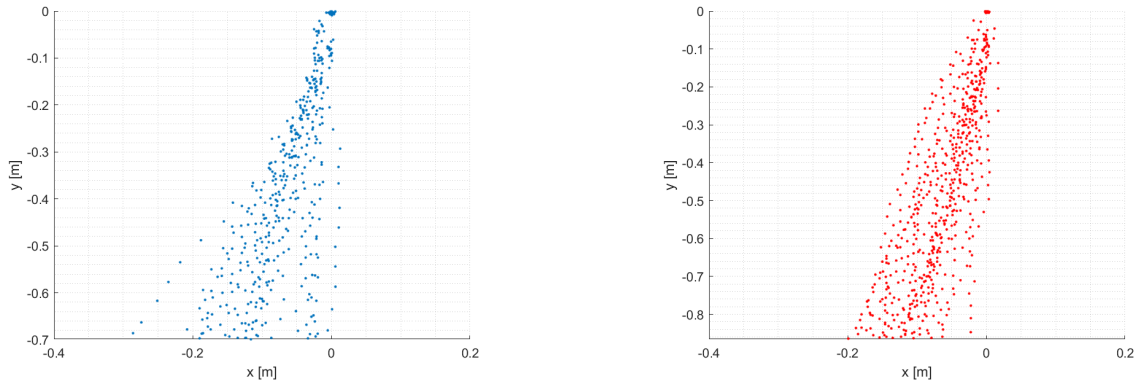


**(a)** Fall experiment scale 1:10

**(b)** Fall experiment scale 1:15

**Figure F.14:** Track positions of Tetrapod in fall experiment

### Cube framework

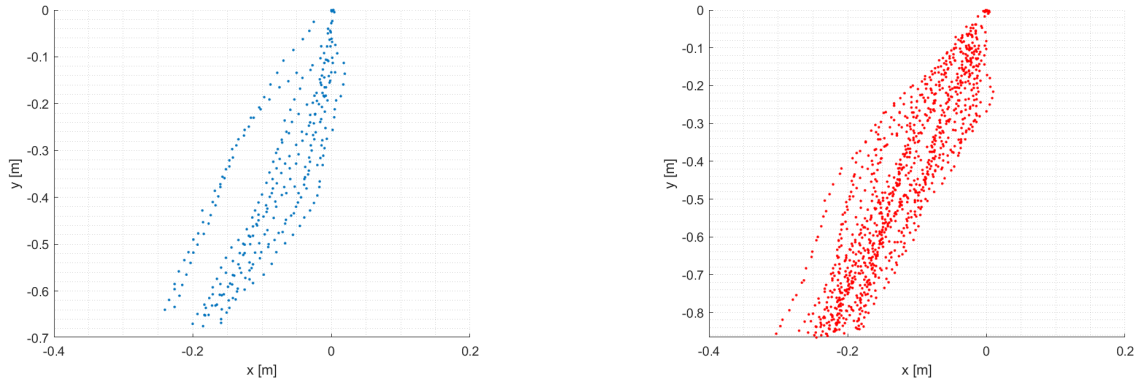


**(a)** Fall experiment scale 1:10

**(b)** Fall experiment scale 1:15

**Figure F.15:** Track positions of Cube framework in fall experiment

### Piebox framework

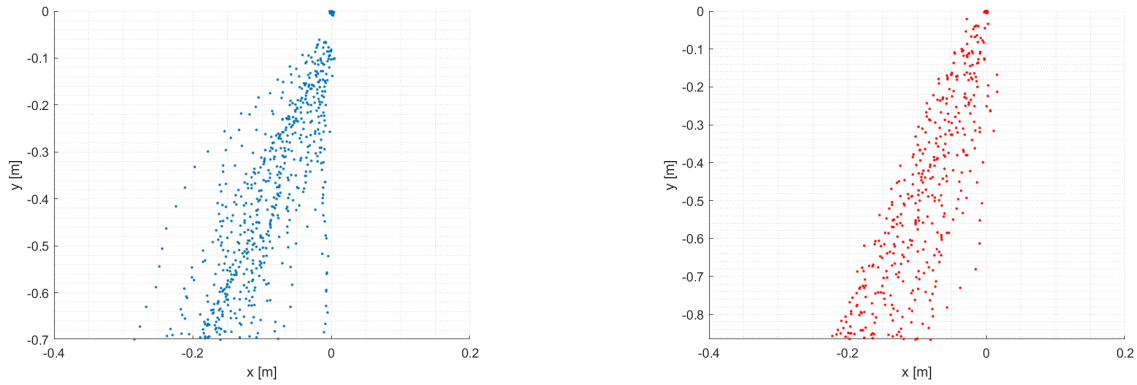


**(a)** Fall experiment scale 1:10

**(b)** Fall experiment scale 1:15

**Figure F.16:** Track positions of Piebox framework in fall experiment

### Anchor long

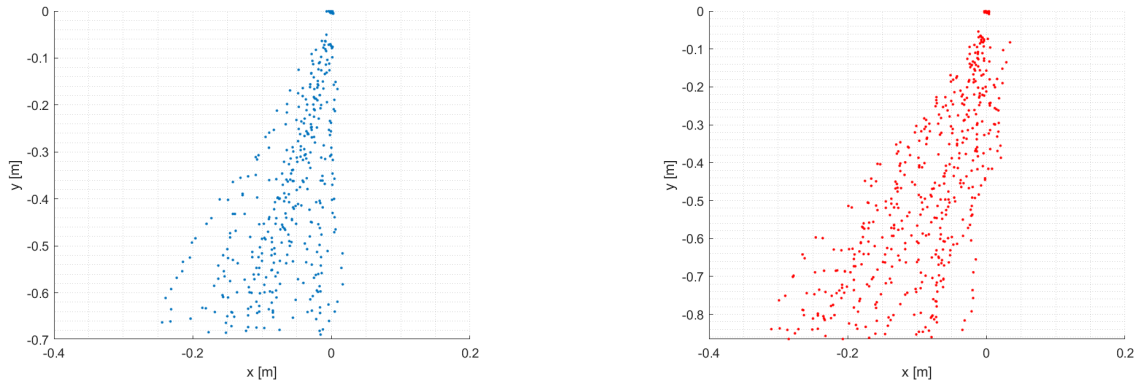


**(a)** Fall experiment scale 1:10 **(b)** Fall experiment scale 1:15

**Figure F.17:** Track positions of Anchor long in fall experiment

### Anchor short

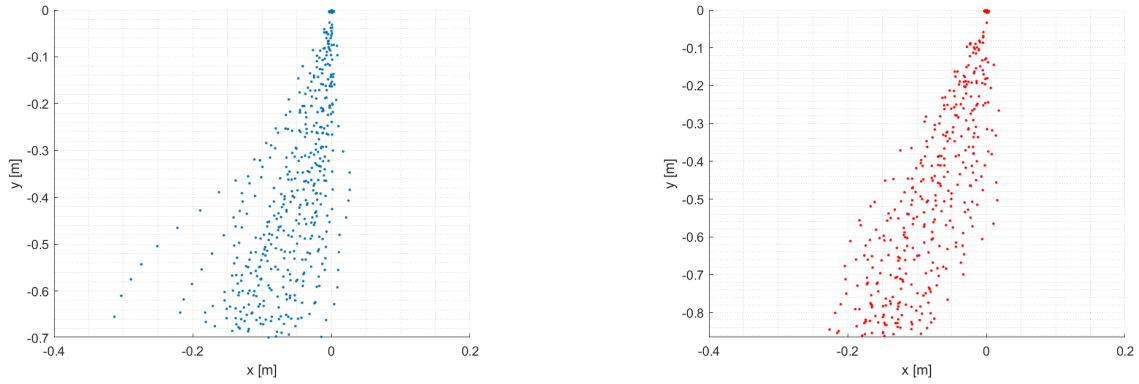


**(a)** Fall experiment scale 1:10 **(b)** Fall experiment scale 1:15

**Figure F.18:** Track positions of Anchor long in fall experiment

### Open table 1

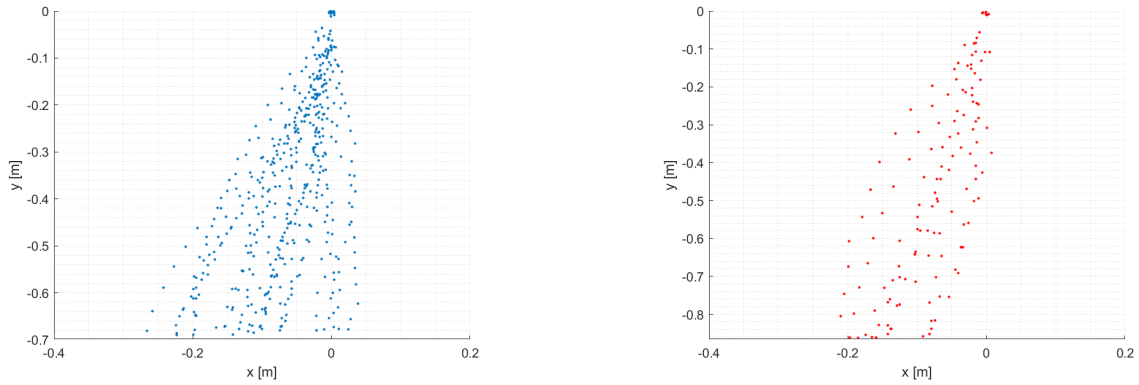


**(a)** Fall experiment scale 1:10 **(b)** Fall experiment scale 1:15

**Figure F.19:** Track positions of Open table 1 in fall experiment

### Open table 2

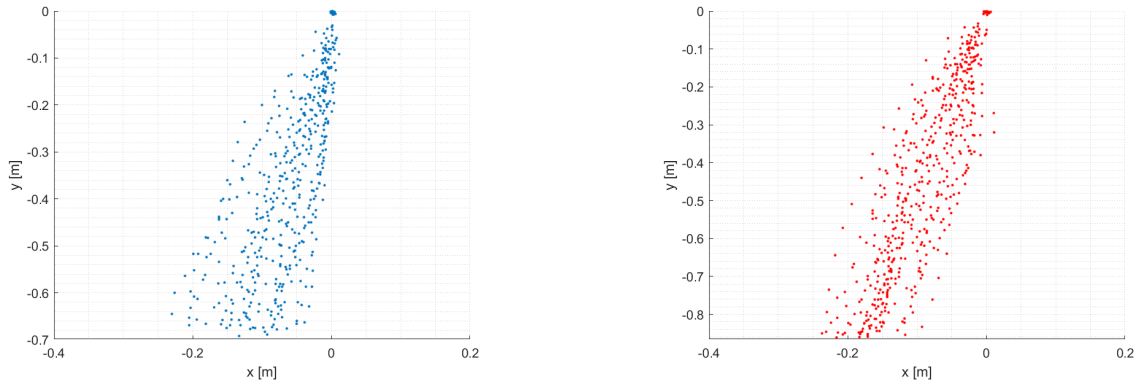


**(a)** Fall experiment scale 1:10

**(b)** Fall experiment scale 1:15

**Figure F.20:** Track positions of Open table 2 in fall experiment

### Open table 3

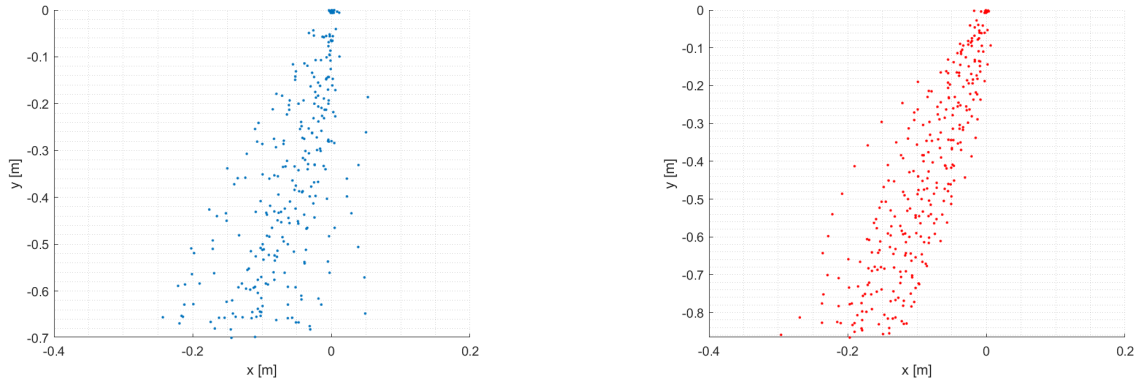


**(a)** Fall experiment scale 1:10

**(b)** Fall experiment scale 1:15

**Figure F.21:** Track positions of Open table 3 in fall experiment

# F.2. Land experiment

## F.2.1. Test conditions

**Table F.5:** Test conditions measured by DASYlab for land experiment on scale 1:15

| | $H_s$ *[m]* | $T_p$ *[s]* | $\bar{u}$ [m/s] |
|---|---|---|---|
| Reference block | 0.018 | 4.7 | 0.08 |
| Xblock | 0.020 | 4.7 | 0.08 |
| Tetrapod | 0.018 | 5.0 | 0.09 |
| Cube framework | 0.018 | 5.0 | 0.08 |
| Piebox framework | 0.020 | 5.1 | 0.09 |
| Anchor short | 0.020 | 4.8 | 0.08 |
| anchor long | 0.018 | 4.5 | 0.08 |
| Open table 1 | 0.022 | 4.8 | 0.07 |
| Open table 2 | 0.017 | 4.4 | 0.08 |
| Open table 3 | 0.021 | 4.8 | 0.08 |

# F.3. Stability experiment

## F.3.1. Test conditions

**Table F.6:** Test conditions measured by DASYlab for stability experiment on scale 1:15

| **SC 1** | | | $H_s$ *[m]* | $T_p$ *[s]* | $\bar{u}$ [m/s] |
|---|---|---|---|---|---|
| | Reference block | 1 | 0.12 | 2.0 | 0.15 |
| | | 2 | 0.13 | 2.0 | 0.15 |
| | Xblock | 1 | 0.13 | 2.0 | 0.15 |
| | | 2 | 0.13 | 2.0 | 0.15 |
| | Tetrapod | 1 | 0.13 | 2.0 | 0.15 |
| | | 2 | 0.13 | 2.0 | 0.15 |
| | Cube framework | 1 | 0.13 | 2.0 | 0.15 |
| | | 2 | 0.13 | 2.0 | 0.15 |
| | | 3 | 0.13 | 2.0 | 0.15 |
| | Piebox framework | 1 | 0.13 | 2.0 | 0.15 |
| | | 2 | 0.13 | 2.0 | 0.15 |
| | Anchor short | 1 | 0.13 | 2.0 | 0.15 |
| | | 2 | 0.13 | 2.0 | 0.16 |
| | Anchor long | 1 | 0.13 | 2.0 | 0.15 |
| | | 2 | 0.13 | 2.0 | 0.15 |
| | Open table 1 | 1 | 0.13 | 2.0 | 0.15 |
| | | 2 | 0.13 | 2.0 | 0.16 |
| | Open table 2 | 1 | 0.13 | 2.0 | 0.15 |
| | | 2 | 0.13 | 2.0 | 0.15 |
| | Open table 3 | 1 | 0.13 | 2.0 | 0.15 |
| | | 2 | 0.13 | 2.0 | 0.15 |

**Table F.7:** Test conditions measured by DASYlab for stability experiment on scale 1:15

| **SC 2** | | *Hs [m]* | *Tp [s]* | *u [m/s]* |
|---|---|---|---|---|
| Reference block | 1 | 0.17 | 2.0 | 0.16 |
| | 2 | 0.17 | 2.0 | 0.15 |
| Xblock | 1 | 0.17 | 2.0 | 0.17 |
| | 2 | 0.17 | 2.0 | 0.17 |
| Tetrapod | 1 | 0.17 | 2.0 | 0.17 |
| | 2 | 0.17 | 2.0 | 0.17 |
| Piebox framework | 1 | 0.18 | 2.0 | 0.17 |
| | 2 | 0.17 | 2.0 | 0.17 |
| | 3 | 0.17 | 2.0 | 0.16 |
| Anchor short | 1 | 0.17 | 2.0 | 0.17 |
| | 2 | 0.18 | 2.0 | 0.17 |
| | 3 | 0.17 | 2.0 | 0.16 |
| | 4 | 0.18 | 2.0 | 0.16 |
| Anchor long | 1 | 0.17 | 2.0 | 0.15 |
| | 2 | 0.17 | 2.0 | 0.16 |
| Open table 1 | 1 | 0.18 | 2.0 | 0.17 |
| | 2 | 0.18 | 2.0 | 0.17 |
| | 3 | 0.17 | 2.0 | 0.16 |
| | 4 | 0.17 | 2.0 | 0.08 |
| Open table 2 | 1 | 0.17 | 2.0 | 0.17 |
| | 2 | 0.18 | 2.0 | 0.17 |
| Open table 3 | 1 | 0.18 | 2.0 | 0.17 |
| | 2 | 0.17 | 2.0 | 0.15 |

**Table F.8:** Test conditions measured by DASYlab for stability experiment on scale 1:15

| **SC 1** | | *Hs [m]* | *Tp [s]* | *u [m/s]* |
|---|---|---|---|---|
| Reference block | 1 | 0.14 | 2.0 | 0.16 |
| | 2 | 0.15 | 2.0 | 0.16 |
| | 3 | 0.14 | 2.0 | 0.16 |
| Tetrapod | 1 | 0.14 | 2.0 | 0.16 |
| | 2 | 0.14 | 2.0 | 0.16 |
| | 3 | 0.15 | 2.0 | 0.16 |
| Anchor short | 1 | 0.14 | 2.1 | 0.16 |
| | 2 | 0.15 | 2.0 | 0.16 |
| | 3 | 0.14 | 2.0 | 0.16 |
| Anchor long | 1 | 0.12 | 1.7 | 0.17 |
| | 2 | 0.13 | 2.0 | 0.16 |
| | 3 | 0.14 | 2.0 | 0.16 |
| Open table 1 | 1 | 0.15 | 2.1 | 0.16 |
| | 2 | 0.16 | 2.1 | 0.16 |
| | 3 | 0.15 | 2.1 | 0.16 |
| | 4 | 0.14 | 2.1 | 0.16 |
| Open table 2 | 1 | 0.15 | 2.0 | 0.16 |
| | 2 | 0.16 | 2.1 | 0.16 |
| | 3 | 0.15 | 2.1 | 0.16 |
| | 4 | 0.14 | 2.1 | 0.16 |
| Open table 3 | 1 | 0.16 | 2.1 | 0.16 |
| | 2 | 0.15 | 2.1 | 0.16 |
| | 3 | 0.14 | 2.1 | 0.16 |

**Table F.9:** Test conditions measured by DASYlab for stability experiment on scale 1:15

| **SC 4** | | *Hs [m]* | *Tp [s]* | *u [m/s]* |
|---|---|---|---|---|
| Tetrapod | 1 | 0.13 | 2.0 | 0.13 |
| | 2 | 0.14 | 2.0 | 0.14 |
| Anchor long | 1 | 0.13 | 2.0 | 0.13 |
| | 2 | 0.14 | 2.0 | 0.14 |
| Open table 2 | 1 | 0.13 | 2.0 | 0.13 |
| | 2 | 0.13 | 2.0 | 0.13 |
| | 3 | 0.14 | 2.0 | 0.13 |
| Open table 3 | 1 | 0.13 | 2.0 | 0.13 |
| | 2 | 0.13 | 2.0 | 0.13 |
| | 3 | 0.14 | 2.0 | 0.13 |

**Table F.10:** Test conditions measured by DASYlab for stability experiment on scale 1:15

| **SC 5** | | *Hs [m]* | *Tp [s]* | *u [m/s]* |
|---|---|---|---|---|
| Open table 2 | 1 | 0.15 | 2.0 | 0.13 |
| | 2 | 0.14 | 2.0 | 0.13 |
| | 3 | 0.15 | 2.0 | 0.13 |
| Open table 3 | 1 | 0.15 | 2.0 | 0.13 |
| | 2 | 0.14 | 2.0 | 0.13 |
| | 3 | 0.15 | 2.0 | 0.13 |

## F.3.2. Storm conditions 1

**Table F.11:** Results of stability test with storm conditions 1

| **Test** | 1 | 2 | 3 |
|---|---|---|---|
| Ref. Block | stable | stable | |
| Xblock | minimal movement | stable | |
| Tetrapod | minimal movement | stable | |
| Piebox fr. | stable | stable | |
| Cube fr. | unstable | unstable | unstable |
| Anchor long | stable | stable | |
| Anchor short | stable | minimal movement | |
| Open table 1 | stable | minimal movement | |
| Open table 2 | stable | stable | |
| Open table 3 | minimal movement | stable | |

## F.3.3. Storm conditions 2

**Table F.12:** Results of stability test with storm conditions 2

| **Test** | 1 | 2 | 3 | 4 |
|---|---|---|---|---|
| Ref. Block | stable | stable | | |
| Xblock | unstable | unstable | | |
| Tetrapod | stable | minimal movement | | |
| Piebox fr. | stable | unstable | unstable | |
| Anchor long | stable | stable | | |
| Anchor short | stable | unstable | stable | stable |
| Open table 1 | unstable | stable | stable | minimal movement |
| Open table 2 | stable | stable | | |
| Open table 3 | stable | stable | | |

## F.3.4. Storm conditions 3

**Table F.13:** Results of stability test with storm conditions 3

| **Test** | 1 | 2 | 3 | 4 |
|---|---|---|---|---|
| Ref. Block | stable | unstable | stable | |
| Tetrapod | stable | minimal movement | stable | |
| Anchor long | minimal movement | minimal movement | stable | |
| Anchor short | unstable | minimal movement | unstable | |
| Open table 1 | minimal movement | minimal movement | minimal movement | unstable |
| Open table 2 | stable | unstable | stable | stable |
| Open table 3 | stable | stable | stable | |

## F.3.5. Storm conditions 4

**Table F.14:** Results of stability test with storm conditions 4

| **Test** | 1 | 2 | 3 |
|---|---|---|---|
| Tetrapod | unstable | unstable | |
| Anchor long | unstable | unstable | |
| Open table 2 | minimal movement | unstable | minimal movement |
| Open table 3 | minimal movement | minimal movement | stable |

## F.3.6. Storm conditions 5

**Table F.15:** Results of stability test with storm conditions 5

| **Test** | 1 | 2 | 3 |
|---|---|---|---|
| Open table 2 | minimal movement | unstable | unstable |
| Open table 3 | stable | unstable | minimal movement |

# F.4. Wave generation

**Table F.16:** Ursell, Keulegan and Carpenter and Reynolds number for each test

| | $U_{ursell}$ [-] | $KC$ [-] | $Re$ [-] |
|---|---|---|---|
| Fall test 1:10 | 12 | 57 | 4534 |
| Fall test 1:15 | 3 | 30 | 2171 |
| Land test | 6 | 21 | 3253 |
| Stability test SC1 | 16 | 108 | 3065 |
| Stability test SC2 | 21 | 142 | 3756 |
| Stability test SC3 | 27 | 138 | 3649 |
| Stability test SC4 | 23 | 119 | 3023 |
| Stability test SC5 | 27 | 137 | 3510 |

# F.5. Fall test

## F.5.1. Horizontal displacement in x-z plane

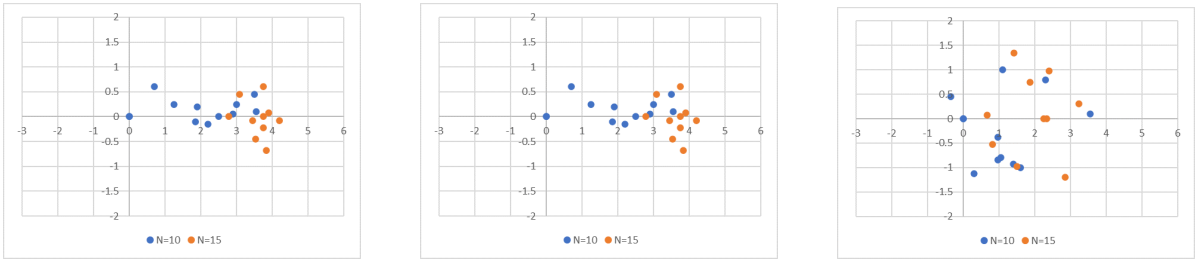


Drop height 1 Drop height 2 Drop height 3

**Figure F.22:** Location of Reference block, after drop for fall experiment N=10

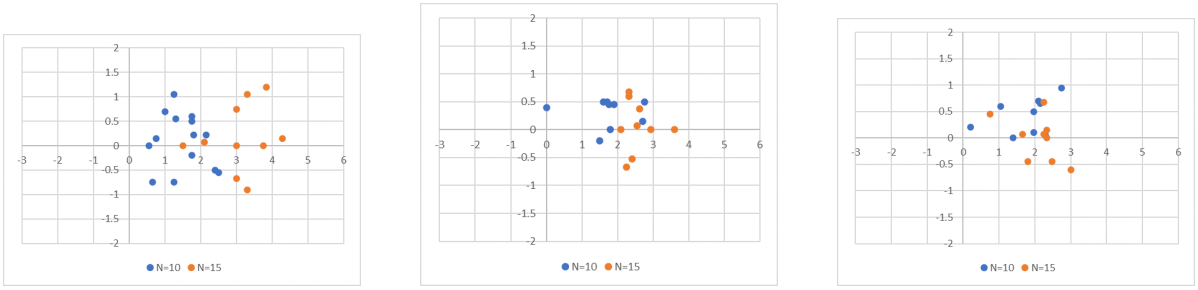


Drop height 1 Drop height 2 Drop height 3

**Figure F.23:** Location of Xblock, after drop for fall experiment N=10

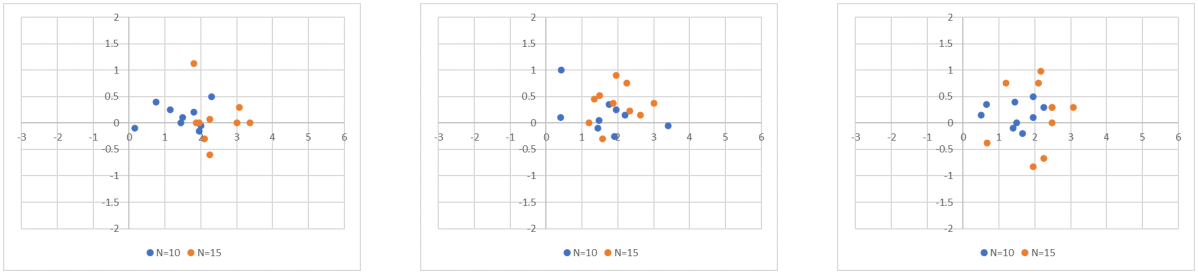


Drop height 1 Drop height 2 Drop height 3

**Figure F.24:** Location of Tetrapod, after drop for fall experiment N=10

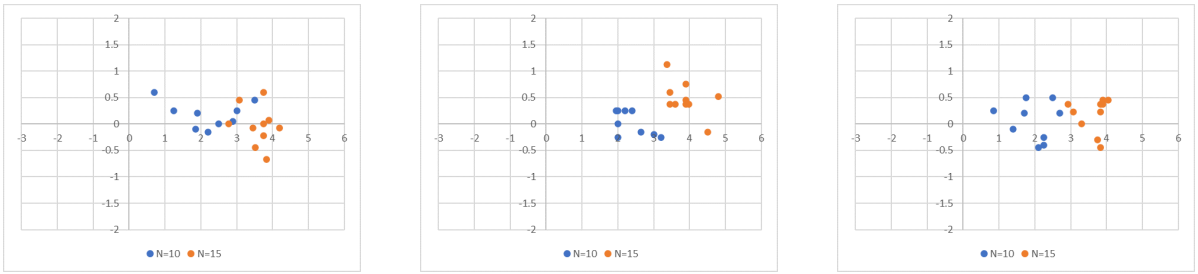


Drop height 1 Drop height 2 Drop height 3

**Figure F.25:** Location of Cube framework, after drop for fall experiment N=10

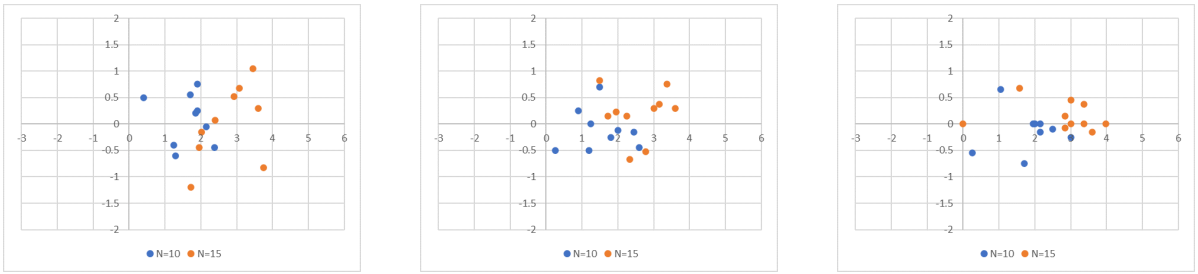


Drop height 1 Drop height 2 Drop height 3

**Figure F.26:** Location of Piebox framework, after drop for fall experiment N=10

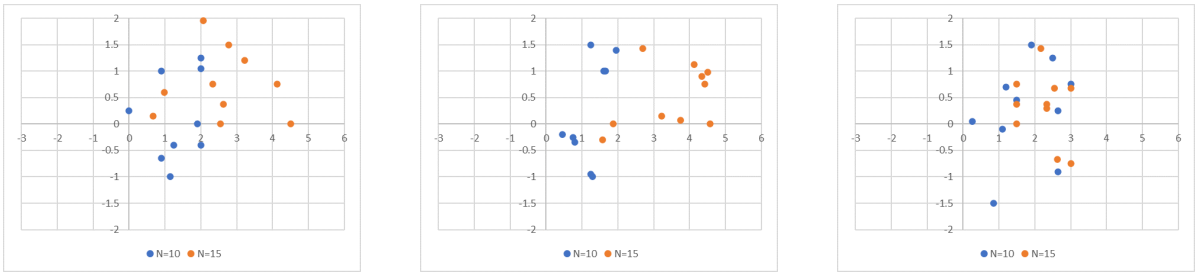


Drop height 1 Drop height 2 Drop height 3

**Figure F.27:** Location of Anchor long, after drop for fall experiment N=10

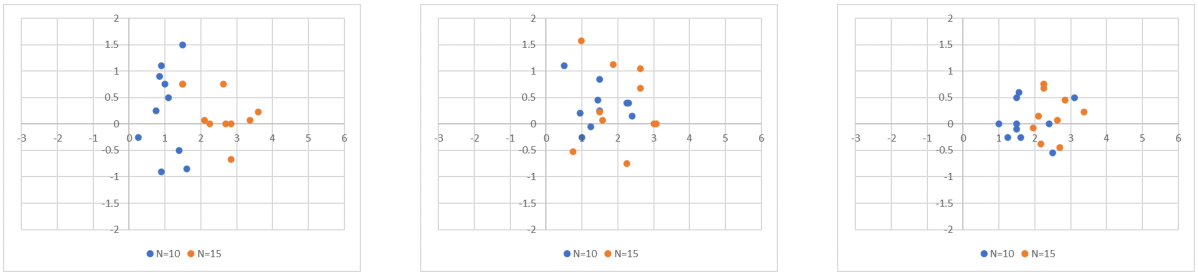


Drop height 1 Drop height 2 Drop height 3

**Figure F.28:** Location of Anchor short, after drop for fall experiment N=10

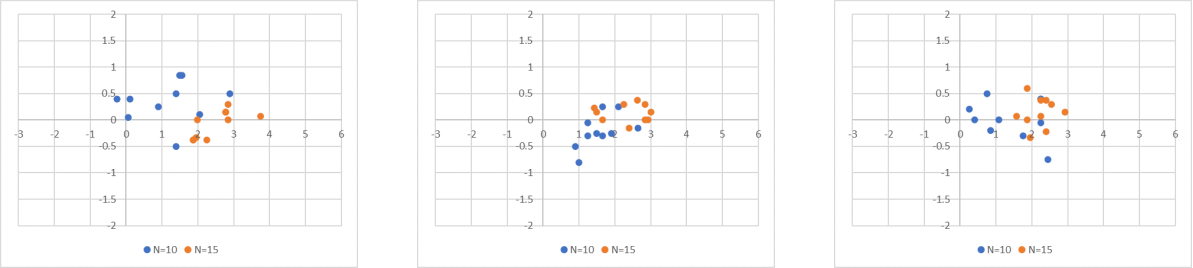


Drop height 1 Drop height 2 Drop height 3

**Figure F.29:** Location of Open table 1, after drop for fall experiment N=10

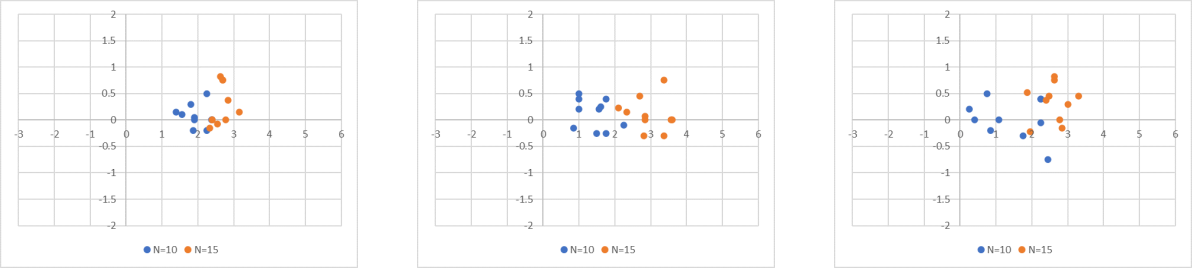


Drop height 1 Drop height 2 Drop height 3

**Figure F.30:** Location of Open table 2, after drop for fall experiment N=10

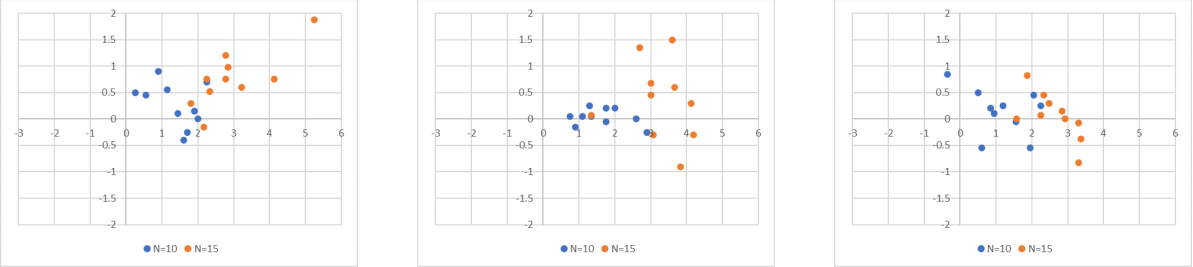


Drop height 1 Drop height 2 Drop height 3

**Figure F.31:** Location of Open table 3, after drop for fall experiment N=10

## F.5.2. Horizontal displacement in x-y plane

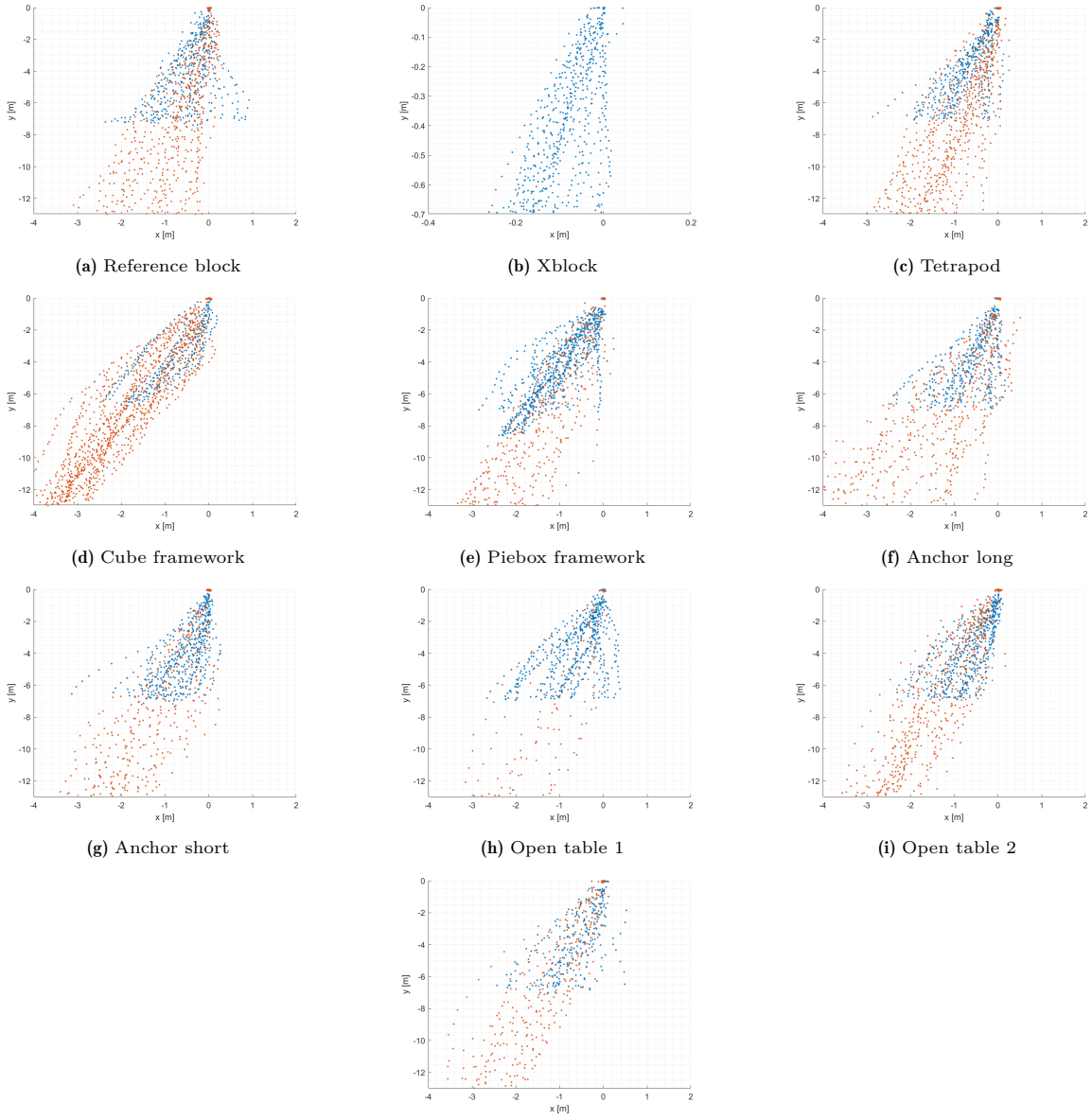


**(a)** Reference block

**(b)** Xblock

**(c)** Tetrapod

**(d)** Cube framework

**(e)** Piebox framework

**(f)** Anchor long

**(g)** Anchor short

**(h)** Open table 1

**(i)** Open table 2

**(j)** Open table 3

**Figure F.32:** Horizontal displacement during fall translated to scale 1:1

### Linear extrapolation

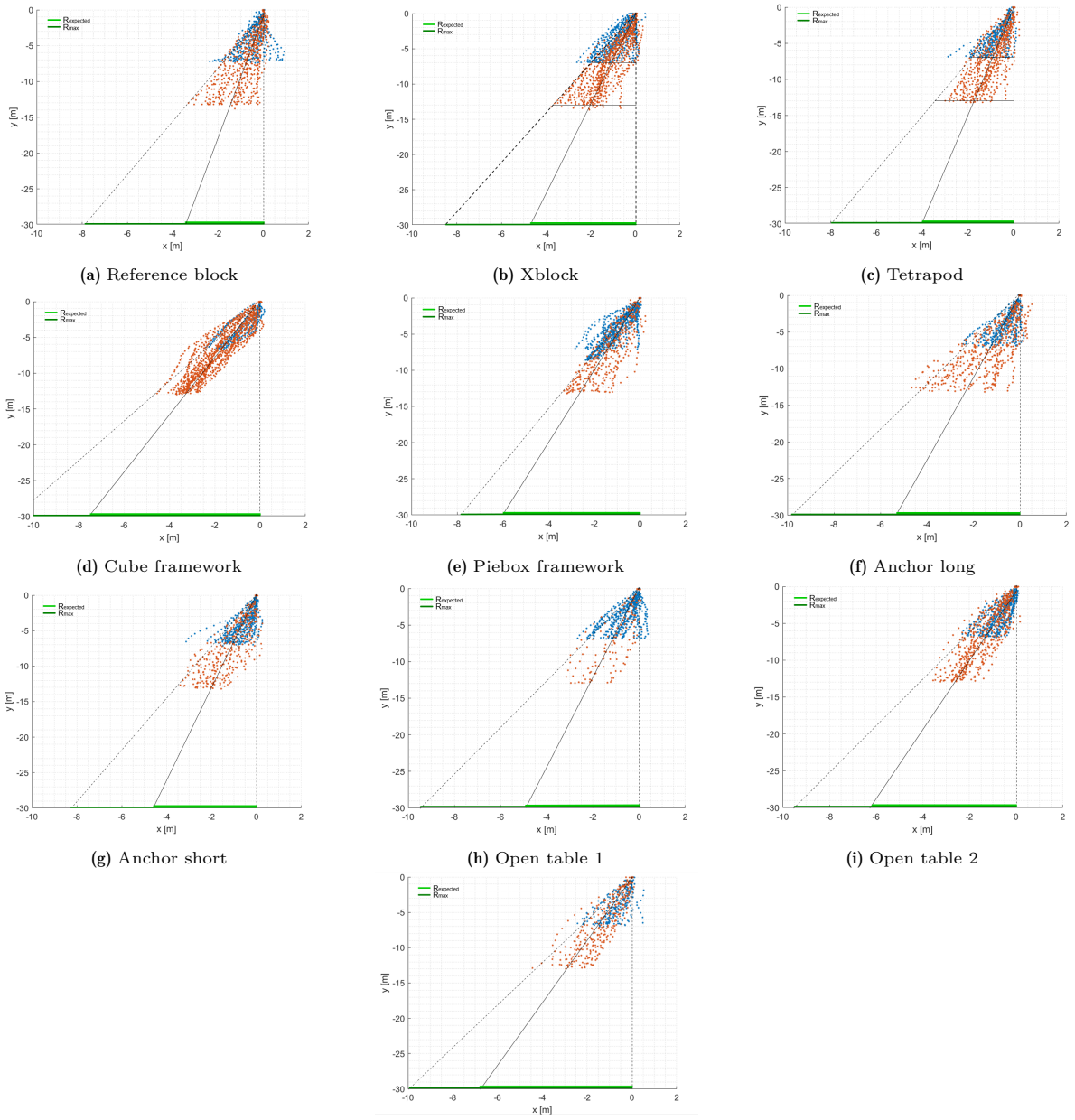


(a) Reference block

(b) Xblock

(c) Tetrapod

(d) Cube framework

(e) Piebox framework

(f) Anchor long

(g) Anchor short

(h) Open table 1

(i) Open table 2

(j) Open table 3

**Figure F.33:** Linear extrapolating of tracking points of concepts during fall, to obtain horizontal displacement radius after fall. $x_{h-mean}$ indicates the most likely location after the fall and the corresponding radius from the drop location of the concept after the fall and $x_{h-max}$ the maximum falling radius of the concept.

The values per concept obtained with linear extrapolation are for all concepts larger than the values per concept obtained with second order extrapolation. The maximum horizontal displacement obtained using linear extrapolation, all exceed the 4 and 5.5 metre lines. For the mean horizontal displacement obtained using linear extrapolation, the Reference block, Tetrapod, Anchor short, Xblock, Open table 1 and Anchor long do not exceed these maximum lines. The linear extrapolation method is assumed to lead to overestimating the radii values.

**Table F.17:** The mean and maximum horizontal displacement at a depth of 30 metres obtained using linear extrapolation.

| | $x_{h-max}$ [m] | $x_{h-mean}$ [m] |
|---|---|---|
| Reference block | 7.8 | 3.9 |
| Xblock | 8.5 | 4.65 |
| Tetrapod | 8 | 4 |
| Cube framework | 10.9 | 7.5 |
| Piebox framework | 7.8 | 6 |
| Anchor long | 9.85 | 5.3 |
| Anchor short | 8.2 | 4.55 |
| Open table 1 | 9.5 | 4.9 |
| Open table 2 | 9.5 | 6.25 |
| Open table 3 | 10 | 6.75 |

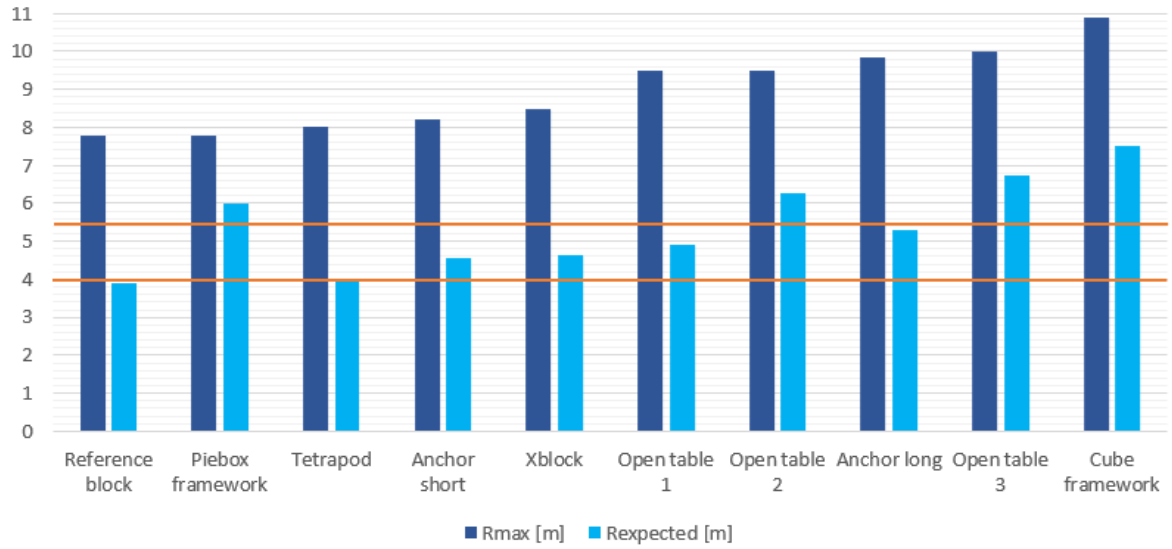


**Figure F.34:** Horizontal displacement results obtained using second order polynomial extrapolating. The orange lines indicate the design criteria values for positioning accuracy.

### 2nd order polynomial extrapolation

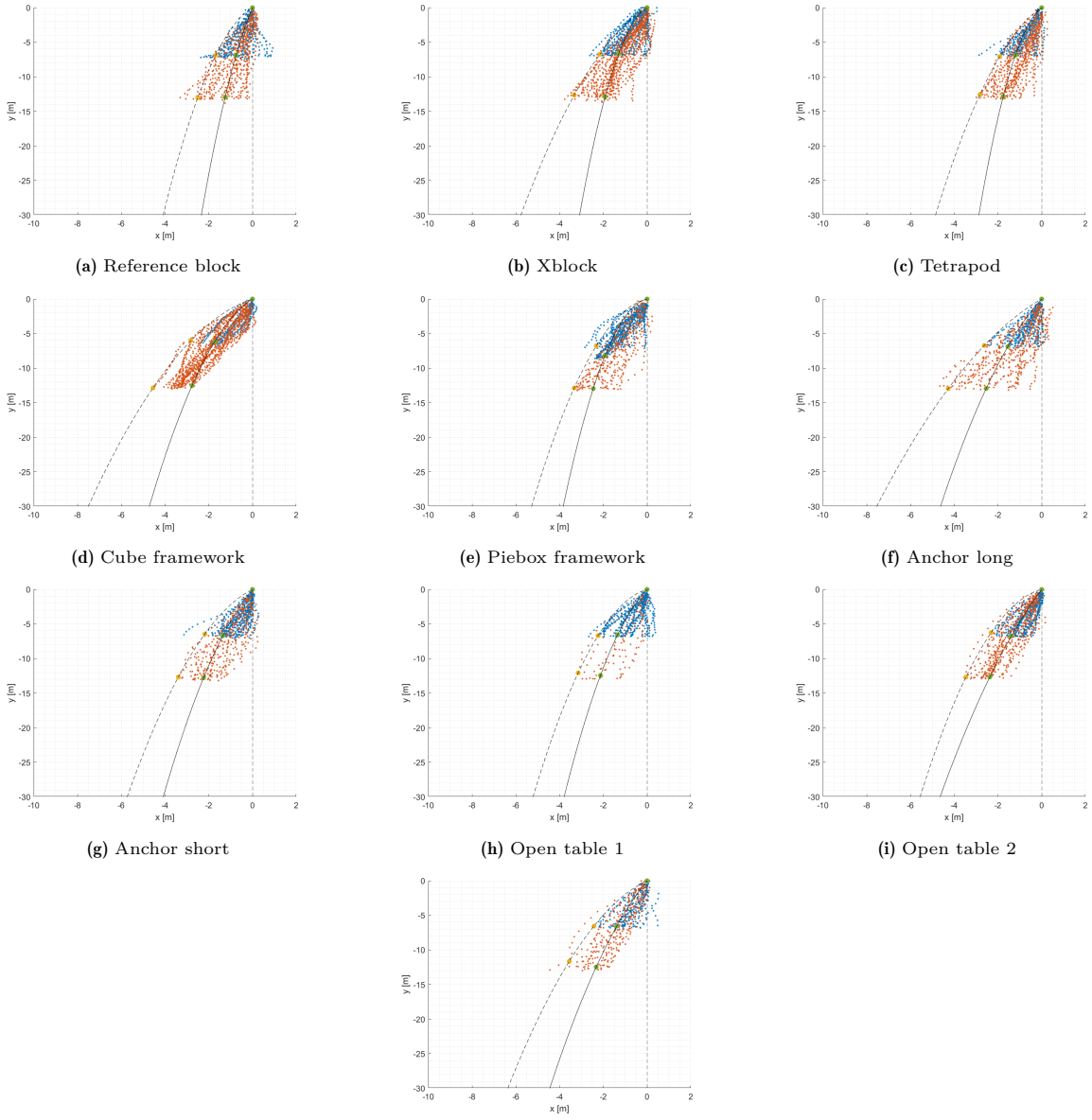


**(a)** Reference block **(b)** Xblock **(c)** Tetrapod

**(d)** Cube framework **(e)** Piebox framework **(f)** Anchor long

**(g)** Anchor short **(h)** Open table 1 **(i)** Open table 2

**(j)** Open table 3

**Figure F.35:** 2nd order polynomial extrapolating of tracking points of concepts during fall, to obtain horizontal displacement radius after fall. $x_{h-mean}$ indicates the most likely location after the fall and the corresponding radius from the drop location of the concept after the fall and $x_{h-max}$ the maximum falling radius of the concept.

# F.6. Land test

**Table F.18:** Number of sides of the concepts hit during the landing experiment per experiment, given in percentage of surface per concept.

| Experiment | 1 | 2 | 3 | 4 | 5 | 6 | 7 | 8 | 9 | 10 | 11 | Average |
|---|---|---|---|---|---|---|---|---|---|---|---|---|
| Ref. Block | 0.17 | 0.33 | 0.33 | 0.33 | 0.17 | 0.50 | 0.33 | | | | | 0.31 |
| Xblock | 0.43 | 0.43 | 0.27 | 0.27 | 0.43 | 0.27 | | | | | | 0.35 |
| Tetrapod | 0.25 | 0.25 | 0.25 | 0.25 | 0.25 | 0.25 | | | | | | 0.25 |
| Piebox fr. | 0.09 | 0.20 | 0.09 | 0.20 | 0.09 | 0.09 | 0.09 | | | | | 0.12 |
| Cube fr. | 0.09 | 0.09 | 0.09 | 0.09 | 0.09 | 0.09 | 0.09 | 0.19 | 0.09 | 0.09 | | 0.10 |
| Anchor long | 0.18 | 0.09 | 0.09 | 0.09 | 0.09 | 0.18 | 0.18 | 0.27 | | | | 0.15 |
| Anchor short | 0.16 | 0.08 | 0.16 | 0.08 | 0.08 | | | | | | | 0.11 |
| Open table 1 | 0.67 | 0.67 | 0.11 | 0.11 | 0.67 | 0.11 | 0.67 | 0.67 | 0.11 | 0.11 | 0.67 | 0.67 |
| Open table 2 | 0.60 | 0.60 | 0.10 | 0.10 | 0.60 | 0.10 | 0.60 | 0.60 | 0.10 | 0.10 | | 0.60 |
| Open table 3 | 0.51 | 0.45 | 0.51 | 0.51 | 0.51 | 0.45 | 0.51 | 0.51 | 0.45 | 0.51 | | 0.49 |

# F.7. Stability test

## F.7.1. Interpretation of output hydraulic conditions generated by the wave flume

**Storm conditions 1**

The current velocity corresponds to a current velocity 1.5 metres above seabed during a storm with a return period of 5 years, at Gemini offshore wind farm. This is a slightly milder current than the current velocity 1.5 metres above seabed during a storm with a 5 year return period, averaged over all three considered offshore wind farms.

The orbital motion generated in the wave flume corresponds to an orbital motion near the bottom generated during a storm with a 10 year return period at Borssele offshore wind farm. At Borssele offshore wind farm, the mildest wave conditions, compared to the other two considered offshore wind farms, occur.

**Storm conditions 2**

The current velocity corresponds to the current 1.5 metres above seabed during a storm with a return period of 10 years, averaged over all three considered offshore wind farms.

The orbital motion generated corresponds to the orbital motion near the bottom generated during a storm with a 10 year return period at HKW offshore wind farm.

**Storm conditions 3**

The current velocity corresponds to the current 1.5 metres above seabed, with a return period of 10 years, averaged over all three considered offshore wind farms.

The orbital motion generated corresponds to the orbital motion near the bottom generated during a storm with a 50 year return period at Borssele offshore wind farm. These wave conditions are slightly milder, than wave conditions during a storm with a 10 year return period at HKW.

**Storm conditions 4**

The current velocity corresponds to the current 1.5 metres above seabed, with a return period of 50 years, averaged over all three considered offshore wind farms.

The orbital motion generated corresponds to the orbital motion near the bottom generated during a storm with a 50 year return period at Gemini offshore wind farm. At Gemini offshore wind farm, the roughest wave conditions, compared to the other two considered offshore wind farms, occur. The wave storm conditions correspond to a storm which is rougher than a storm with a 50 year return period, averaged over all three offshore wind farms.

**Storm conditions 5**

The current velocity corresponds to the current 1.5 metres above seabed, with a return period of 50 years, averaged over all three considered offshore wind farms.

The orbital motion generated corresponds to the larger orbital motion near the bottom generated during a storm with a 50 year return period at Gemini offshore wind farm and a storm with a return period of 50 years averaged over all three wind farms.

**Table F.19:** For each concept it is presented whether the concept is to remain stable during prevailing conditions per considered offshore wind farm. + indicates that the concept remains stable, - indicates that the concept does not remain stable, ? indicates that it is unknown whether the concept remains stable during these storm conditions

| Storm conditions at OWF | Borssele | | HKW | | Gemini | | Averaged | |
|---|---|---|---|---|---|---|---|---|
| T [years] | 10 | 50 | 10 | 50 | 10 | 50 | 10 | 50 |
| Reference block | + | + | + | - | - | - | | - |
| Xblock | + | - | - | - | - | - | - | - |
| tetrapod | + | + | + | + | + | - | + | ? |
| Cube framework | - | - | - | - | - | - | - | - |
| Piebox framework | + | - | - | - | - | - | - | - |
| Anchor long | + | + | + | + | + | - | + | ? |
| Anchor short | + | - | - | - | - | - | - | - |
| Open table 1 | + | - | - | - | - | - | - | - |
| Open table 2 | + | + | + | + | + | + | + | + |
| Open table 3 | + | + | + | + | + | + | + | + |